Sources and fate of microplastics and nanoplastics: detection and characterization methods

Laura María Hernández Rodríguez

Department of Chemical Engineering

McGill University

Montreal, Canada

August 2021

A thesis submitted to McGill University in partial fulfillment of the requirement of the degree of

Doctor of Philosophy

Preface

In accordance with the “McGill Guidelines for Thesis Preparation”, this thesis is presented in a manuscript-based format. A brief introduction to the subject matter of this thesis, its objectives, and a summary of the presented manuscripts and the authors’ contributions are presented in Chapter 1. Chapter 2 presents a brief literature review on the topic. Chapters 3-7 present five original research manuscripts. Finally, Chapter 8 contains the thesis conclusions and suggestions for future work.

Acknowledgments

Firstly, I would like to thank my supervisor and mentor Dr. Nathalie Tufenkji. I have been blessed to have met such a wonderful woman in my path. I will be always thankful for all your knowledge, guidance, kind words, and support during this Ph.D.

I would also like to thank the committee members Dr. Berk, Dr. Wheeler, and Dr. Yaylayan for taking the time to read this manuscript and for attending my defense.

Furthermore, I'd like to acknowledge McGill University (McGill Engineering doctoral award, Eugenie Ulmer-Lamothe award), the Natural Science and Engineering Research Council of Canada (PURE CREATE program, NSERC Strategic and Discovery programs), the Fonds de recherche du Quebec, the Canada Foundation for Innovation, and the Department of Fisheries and Oceans for their generous funding.

I would like to thank Dr. Varoujan Yaylayan for welcoming me to his lab for my Py-GC-MS experiments. I learned so much from you and your lab, and I will always be grateful. I would also like to thank Dr. Kevin Wilkinson for the access to his lab and his continuous support. Dr. Liisa Jantunen for her help with collecting Arctic samples, I hope to be able to join you in the Arctic one day. I would like to thank Dr. Hans Larsson for giving us access to his lab and equipment.

To Dr. Watson Vargas, I do not have the words to thank you for receiving me in your research group when I was an undergrad. That opportunity changed my life. To Dr. Kretzschmar, thank you for encouraging me to take the path of research and pursue my Ph.D. I promise this is the last time I will call you Dr., we can finally be on a first-name basis (as per your multiple requests). To Dr. Sepideh Razavi, thanks for sharing your experience and encouraging me.

To all the past and present members of the biocolloids and surfaces group, thank you for all the fruitful discussions. Thanks to the chemical engineering staff for your help and support: Frank, Ranjan, Gerald, Lisa, Anna, Andrew, and Lu. To the members of GEEC, thanks for helping me fight the good fight, aiming for a more equitable diverse, and inclusive world.

Jeff, this thesis would not have been possible without your help and encouragement. I will always be thankful we were assigned to the same office. You are very much missed in Montreal.

To the friends I have made during my Ph.D., you are my Montreal family. Rapha and Ade: you are the two sisters the universe has given me, I thank life for you gals, I hope I can always be there for you as you have been here for me. Jacky and Mike: thanks for all the support, the long hours of talking, all the love, I love you guys. Oscar, and Karlita: thanks for always welcoming me at your home, your unconditional support, and for the all the great times, my Latin family in Montreal. Jenny and Ele: mis amigas que me cuidan, I love you guys so much. Maya, Asmara, Jesus, and Ale: thanks for all the dances (God knows they kept me sane through this Ph.D.), and believing unconditionally on me. Nia: Thanks for encouraging me to be a better human. Sharmaine, and Georges: short friendship, lots of feelings, I will miss having lunch with you guys every day. Nico, Buki, and Eva: my college-friends, thanks for your unconditional support both emotionally and technically. Friends, your support, encouragement, and energy have kept me going through thick and thin.

To my friends back home, thanks for always believing in me, all the long hours on video calls, and your unconditional encouragement. Vane, Vale, Pin, Danielita, Geme, Nany, Melucha, Kyris, Natis, Dani Duran, Mapao, and “aja” Dani: your friendship is invaluable to me. Jorge and Caro, my family in Canada, thanks for always being there for me when I have needed a hug, just a quick 6 hours away.

Finally, this thesis is dedicated to my family. Papito, thanks for pushing me to always question everything and learn more. Mamita, your support has been invaluable during the hard times and the good times. Juancho and Dani, I'm so proud of you both, thanks for teaching me lessons every day, thanks for all the fun we have had together, you guys make me happy. Tio JR, thanks for always believing in me and your support. Tia MT thanks for all the talks and advice. Abue, gracias por tu apoyo y por siempre quererme tanto. Manu, and Juani: thanks for being the sisters I don't have. Clau, thanks for all the long calls while I was in window-less rooms doing characterizations. I will always miss you; you will always live in my memories. Rodriguez family, thanks for your support and the long phone calls, especially to Paul and Michelle (and their families) for welcoming me on weekends in their homes. Last but not least: Adri, I am so glad I changed my office that first year of my Ph.D., who would have known I would meet the love of my life in the lab across the hallway? You are by far the best thing that happened to me during my Ph.D. Thanks for your support: emotional and polymer-science related. I love you so much.

Abstract

Widespread environmental contamination by plastic is an issue of global concern. While governments, companies, and individuals are shifting towards increased sustainability, for instance by reducing the consumption of single-use plastics, the use and mismanagement of plastics remain common.

Several studies have confirmed the presence of microplastics in consumer products and other sources, however, nanoplastics <100 nm have rarely been identified. Their small size adds a significant barrier to detection in complex matrices such as natural soils, waters, and foods. The objective of this thesis was to combine existing technologies and explore their detection limits to characterize micro- and nanoplastics in commercial goods and environmental samples.

One approach to meet this goal is to analyze products known to contain plastic particles. While the presence of primary microplastics in facial scrubs has been reported; in this work, the presence of nanoplastics was confirmed for the first time. Scanning electron microscopy (SEM), X-ray photoelectron spectroscopy, and Fourier Transform Infrared Spectroscopy (FTIR) were used to identify polyethylene nanoparticles.

While it may not be surprising to find nanoplastics as part of the size distribution in facial scrubs, this work also shows that micro- and nanoplastics can be produced from products that do not contain plastic particles but are rather packaged in plastic. Teabags made of polyethylene terephthalate and nylon were identified as a direct source of micro- and nanoplastics to humans. It was found that approximately 11.6 billion microplastics and 3.1 billion nanoplastics can be released into a single cup of tea, highlighting the importance of considering the fate of food packagings.

While it has been established that bulk plastics can break down and release secondary microplastics, the fragmentation of these particles into nanoplastics has yet to be thoroughly studied. Four types of microplastics were placed in water and under UV-light or thermal degradation stimuli for 18 weeks. The leachate was subsequently analyzed using nanoparticle tracking analysis, SEM, and FTIR and it was found that all four plastics released some fraction of smaller particulate material. This study contributes to our understanding of the breakdown of microplastics into smaller micro- and nanoplastics.

The most commonly used techniques for identifying microplastics are Fourier transform infrared microspectroscopy and Raman microscopy. Unfortunately, characterization using such techniques is costly, time-consuming, and limited to larger particles. There is a need for rapid on-site identification of microplastics, as governments move towards requiring the screening of drinking water for microplastic presence.

One potential alternative to the laborious and time-intensive methods is Pyrolysis-gas chromatography-mass spectroscopy (Py-GC-MS). Py-GC-MS was used for a fast and qualitative screening of microplastics (> 1.5 µm) in drinking water and Arctic water. The analysis of Py-GC-MS spectra is ambiguous as different scientists have different benchmarks to confirm the presence of plastics in samples. In this study, a scoring system was proposed with which the presence of plastics can be evaluated. This system in combination with FTIR and Nile red dye were used to propose a fast, low-cost, screening method for microplastics in bottled water.

Overall, this work identified micro- and nanoplastics released from consumer goods using conventional characterization techniques, while acknowledging their limitations. Findings illustrate the importance of monitoring micro- and nanoplastics in consumer goods, as they lead to direct contact with humans and in some cases ingestion. This work also contributes to the field of

microplastic identification by developing rapid and low-cost methods to identify microplastics in environmental samples.

Résumé

La contamination de l'environnement par les plastiques est une problématique mondiale. Les gouvernements, entreprises et individus s'engagent progressivement dans un combat contre la pollution environnementale, en réduisant par exemple la consommation de plastiques à usage unique. Toutefois, l'utilisation et la mauvaise gestion des plastiques restent courantes.

Plusieurs études ont confirmé la présence de microplastiques dans des produits de consommation et autres. Cependant, des nanoplastiques (< 100 nm) ne furent que rarement identifiés. Leur toute petite taille est un obstacle à leur détection dans des milieux complexes comme la terre, l'eau et la nourriture. L'objectif de cette thèse fut de caractériser les micro- et nanoplastiques d'articles commerciaux et d' échantillons environnementaux en combinant les technologies existantes de détection.

Notre première approche fut d'analyser des produits déjà connus pour contenir des particules de plastique. Alors que la présence de microplastiques primaires dans des crèmes exfoliantes pour le visage fut préalablement rapportée, des nanoparticules de poly(éthylène) furent détectées dans notre étude. La microscopie élecronique à balayage (SEM), la spectrométrie photoélectronique par rayons X et la spectroscopie infrarouge à transformée de Fourier (FTIR) furent employées pour l'identification.

Ce projet montre également que des micro- et nanoplastiques peuvent se former dans des produits qui ne contiennent pas à l'origine des particules de plastique mais dont l'emballage est en plastique. Des sachets de thé en polytéréphtalate d'éthylène et nylon furent identifiés comme une source directe de production de micro- et nanoplastiques. Il fut estimé qu'environ 11,6 milliards de microplastiques et 3,1 milliards de nanoplastiques peuvent être relargués dans une tasse de thé.

Bien qu'il soit connu que les plastiques peuvent se décomposer et relâcher des microplastiques secondaires, la fragmentation de ces particules en nanoplastiques n'a pas été très étudiée. Quatre types de microplastiques furent immergés dans l'eau pendant 18 semaines et un rayonnement UV ou de la chaleur furent appliqués. Des échantillons furent caracterisés par analyse de suivi des nanoparticules, SEM et FTIR. Il fut démontré que les quatre types de plastique relâchent des particules plus petites. Cette étude a ainsi permis d'élargir notre compréhension de la décomposition des microplastiques, en microplastiques plus petits et en nanoplastiques.

Les microspectroscopies Raman et infrarouge à transformée de Fourier correspondent aux techniques les plus utilisées pour l'identification des microplastiques. Néanmoins, ce sont des méthodes coûteuses, qui prennent du temps et qui ne peuvent pas être utilisées pour des particules très petites. L'identification rapide et sur le site des microplastiques est un réel besoin. Cela permettrait par exemple le contrôle de l'eau potable via la détection de microplastiques.

Une solution envisagée est l'utilisation de la pyrolyse couplée à la spectrométrie de masse (Py-GC-MS). La Py-GC-MS fut employée pour une analyse rapide et qualitative de microplastiques (> 1.5 μm) présents dans l'eau potable et dans de l'eau de l'Arctique. L'interprétation des spectres obtenus reste délicate car différentes références sont utilisées dans la littérature pour confirmer la présence de plastiques. Dans cette étude, un système de notation fut mise en vigueur afin d'évaluer la présence de plastiques. Ce système combiné avec le FTIR et un colorant rouge type Nile furent proposés comme une technique rapide et economique pour la détection des microplastiques dans les bouteilles d'eau.

Cette thèse permit donc d'identifier des micro- et nanoplastiques présents dans des articles commerciaux en utilisant des techniques de caractérisation conventionnelles, tout en reconnaissant leurs limites. Les résultats obtenus montrent l'importance du contrôle des micro- et nanoplastiques

dans les biens de consommation puisque ces derniers sont en contact direct avec les individus et, dans certains cas, peuvent être ingérés. Ce projet de recherche contribua aussi dans le domaine de l'identification des microplastiques en développant des méthodes rapides et économiques pour identifier les microplastiques dans des échantillons environnementaux.

Table of Contents

Preface i
Acknowledgments ii
Abstract v
Résumé viii
Table of Contents xi
List of Figures xviii
List of Tables xxix
List of Abbreviations xxxiii
Chapter 1: Introduction 1
1.1 Research objectives 2
1.2 Thesis organization 2
1.3 Contribution of the Authors 5
Chapter 2: Literature review 9
2.1 Sources and sinks of microplastics 9
2.1.1 Primary microplastics 9
2.1.2 Secondary microplastics 10
2.1.3 Air, water, soil, and food; microplastics are everywhere 11
2.2 Nanoplastics, where do they come from? 13
2.3 Identification and quantification of microplastics and nanoplastics 16
2.3.1 Visual characterization: size and morphology of micro- and nanoplastics 16
2.3.2 Chemical confirmation of micro- and nanoplastics composition 18
2.3.2.1 Vibration spectroscopy and microspectroscopy 18

2.3.2.1.1 Fourier-transform infrared spectroscopy (FTIR) 18
2.3.2.1.2 Raman microscopy 19
2.3.2.2 Mass spectroscopy methods 20
2.3.2.2.1 Thermal desorption coupled with gas chromatography-mass spectrometry (TDS-GC-MS) 21
2.3.2.2.2 Pyrolysis-gas chromatography-mass spectrometry (Py-GC-MS) 21
2.3.2.3 Signal processing 22
2.3.3 Emerging characterization techniques 23
2.4 Blank and spike controls 24
2.5 References 25
Preface to Chapter 3 44
Chapter 3: Are There Nanoplastics in Your Personal Care Products? 45
Abstract 45
3.1 Introduction 46
3.2 Materials and methods 47
3.2.1 Isolation of nanoparticles from facial scrubs 47
3.2.2 Characterization of recovered nano-sized materials 49
3.2.3 Control experiments 50
3.3 Results and discussion 51
3.3.1 Nanosized particles are detected in commercial scrubs 51
3.3.2 FITR and XPS characterization of the isolated nanomaterial 54

3.4 Environmental implications 56
3.5 Acknowledgements 57
3.6 References 57
3.7 Supporting information 64
Preface to Chapter 4 69
Chapter 4: Plastic teabags release billions of microparticles and nanoparticles into tea 70
Abstract 70
4.1 Introduction 71
4.2 Materials and Methods 72
4.2.1 Release of particles from teabags 72
4.2.2 Characterization of debris leached from teabags 73
4.2.3 Control experiments with teabags 74
4.2.4 Concentrated leachate preparation for preliminary toxicity assays 76
4.2.5 Characterization of leachates and teabags using ICP-MS 77
4.2.6 Toxicity assays using *D. magna* 77
4.3 Results 79
4.3.1 Plastic teabags and their leachates contain micro- and nanoparticles 79
4.3.2 Particles originate from plastic teabags 82
4.3.3 Adverse biological effects of dialyzed leachates of the plastic teabags 86
4.3.4 Identification of metal(loid)s in the teabag leachate 89
4.3.5 Biological effects of non-dialyzed leachates 89

4.4 Discussion 90

4.5 Acknowledgments 95

4.6 References 95

4.7 Supporting Information 107

4.7.1 Description of Control Experiments. 107

4.7.1.1 (i) Sample preparation for SEM imaging to avoid coffee ring effect 107

4.7.1.2 (ii-v) Confirming that particles are not released due to cutting or from the apparatus or from tea leaves, and that particle release is enhanced at high temperature 108

4.7.2 Description of *D. magna* Swimming Assay. 112

4.7.3 Description of ICP-MS analysis of leachates. 114

4.7.4 Immobility assessment, body size, X-ray computed tomography scanning, and optical imaging of D. magna exposed to non-dialyzed teabag leachate. 117

Preface to Chapter 5 121

Chapter 5: Photolytic and thermal weathering of four commonly used plastics 122

Abstract 122

5.1 Introduction 122

5.2 Materials and Methods 125

5.2.1 Weathering microplastics with UV radiation or thermal stimulus 125

5.2.2 Analysis of particles in leachates using SEM and NTA 126

5.2.3 Characterization of the chemical composition of leachates and prepared microplastics 128

5.2.4 Vickers microhardness (H_v, kg mm^{-2}) of pristine and weathered prepared microplastics 128
5.3 Results and discussion 128
5.3.1 Size and number of particles in the leachate 128
5.3.2 FTIR analysis of the prepared microplastics and their leachates 135
5.3.3 Microhardness changes in prepared microplastics after weathering 139
5.4 Environmental implications 141
5.5 Acknowledgements 143
5.6 References 144
Preface to Chapter 6 150
Chapter 6: Detection of widespread microplastics using pyrolysis gas chromatography-mass spectrometry 151
Abstract 151
6.1 Introduction 151
6.2 Materials and Methods 155
6.2.1 Commercial bulk plastics to create polymer library and evaluate the sensitivity of the equipment 155
6.2.1.1 Bulk plastics 155
6.2.1.2 Commercial micro and nanobeads 160
6.2.2 Environmental samples 162
6.2.2.1 Sampling campaign at drinking water treatment plants (DWTPs) 162
6.2.2.1.1 Preparation of blanks for DWTP 163

6.2.2.2 Arctic water sampling 164
6.2.2.3 Preparation of samples for Py-GC-MS analysis and injection 169
6.2.2.4 Analysis of Py-GC-MS data 169
6.3 Results 170
6.3.1 DWTP waters can contain plastics 170
6.3.2 Analysis of Arctic water samples 179
6.4 Limitations of the technique and future work 186
6.5 Acknowledgements 189
6.6 References 189
Preface to Chapter 7 196
Chapter 7: Optimizing the concentration of Nile red for screening of microplastics in bottled water 197
Abstract 197
7.1 Introduction 197
7.2 Materials and methods 200
7.2.1 Bottled water samples 200
7.2.1.1 Approach 1 - imaging and FTIR analysis 201
7.2.1.1.1 Staining and filtration 201
7.2.1.1.2 Method development (positive and negative controls) 202
7.2.1.1.3 Imaging 204
7.2.1.1.4 Particle counts 205
7.2.1.1.5 FTIR analysis 206

7.2.1.2 Approach 2 - Py-GC-MS 206
7.2.1.2.1 Filtration and staining for sample preparation 206
7.2.1.2.2 Py-GC-MS analysis 207
7.3 Results and discussion 208
7.3.1 Nile red staining optimization 208
7.3.2 Particles in bottled water samples 212
7.3.3 Analysis of particles > 1.5 µm and < 100 µm using Py-GC-MS 215
7.4 Environmental implications 217
7.5 Acknowledgements 219
7.6 References 220
7.7 Supporting information 229
7.7.1 References 242
Chapter 8: Conclusions and future work 244
8.1 Conclusions 244
8.2 Perspectives 246
References 248

List of Figures

Figure 2.1. Shows the transformations and subsequent characteristics of plastic particles in the environment. Figure taken with permission from "Nanoplastics are neither microplastics nor engineered nanoparticles", Gigault et al., Nature Nanotechnology.

Figure 3.1. Scheme of the filtration process to which the scrubs were subjected.

Figure 3.2. SEM images of samples taken at different filtration steps of the commercial scrubs: (a) Retentate 1 from scrub A, (b) Filtrate 5 from scrub A, (c) Retentate 1 from scrub B, (d) Filtrate 5 from scrub B, (e) Retentate 1 from scrub C, (f) Filtrate 5 from scrub C. Samples of Retentate 1 for each scrub were dried and fixed onto carbon tape for imaging. Samples of Filtrate 5 for each scrub were filtered through 10-nm polycarbonate membranes for imaging.

Figure 3.3. (a) FTIR spectra of commercial PE beads (250 µm) and Filtrate 5 of scrubs A, B and C. (b) XPS valence band scan of commercial PE beads and Filtrate 5 of scrubs A, B and C.

Figure S3.1. Dynamic light scattering number weight distribution for Filtrate 4 of Scrubs A, B and C. The distribution has a significant portion above 100 nm.

Figure S3.2. Picture of Scrub A and its 5 filtrates.

Figure S3.3. (a) Dynamic light scattering number weighted distribution of particles in Filtrate 5 of scrubs A, B and C. (b) Particle size distributions from (a) are shown on a different x-axis scale for improved clarity.

Figure S3.4. TEM images of Filtrate 5 for (a) Scrub A, (b) Scrub B, (c) Scrub C.

Figure S3.5. SEM images of commercial polyethylene scrub beads and their corresponding Filtrate 5 obtained in the control experiment. (a) Commercial PE beads (50 µm), (b) Filtrate 5 of

commercial PE (50 µm), (c) commercial PE beads (250 µm), (d) Filtrate 5 of commercial PE (250 µm), (e) commercial PE beads (800 µm). (f) Filtrate 5 of commercial PE (800 µm).

Figure S3.6. SEM image of Filtrate 5 sample when filtering RO water as a negative control. No particles are observed. The black dots are the holes in the 10 nm filtration membrane that is used to fix the sample for observation. The observation was made at 200 kV.

Figure S3.7. XPS survey scan of Filtrate 5 for scrubs A, B and C.

Figure 4.1. Teabag and leachate preparation for analysis with SEM, FTIR and XPS. (a) Schematic showing the preparation of teabag samples. (b-qm) SEM images of original teabags and their leachates after steeping. Empty plastic teabags were fixed onto carbon tape and the leachates (100 µL) were drop cast onto silicon wafers. (b, f, j, n) Imaging at 1,000× of the original teabags before steeping shows a net-like structure (~30-70 µm) that appears to have a smooth surface, whereas at higher magnification (30,000× insets) surface roughness and small particles (~200-1,000 nm) are observed. (c, g, k, o) Imaging at 1,000× of the teabags after steeping reveals a rougher surface, at higher magnification (30,000× insets) dents and fractures are observed. (d, h, l, p) Teabag leachates: irregularly shaped microparticles (~1-200 µm) are observed at 1,000×. Micron-sized particle size distribution is shown in the insets. (e, i, m, q) Increasing the magnification to 100,000× confirms the presence of sub-micron and nano-sized particles in the teabag leachates. Sub-micron particle size distribution is shown in the insets.

Figure 4.2. FTIR spectra and XPS scans for nylon 6,6, PET, the original teabags and their corresponding leachates. (a) The FTIR peak at 3289 cm^{-1} corresponds to the stretching vibration frequency of N–H groups in nylon 6,6 and the peaks detectable at 2932 cm^{-1} and 2860 cm^{-1} can be associated to those of the ethylene sequence in nylon 6,6 (CH_2 asymmetric stretching). Teabags A

and B, and their leachates, also present characteristic peaks of nylon 6,6 in the fingerprint region of their FTIR spectra (2,000 to 500 cm^{-1}): 1634 cm^{-1} (amide I band, having a main contribution of the C=O stretching), 1535 cm^{-1} (amide II band, bending vibration frequency of N-H), 1371 cm^{-1} (amide III band, CH_2 wagging), and 681 cm^{-1} (bending vibration frequency of N-H). (b) Peaks can be observed at 1748 cm^{-1} (acid ester C=O group), 1375 and 1347 cm^{-1} (CH_2 wagging of glycol, sample D specifically), 1226 and 1089 cm^{-1} (broad bands, asymmetric C-C-O and O-C-C stretching, respectively), 1025 cm^{-1} (in-plane vibration of benzene), and 730 cm^{-1} (C-H wagging vibrations from the aromatic structure, out of plane of benzene group). (c, e, g) C1s, O1s, and N1s XPS spectra of teabags A and B and their corresponding leachates. The peaks observed confirm that the composition of these teabags is nylon. (d, f) C1s and O1s XPS spectra of teabags C and D and their corresponding leachates. The observed peaks confirm that the composition of these teabags is PET.

Figure 4.3. Teabag leachates affect the morphology and swimming behavior of *Daphnia magna*. (a) Microparticles identified in *D. magna* exposed to dialyzed teabag B and D leachates, as well as in raw leachates are marked with arrows. Optical images of *D. magna* were taken using an Olympus DP80 microscope digital camera at 60× magnification focusing on the intestine. (b) CT images of *D. magna* exposed to dialyzed teabag B and D leachates. Top images show the 3-D morphology and bottom images show 2-D internal sections. (c) Representative swimming tracks of *D. magna* exposed to dialyzed teabag D leachate. (d, e) The swimming distance of *D. magna* after exposure to teabag B and teabag D leachates. Asterisk indicates that the measurement is statistically significantly different (p-value<0.05, one-way analysis of variance (ANOVA) followed by the *post-hoc* Tukey's multiple comparison test) from the control; n=9 for dialyzed

teabag B, dialyzed leachate D, and non-dialyzed leachate B, and n=6-9 for non-dialyzed teabag D leachate.

Figure S4.1. Deposition of particles for SEM imaging. (a) Following deposition of 100 µL of leachate as a single droplet onto an untreated silicon wafer, a coffee ring effect can be observed as a result of the accumulation of particles at the edge of the droplet. (b) Following deposition of 100 µL of leachate in ten successive droplets of 10 µL over a silicon wafer washed with ethanol to increase hydrophilicity of the surface by oxidation. No coffee ring effect is observed as the sample dries uniformly over the silicon wafer.

Figure S4.2. Filtration set-up used to process leachate from the unopened teabag (with loose leaf tea inside) and SEM images from control experiments. (a) This process was necessary to remove tea debris and organics; however, it adds steps to the sample processing. Therefore, counts should not be directly compared with those obtained in the main experiment because samples were not processed in the exact same way. First, leaf and twig fragments are removed using a 0.45 µm EMD Millipore Millex sterile syringe filter. Subsequently, dissolved organics are removed using a 50 mL Amicon stirred cell. This procedure is carried out to remove the dissolved organics in order to adequately characterize the leachate. Imaging at 1,000× of dried leachate from (b) control experiment with uncut teabag B and (c) control experiment with uncut teabag D. Both samples were prepared by following the process described in Fig. 4.1a (with the exception of opening and emptying the teabag). Subsequently, the leachates were processed as shown in Fig. S4.2a to remove dissolved organics. Particulate material is observed in both images, supporting the hypothesis that particles are leaching from teabags even when they are unopened. Imaging at 50,000× of (d) unheated leachate B and (e) unheated leachate D. Both samples were prepared by following the process described in Fig. 4.1a with the exception that the temperature of the water

in which the teabags were steeped was at 22 °C instead of 95 °C. (f) Imaging at 50,000× of filtrate from the control experiment in which RO water was processed through the system described in Fig. 4.1a. The image shows no micro- or nanoparticles in the filtrate, confirming that the particles are not released from the experimental system (tubing, filters, etc). (g) Imaging at 30,000× of the filtrate from the control experiment conducted using a metallic steeper and loose tea leaves (which were not previously packaged in individual teabags). The image shows no micro- or nanoparticles in the filtrate, confirming that the particles are not released from the tea leaves. (h) SEM image at 50,000× of negative control experiment where RO water was processed through the system described in Figure S4.2a. Results show no micro- or nanoparticles in the filtrate, confirming that there are no particles released by the EMD Millipore Millex sterile syringe filter or the Amicon stirred cell.

Figure S4.3. FTIR spectra for control experiments. FTIR spectra for the original (cut) teabag and the corresponding leachates prepared without cutting the teabag and removing the tea. FTIR peaks identified for the dried leachates match with those observed for the original teabag material. This confirms that the particles leaching out of uncut teabags are plastic. This also confirms that teabags leach micro- and nanoplastics even when they are not cut.

Figure S4.4. XPS analysis of the original (cut and emptied) teabag and leachates prepared without cutting the teabag and removing the tea. (a,b,c) C1s, O1s and N1s spectra of the original teabag B and the leachate obtained by steeping an unopened teabag B (with tea inside) and further processing the leachate as shown in Fig. S4.2a to remove dissolved organics. The measurements confirm that the particles in the leachate are nylon. (d,e) C1s and O1s spectra of the original teabag D and the leachate obtained by steeping an unopened teabag D (with tea inside) and further

processing the leachate as shown in Fig. S4.2a to remove dissolved organics. The signals confirm that the particles in the leachate are PET.

Figure S4.5. Swimming track density of *Daphnia magna* after exposure to different concentrations of (a) non-dialyzed teabag B leachate and (b) teabag D leachate, and (c) dialyzed teabag B leachate and (d) teabag D leachate. Swimming track density was determined by the image analysis of the trails left by *D. magna* during one-minute video recording. The tracks in each image were transformed to black pixels and background as white, and then the percentage of black pixels from each image was calculated using ImageJ 1.8.0. Asterisk indicates that the measurement is significantly different (p-value <0.05) from the control; n=9 for dialyzed teabag B, dialyzed leachate D, and non-dialyzed leachate B, and n=6-9 for non-dialyzed teabag D leachate.

Figure S4.6. ICP-MS measurements of concentrations of (a) aluminum, (b) arsenic, (c) chromium and (d) lead found in the concentrated (100%) leachate before and after dialysis. The negative control was prepared by performing the complete digestion process without any leachate sample (adding acids and performing the temperature ramps). Asterisk indicates that the measurement is significantly (p-value <0.05) different from the control using a t-test. Statistics were not performed on the arsenic measurements as n=2 for those samples. Al and Cr are the most abundant metal(loid)s detected, with concentrations up to 2.3 and 3.7 ppm, respectively. In contrast, the concentrations of As and Pb are more than one order of magnitude lower (0.05-0.3 ppm).

Figure S4.7. ICP-MS measurements of total mass of (a) aluminum, (b) arsenic, (c) chromium and (d) lead detected in a single empty plastic teabag (cleaned with RO water) and one full plastic teabag (containing loose leaf tea) for brands B and D. The negative control was prepared by performing the complete digestion without any leachate sample (i.e., acids were added to empty tubes and temperature ramps were performed). Asterisk indicates that the measurement is

significantly (p-value <0.05) different from the control using a t-test. Statistics were not performed on the arsenic measurements as n=2 for those samples. Note that the lead content of full teabag D and empty teabag D are not significantly (p-value <0.05) different from each other using a t-test. The presence of tea leaves significantly increases the levels of Al and As. The concentration of Al is two orders of magnitude higher (18-25 µg per empty teabag compared to 1200-3700 µg per cup of tea), whereas the concentration of As is two-fold greater (from 0.7-1.0 µg per teabag compared to 1.6-1.7 µg per cup of tea). The levels of Pb and Cr are comparable for the empty and full teabags; therefore, the source of these metal(loid)s could be either the tea leaves or the plastic teabags.

Figure S4.8. Mean immobility and body size of *Daphnia magna*. *D. magna* was exposed to different concentrations (0.5%, 5%, and 50%) of non-dialyzed (a, c) teabag B and (b, d) D leachate for 24 h and 48 h. Asterisk indicates that the measurement is significantly different (p-value <0.05) from the control.

Figure S4.9. CT images of *Daphnia magna* exposed to 5% and 50% non-dialyzed teabag D leachate. Random samples were stained with phosphotungstic acid and scanned using a Zeiss Xradia 520 Versa. Scale bar, 100 µm.

Figure S4.10. The presence of micro-particles in *Daphnia magna* exposed to non-dialyzed teabag D leachate. The particles are indicated with white arrows in intestine (a-c) and abdominal setae (d). Following 48 h of exposure to non-dialyzed leachates, and after the swimming assessment, a subsample of *D. magna* was randomly selected and fixed in 70% ethanol overnight. *D. magna* preserved in ethanol is carefully rinsed 6 times with DI water before imaging. Representative images are taken using an Olympus DP80 microscope digital camera at 60× magnification. Scale bar, 10 µm. Intestine is focused for imaging, as shown in a-c. Foreign microparticles are only found in the leachate-treated *D. magna* (b, c) but not in the control (a). The microparticles are also found

on the hair-like abdominal setae close to anus (d). The observed microparticles in (d) may be egested from anus and attach onto the abdominal setae. The size and shape of these microparticles are similar to those of particles we observed in the leachate.

Figure 5.1. SEM images of the leachates of plastics exposed to UV or high temperature weathering. (a, e, i, m) Imaging at low magnification of leachates of UV-weathered plastics. Particle size distributions shown in insets. (b, f, j, n) Imaging at high magnification of leachates of UV-weathered plastics. Nanoparticle size distribution shown in insets. (c, g, k, o) Imaging at low magnification of leachates of plastics weathered at high temperature. Microparticle distribution shown in insets. (d, h, l, p) Imaging at high magnification of leachates of plastics weathered at high temperature. Nanoparticle size distribution shown in insets.

Figure 5.2. NTA measurements of the leachates for each UV and T weathering. Results were obtained by tracking > 200 particles. The tracks were processed using the NanoSight software. Three samples were measured three times, for a total of 9 measurements per leachate. Asterisk indicates that the average of the 9 measurements for UV-weathered and T-weathered were statistically significantly different (p-value < 0.05, Student t-test, n=9).

Figure 5.3. SEM images of fridge-controls and fridge-procedural blanks. (a, e, i, m) Imaging at 1,200× of leachate of fridge-controls of plastics. (b, f, j, n) Imaging at 25,000× of leachate of fridge-controls for plastics. (c, g, k, o) Imaging at 1,200× of leachate of fridge-procedural blanks of plastics. (d, h, l, p) Imaging at 25,000× of leachate of fridge-procedural blanks of plastics.

Figure 5.4. SEM images of procedural blanks. (a, e, i, m) Imaging at 1,200× of leachate of procedural blank for UV-weathering of plastics. (b, f, j, n) Imaging at 25,000× of leachate of procedural blank for UV-weathering of plastics. (c, g, k, o) Imaging at 1,200× of leachate of

procedural blank for T-weathering of plastics. (d, h, l, p) Imaging at 25,000× of leachate of procedural blank for T-weathering of plastics.

Figure 5.5. FTIR spectra for bulk plastics (before and after weathering) and their corresponding films for (a,b) PS, (c,d) PP, (e,f) HDPE, and (g,h) LDPE. It can be observed that the signal for each film corresponds to that of their parent plastic.

Figure 5.6. Vickers microhardness measurements for PS, PP, LDPE and HDPE microplastics. Each prepared microplastic sample, exposed to UV irradiation, heated or fridge-control, was compared to its pristine form, except HDPE and LDPE which were also compared to each other. Five UV-weathered, T-weathered, and fridge-control samples were analyzed (N=5). Ten pristine samples were analyzed (N=10). Error bars represent the standard deviation. Letters denote results of a 1-way ANOVA test performed with post hoc Tukey's HSD $\alpha = 0.05$.

Figure 6.1. 0.005 ng to 5000 ng of 20 nm commercial PS nanobeads were analyzed using Py-GC-MS. Using the XCalibur software the area under the curve for the styrene peak was calculated with an ICIS integration algorithm. The area under the curve was plotted in a log-log scale to show the correlation with the mass of plastic. Samples were analyzed in triplicate.

Figure 6.2. Map showing the pinned locations where surface water was sampled on the Amundsen expedition ship.

Figure 7.1. (a) Schematic showing the process followed to analyze bottled water. Approach 1 for counting and identification of particles > 100 μm with FTIR, and Approach 2 for identification of particles < 100 μm with Py-GC-MS. (b) Average particle counts observed in LC/MS water negative controls versus NR concentration. No statistically significant difference is observed

between NR concentrations ($p > 0.05$, $n = 10$). (c) Effect of NR concentration on the average recovery from positive controls spiked with 20 µm PS particles in LC/MS water at 2000 particles/L ($n = 5$). The solid bar has been corrected by subtracting the counts from the negative control, the hatched bar represents the raw positive control counts. (d) Average total number of particles (>5 µm) observed in each type of bottled water using a NR concentration of 0.1 mg L^{-1}. Letters indicate that the measurement is statistically significantly different ($p > 0.05$, $n = 7$) from the other letter groups. Counts are not corrected with the negative control, however, the values for the negative controls are shown in red. Raw data shown in Table S7.4. (e) Polymers identified using FTIR and total number of particles identified of each type (for all bottled water samples combined $n = 49$). A maximum of 20 particles per sample were analyzed by FTIR. Raw data shown in Table S7.5. All error bars represent standard deviation.

Figure 7.2. FTIR identification of particles and fibers >100 µm found in each bottled water sample. n refers to the number of particles analyzed for each bottled water. Raw data shown in Table S7.6. P=plastic bottle, G=glass bottle, C=carbonated water.

Figure S7.1. Whatman binder-free glass microfiber filter placed on Buchner funnel in a coffee-filter formation before and after filtration of the samples.

Figure S7.2. Schematic that shows the division in which the imaging was divided. This approach ensured that the entire area of the filter was imaged.

Figure S7.3. Representative filters of negative controls at varying NR concentrations. Row 1 - filters under ambient light with no emission filter. Row 2 - filters under blue light with an orange emission filter. Row 3 - filters under blue light with an orange emission filter taken at 40× total magnification.

Figure S7.4. Representative images of the particles observed in (a) the positive control (which was spiked with 20 µm PS), (b) bottled water samples, and (c) bottled water sample 2, which contained an unusually large amount of fibers. All samples shown were spiked with 0.1 mg NR/L.

List of Tables

Table 6.1. Common plastics were chosen to generate a small library of bulk plastics. These standards served as references when analyzing environmental samples. The plastics chosen were determined based on other studies where larger plastics were identified in drinking water using FTIR (Chapter 7).

Table 6.2. Common plastics and fibers and their characteristic pyrolysis products. Each characteristic pyrolysis product is identified by its indicator ions at the retention time. Only indicator ions with mass above 50 were considered to preserve the integrity of the MS detector (the instrument was tuned between 50-250 amu). We did not observe notable differences between the pyrograms of HDPE and LDPE, therefore we consolidated these two materials into simply polyethylene (PE).

Table 6.3. Single ion monitoring (SIM) groups used in this study.

Table 6.4. Information regarding section of the Amundsen cruise, station ID where samples were taken, exact location (latitude and longitude), and the volume filtered. Samples were taken wearing only a neoprene suit unless otherwise specified in the notes. Samples 2B-5 and 2B-11 are missing due to procedural or processing mistakes on the ship and/or laboratory.

Table 6.5. Detailed Py-GC-MS results of SIM 1 for each replicate of DWTP samples.

Table 6.6. Detailed Py-GC-MS results of SIM 2 for each replicate of DWTP samples.

Table 6.7. Detailed Py-GC-MS results of SIM 3 for each replicate of DWTP samples (rayon and cellulose acetate).

Table 6.8. Detailed Py-GC-MS results of SIM 3 for each replicate of DWTP samples (kraton and cellulose).

Table 6.9. Detailed Py-GC-MS results of SIM 3 for each replicate of DWTP samples (polypropylene, Nylon and poly(methylmethacrylate)).

Table 6.10. Chemical identification via Py-GC-MS of particles between 1.5 and 106 μm present in DWTP samples collected from the effluent and distribution lines for 5 locations. The presence of a certain polymer is confirmed (✓) when at least one of the triplicates had a percentage match ≥83.3%. If the percentage match was below 83.3% it is marked with ×.

Table 6.11. Detailed Py-GC-MS results of SIM 1 for all filters with Arctic samples.

Table 6.12. Detailed Py-GC-MS results of SIM 2 for all filters with Arctic samples.

Table 6.13. Detailed Py-GC-MS results of SIM 3 for all filters with Arctic samples (rayon and cellulose acetate).

Table 6.14. Detailed Py-GC-MS results of SIM 3 for all filters with Arctic samples (kraton and cellulose).

Table 6.15. Detailed Py-GC-MS results of SIM 3 for all filters with Arctic samples (polypropylene, Nylon and poly(methylmethacrylate)).

Table 6.16. Chemical identification via Py-GC-MC of particles between 1.5 and 106 μm present in Arctic samples. The presence of a certain polymer is confirmed (✓) when at least one of the triplicates had a percentage match ≥83.3%. If the percentage match was below 83.3%, it is marked with ×.

Table 7.1. Preparation of negative controls, positive controls and bottled water samples used in imaging, counting and FTIR analysis

Table 7.2. Polymers <100 µm identified by Py-GC-MS for each bottled water sample and negative controls. Polymers were positively identified when a sample resulted in ≥83.3% match with the characteristic pyrolysis products (see SI for detailed explanation). A ✓ indicates a positive match, while the × means either the polymer was not observed, or the match was below the threshold. Raw data in Tables S7.7 to S7.11.

Table S7.1. Most common plastics and fibers found with FTIR and their characteristic pyrolysis products. Each characteristic pyrolysis product is identified in the MS by finding the indicator ions at the retention time. References indicate pyrolysis product information taken from literature.

Table S7.2. Plastics and fibers were placed into single ion monitoring (SIM) groups according to similar mass of ion ranges for their characteristic pyrolysis products.

Table S7.3. Specifications for the standards used for each polymer.

Table S7.4. Total particle counts from bottled water samples. Data plotted in Figure 7.1c.

Table S7.5. Plastics and fibers identified using FTIR and total number of particles identified of each type (for all bottled water samples combined n = 49). A maximum of 20 particles per sample were analyzed by FTIR. Data plotted in Figure 7.1d.

Table S7.6. Plastic particle counts from FTIR identification of particles >100 µm found in each bottled water sample. Data plotted in Figure 7.4.

Table S7.7. Detailed Py-GC-MS results from SIM 1 plastics and fibers. Each characteristic pyrolysis product is given a match score: perfect match (green = 1 point), partial match (yellow = 0.5 points), no match (red = 0 points).

Table S7.8. Detailed Py-GC-MS results from SIM 2 plastics and fibers. Each characteristic pyrolysis product is given a match score: perfect match (green = 1 point), partial match (yellow = 0.5 points), no match (red = 0 points).

Table S7.9. Detailed Py-GC-MS results from SIM 3 plastics and fibers. See also Table S7.10. Each characteristic pyrolysis product is given a match score: perfect match (green = 1 point), partial match (yellow = 0.5 points), no match (red = 0 points).

Table S7.10. Detailed Py-GC-MS results from SIM 3 plastics and fibers. Each characteristic pyrolysis product is given a match score: perfect match (green = 1 point), partial match (yellow = 0.5 points), no match (red = 0 points).

Table S7.11. Detailed Py-GC-MS results from SIM 4 plastics and fibers. Each characteristic pyrolysis product is given a match score: perfect match (green = 1 point), partial match (yellow = 0.5 points), no match (red = 0 points).

List of Abbreviations

D. magna	*Daphnia magna*
DWTP	Drinking Water Treatment Plant
FTIR	Fourier Transform Infrared Spectroscopy
HDPE	High Density Polyethylene
Hv	Vickers microhardness
ICP-MS	Inductively Coupled Plasma- Mass Mpectroscopy
LDPE	Low Density Polyethylene
NR	Nile red
NTA	Nanoparticle tracking analysis
PE	Polyethylene
PET	Polyethylene Teraphtalete
PS	Polystyrene
RO	Reverse Osmosis
SEM	Scanning Electron Microscopy
T	Temperature
TDS-GC-MS	Thermal desorption coupled with gas chromatography-mass spectrometry
TEM	Transmission Electron Microscopy
UV	Ultra-violet
WWTP	Waste-water Treatment Plant
XPS	X-ray Photoelectron Spectroscopy

Chapter 1: Introduction

Microplastics have been widely detected in the environment, including in plants and animals as well as in soils, sediments, and waters. Additionally, discarded consumer products lead to the release or introduction of microplastics into the food web. As humans, we are exposed to micro- and nanoplastics in our daily lives through our food but also the products we use.

One of the greatest challenges when identifying micro- and nanoplastics is that the instruments typically used in the observation and identification of traditional nanoparticles (e.g., gold, silver, titanium dioxide, etc.), are not able to chemically identify small plastic particles. For instance, characterization techniques like scanning electron microscopy (SEM) and transmission electron microscopy (TEM) cannot confirm nanoplastic composition in a sample. These electron microscopy techniques when coupled with energy dispersive X-ray spectroscopy only go as far as identifying the elemental composition, but this is not particularly useful to identify plastics, as they are mainly composed of similar alkyl groups. Another major challenge is that instruments, used traditionally for the characterization of macro-plastics (diameter $\geq$ 5 mm), do not have the spatial resolution to identify small particles, especially below 1 μm.

Some other challenges in the characterization of micro- and nanoplastics include degradation of the surface, presence of sorbed chemicals, and pre-selection of a sub-sample for analysis. The research field is developing rapidly, making available several techniques that are useful to identify sub-samples of large microplastics. However, for smaller micro- and nanoplastics, there is much room for improvement.

This work explores different sources of micro- and nanoplastics in the environment. By combining traditional characterization methods and pushing their limitations, the research evaluates and

confirms the presence of micro- and nanoplastics in environmental samples. It is shown that when the particles of a single type of nanoplastic are accumulated into a film, the film can be characterized using X-ray photoelectron spectroscopy (XPS) and Fourier transform infrared spectroscopy (FTIR). The number of particles was estimated using SEM complemented with nanoparticle tracking analysis (NTA). These micro- and nanoplastics were found in both consumer products and breaking off larger plastics when they are weathered. Both sources end up in the environment, where they are more biologically available than larger plastics. Additionally, methods were developed to evaluate environmental samples for the presence of plastic particles.

1.1 Research objectives

1. To evaluate existing technologies for their ability to characterize micro- and nanoplastics in commercial goods and environmental samples.
2. To propose a systematic rigorous approach for the identification of plastics using pyrolysis coupled with gas chromatography-mass spectroscopy.
3. To propose a reliable and reproducible visual identification method for pre-screening microplastics in clean water matrices.
4. To understand the relative importance of UV versus temperature exposure in the weathering of microplastics and evaluate their potential to fragment into a substantial number of micro- and nanoparticles.

1.2 Thesis organization

- Chapter 2 provides a brief literature review of micro- and nanoplastics, their sources, fate, and detection methods. The impacts that plastic particles have on the environment are

discussed. Additionally, the most common techniques are explained, and their advantages and limitations are evaluated.

- In Chapter 3, three brands of facial scrubs containing polyethylene microbeads as a listed ingredient were purchased. The diluted facial scrubs were subjected to serial filtrations which removed all particles larger than 100 nm. In this remaining fraction, SEM, X-ray photoelectron spectroscopy (XPS), and Fourier Transform Infrared Spectroscopy (FTIR) were used to identify polyethylene nanoparticles. The presence of nanoparticles ranging from 24 ± 6 nm to 52 ± 14 nm was confirmed. Subsequently, these nanoparticles were dried to form a film that was characterized with X-ray photoelectron spectroscopy (XPS) and Fourier Transform Infrared Spectroscopy (FTIR) to confirm the particles were indeed polyethylene. Although the source of these nanoplastics was not simple to identify, they were likely produced by the breakdown of the larger microbeads during the emulsification process.

- In Chapter 4, teabags made of polyethylene terephthalate (PET) and nylon were identified as a direct source of micro- and nanoplastics to humans. Teabags made of PET and nylon were tested for their release of plastic particles. Briefly, emptied teabags were placed in RO water at 95 °C for 5 minutes to simulate the preparation of tea. The teabag leachate was analyzed using SEM to identify micro- and nanoparticles that had detached from the original teabag. Using SEM and NTA, it was found that approximately 11.6 billion microplastics and 3.1 million nanoplastics could be released from a single teabag. Furthermore, the leachate was divided into large microplastics (> 2.5 μm), and small microplastics and nanoplastics (< 2.5 μm). The composition of each fraction was matched with the parent teabag, thus confirming that the particles were made of plastic and therefore

released from the teabag. An initial acute invertebrate toxicity experiment showed dose-dependent behavioral effects in *Daphnia magna* upon exposure to the particles released from the teabags.

- In Chapter 5, we studied the breakdown of large microplastics into small micro- and nanoplastics. Large microplastics of PS, PP, HDPE, and LDPE were placed in RO water and then subjected to degradation stimuli. For 18 weeks, half of the samples were placed under UV-A at a constant temperature, whereas the other half were placed at 37 °C in the dark. All degraded large microplastics were tested for the release of small micro- and nanoplastics, as well as for changes in their superficial hardness. It was found that all large microplastics released some level of small micro- and nanoplastics into the water when stimulated with UV or temperature.

- In Chapter 6, pyrolysis coupled with gas chromatography- mass spectroscopy (Py-GC-MS) was used for the analysis of environmental samples of drinking water treatment plant (DWTP) water and Arctic water. Samples were filtered onto a glass fiber filter and then were pyrolyzed at 500 °C for 20 seconds. The results were then analyzed using a simple yet systematic scoring system that was created for the analysis of Py-GC-MS data. This is an important contribution to literature, as there is a lack of consistency in the scientific community when analyzing Py-GC-MS data.

- In Chapter 7, Py-GC-MS and the scoring system were used in combination with a benchtop FTIR for the fast, low-cost screening of plastics in seven types of bottled water. Additionally, the dye Nile red was used to attempt the quantification of particles > 5.1 µm. The concentration of Nile red required to stain samples was studied to reduce false positives in negative controls, without compromising the fluorescence signal of particles

in real samples. A low-cost and simple method was also proposed for screening microplastics in clean water samples which can be used on-site at DWTP.

- Chapter 8 provides a concise conclusion of the thesis and gives suggestions for future studies.

1.3 Contribution of the Authors

This thesis comprised 5 manuscripts. The original contributions of the authors are summarized below.

1. "Are There Nanoplastics in Your Personal Care Products?", Environmental Science & Technology Letters 4 (7), 280-285

Authors: Laura M. Hernandez, Nariman Yousefi, Nathalie Tufenkji

Contributions: L. M. Hernandez did the experimental work, SEM, FTIR, and wrote the manuscript. N. Yousefi did the XPS analysis. N. Tufenkji supervised the project, read, commented on, and edited the manuscript.

2. "Plastic Teabags Release Billions of Microparticles and Nanoparticles into Tea", *Environmental Science & Technology 53 (21), 12300-12310*

Authors: Laura M. Hernandez, Elvis Genbo Xu, Hans C. E. Larsson, Rui Tahara, Vimal B. Maisuria, and Nathalie Tufenkji

Contributions: L. M. Hernandez prepared the teabag leachates and controls and characterized the leachates with FTIR, XPS, SEM, and ICP-MS (data analysis only). L. M. Hernandez also put together the figures and wrote the manuscript except for the biology-related part. E. Genbo Xu

designed and conducted the exposure experiments using *D. magna*, did microscopy on the *D. magna*, analyzed the *D. magna* results and statistical analysis, and wrote the related part of the manuscript. V.B. Maisuria contributed to experimental design and execution of teabag leachate toxicity experiments. H.C.E. Larsson and R. Tahara did the CT-scan images of the *D. magna*. N. Tufenkji supervised the project, read, commented on, and edited the manuscript.

3. "Photolytic and thermal degradation weathering of four commonly used plastics", to be submitted to *Environmental Science & Technology*

Authors: Laura M. Hernandez, Joel Grant, Parvin Shakeri Fard, Richard Chromik, Jeffrey Farner, and Nathalie Tufenkji

Contributions: L. M. Hernandez prepared the experimental design, prepared the experimental setup, prepared and analyzed the samples for SEM, analyzed the samples with NTA, analyzed the films with FTIR, and wrote the manuscript. J. Grant prepared the experimental setup, prepared the samples for analysis, and did the microhardness measurements. P. Shakeri Fard prepared the films for FTIR. R. Chromik contributed to analysis of material characterization. J. Farner helped in the experimental design, did the statistical analysis, edited the manuscript, and supervised the project. N. Tufenkji supervised the project, read, commented on, and edited the manuscript.

4. "Detection of widespread microplastics using Pyrolysis Gas Chromatography-Mass Spectrometry", to be submitted to *Journal of Hazardous Materials*.

Authors: Laura M. Hernandez, Jeffrey Farner, Laura Rowenczyk, Liisa Jantunen, Varoujan Yaylayan, Nathalie Tufenkji

Contributions: L. M. Hernandez did the experimental design, performed all experimental work, analyzed all data, and prepared the manuscript. J. Farner helped with processing water samples and the edition of the manuscript. L. Rowenczyk participated in the sample collection of DWTP water. L. Jantunen provided the Arctic samples. V. Yaylayan and N. Tufenkji supervised the project, read, commented on, and edited the manuscript.

5. "Optimizing the Concentration of Nile Red for Screening of Microplastics in Bottled Water", to be submitted to *Environmental Science & Technology*

Authors: Laura M. Hernandez, Jeffrey M. Farner, Dominique Claveau-Mallet, Mira Okshevsky, Heidi Jahandideh, Sara Matthews, Ranjan Roy, Varoujan Yaylayan, and Nathalie Tufenkji

Contributions: L. M. Hernandez did the experimental design, performed counts, did the characterization using FTIR, performed the analysis of samples using Py-GC-MS, analyzed FTIR and Py-GC-MS data, and the related sections of the manuscript. J. Farner helped in the experimental design, sample preparation, and preparation and edition of the manuscript. D. Claveau-Mallet took images of the samples for counting and helped in the preparation of the manuscript. M. Okshevsky contributed to the method development of the project. H. Jahandideh took images of the samples for counting and helped in editing the manuscript. S. Matthews helped in the sample preparation. R. Roy contributed to the method development of the Py-GC-MS technique. V. Yaylayan guided the data analysis of Py-GC-MS, commented on it, and edited the manuscript. N. Tufenkji supervised the project, read, commented on, and edited the manuscript.

Chapter 2: Literature review

In 2017, it was estimated that the world plastic production was 348 million tons, a 230-fold increase from the plastic production in 1950.[1] Yet, only 6-26% of this plastic is recycled, meaning 74-94% ends up in environmental compartments including landfills.[2–4] Microplastics are defined in literature as plastics smaller than 5 mm in diameter.[5,6] Since 2004, microplastics have been detected in air,[7–10] oceans,[11–18] soils,[19–21] sediments,[22,23] and surface waters worldwide.[24–28]

While microplastics can be purposefully manufactured, a major source of microplastics in the environment is actually the breakdown of larger pieces of plastic. In order to distinguish between industrial sources and larger plastic breaking down, microplastics have been categorized into primary and secondary.[29] Primary microplastics are particles that are originally manufactured to be less than 5 mm, whereas secondary microplastics are the product of degradation or fragmentation of larger plastics in the environment.[6] This distinction is important, the different sources will have implications in the particle shape, irregularities and heterogeneity of the populations. Identifying the potential sources can help at designing mitigation measures to reduce microplastic influx to the environment.

2.1 Sources and sinks of microplastics

2.1.1 Primary microplastics

Primary microplastics are introduced into the environment either intentionally, due to their applications in various commercial products, or incidentally, because of accidental spillage of pellets.[30] In commercial goods, microplastics are added in a wide variety of products, including personal care products such as creams, soaps, toothpaste, household detergent and facial scrubs. They are added to these products to serve as exfoliants, in order to replace natural exfoliants (e.g.

oats, apricots, etc.) due to their short shelf life.[31] Once these products are used, microplastics are directly disposed through the wastewater streams and travel in wastewater. It is estimated that approximately 95-99% of microplastics are retained in the sludge of the waste-water treatment plant (WWTP).[31] The remaining billions of microplastics that bypass the WWTP enter the aquatic environment every day.[31] Recently, the use of microplastics in personal care products has been banned in several countries including the US and Canada.[31,32] Despite the benefits of this ban, it is important to note that microplastics are still widely used in personal care products around the globe.

Other consumer products that contain primary microplastics are lubricants, industrial abrasives, paints, fertilizers, industrial detergents, infill material (e.g. artificial turf for sports), and the oil and gas industry.[33] Their function varies from exfoliating agents to controlling the appearance and stability of products.[33] Similarly to exfoliating beads, release of microplastics from other sources has been observed. For instance, infill material used in artificial turf will release particles into wastewater systems through rain, and paint will degrade with time.

2.1.2 Secondary microplastics

Secondary microplastics are those which result from the breakdown of macroplastics. There are various sources of secondary microplastics such as degradation of car tires, microfibers sheading textiles, and degradation of larger plastics in the ocean.[30,34] There are several mechanisms for secondary microplastic release, for instance in the case of tires, microplastics are released from the friction between the tire and the road. In the case of microfibers shedding from textiles, the mechanical action of washing the textile will pull out microfibers. However, in the case of large plastics breaking down in the environment, the mechanisms are not simple, as there are many factors contributing.

Degradation of plastics occurs due to a variety of stressors such as hydrolysis, photolytic oxidation (due to light and UV exposure), mechanical abrasion (by sand or wave action), and biodegradation.[35] These processes possibly work synergistically, as in the environment all these stressors are present. For example, ultra-violet light exposure impacts the mechanical properties of plastics, rendering the materials more brittle and making mechanical degradation more likely.[35] Mimicking realistic environmental conditions is complex, as organic matter and other contaminants should be considered. Later, removing this complex matrix from the microplastics can be challenging. Therefore, it is unsurprising that scientists have focused on understanding the individual effects of degradation stressors, instead of the synergistic effects in representative environmental conditions.

2.1.3 Air, water, soil, and food; microplastics are everywhere

An increasing number of studies have documented the presence and effects of microplastics in the natural environment.[36–38] In 2017, the European Chemical Agency estimated that about 145,000 tons of primary microplastics are used in the EU per year, from which 42,000 tons are predicted to end up in the environment.[33] Infill material such as artificial turf make up the largest source of primary microplastics .[33] The same agency has estimated that around 176,000 tons per year of secondary microplastics are released to European surface waters.[33] Microplastics in the oceans and their effects on marine life have received much attention, however, microplastics can be found in many other environmental compartments including: fresh water sources, terrestrial environments, and the air. There is limited but growing information on the effects of microplastics in these other compartments.[9,10,19,20,39]

When primary microplastics are discarded to wastewater, for instance when a face exfoliant is used, it is known that the majority of them will be retained in the WWTP sewage sludge. Microplastics have been confirmed in sewage sludge across the world, and this sludge is commonly used for agricultural purposes.[40] In fact, studies have found that agricultural soils with a history of sewage sludge application contained a higher concentration of synthetic microfibers when compared to fields that had never been treated with sludge.[21,39–45] This route is the primary input of microplastics into terrestrial compartments of the environment.

Microplastics have also been detected in all marine, freshwater and estuary ecosystems. [15,22,36,46–50] Experiments in fish, marine mammals, and other aquatic organisms have found that indeed these organisms will ingest microplastics when exposed to them. There are several consequences that microplastics will cause in organisms, including bioaccumulation,[37] disruption of locomotor activity,[51] and chronic effects.[52] To date, these studies have been mainly carried out in laboratory environments mainly with marine aquatic organisms.[53] Studies have found that exposure of fish to microplastics can cause decrease in growth rates,[54] induced inflammatory responses,[52] changes in metabolism,[52,55] and disturbance of the immune system.[56]

It is important to note that microplastics may have both physical and chemical effects. Microplastics can either pass through the gut or be retained in the digestive track of certain bivalves.[46–48,57] The accumulation of particles can lead to physical blockages in the gastrointestinal system, and even decreased food consumption.[58] On the other hand, plastics are made with various chemicals and additives that can be harmful to humans and other species. Additionally, plastics can sorb and de-sorb chemicals, which can represent an additional risk as the plastic could sorb an environmental pollutant and then desorb it after being ingested by an organism.[59,60]

More concerning, microplastics have been detected directly in human food chain in products such as beverages,[1,61–64] honey,[65] seafood,[66] table salt,[67–70] and tap water.[68] Their effects are yet to be thoroughly studied.

2.2 Nanoplastics, where do they come from?

The definition of nanoplastics is still debated, however, it has been suggested that it should not follow an arbitrary size cut-off, but instead depend on the characteristics such as Brownian motion (Figure 2.1-1), interaction with light (Figure 2.1-2), physical interactions (Figure 2.1-3), size in comparison to other environmental macromolecules (Figure 2.1-4), bio-uptake and translocations (Figure 2.1-5), and diffusion rates (Figure 2.1-6),.[71] Additionally, Gigault *et al*. propose a differentiation between nanoplastics and engineered nanomaterials. Nanoplastics have a higher particle heterogeneity due to their variable sources and degradation conditions (Figure 2.1-7), and incidental nanoplastics can be a product of fragmentation of other primary nanoplastics in the environment (Figure 2.1-8).[71]

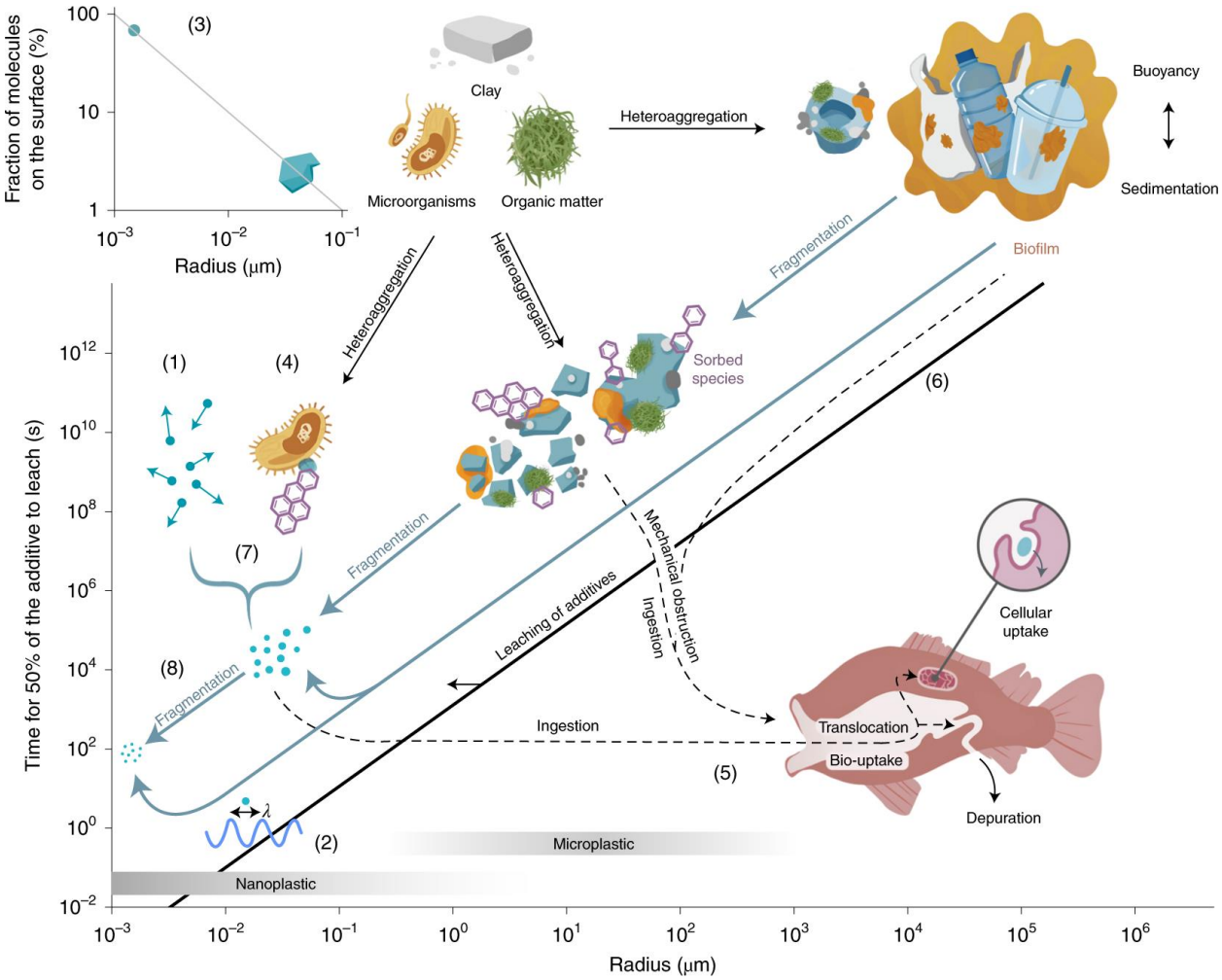

Figure 2.1. Shows the transformations and subsequent characteristics of plastic particles in the environment. Figure taken with permission from "Nanoplastics are neither microplastics nor engineered nanoparticles", Gigault *et al.*, Nature Nanotechnology.

Recently nanoplastics have been found in consumer products, human food, and the environment.[19,71–73] Studies have shown that a source of nanoplastics can be consumer products, either as a result of polydisperse raw material or breakdown of microplastics during processing.[72] Additionally, the degradation of macro- and microplastics has been shown to produce nanoplastics. Researchers have shown that nanoplastics can break down from larger plastics when these are subjected to stressors such as mechanical,[74] heat,[61] or UV-light [75]. Recently, researchers have tried

to understand the formation of nanoplastics by emulating environmental conditions. For instance, Lambert and Wagner simulated the weathering of a polystyrene coffee cup lid for 56 days.[76] UV irradiation and agitation were used to simulate wave action and light exposure in the marine environment.[76] Nanoparticle tracking analysis (NTA) confirmed the formation of nanoplastics with particle sizes spanning a range of values from 30-2000 nm.[76] It is also important to acknowledge that the nanoplastics formed contained chemical products such as residual monomer, plasticizers (such as phthalates), surfactants, oxidation preventers, pigments, and flame retardants, all of which were likely added to the original plastic during manufacturing or processing.[77]

To date, there is no comprehensive set of environmental field data of the formation of nanoplastics in the environment. Neither is there a complete understanding of how nanoplastics behave in the environment or the potential impacts they may have.[78] Several studies have attempted to assess the toxicity of nanoplastics, however, many of these use commercial particles which are not necessarily environmentally relevant.[79]

Nanoplastics are still a topic of concern. There are many questions that remain unanswered. Researchers are working towards answering enquiries such as how much nanoplastics exist in the environment, where are these coming from, and what their impact is in each ecosystem that they reach.[78] With these answers, government and policy makers will have a better understanding on how to deal with this issue.

The main reason why these questions have remained unanswered is due to the current sampling and identification techniques which are not suitable for retaining the very small size fractions (nanoplastics).[35,80] The current sampling methods are too coarse to separate nanoplastics from the environmental matrix (e.g. beach combing, filtering with nets), and are more suitable at collecting the larger size fractions of plastics. As a result, virtually no information is reported on

environmental concentrations of nanoplastics. Even when nanoplastics are found, characterization techniques that have been traditionally applied to plastics do not have the sensitivity to characterize nanoplastics. Therefore, there is a need to develop new techniques and optimize current techniques to be able to identify nanoplastics.

2.3 Identification and quantification of microplastics and nanoplastics

As micro- and nanoplastics are emerging contaminants, methods for their analysis have been in rapid development. Most techniques currently used to identify the type of plastics in these small particles were previously used to characterize bulk plastics. One problem, however, is that at the micro- and, even more so, at the nanoscale, the size and mass of sample is orders of magnitude smaller when compared to the bulk analysis. Therefore, advances are needed to make common analytical techniques more precise and sensitive. These analytical techniques fall into two main categories: visual characterization, in which the sample's size and morphology are observed; and chemical characterization, in which the composition of the sample is analyzed.

2.3.1 Visual characterization: size and morphology of micro- and nanoplastics

Visual characterization was used as the initial step in 79 percent of the studies that were assessed to screen for microplastics in environmental samples.[81] Visual characterization techniques are a cost-effective and practical way to reduce the number of particles that will subsequently be analyzed using chemical methods. These methods entail determining the physical features of plastic-associated particles (i.e., morphology, color, lack of cell structure, response to physical stress, response to the hot-needle test, etc.).[82] There are a wide number of studies in literature that use visual characterization only for particles larger than 500 µm.[83] However, for particles below the 500 µm threshold, visual characterization solely is unreliable.[81,84]

Aggregated 12 nm Eu-luminescence-labeled nanoplastics inside *Murraya exotica* were observed non-invasively with two-photon excitation and time-resolved detection.[85] This technique has advantages in simplifying sample preparation compared to electron microscopy, however the technique is still diffraction limited. Staining with Nile Red for fluorescence microscopy has been used to identify microplastics.[86] While Nile Red can be inconsistent and is not plastic-specific,[87,88] it is effective in clean samples, and a better understanding of plastic-dye interactions may lead to the use of more plastic-specific and plastic-sensitive dyes and dye combinations.

Observation with conventional light microscopy is limited by the fundamental 200 nm diffraction limit, even with ideal optics.[89] Scanning electron microscopy (SEM) has been frequently used for visual characterization of small microplastics and nanoplastics, as it allows for more detailed observation of surfaces.[90] Nevertheless, the complicated and time consuming sample preparation and the high cost of the equipment required decreases the simplicity that makes visual characterization appealing.[90,91] Additionally, SEM is not able to confirm the presence of plastic as even when coupled with energy dispersive X-ray spectroscopy, only the elemental composition can be obtained. In the case of plastic particles, elemental information is not valuable, as most plastics are comprised of chains of primarily carbon in different bonding conformations. Transmission electron microscopy (TEM), which is frequently used for particles at the same length scales (e.g. nanomaterials, colloids) is not a useful technique in this case either. Nanoplastics have an amorphous crystalline structure resulting in low contrast between the sample and the background and require heavy metal stains for observation.[92]

NTA is a light scattering technique that uses Brownian motion to measure concentration and size distribution of suspended nanoplastics down to 10 nm.[76] Suspended particles are illuminated by a laser beam, light scattered in collected using a microscope with a digital camera. The NTA

software then analyzes particles using the Stokes-Einstein equation and calculates hydrodynamic diameters. By analyzing the particle densities, it is also able to calculate the count-based concentration of the sample.[93,94]

2.3.2 Chemical confirmation of micro- and nanoplastics composition

Characterization of the chemical composition of micro- and nanoplastics is of considerable importance, as studies have shown visual characterization can only be reliable for microplastics > 500 μm. There is a wide variety of techniques available to characterize the composition of micro- and nanoplastics. Although there are some that are more widely used and established (e.g. infrared spectroscopy and Raman spectroscopy), others are emerging techniques that show great promise. In this review, chemical characterization techniques are classified into two categories, (1) Vibration spectroscopy and microspectroscopy capable of analyzing a single particle or an accumulation of several particles of the same kind, and (2) mass-based methods in which several particles of different compositions can be analyzed simultaneously, and the signal depends on the mass of the samples.

2.3.2.1 Vibration spectroscopy and microspectroscopy

Vibration spectroscopy is a common method in polymer science to identify the bonds present in a sample. However, most of these techniques have traditionally been applied to larger pieces of polymer. Vibration spectroscopy coupled with optical microscopy is commonly known as microspectroscopy, these techniques can provide both visual information and composition of plastic particles. However, the signal obtained is dependent on the size of the particles analyzed and typically a well-separated sample is required.

2.3.2.1.1 Fourier-transform infrared spectroscopy (FTIR)

Since 2004, infrared spectroscopy has been used for identification of microplastics.[23] Fourier-transform infrared spectroscopy is one of the most commonly used techniques, as it is reliable and reproducible for detection of polymers. The FTIR signal is generated when functional groups in a molecule absorb of IR light, resulting in the change in the permanent dipole moment of a chemical bond. As a result, detection of polar functional groups such as those contained in polymers is straightforward. Modern FTIR microscopes can couple visual and chemical characterization of microparticles with a spatial resolution down to 5 µm (in optimal conditions).[95] However, it is important to note that FTIR requires the sample to have a minimum thickness (~150 nm[96]) and to be deposited onto an IR transparent substrate.[97] The most commonly used substrates are aluminum oxide filters. [98] The issue with these substrates is that they interfere with the IR signal below 1300 cm^{-1}, thus losing information in the fingerprint region.[98] Other substrates are proposed to replace aluminum oxide but research is still ongoing.[2] Due to the limitations of this technique, it is mostly used when particles are larger than 20 µm. For smaller particles other techniques that are better at subtracting background noise are used.[90] However, agglomerates of smaller particles of the same polymer nature may be analyzed, as the cumulative absorbance is enough to provide a detectable signal.[72]

2.3.2.1.2 Raman microscopy

Raman spectroscopy is one of the most commonly used methods in literature to characterize microplastics, especially the fraction of particles below 20 µm.[99] Studies have shown Raman is better suited to individually analyze small microplastics than FTIR. FTIR can lead to up to a 35% underestimation of the number of microplastics in comparison to Raman.[100] In Raman active materials, molecular vibrations cause the scattering of polarized light.[101] An advantage of this technique is that the complete wavelength region can be scanned and used for identification,

therefore amorphous carbon can be detected. As a result, the Raman spectra of microplastics exposed to UV degradation is not significantly altered.[101] The theoretical spatial resolution is as low as 1 µm, therefore it has greater sensitivity than other commonly used techniques such as FTIR.[97] Another advantage is that the particle shape and thickness will not influence the measurement. However, some materials exhibit Raman fluorescence, masking vibrational information. Additionally, the Raman signal can be heavily interfered by fluorescent dyes,[101], microbiological,[100] organic,[95] and inorganic substances.[95] Due to this, microplastic samples have to be separated from the matrix and processed beforehand.[95,100] Below the 1 µm limit, mass-based methods should be used, as single-particle characterization lacks sensitivity.

2.3.2.2 Mass spectroscopy methods

Mass spectroscopy-based methods are those in which the sample is analyzed in bulk. The main advantage of these methods is the ability to identify nanoparticles of various plastics simultaneously, given there is enough mass of each nanoplastic in the sample. The signal in these methods depends mainly on the mass of plastics. However, other factors can influence the signal such as the organics in the matrix, additives in the plastic, sorbed contaminants, and coatings. Samples which contain high amounts of these should be previously cleaned to enhance the signal of the plastic. These methods are broadly suitable to qualitatively identify the types of plastics in a sample. However, only specific configurations allow for quantification of samples, returning a mass-based result. This is in comparison with visual analysis which provides number-based particle counts. The trade-off when using mass spectroscopy-based methods in comparison to visual characterizations and some types of vibration spectroscopy, is that visual information and spatial resolution are lost.

2.3.2.2.1 Thermal desorption coupled with gas chromatography-mass spectrometry (TDS-GC-MS)

TDS-GC-MS is a technique that was first used by Duemichen *et al.* in 2014 to detect unknown organic substances.[102] The sample is placed onto a thermogravimetric balance and subsequently heated to temperatures up to 1000 °C.[103] This heating produces degradation products which are absorbed onto a solid-phase substrate and subsequently transferred to a thermal desorption unit. Degradation products, mostly in the form of organic molecules, are desorbed and injected onto a chromatography column and analyzed with a mass spectrometer. In comparison to other mass-based techniques, TDS-GC-MS can analyze large masses of up to 100 mg, however, in practice only qualitative analysis is possible. [102,104,105]

2.3.2.2.2 Pyrolysis-gas chromatography-mass spectrometry (Py-GC-MS)

Py-GC MS is another mass-based analytical technique where the sample is decomposed at high temperatures (pyrolysis). Inter-lab reproducibility is challenging with this technique, as results are highly dependent on sample preparation, pyrolizer type, pyrolizate transfer, and the specifications of the GC column.[106] The three main types of pyrolizer that are commonly used in literature: filament, furnace, and Curie-point. In a filament pyrolizer, the sample is inserted into a quartz tube which is then placed inside the coiled filament. An electrical current is then passed through the filament and due to its resistance, it will instantaneously heat the sample up to a specific temperature. [107] In a furnace pyrolizer, the solid sample is dried onto sample holders (reusable cups), subsequently these are dropped into a pre-heated furnace for pyrolysis.[107] Curie-point pyrolysis uses induction: the solid sample is placed inside a ferromagnetic foil which is later placed in a high frequency magnetic field.[106,108]

In all cases, the pyrolysis is performed in a controlled atmosphere with an inert gas. In filament and Curie-point pyrolizers, a disposable substrate is used, this can be an advantage as it facilitates the sample preparation of simultaneous samples. Suspensions with micro- and nanoplastics can be dried onto these substrates, and samples can be stored for prolonged times. This is not possible in furnace pyrolysis as the fused quartz sample container is reusable, therefore the sample must be placed in as a solid or powder making it inconvenient when analyzing nanoplastic samples which are normally in suspension. The main advantage of the Curie-point pyrolizer is that the composition of the pyrolysis products does not change in the range of 480-980°C, whereas in the other pyrolizers the composition of pyrolysis products is temperature dependent. [109] Additionally, Curie-point pyrolizers are faster to reach and maintain accurately the target temperature. In Curie-point and furnace pyrolysis, quantification is possible when high temperatures are used as no un-pyrolyzed sample remains as residue. Quantification is harder in filament pyrolysis, as some of the pyrolysis products will condense in the quartz tube.

In comparison to other techniques like TED-GC MS, Py-GC-MS offers more sensitivity, making it appealing when trying to identify nanoplastics (down to 50 µg of sample).[107] However, this can be a drawback when analyzing environmental samples such as sediments and tissues, as the amount of sample that can be injected is restricted by the size of the pyrolizer. Additionally, the success of Py-GC-MS in detecting micro- and nanoplastics is highly dependent on the matrix in which these are embedded. In high organic content matrices, digestions and other separation methods are necessary.

2.3.2.3 Signal processing

With all these spectroscopic/spectrometric techniques, obtaining useful information requires interpretation of the raw data. There are many libraries commercially available, however, each

equipment has different specifications (e.g. column type, column length, sample degradation temperature, thermal desorption, cryo-focusing of degradation products etc.). Due to these differences, it is often better to build an equipment-specific library. This makes it simpler to optimize identification and attempt quantification. It is also valuable to have a thorough understanding of the fundamental chemical implications of the spectra in order to decode the signal and identify contaminants.

2.3.3 Emerging characterization techniques

Recently, there has been a spike in emerging technologies to identify micro- and nanoplastics in the nanometer range. Photothermal Spectroscopy Corporation has developed a system with overcomes the diffraction limit of IR spectroscopy. This is achieved using a pulsating mid-IR laser which induces photothermal activity at the sample surface. This microspectroscopy technique can perform IR and Raman simultaneously, as it is also able to collect the Raman shifted light produced by the photothermal activity. They claim that their instrument can achieve spatial resolution of less than 1 μm.[110] Time-of-flight secondary ions mass spectrometry (TOF-SIMS) has also been proposed as a potential technique to identify small micro- and nanoplastics. In other materials, TOF-SIMS can provide a spatial resolution down to 70 nm. However, this has not been achieved in plastics.[111]

Other researchers have tackled the problem of identifying and recovering nanoplastics by doping them with metals. These metals can be used as tracers which facilitate detection and even allows for quantification. Mitrano *et al*. detailed a synthesis method that can be used to produce polyacrylonitrile particles doped with Pd. The fate of these particles was later evaluated in a simulated wastewater treatment plant liquor.[112]

2.4 Blank and spike controls

When assessing a sample for the presence of micro- and nanoplastics, there is a crucial need for quality controls that include: blanks, spike recoveries, and contamination assessment. Dris *et al*. found that indoor environments contain 1.0-60.0 fibers per m^3, of these, 33% were synthetic polymers.[113] This and other studies highlight the importance of blanks undergoing some or all extraction steps and analyzed under the same conditions as samples.[114–117] Background levels can represent a significant portion of the signal in low concentration samples.[115] Positive controls (spiked samples) are used for both solid and liquid samples[41,115,117–120] with recoveries between 70 and 95% in most studies, though comparison between biota studies is still hampered by variation in recovery rates across size fractions and processing methods.[121] Spikes are generally limited to only a few types of particles, with polystyrene most commonly employed. Spiked particles are typically 100-500 μm.[39,115,120] While satisfactory recovery was sometimes reported using spikes as small as 10-45 μm,[118] studies using nanometer-sized spike controls are lacking. Few[119] studies spike samples with fibers. Frequently, recoveries for positive controls are solely analyzed visually, but ideally, chemical analysis should be conducted to identify transformations due to extraction. Airborne contamination controls using clean petri dishes or filters have been employed, leading researchers to count fibers depending on colour.[119,122] Using laminar flow hoods, clean environments and/or dyed natural fiber clothing can limit microfiber contamination.[123] Contamination is especially problematic in nanoplastic detection with mass spectroscopy methods due to the bulk nature of the analysis.

Micro- and nanoplastics have been found in environmental samples of all compartments. Their effects have been studied mostly in laboratory settings, and there is still much to understand.

Detection of these, especially in complex matrices such as organisms is challenging and new technological developments are needed to advance research on microplastics pollution.

2.5 References

(1) Shruti, V. C.; Pérez-Guevara, F.; Elizalde-Martínez, I.; Kutralam-Muniasamy, G. Toward a Unified Framework for Investigating Micro(Nano)Plastics in Packaged Beverages Intended for Human Consumption. *Environmental Pollution* **2021**, *268*, 115811. https://doi.org/10.1016/j.envpol.2020.115811.

(2) Alimi, O. S.; Farner Budarz, J.; Hernandez, L. M.; Tufenkji, N. Microplastics and Nanoplastics in Aquatic Environments: Aggregation, Deposition, and Enhanced Contaminant Transport. *Environmental Science & Technology* **2018**. https://doi.org/10.1021/acs.est.7b05559.

(3) Kanhai, L. D. K.; Gårdfeldt, K.; Lyashevska, O.; Hassellöv, M.; Thompson, R. C.; O'Connor, I. Microplastics in Sub-Surface Waters of the Arctic Central Basin. *Marine Pollution Bulletin* **2018**, *130*, 8–18. https://doi.org/10.1016/j.marpolbul.2018.03.011.

(4) World Economic Forum. The New Plastics Economy - Rethinking the Future of Plastics; 2016.

(5) Law, K. L.; Thompson, R. C. Microplastics in the Seas. *Science* **2014**, *345* (6193), 144–145. https://doi.org/10.1126/science.1254065.

(6) Koehler, A.; Anderson, A.; Andrady, A.; Arthur, C.; Baker, J.; Bouwman, H.; Gall, S.; Hidalgo-Ruz, V.; Köhler, A.; Law, K. L.; Leslie, H.; Kershaw, P.; Pahl, S.; Potemra, J.; Ryan, P.; Shim, W. J.; Thompson, R.; Hideshige Takada; Turra, A.; Vethaak, D.; Wyles, K. Sources, Fate

and Effects of Microplastics in the Marine Environment: a Global Assessment. **2015**. https://doi.org/10.13140/RG.2.1.3803.7925.

(7) Panko, J. M.; Chu, J.; Kreider, M. L.; Unice, K. M. Measurement of Airborne Concentrations of Tire and Road Wear Particles in Urban and Rural Areas of France, Japan, and the United States. *Atmospheric Environment* **2013**, *72*, 192–199. https://doi.org/10.1016/j.atmosenv.2013.01.040.

(8) Abbasi, S.; Keshavarzi, B.; Moore, F.; Turner, A.; Kelly, F. J.; Dominguez, A. O.; Jaafarzadeh, N. Distribution and Potential Health Impacts of Microplastics and Microrubbers in Air and Street Dusts from Asaluyeh County, Iran. *Environmental Pollution* **2019**, *244*, 153–164. https://doi.org/10.1016/j.envpol.2018.10.039.

(9) Biber, N. F. A.; Foggo, A.; Thompson, R. C. Characterising the Deterioration of Different Plastics in Air and Seawater. *Marine Pollution Bulletin* **2019**, *141*, 595–602. https://doi.org/10.1016/j.marpolbul.2019.02.068.

(10) Gasperi, J.; Wright, S. L.; Dris, R.; Collard, F.; Mandin, C.; Guerrouache, M.; Langlois, V.; Kelly, F. J.; Tassin, B. Microplastics in Air: Are We Breathing It In? *Current Opinion in Environmental Science & Health* **2018**, *1*, 1–5. https://doi.org/10.1016/j.coesh.2017.10.002.

(11) Costa, M. F.; Barletta, M. Microplastics in Coastal and Marine Environments of the Western Tropical and Sub-Tropical Atlantic Ocean. *Environ. Sci.: Processes Impacts* **2015**, *17* (11), 1868–1879. https://doi.org/10.1039/C5EM00158G.

(12) Cozar, A.; Echevarria, F.; Gonzalez-Gordillo, J. I.; Irigoien, X.; Ubeda, B.; Hernandez-Leon, S.; Palma, A. T.; Navarro, S.; Garcia-de-Lomas, J.; Ruiz, A.; Fernandez-de-Puelles, M. L.;

Duarte, C. M. Plastic Debris in the Open Ocean. *Proceedings of the National Academy of Sciences* **2014**, *111* (28), 10239–10244. https://doi.org/10.1073/pnas.1314705111.

(13) Cózar, A.; Martí, E.; Duarte, C. M.; García-de-Lomas, J.; van Sebille, E.; Ballatore, T. J.; Eguíluz, V. M.; González-Gordillo, J. I.; Pedrotti, M. L.; Echevarría, F.; Troublè, R.; Irigoien, X. The Arctic Ocean as a Dead End for Floating Plastics in the North Atlantic Branch of the Thermohaline Circulation. *Sci. Adv.* **2017**, *3* (4), e1600582. https://doi.org/10.1126/sciadv.1600582.

(14) Eriksen, M.; Lebreton, L. C. M.; Carson, H. S.; Thiel, M.; Moore, C. J.; Borerro, J. C.; Galgani, F.; Ryan, P. G.; Reisser, J. Plastic Pollution in the World's Oceans: More than 5 Trillion Plastic Pieces Weighing over 250,000 Tons Afloat at Sea. *PLoS ONE* **2014**, *9* (12), e111913. https://doi.org/10.1371/journal.pone.0111913.

(15) Hirai, H.; Takada, H.; Ogata, Y.; Yamashita, R.; Mizukawa, K.; Saha, M.; Kwan, C.; Moore, C.; Gray, H.; Laursen, D.; Zettler, E. R.; Farrington, J. W.; Reddy, C. M.; Peacock, E. E.; Ward, M. W. Organic Micropollutants in Marine Plastics Debris from the Open Ocean and Remote and Urban Beaches. *Marine Pollution Bulletin* **2011**, *62* (8), 1683–1692. https://doi.org/10.1016/j.marpolbul.2011.06.004.

(16) Ross, P. S.; Chastain, S.; Vassilenko, E.; Etemadifar, A.; Zimmermann, S.; Quesnel, S.-A.; Eert, J.; Solomon, E.; Patankar, S.; Posacka, A. M.; Williams, B. Pervasive Distribution of Polyester Fibres in the Arctic Ocean Is Driven by Atlantic Inputs. *Nat Commun* **2021**, *12* (1), 106. https://doi.org/10.1038/s41467-020-20347-1.

(17) Kaiser, J. The Dirt on Ocean Garbage Patches. *Science* **2010**, *328* (5985), 1506–1506. https://doi.org/10.1126/science.328.5985.1506.

(18) Jambeck, J. R.; Geyer, R.; Wilcox, C.; Siegler, T. R.; Perryman, M.; Andrady, A.; Narayan, R.; Law, K. L. Plastic Waste Inputs from Land into the Ocean. *Science* **2015**, *347* (6223), 768–771. https://doi.org/10.1126/science.1260352.

(19) Kwak, J. I.; An, Y.-J. Microplastic Digestion Generates Fragmented Nanoplastics in Soils and Damages Earthworm Spermatogenesis and Coelomocyte Viability. *Journal of Hazardous Materials* **2021**, *402*, 124034. https://doi.org/10.1016/j.jhazmat.2020.124034.

(20) Nizzetto, L.; Futter, M.; Langaas, S. Are Agricultural Soils Dumps for Microplastics of Urban Origin? *Environmental Science & Technology* **2016**, *50* (20), 10777–10779. https://doi.org/10.1021/acs.est.6b04140.

(21) Zubris, K. A. V.; Richards, B. K. Synthetic Fibers as an Indicator of Land Application of Sludge. *Environmental Pollution* **2005**, *138* (2), 201–211. https://doi.org/10.1016/j.envpol.2005.04.013.

(22) Hidalgo-Ruz, V.; Gutow, L.; Thompson, R. C.; Thiel, M. Microplastics in the Marine Environment: A Review of the Methods Used for Identification and Quantification. *Environmental Science & Technology* **2012**, *46* (6), 3060–3075. https://doi.org/10.1021/es2031505.

(23) Thompson, R. C. Lost at Sea: Where Is All the Plastic? *Science* **2004**, *304* (5672), 838–838. https://doi.org/10.1126/science.1094559.

(24) Dris, R.; Imhof, H.; Sanchez, W.; Gasperi, J.; Galgani, F.; Tassin, B.; Laforsch, C. Beyond the Ocean: Contamination of Freshwater Ecosystems with (Micro-)Plastic Particles. *Environ. Chem.* **2015**, *12* (5), 539. https://doi.org/10.1071/EN14172.

(25) Ji, X.; Ma, Y.; Zeng, G.; Xu, X.; Mei, K.; Wang, Z.; Chen, Z.; Dahlgren, R.; Zhang, M.; Shang, X. Transport and Fate of Microplastics from Riverine Sediment Dredge Piles: Implications for Disposal. *Journal of Hazardous Materials* **2021**, *404*, 124132. https://doi.org/10.1016/j.jhazmat.2020.124132.

(26) McCormick, A.; Hoellein, T. J.; Mason, S. A.; Schluep, J.; Kelly, J. J. Microplastic Is an Abundant and Distinct Microbial Habitat in an Urban River. *Environ. Sci. Technol.* **2014**, *48* (20), 11863–11871. https://doi.org/10.1021/es503610r.

(27) Morritt, D.; Stefanoudis, P. V.; Pearce, D.; Crimmen, O. A.; Clark, P. F. Plastic in the Thames: A River Runs through It. *Marine Pollution Bulletin* **2014**, *78* (1–2), 196–200. https://doi.org/10.1016/j.marpolbul.2013.10.035.

(28) Sanchez, W.; Bender, C.; Porcher, J.-M. Wild Gudgeons (*Gobio Gobio*) from French Rivers Are Contaminated by Microplastics: Preliminary Study and First Evidence. *Environmental Research* **2014**, *128*, 98–100. https://doi.org/10.1016/j.envres.2013.11.004.

(29) Lee, J.; Hong, S.; Song, Y. K.; Hong, S. H.; Jang, Y. C.; Jang, M.; Heo, N. W.; Han, G. M.; Lee, M. J.; Kang, D.; Shim, W. J. Relationships among the Abundances of Plastic Debris in Different Size Classes on Beaches in South Korea. *Marine Pollution Bulletin* **2013**, *77* (1–2), 349–354. https://doi.org/10.1016/j.marpolbul.2013.08.013.

(30) McDevitt, J. P.; Criddle, C. S.; Morse, M.; Hale, R. C.; Bott, C. B.; Rochman, C. M. Addressing the Issue of Microplastics in the Wake of the Microbead-Free Waters Act—A New Standard Can Facilitate Improved Policy. *Environ. Sci. Technol.* **2017**, *51* (12), 6611–6617. https://doi.org/10.1021/acs.est.6b05812.

(31) Rochman, C. M.; Kross, S. M.; Armstrong, J. B.; Bogan, M. T.; Darling, E. S.; Green, S. J.; Smyth, A. R.; Veríssimo, D. Scientific Evidence Supports a Ban on Microbeads. *Environmental Science & Technology* **2015**, *49* (18), 10759–10761. https://doi.org/10.1021/acs.est.5b03909.

(32) Burton, G. A. Losing Sight of Science in the Regulatory Push to Ban Microbeads from Consumer Products and Industrial Use. *Integrated Environmental Assessment and Management* **2015**, *11* (3), 346–347. https://doi.org/10.1002/ieam.1645.

(33) European Chemical Agency. *Microplastics*; 2017.

(34) Hernandez, E.; Nowack, B.; Mitrano, D. M. Polyester Textiles as a Source of Microplastics from Households: A Mechanistic Study to Understand Microfiber Release During Washing. *Environ. Sci. Technol.* **2017**, *51* (12), 7036–7046. https://doi.org/10.1021/acs.est.7b01750.

(35) Mattsson, K.; Hansson, L.-A.; Cedervall, T. Nano-Plastics in the Aquatic Environment. *Environ. Sci.: Processes Impacts* **2015**, *17* (10), 1712–1721. https://doi.org/10.1039/C5EM00227C.

(36) Boerger, C. M.; Lattin, G. L.; Moore, S. L.; Moore, C. J. Plastic Ingestion by Planktivorous Fishes in the North Pacific Central Gyre. *Marine Pollution Bulletin* **2010**, *60* (12), 2275–2278. https://doi.org/10.1016/j.marpolbul.2010.08.007.

(37) Eriksson, C.; Burton, H. Origins and Biological Accumulation of Small Plastic Particles in Fur Seals from Macquarie Island. *Ambio* **2003**, *32* (6), 380–384.

(38) Murray, F.; Cowie, P. R. Plastic Contamination in the Decapod Crustacean Nephrops Norvegicus (Linnaeus, 1758). *Marine Pollution Bulletin* **2011**, *62* (6), 1207–1217. https://doi.org/10.1016/j.marpolbul.2011.03.032.

(39) Mahon, A. M.; O'Connell, B.; Healy, M. G.; O'Connor, I.; Officer, R.; Nash, R.; Morrison, L. Microplastics in Sewage Sludge: Effects of Treatment. *Environ. Sci. Technol.* **2017**, *51* (2), 810–818. https://doi.org/10.1021/acs.est.6b04048.

(40) Rolsky, C.; Kelkar, V.; Driver, E.; Halden, R. U. Municipal Sewage Sludge as a Source of Microplastics in the Environment. *Current Opinion in Environmental Science & Health* **2020**, *14*, 16–22. https://doi.org/10.1016/j.coesh.2019.12.001.

(41) Li, X.; Chen, L.; Mei, Q.; Dong, B.; Dai, X.; Ding, G.; Zeng, E. Y. Microplastics in Sewage Sludge from the Wastewater Treatment Plants in China. *Water Research* **2018**, *142*, 75–85. https://doi.org/10.1016/j.watres.2018.05.034.

(42) Bayo, J.; Olmos, S.; López-Castellanos, J.; Alcolea, A. Microplastics and Microfibers in the Sludge of a Municipal Wastewater Treatment Plant. *Int. J. SDP* **2016**, *11* (5), 812–821. https://doi.org/10.2495/SDP-V11-N5-812-821.

(43) El Hayany, B.; El Fels, L.; Quénéa, K.; Dignac, M.-F.; Rumpel, C.; Gupta, V. K.; Hafidi, M. Microplastics from Lagooning Sludge to Composts as Revealed by Fluorescent Staining-Image Analysis, Raman Spectroscopy and Pyrolysis-GC/MS. *Journal of Environmental Management* **2020**, *275*, 111249. https://doi.org/10.1016/j.jenvman.2020.111249.

(44) Zhang, Z.; Chen, Y. Effects of Microplastics on Wastewater and Sewage Sludge Treatment and Their Removal: A Review. *Chemical Engineering Journal* **2020**, *382*, 122955. https://doi.org/10.1016/j.cej.2019.122955.

(45) Zhong, H.; Yang, S.; Zhu, L.; Liu, C.; Zhang, Y.; Zhang, Y. Effect of Microplastics in Sludge Impacts on the Vermicomposting. *Bioresource Technology* **2021**, *326*, 124777. https://doi.org/10.1016/j.biortech.2021.124777.

(46) Browne, M. A.; Dissanayake, A.; Galloway, T. S.; Lowe, D. M.; Thompson, R. C. Ingested Microscopic Plastic Translocates to the Circulatory System of the Mussel, *Mytilus Edulis* (L). *Environ. Sci. Technol.* **2008**, *42* (13), 5026–5031.

(47) Van Cauwenberghe, L.; Claessens, M.; Vandegehuchte, M. B.; Janssen, C. R. Microplastics Are Taken up by Mussels (*Mytilus Edulis*) and Lugworms (*Arenicola Marina*) Living in Natural Habitats. *Environmental Pollution* **2015**, *199*, 10–17. https://doi.org/10.1016/j.envpol.2015.01.008.

(48) von Moos, N.; Burkhardt-Holm, P.; Köhler, A. Uptake and Effects of Microplastics on Cells and Tissue of the Blue Mussel *Mytilus Edulis* L. after an Experimental Exposure. *Environmental Science & Technology* **2012**, *46* (20), 11327–11335. https://doi.org/10.1021/es302332w.

(49) Watts, A. J. R.; Urbina, M. A.; Goodhead, R.; Moger, J.; Lewis, C.; Galloway, T. S. Effect of Microplastic on the Gills of the Shore Crab *Carcinus Maenas*. *Environmental Science & Technology* **2016**, *50* (10), 5364–5369. https://doi.org/10.1021/acs.est.6b01187.

(50) Andrady, A. L. Microplastics in the Marine Environment. *Marine pollution bulletin* **2011**, *62*, 1596–1605.

(51) Chen, Q.; Gundlach, M.; Yang, S.; Jiang, J.; Velki, M.; Yin, D.; Hollert, H. Quantitative Investigation of the Mechanisms of Microplastics and Nanoplastics toward Zebrafish Larvae Locomotor Activity. *Science of The Total Environment* **2017**, *584–585*, 1022–1031. https://doi.org/10.1016/j.scitotenv.2017.01.156.

(52) Lu, Y.; Zhang, Y.; Deng, Y.; Jiang, W.; Zhao, Y.; Geng, J.; Ding, L.; Ren, H. Uptake and Accumulation of Polystyrene Microplastics in Zebrafish (*Danio Rerio*) and Toxic Effects in Liver. *Environ. Sci. Technol.* **2016**, *50* (7), 4054–4060. https://doi.org/10.1021/acs.est.6b00183.

(53) Wang, W.; Ge, J.; Yu, X. Bioavailability and Toxicity of Microplastics to Fish Species: A Review. *Ecotoxicology and Environmental Safety* **2020**, *189*, 109913. https://doi.org/10.1016/j.ecoenv.2019.109913.

(54) Yin, L.; Chen, B.; Xia, B.; Shi, X.; Qu, K. Polystyrene Microplastics Alter the Behavior, Energy Reserve and Nutritional Composition of Marine Jacopever (Sebastes Schlegelii). *Journal of Hazardous Materials* **2018**, *360*, 97–105. https://doi.org/10.1016/j.jhazmat.2018.07.110.

(55) Mattsson, K.; Ekvall, M. T.; Hansson, L.-A.; Linse, S.; Malmendal, A.; Cedervall, T. Altered Behavior, Physiology, and Metabolism in Fish Exposed to Polystyrene Nanoparticles. *Environ. Sci. Technol.* **2015**, *49* (1), 553–561. https://doi.org/10.1021/es5053655.

(56) Greven, A.-C.; Merk, T.; Karagöz, F.; Mohr, K.; Klapper, M.; Jovanović, B.; Palić, D. Polycarbonate and Polystyrene Nanoplastic Particles Act as Stressors to the Innate Immune System of Fathead Minnow (*Pimephales Promelas*): Nanoplastics' Effect on the Immune System of Fish. *Environ Toxicol Chem* **2016**, *35* (12), 3093–3100. https://doi.org/10.1002/etc.3501.

(57) Fabbri, D.; Rombolà, A. G.; Vassura, I.; Torri, C.; Franzellitti, S.; Capolupo, M.; Fabbri, E. Off-Line Analytical Pyrolysis GC–MS to Study the Accumulation of Polystyrene Microparticles in Exposed Mussels. *Journal of Analytical and Applied Pyrolysis* **2020**, *149*, 104836. https://doi.org/10.1016/j.jaap.2020.104836.

(58) Lusher, A. L.; McHugh, M.; Thompson, R. C. Occurrence of Microplastics in the Gastrointestinal Tract of Pelagic and Demersal Fish from the English Channel. *Marine Pollution Bulletin* **2013**, *67* (1–2), 94–99. https://doi.org/10.1016/j.marpolbul.2012.11.028.

(59) Rios*, L. M.; Jones, P. R.; Moore, C.; Narayan, U. V. Quantitation of Persistent Organic Pollutants Adsorbed on Plastic Debris from the Northern Pacific Gyre's "Eastern Garbage Patch." *Journal of Environmental Monitoring* **2010**, *12* (12), 2226. https://doi.org/10.1039/c0em00239a.

(60) Holmes, L. A.; Turner, A.; Thompson, R. C. Adsorption of Trace Metals to Plastic Resin Pellets in the Marine Environment. *Environmental Pollution* **2012**, *160*, 42–48. https://doi.org/10.1016/j.envpol.2011.08.052.

(61) Hernandez, L. M.; Xu, E. G.; Larsson, H. C. E.; Tahara, R.; Maisuria, V. B.; Tufenkji, N. Plastic Teabags Release Billions of Microparticles and Nanoparticles into Tea. *Environ. Sci. Technol.* **2019**, *53* (21), 12300–12310. https://doi.org/10.1021/acs.est.9b02540.

(62) Evandri, M. G.; Tucci, P.; Bolle, P. Toxicological Evaluation of Commercial Mineral Water Bottled in Polyethylene Terephthalate: A Cytogenetic Approach with *Allium Cepa*. *Food Additives and Contaminants* **2000**, *17* (12), 1037–1045. https://doi.org/10.1080/02652030010014411.

(63) Makhdoumi, P.; Amin, A. A.; Karimi, H.; Pirsaheb, M.; Kim, H.; Hossini, H. Occurrence of Microplastic Particles in the Most Popular Iranian Bottled Mineral Water Brands and an Assessment of Human Exposure. *Journal of Water Process Engineering* **2021**, *39*, 101708. https://doi.org/10.1016/j.jwpe.2020.101708.

(64) Mason, S. A.; Welch, V. G.; Neratko, J. Synthetic Polymer Contamination in Bottled Water. *Frontiers in Chemistry* **2018**, *6*. https://doi.org/10.3389/fchem.2018.00407.

(65) Diaz-Basantes, M. F.; Conesa, J. A.; Fullana, A. Microplastics in Honey, Beer, Milk and Refreshments in Ecuador as Emerging Contaminants. *Sustainability* **2020**, *12* (14), 5514. https://doi.org/10.3390/su12145514.

(66) Rochman, C. M.; Tahir, A.; Williams, S. L.; Baxa, D. V.; Lam, R.; Miller, J. T.; Teh, F.-C.; Werorilangi, S.; Teh, S. J. Anthropogenic Debris in Seafood: Plastic Debris and Fibers from Textiles in Fish and Bivalves Sold for Human Consumption. *Sci Rep* **2015**, *5* (1), 14340. https://doi.org/10.1038/srep14340.

(67) Karami, A.; Golieskardi, A.; Keong Choo, C.; Larat, V.; Galloway, T. S.; Salamatinia, B. The Presence of Microplastics in Commercial Salts from Different Countries. *Scientific Reports* **2017**, *7*, 46173. https://doi.org/10.1038/srep46173.

(68) Kosuth, M.; Mason, S. A.; Wattenberg, E. V. Anthropogenic Contamination of Tap Water, Beer, and Sea Salt. *PLoS ONE* **2018**, *13* (4), e0194970. https://doi.org/10.1371/journal.pone.0194970.

(69) Peixoto, D.; Pinheiro, C.; Amorim, J.; Oliva-Teles, L.; Guilhermino, L.; Vieira, M. N. Microplastic Pollution in Commercial Salt for Human Consumption: A Review. *Estuarine, Coastal and Shelf Science* **2019**, *219*, 161–168. https://doi.org/10.1016/j.ecss.2019.02.018.

(70) Yang, D.; Shi, H.; Li, L.; Li, J.; Jabeen, K.; Kolandhasamy, P. Microplastic Pollution in Table Salts from China. *Environmental Science & Technology* **2015**, *49* (22), 13622–13627. https://doi.org/10.1021/acs.est.5b03163.

(71) Gigault, J.; El Hadri, H.; Nguyen, B.; Grassl, B.; Rowenczyk, L.; Tufenkji, N.; Feng, S.; Wiesner, M. Nanoplastics Are Neither Microplastics nor Engineered Nanoparticles. *Nat. Nanotechnol.* **2021**, *16* (5), 501–507. https://doi.org/10.1038/s41565-021-00886-4.

(72) Hernandez, L. M.; Yousefi, N.; Tufenkji, N. Are There Nanoplastics in Your Personal Care Products? *Environmental Science & Technology Letters* **2017**, *4* (7), 280–285. https://doi.org/10.1021/acs.estlett.7b00187.

(73) *Analysis of Nanoplastics and Microplastics in Food*, First edition.; Nollet, L. M. L., Siddiqi, K. S., Eds.; Food analysis & properties; CRC Press / Taylor & Francis Group: Boca Raton, 2021.

(74) Ekvall, M. T.; Lundqvist, M.; Kelpsiene, E.; Šileikis, E.; Gunnarsson, S. B.; Cedervall, T. Nanoplastics Formed during the Mechanical Breakdown of Daily-Use Polystyrene Products. *Nanoscale Adv.* **2019**, *1* (3), 1055–1061. https://doi.org/10.1039/C8NA00210J.

(75) Lambert, S.; Wagner, M. Formation of Microscopic Particles during the Degradation of Different Polymers. *Chemosphere* **2016**, *161*, 510–517. https://doi.org/10.1016/j.chemosphere.2016.07.042.

(76) Lambert, S.; Wagner, M. Characterisation of Nanoplastics during the Degradation of Polystyrene. *Chemosphere* **2016**, *145*, 265–268. https://doi.org/10.1016/j.chemosphere.2015.11.078.

(77) Bouwmeester, H.; Hollman, P. C. H.; Peters, R. J. B. Potential Health Impact of Environmentally Released Micro- and Nanoplastics in the Human Food Production Chain: Experiences from Nanotoxicology. *Environmental Science & Technology* **2015**, *49* (15), 8932–8947. https://doi.org/10.1021/acs.est.5b01090.

(78) Wagner, S.; Reemtsma, T. Things We Know and Don’t Know about Nanoplastic in the Environment. *Nat. Nanotechnol.* **2019**, *14* (4), 300–301. https://doi.org/10.1038/s41565-019-0424-z.

(79) Pikuda, O.; Xu, E. G.; Berk, D.; Tufenkji, N. Toxicity Assessments of Micro- and Nanoplastics Can Be Confounded by Preservatives in Commercial Formulations. *Environmental Science & Technology Letters* **2018**. https://doi.org/10.1021/acs.estlett.8b00614.

(80) Nguyen, B.; Claveau-Mallet, D.; Hernandez, L. M.; Xu, E. G.; Farner, J. M.; Tufenkji, N. Separation and Analysis of Microplastics and Nanoplastics in Complex Environmental Samples. *Accounts of Chemical Research* **2019**, *52* (4), 858–866. https://doi.org/10.1021/acs.accounts.8b00602.

(81) Renner, G.; Schmidt, T. C.; Schram, J. Analytical Methodologies for Monitoring Micro(Nano)Plastics: Which Are Fit for Purpose? *Current Opinion in Environmental Science & Health* **2018**, *1*, 55–61. https://doi.org/10.1016/j.coesh.2017.11.001.

(82) Galgani, F.; Hanke, G.; Werner, S.; De Vrees, L. Marine Litter within the European Marine Strategy Framework Directive. *ICES Journal of Marine Science* **2013**, *70* (6), 1055–1064. https://doi.org/10.1093/icesjms/fst122.

(83) Rocha-Santos, T.; Duarte, A. C. A Critical Overview of the Analytical Approaches to the Occurrence, the Fate and the Behavior of Microplastics in the Environment. *TrAC Trends in Analytical Chemistry* **2015**, *65*, 47–53. https://doi.org/10.1016/j.trac.2014.10.011.

(84) European Commission. Joint Research Centre. Institute for Environment and Sustainability.; MSFD Technical Subgroup on Marine Litter. *Guidance on Monitoring of Marine Litter in European Seas.*; Publications Office: LU, 2013.

(85) Zhang, T.-R.; Wang, C.-X.; Dong, F.-Q.; Gao, Z.-Y.; Zhang, C.-J.; Zhang, X.-J.; Fu, L.-M.; Wang, Y.; Zhang, J.-P. Uptake and Translocation of Styrene Maleic Anhydride Nanoparticles

in *Murraya Exotica* Plants As Revealed by Noninvasive, Real-Time Optical Bioimaging. *Environ. Sci. Technol.* **2019**, *53* (3), 1471–1481. https://doi.org/10.1021/acs.est.8b05689.

(86) Shim, W. J.; Song, Y. K.; Hong, S. H.; Jang, M. Identification and Quantification of Microplastics Using Nile Red Staining. *Marine Pollution Bulletin* **2016**, *113* (1–2), 469–476. https://doi.org/10.1016/j.marpolbul.2016.10.049.

(87) Erni-Cassola, G.; Gibson, M. I.; Thompson, R. C.; Christie-Oleza, J. A. Lost, but Found with Nile Red: A Novel Method for Detecting and Quantifying Small Microplastics (1 Mm to 20 Mm) in Environmental Samples. *Environ. Sci. Technol.* **2017**, *51* (23), 13641–13648. https://doi.org/10.1021/acs.est.7b04512.

(88) Maes, T.; Jessop, R.; Wellner, N.; Haupt, K.; Mayes, A. G. A Rapid-Screening Approach to Detect and Quantify Microplastics Based on Fluorescent Tagging with Nile Red. *Sci Rep* **2017**, *7* (1), 44501. https://doi.org/10.1038/srep44501.

(89) Betzig, E.; Patterson, G. H.; Sougrat, R.; Lindwasser, O. W.; Olenych, S.; Bonifacino, J. S.; Davidson, M. W.; Lippincott-Schwartz, J.; Hess, H. F. Imaging Intracellular Fluorescent Proteins at Nanometer Resolution. *Science* **2006**, *313* (5793), 1642–1645. https://doi.org/10.1126/science.1127344.

(90) Silva, A. B.; Bastos, A. S.; Justino, C. I. L.; da Costa, J. P.; Duarte, A. C.; Rocha-Santos, T. A. P. Microplastics in the Environment: Challenges in Analytical Chemistry - A Review. *Analytica Chimica Acta* **2018**, *1017*, 1–19. https://doi.org/10.1016/j.aca.2018.02.043.

(91) Shim, W. J.; Hong, S. H.; Eo, S. E. Identification Methods in Microplastic Analysis: A Review. *Anal. Methods* **2017**, *9* (9), 1384–1391. https://doi.org/10.1039/C6AY02558G.

(92) Gigault, J.; Pedrono, B.; Maxit, B.; Ter Halle, A. Marine Plastic Litter: The Unanalyzed Nano-Fraction. *Environ. Sci.: Nano* **2016**, *3* (2), 346–350. https://doi.org/10.1039/C6EN00008H.

(93) Filipe, V.; Hawe, A.; Jiskoot, W. Critical Evaluation of Nanoparticle Tracking Analysis (NTA) by NanoSight for the Measurement of Nanoparticles and Protein Aggregates. *Pharm Res* **2010**, *27* (5), 796–810. https://doi.org/10.1007/s11095-010-0073-2.

(94) NanoSight. NanoSight NTA 2.1 Analytical Software. Operating Manual. **2010**.

(95) Elert, A. M.; Becker, R.; Duemichen, E.; Eisentraut, P.; Falkenhagen, J.; Sturm, H.; Braun, U. Comparison of Different Methods for MP Detection: What Can We Learn from Them, and Why Asking the Right Question before Measurements Matters? *Environmental Pollution* **2017**, *231*, 1256–1264. https://doi.org/10.1016/j.envpol.2017.08.074.

(96) Mallikarjunachari, G.; Ghosh, P. Analysis of Strength and Response of Polymer Nano Thin Film Interfaces Applying Nanoindentation and Nanoscratch Techniques. *Polymer* **2016**, *90*, 53–66. https://doi.org/10.1016/j.polymer.2016.02.042.

(97) Löder, M. G. J.; Gerdts, G. Methodology Used for the Detection and Identification of Microplastics—A Critical Appraisal. In *Marine Anthropogenic Litter*; Bergmann, M., Gutow, L., Klages, M., Eds.; Springer International Publishing: Cham, 2015; pp 201–227. https://doi.org/10.1007/978-3-319-16510-3_8.

(98) Löder, M. G. J.; Kuczera, M.; Mintenig, S.; Lorenz, C.; Gerdts, G. Focal Plane Array Detector-Based Micro-Fourier-Transform Infrared Imaging for the Analysis of Microplastics in Environmental Samples. *Environ. Chem.* **2015**, *12* (5), 563. https://doi.org/10.1071/EN14205.

(99) Ribeiro-Claro, P.; Nolasco, M. M.; Araújo, C. Characterization of Microplastics by Raman Spectroscopy. In *Comprehensive Analytical Chemistry*; Elsevier, 2017; Vol. 75, pp 119–151. https://doi.org/10.1016/bs.coac.2016.10.001.

(100) Käppler, A.; Fischer, D.; Oberbeckmann, S.; Schernewski, G.; Labrenz, M.; Eichhorn, K.-J.; Voit, B. Analysis of Environmental Microplastics by Vibrational Microspectroscopy: FTIR, Raman or Both? *Anal Bioanal Chem* **2016**, *408* (29), 8377–8391. https://doi.org/10.1007/s00216-016-9956-3.

(101) Lenz, R.; Enders, K.; Stedmon, C. A.; Mackenzie, D. M. A.; Nielsen, T. G. A Critical Assessment of Visual Identification of Marine Microplastic Using Raman Spectroscopy for Analysis Improvement. *Marine Pollution Bulletin* **2015**, *100* (1), 82–91. https://doi.org/10.1016/j.marpolbul.2015.09.026.

(102) Duemichen, E.; Braun, U.; Senz, R.; Fabian, G.; Sturm, H. Assessment of a New Method for the Analysis of Decomposition Gases of Polymers by a Combining Thermogravimetric Solid-Phase Extraction and Thermal Desorption Gas Chromatography Mass Spectrometry. *Journal of Chromatography A* **2014**, *1354*, 117–128. https://doi.org/10.1016/j.chroma.2014.05.057.

(103) Dümichen, E.; Eisentraut, P.; Bannick, C. G.; Barthel, A.-K.; Senz, R.; Braun, U. Fast Identification of Microplastics in Complex Environmental Samples by a Thermal Degradation Method. *Chemosphere* **2017**, *174*, 572–584. https://doi.org/10.1016/j.chemosphere.2017.02.010.

(104) Dümichen, E.; Barthel, A.-K.; Braun, U.; Bannick, C. G.; Brand, K.; Jekel, M.; Senz, R. Analysis of Polyethylene Microplastics in Environmental Samples, Using a Thermal Decomposition Method. *Water Research* **2015**, *85*, 451–457. https://doi.org/10.1016/j.watres.2015.09.002.

(105) Duemichen, E.; Javdanitehran, M.; Erdmann, M.; Trappe, V.; Sturm, H.; Braun, U.; Ziegmann, G. Analyzing the Network Formation and Curing Kinetics of Epoxy Resins by in Situ Near-Infrared Measurements with Variable Heating Rates. *Thermochimica Acta* **2015**, *616*, 49–60. https://doi.org/10.1016/j.tca.2015.08.008.

(106) *Encyclopedia of Spectroscopy and Spectrometry*; Lindon, J. C., Ed.; Academic Press: San Diego, 20.

(107) Hammond, T.; Lehrle, R. S. Pyrolysis GLC. In *Comprehensive Polymer Science and Supplements*; Elsevier, 1989; pp 589–612. https://doi.org/10.1016/B978-0-08-096701-1.00027-6.

(108) Roussis, S. G.; Fedora, J. W. Use of a Thermal Extraction Unit for Furnace-Type Pyrolysis: Suitability for the Analysis of Polymers by Pyrolysis/GC/MS. *Rapid Communications in Mass Spectrometry* **1996**, *10* (1), 82–90. https://doi.org/10.1002/(SICI)1097-0231(19960115)10:1<82::AID-RCM449>3.0.CO;2-N.

(109) Alexeeva, K. V.; Khramova, L. P. Comparison of Various Pyrolyzers in the Study of Polymer Compositions. *Journal of Chromatography A* **1972**, *69* (1), 65–70. https://doi.org/10.1016/S0021-9673(00)83084-8.

(110) Baden, N.; Kobayashi, H.; Urayama, N. Submicron-Resolution Polymer Orientation Mapping by Optical Photothermal Infrared Spectroscopy. *International Journal of Polymer Analysis and Characterization* **2020**, *25* (1), 1–7. https://doi.org/10.1080/1023666X.2020.1735851.

(111) Physical electronics ULVAC-PHI. Phi NanoTOF II.

(112) Mitrano, D. M.; Beltzung, A.; Frehland, S.; Schmiedgruber, M.; Cingolani, A.; Schmidt, F. Synthesis of Metal-Doped Nanoplastics and Their Utility to Investigate Fate and Behaviour in Complex Environmental Systems. *Nat. Nanotechnol.* **2019**, *14* (4), 362–368. https://doi.org/10.1038/s41565-018-0360-3.

(113) Dris, R.; Gasperi, J.; Mirande, C.; Mandin, C.; Guerrouache, M.; Langlois, V.; Tassin, B. A First Overview of Textile Fibers, Including Microplastics, in Indoor and Outdoor Environments. *Environmental Pollution* **2017**, *221*, 453–458. https://doi.org/10.1016/j.envpol.2016.12.013.

(114) Talvitie, J.; Mikola, A.; Koistinen, A.; Setälä, O. Solutions to Microplastic Pollution – Removal of Microplastics from Wastewater Effluent with Advanced Wastewater Treatment Technologies. *Water Research* **2017**, *123*, 401–407. https://doi.org/10.1016/j.watres.2017.07.005.

(115) Ziajahromi, S.; Neale, P. A.; Rintoul, L.; Leusch, F. D. L. Wastewater Treatment Plants as a Pathway for Microplastics: Development of a New Approach to Sample Wastewater-Based Microplastics. *Water Research* **2017**, *112*, 93–99. https://doi.org/10.1016/j.watres.2017.01.042.

(116) Tagg, A. S.; Harrison, J. P.; Ju-Nam, Y.; Sapp, M.; Bradley, E. L.; Sinclair, C. J.; Ojeda, J. J. Fenton's Reagent for the Rapid and Efficient Isolation of Microplastics from Wastewater. *Chem. Commun.* **2017**, *53* (2), 372–375. https://doi.org/10.1039/C6CC08798A.

(117) Simon, M.; van Alst, N.; Vollertsen, J. Quantification of Microplastic Mass and Removal Rates at Wastewater Treatment Plants Applying Focal Plane Array (FPA)-Based Fourier Transform Infrared (FT-IR) Imaging. *Water Research* **2018**, *142*, 1–9. https://doi.org/10.1016/j.watres.2018.05.019.

(118) Carr, S. A.; Liu, J.; Tesoro, A. G. Transport and Fate of Microplastic Particles in Wastewater Treatment Plants. *Water Research* **2016**, *91*, 174–182. https://doi.org/10.1016/j.watres.2016.01.002.

(119) Gies, E. A.; LeNoble, J. L.; Noël, M.; Etemadifar, A.; Bishay, F.; Hall, E. R.; Ross, P. S. Retention of Microplastics in a Major Secondary Wastewater Treatment Plant in Vancouver, Canada. *Marine Pollution Bulletin* **2018**, *133*, 553–561. https://doi.org/10.1016/j.marpolbul.2018.06.006.

(120) Dyachenko, A.; Mitchell, J.; Arsem, N. Extraction and Identification of Microplastic Particles from Secondary Wastewater Treatment Plant (WWTP) Effluent. *Anal. Methods* **2017**, *9* (9), 1412–1418. https://doi.org/10.1039/C6AY02397E.

(121) Hermsen, E.; Mintenig, S. M.; Besseling, E.; Koelmans, A. A. Quality Criteria for the Analysis of Microplastic in Biota Samples: A Critical Review. *Environ. Sci. Technol.* **2018**, *52* (18), 10230–10240. https://doi.org/10.1021/acs.est.8b01611.

(122) McIlwraith, H. K.; Lin, J.; Erdle, L. M.; Mallos, N.; Diamond, M. L.; Rochman, C. M. Capturing Microfibers – Marketed Technologies Reduce Microfiber Emissions from Washing Machines. *Marine Pollution Bulletin* **2019**, *139*, 40–45. https://doi.org/10.1016/j.marpolbul.2018.12.012.

(123) Murphy, F.; Ewins, C.; Carbonnier, F.; Quinn, B. Wastewater Treatment Works (WwTW) as a Source of Microplastics in the Aquatic Environment. *Environ. Sci. Technol.* **2016**, *50* (11), 5800–5808. https://doi.org/10.1021/acs.est.5b05416.

Preface to Chapter 3

Following the literature review presented in Chapter 3, it is evident that there is a need to search for techniques that have the resolution to detect nanoplastics. Additionally, there is a need to detect nanoplastics < 100 nm that could be coming from primary sources, as these have been commonly overlooked and rarely identified. This chapter approached these issues by analyzing a product that is known to contain microplastics as an added ingredient. We hypothesized that the product would contain a continuum of sizes of plastic particles, which would be smaller than 100 nm. Using sequential filtration, we were able to remove all particles above 100 nm. A film formed from the nanoplastics < 100 nm in size was linked to the primary microplastics using traditional spectroscopy methods. Although the source of these nanoplastic particles was not simple to identify, we hypothesized that they were produced by the breakdown of larger beads during the emulsification process of the product. This chapter was published in *Environmental Science & Technology Letters* in 2017.

Chapter 3: Are There Nanoplastics in Your Personal Care Products?

Abstract

Fragmentation of plastic debris and the commercial use of plastic microbeads have led to the widespread distribution of microplastics in natural environments. Several studies have reported on the occurrence and toxicity of microplastics in soils and waters; however, due to methodological challenges, the presence and impact of nanoplastics (<100 nm) in natural systems have been largely ignored. Microbeads used in consumer products such as scrubs and shampoos are processed by mechanical means that may lead to their fragmentation into potentially more hazardous nanoplastics. In this study, three commercial facial scrubs containing polyethylene microbeads (~0.2 mm diameter) were examined to verify whether they contained nanoplastics. Particulates in the scrubs were fractionated using sequential filtration to isolate particles smaller than 100 nm. Scanning electron microscopy was used to confirm the presence of nanoparticles ranging in size from 24 ± 6 nm to 52 ± 14 nm. X-ray Photoelectron Spectroscopy and Fourier Transform Infrared Spectroscopy were used to confirm that the identified nanoparticles consisted of polyethylene. This study confirms the (unexpected) presence of nanoplastics in personal care products containing polyethylene microbeads and highlights the need for further studies to characterize the release and distribution of nanoplastic litter in natural aquatic and soil environments.

3.1 Introduction

The existence of milli- and micron-sized plastic waste in marine and freshwater bodies and its potential impact on aquatic life has recently become a major concern.[1,2] Small particulate plastics have found their way into aquatic bodies via two major routes. In the marine environment, larger plastic debris is fragmented by UV photodegradation, biodegradation, and chemical degradation processes (secondary microplastics).[3–6] Large plastic debris are reduced in size to form macroplastics (>25mm), mesoplastics (5–25 mm) and microplastics (<5 mm).[7] Most plastic debris eventually fragment into microplastics; in subtropical gyres, concentrations up to 10^6 microplastic particles per km^2 have been observed.[8] Another source of microplastics is synthetic microbeads, plastic particles of 5 μm–1 mm in diameter, incorporated into cosmetic and personal care products such as shampoos and scrubs (primary microplastics). Personal care products and cosmetics containing microbeads were recently banned in the US, Canada, and the European Union;[9,10] nonetheless, they are still widely used in many other countries and their impact may be felt over several future generations.[10]

Primary microplastics are usually made of polyethylene (PE) or polystyrene, whereas secondary microplastics have a more versatile chemistry due to the variety of plastics that are discharged into water bodies.[3] The degradation of microplastics via physical, chemical, and biological processes is likely to lead to the formation of nanoplastics (particles <100 nm in size),[11,12] exacerbating the associated environmental hazards.[13] In addition, the small size of nanoplastics poses a unique risk as it is comparable to that of cell membranes and other cellular components.[14,15] The hydrophobic nature of nanoplastics combined with their size should enable their entry into cells through poration or disruption of cell walls, which may lead to cytotoxicity.[16–19] The cytotoxic effect of a range of nanomaterials including carbon nanotubes, quantum dots, and silver is also well

documented,[20,21] and concerns have been raised about the lack of regulations on the use of nanoparticles in cosmetics and foods in North America[22,23] and Europe.[24] Despite the potential severity of its environmental and health impacts, pollution with nanoplastics of marine and freshwater bodies as well as soils has been generally neglected. Likely due to methodological challenges, the presence and impacts of nanoplastics in natural systems have been largely ignored[25,26] Furthermore, the presence of nanoplastics in consumer products has not been considered as a potential source of pollution to the natural environment.

Consumer products containing microbeads such as scrubs and shampoos are mechanically processed and emulsified using high shear mixers.[27] We thus hypothesized that physical degradation and breakdown of the microbeads during their manufacture or during preparation of the personal care products could lead to the formation of nanoplastics.

This study investigated the presence of nanoplastics in three different commercially available personal scrubs that were declared by the manufacturers to contain PE microbeads. The particulate material in the commercial products was fractionated using sequential filtration with various pore sizes. The separated particles were then characterized by electron microscopy and spectroscopy techniques to confirm the presence of considerable quantities of nanoplastics in personal care products containing microbeads.

3.2 Materials and methods

3.2.1 Isolation of nanoparticles from facial scrubs

Three commercial facial scrubs containing PE were purchased off the shelf from a drugstore in Montreal, Canada (July 2016). Diluted samples of the facial scrubs (herein referred to as scrubs

A, B, and C) were then subjected to sequential filtration to remove all particles larger than 100 nm. Scrub samples (0.2 g) were first diluted with 10 mL of reverse osmosis (RO) water. The intention of diluting at this ratio was to reduce the viscosity of the facial scrub while maintaining the particle concentration as high as possible. This suspension was subjected to five filtration steps (Figure 3.1). The first two steps used Whatman® filter paper and negative pressure filtration. In filtration step 1, Grade 2 Whatman® filter paper (20-25 µm) was used, and in filtration step 2, Grade 41 Whatman® filter paper (2.5 µm) was used. For steps 3-5, EMD Millipore Millex™ Sterile Syringe Filters of 0.45 µm and 0.1 µm were used applying positive pressure with a 10 mL syringe. A 0.1 µm syringe filter was used in step 4. DLS analysis of Filtrate 4 indicated the presence of particles larger than 100 nm (Figure S3.1), most likely due to imperfections in the syringe filter. For this reason, a second 0.1 µm filtration step was added as Step 5. All filter papers and syringe filters were rinsed three times with RO water before use. An image of Scrub A and the five subsequent filtrates is shown in Figure S3.2 to better illustrate how material is removed in each of the five steps. All experiments were done in triplicate.

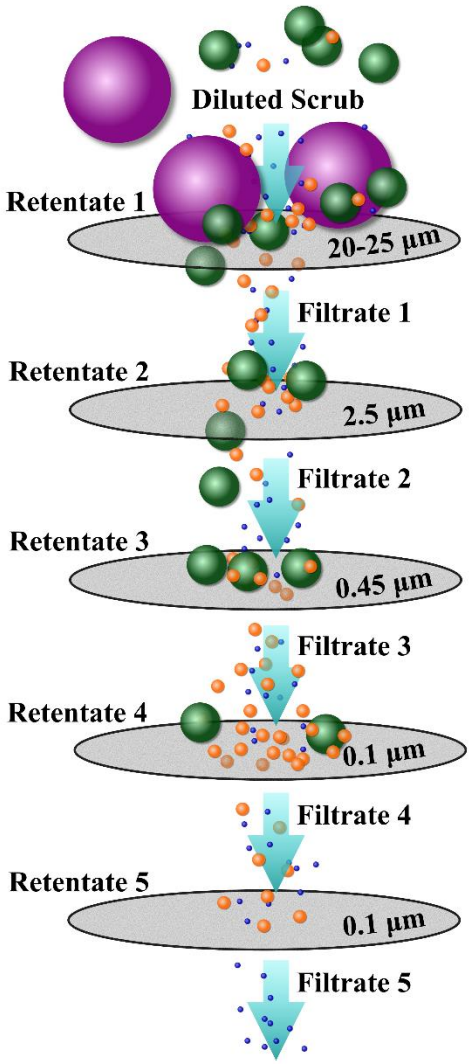

Figure 3.1. Scheme of the filtration process to which the scrubs were subjected.

3.2.2 Characterization of recovered nano-sized materials

Dynamic light scattering (DLS) (Zetasizer Nano ZS, Malvern Instruments) was used as a preliminary technique to confirm the presence of nanoparticles in Filtrate 5. For further confirmation, the particles isolated in Retentate 1 and Filtrate 5 were imaged using an FEI Quanta 450 Environmental Scanning Electron Microscope (FE-ESEM). Samples from Retentate 1 were collected for observation by first drying the Grade 2 Whatman® filter paper at room temperature

in a glass dish, then removing the dried powder of particles from the filtration membrane using a metallic spatula and finally fixing the powder onto adhesive carbon tape. The suspensions obtained as Filtrate 5 were fixed by filtering 100 µL of sample through a polycarbonate membrane (Sterlitech) with a 10-nm pore size. The carbon tape (coated with Retentate 1 powder) and the polycarbonate membrane (coated with Filtrate 5 particles) were both coated with a 3 nm layer of platinum (Leica Microsytems EM ACE600 Sputter Coater) for SEM imaging. Filtrate 5 samples were also imaged using Philips CM200 Transmission Electron Microscope. For observation, a drop of sample was fixed onto a Lacey carbon grid.

The composition of the material obtained in Filtrate 5 (<100 nm) was determined by Fourier Transform Infrared Spectroscopy (FTIR). The suspension (3 mL) was dried over aluminum foil in a desiccator, yielding a thin powder film of particles. The white powder was characterized using a Spectrum TWO FTIR with single bounce diamond (Perkin Elmer, Massachusetts, USA) in Attenuated Total Reflection (ATR) mode and a K-Alpha X-Ray Photoelectron Spectrometer (XPS) (Thermo Scientific, Massachusetts, USA) in the valence band range (0-25 eV). Additionally, commercial PE beads (250 µm diameter) were also analyzed as a positive control.

3.2.3 Control experiments

To verify whether the filtration process could result in fragmentation of PE microbeads, three types of commercial PE beads (50 µm, 250 µm, 800 µm) were acquired. These beads (0.1 g) were suspended in 10 mL of a 1:3 solution of commercial soap (Decon™ Bacdown™, Fisher) to RO water and then subjected to the same sequential filtration described in Figure 3.1. Filtrate 5 from these control samples was evaluated using DLS and SEM. As a negative control, RO water was processed through the filtration system described in Figure 3.1 and the resulting Filtrate 5 was also analyzed by DLS and SEM.

3.3 Results and discussion

3.3.1 Nanosized particles are detected in commercial scrubs

Using DLS, the number-weighted particle size distribution (Figure S3.3a) indicated that most of the particles are smaller than 100 nm in the Filtrate 5 from the sequential filtration of each of the diluted scrub samples. SEM was used to further characterize the size and shape of the detected nanomaterials in all three scrub samples. It is worth noting that DLS measurements are strongly biased by scattering of larger particles in a population.[28] This results in a higher mean particle size for a polydisperse suspension and would thus explain the differences in sizes measured by SEM and DLS. SEM imaging indicates the presence of large particles (~20 μm in diameter) in all three Retentate 1 samples (Figure 3.2a, c and e) as expected; however, smaller particles (~300 nm in diameter) are also observed (see insets). The particles present in Retentate 1 were observed to have irregular shapes and sizes; this can be evidence that larger beads were fragmented into smaller particles. Moreover, for each scrub, nanoparticles can be observed in images of Filtrate 5 (Figure 3.2b, d and f). The particles observed in Filtrate 5 appear more uniform in size because the samples went through several filtration steps (Figure 3.1) and because of limitations in microscope resolution at this high magnification. Although at first glance, most particles seem spherical, some shape irregularities and surface roughness are likely "hidden" by the Pt coating and cannot be resolved using SEM. To avoid these artefacts, the particles were also imaged by TEM (Figure S3.4); however, image analysis for size and shape characterization is challenging due to low contrast between the carbon grid and the carbon-based nanoparticles.

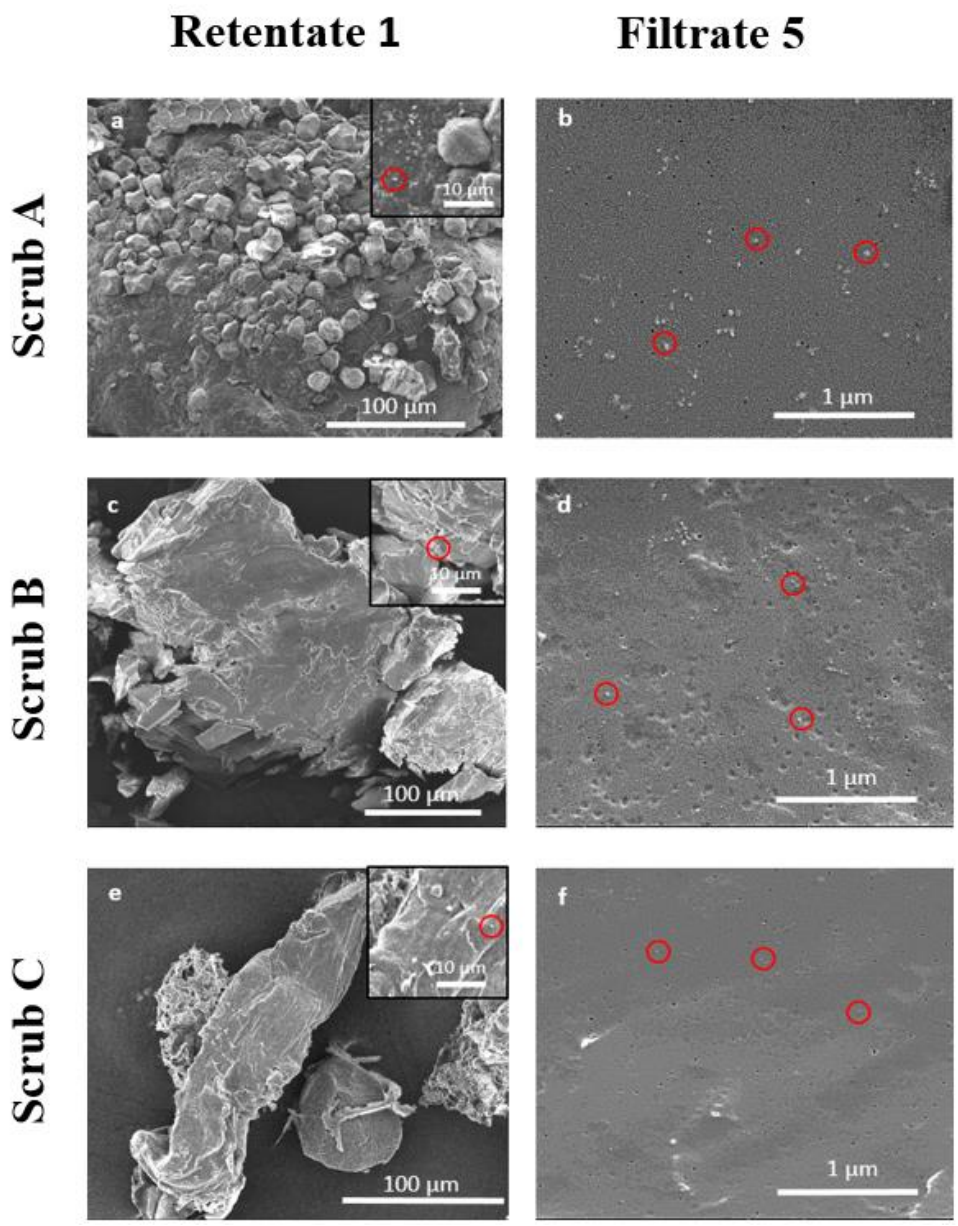

Figure 3.2. SEM images of samples taken at different filtration steps of the commercial scrubs: (a) Retentate 1 from scrub A, (b) Filtrate 5 from scrub A, (c) Retentate 1 from scrub B, (d) Filtrate 5 from scrub B, (e) Retentate 1 from scrub C, (f) Filtrate 5 from scrub C. Samples of Retentate 1 for each scrub were dried and fixed onto carbon tape for imaging. Samples of Filtrate 5 for each scrub were filtered through 10-nm polycarbonate membranes for imaging.

ImageJ software was used to estimate particle sizes from the SEM images. Analysis of over 1000 particles in Filtrate 5 from each of the three facial scrubs yielded equivalent particle diameters of 32±10 nm, 24±6 nm and 52±14 nm for scrubs A, B and C, respectively. Moreover, the surface coverage of nanoparticles on the 10-nm polycarbonate membrane was determined for each Filtrate 5 sample yielding an average count of 1.25 million particles/mm^2 of the polycarbonate membrane. Considering that 0.2 g of facial scrub was diluted into 10 mL of water and subsequently 0.1 mL of this dilution was filtered through the 10-nm polycarbonate membrane for SEM observation, it can be determined that the scrubs contain at the very least 300 billion nanoparticles per gram. By weighing the microparticles isolated in Retentate 1 and assuming a bead density of 0.97 g/cm^3, it was calculated that 0.03% w/w of the plastic contained in the scrubs is nanosized. This calculation was made by assuming that the weight of the microplastics found in Retentate 1 can be approximated to be ~100% of the total weight of the plastic component of the scrub. It is worth noting that it was not within the scope of this work to rigorously quantify the potential loss of particles in the syringe filter due to electrostatic, edge and other effects.[29] Clearly, there is significant loss of nanoparticles in the syringe filter due to these effects; therefore, the amount of nanoparticles estimated should be considered as the lower threshold present in the original scrub matrix.

Control experiments were conducted to evaluate the possibility of plastic microbeads breaking due to the force used in the sequential filtration process or the possibility of micro- or nanoplastic emanating from the filtration materials used. To test this hypothesis, samples of commercially available PE beads (50 µm, 250 µm, 800 µm) were sequentially filtered through the same process used for commercial scrubs (Figure 3.1). SEM images show the original commercial microbeads used (Figure S3.5a, c and e) and Filtrate 5 of this control experiment (Figure S3.5b, d and f). No

nanomaterials were detected in Filtrate 5 for all three commercial samples. Attempts to characterize Filtrate 5 of these control samples using DLS revealed unreliable correlation functions, indicating the absence of particles in the samples. This supports the hypothesis that the sequential filtration process did not cause the breakage of PE beads in the commercial scrubs into nano-sized particles. Moreover, the results suggest that nanoplastics form during the production of personal care products, e.g., during the mixing stage of ingredients of shampoos and soaps. This finding highlights the need for post-production monitoring of personal care products (among many other products that contain microparticles) for formation of nanoparticulates during the production process.

As a negative control, RO water was processed through the filtration system described in Figure 3.1. Filtrate 5 for this control was analyzed by DLS and SEM. As previously experienced, attempts to characterize Filtrate 5 using DLS resulted in unreliable correlation functions indicating the absence of nanoparticles in the RO water filtrate. SEM images (Figure S3.6) confirm that no nanomaterials leach from the membranes during the sequential filtration of RO water.

3.3.2 FITR and XPS characterization of the isolated nanomaterial

The composition of the isolated nanomaterial was analyzed using FTIR; the infrared spectra in transmittance from 500 to 4000 cm^{-1} are shown in Figure 3.3a. PE exhibits characteristic absorption bands at 720-731 cm^{-1} (rocking deformation, medium intensity), 1463 cm^{-1} and 1473 cm^{-1} (bending deformation, strong intensities) and 2851 cm^{-1} and 2919 cm^{-1} (CH_2 symmetric and asymmetric stretching respectively, strong intensities), which can be used as PE markers.[30] FTIR spectra of the commercial 250 µm PE beads and the three scrubs characterized under the same experimental conditions reveal the presence of the same bands, confirming the presence of PE in the scrub filtrates.

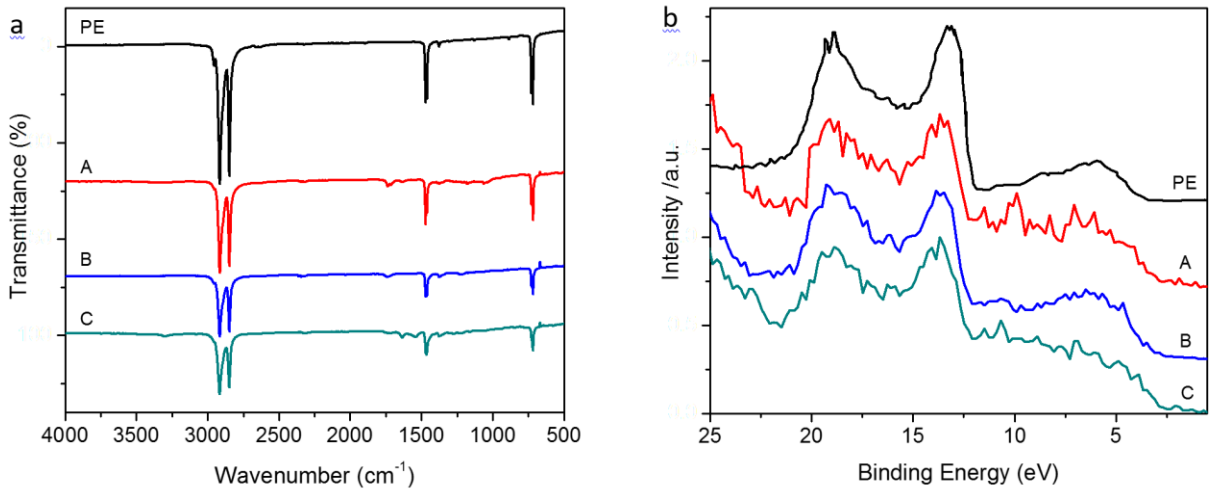

Figure 3.3. (a) FTIR spectra of commercial PE beads (250 µm) and Filtrate 5 of scrubs A, B and C. (b) XPS valence band scan of commercial PE beads and Filtrate 5 of scrubs A, B and C.

Elemental identification was implemented using surface-sensitive XPS. Typical C_{1s} peaks in the range of 280-300 eV were not chosen since polyolefins tend to have identical C_{1s} peaks. For example, PE and polypropylene (PP) cannot be differentiated using the core level spectra. Accordingly, the valence band photoelectrons in the 0-25 eV range were studied (Figure 3.3b). The molecular structure of PE consists of repeating $–CH_2–$ units; the C_{2s} contribution is seen as the two intense bands at binding energies of ~13 eV (antibonding molecular orbital) and ~19 eV (bonding analogue).[31] The broad band detectable from 3 to 11 eV is associated with the C_{2p} contribution.[31] The similarity of valence band spectra obtained for scrubs A, B and C with that of the control PE beads confirms the presence of PE in the studied scrubs. Moreover, the absence of a third intense peak in each scrub spectrum within the C_{2s} feature at ~16-17 eV (representing the methyl side-chain), indicates that the scrubs do not contain PP. XPS survey scans show the elemental composition of Filtrate 5 for scrubs A, B and C (Figure S3.7). No phosphorus, nitrogen or metal oxides were detected and therefore we can assume that there was no significant source of

contamination from surfactant, salts, or other colloids that may be mistaken as nanoplastics in the SEM or DLS analyses.

3.4 Environmental implications

The presence of nanoplastics in the environment is of growing concern;[32,33] yet, their detection, quantification, and characterization present important methodological challenges which have limited our understanding of their potential consequences. This study reveals for the first time the (unexpected) presence of nanoplastics (<100 nm) in commercial facial scrubs, which are present in the product as manufactured rather than as the result of microplastics breaking down in the environment. The source of the nanoplastics is unknown but may be linked to a broad size distribution of the starting microbead material, or larger particles breaking down in the emulsification process during manufacture of the scrubs. Microbeads also undergo mechanical stresses during consumer use, and possible fragmentation into nano-sized particles should be studied. This is of significant concern as facial scrubs are applied directly on skin, providing a direct route of exposure to the nanoplastics. Earlier studies have demonstrated the toxicity of PE in blue mussels,[34] *Hyalella azteca*[35] and marine larva[36] which highlights the potential risks of these nanomaterials. Although the complex mechanisms are not well understood and more research is needed, the release of nanoplastics to the natural environment and subsequent organismal exposure may also lead to enhanced biouptake of adsorbed co-contaminants.[40–43]

While the occurrence of nanoplastics in the environment has been hypothesized in the literature,[23,25,32,44,45] there are no reports of successful identification and characterization of particulate plastics with a diameter of less than 100 nm in the environment. There is increasing concern over the release of microplastics into lakes, rivers, and seas; however, this work demonstrates that nanoplastics are also being introduced in important quantities to the natural

environment. Although a few countries are starting to phase out microbead-containing consumer products, their global production and use over several decades does raise questions and concerns. Given the potential severity of the health and environmental impacts of nanoplastics, the findings presented here suggest that this smallest fraction of plastics deserves further study and scrutiny by researchers and policy makers. With the likely prevalence of nanoplastics in consumer products, ongoing work in our laboratory is aimed at investigating the presence of nanoplastics in wastewater sludges and treated effluents.

3.5 Acknowledgements

The authors acknowledge the financial support of the Canada Research Chairs program, Natural Sciences and Engineering Research Council of Canada, the FRQNT, and McGill University for MEDA awards to LMH and NY. The authors thank Nicholas Lin and Sunny Weng for assistance with preparation of graphics and Jeffrey Farner for helpful discussions and manuscript editing.

3.6 References

(1) Eerkes-Medrano, D.; Thompson, R. C.; Aldridge, D. C. Microplastics in freshwater systems: A review of the emerging threats, identification of knowledge gaps and prioritisation of research needs. *Water Res.* **2015**, *75*, 63–82 DOI: 10.1016/j.watres.2015.02.012.

(2) Hidalgo-Ruz, V.; Gutow, L.; Thompson, R. C.; Thiel, M. Microplastics in the Marine Environment: A Review of the Methods Used for Identification and Quantification. *Environ. Sci. Technol.* **2012**, *46*, 3060–3075 DOI: 10.1021/es2031505.

(3) Browne, M. A.; Galloway, T.; Thompson, R. Microplastic-an emerging contaminant of potential concern? *Integr. Environ. Assess. Manag.* **2007**, *3*, 559–561 DOI: 10.1002/ieam.5630030412.

(4) Andrady, A. L. Microplastics in the marine environment. *Mar. Pollut. Bull.* **2011**, *62*, 1596–1605.

(5) Barnes, D. K. A.; Galgani, F.; Thompson, R. C.; Barlaz, M. Accumulation and fragmentation of plastic debris in global environments. *Philos. Trans. R. Soc. B Biol. Sci.* **2009**, *364*, 1985–1998 DOI: 10.1098/rstb.2008.0205.

(6) Thompson, R. C. Lost at Sea: Where Is All the Plastic? *Science* **2004**, *304*, 838–838 DOI: 10.1126/science.1094559.

(7) Lee, J.; Hong, S.; Song, Y. K.; Hong, S. H.; Jang, Y. C.; Jang, M.; Heo, N. W.; Han, G. M.; Lee, M. J.; Kang, D.; et al. Relationships among the abundances of plastic debris in different size classes on beaches in South Korea. *Mar. Pollut. Bull.* **2013**, *77*, 349–354 DOI: 10.1016/j.marpolbul.2013.08.013.

(8) Law, K. L.; Thompson, R. C. Microplastics in the seas. *Science* **2014**, *345*, 144–145 DOI: 10.1126/science.1254065.

(9) Rochman, C. M.; Kross, S. M.; Armstrong, J. B.; Bogan, M. T.; Darling, E. S.; Green, S. J.; Smyth, A. R.; Veríssimo, D. Scientific Evidence Supports a Ban on Microbeads. *Environ. Sci. Technol.* **2015**, *49*, 10759–10761 DOI: 10.1021/acs.est.5b03909.

(10) Burton, G. A. Losing sight of science in the regulatory push to ban microbeads from consumer products and industrial use. *Integr. Environ. Assess. Manag.* **2015**, *11*, 346–347 DOI: 10.1002/ieam.1645.

(11) Bouwmeester, H.; Hollman, P. C. H.; Peters, R. J. B. Potential Health Impact of Environmentally Released Micro- and Nanoplastics in the Human Food Production Chain: Experiences from Nanotoxicology. *Environ. Sci. Technol.* **2015**, *49*, 8932–8947 DOI: 10.1021/acs.est.5b01090.

(12) Cozar, A.; Echevarria, F.; Gonzalez-Gordillo, J. I.; Irigoien, X.; Ubeda, B.; Hernandez-Leon, S.; Palma, A. T.; Navarro, S.; Garcia-de-Lomas, J.; Ruiz, A.; et al. Plastic debris in the open ocean. *Proc. Natl. Acad. Sci.* **2014**, *111*, 10239–10244 DOI: 10.1073/pnas.1314705111.

(13) Velzeboer, I.; Kwadijk, C. J. A. F.; Koelmans, A. A. Strong Sorption of PCBs to Nanoplastics, Microplastics, Carbon Nanotubes, and Fullerenes. *Environ. Sci. Technol.* **2014**, *48*, 4869–4876 DOI: 10.1021/es405721v.

(14) Hoet, P. H. M.; Nemmar, A.; Nemery, B. Health impact of nanomaterials? *Nat. Biotechnol.* **2004**, *22*, 19–19 DOI: 10.1038/nbt0104-19.

(15) Oberdörster, G.; Oberdörster, E.; Oberdörster, J. Nanotoxicology: an emerging discipline evolving from studies of ultrafine particles. *Environ. Health Perspect.* **2005**, *113*, 823–839.

(16) Bothun, G. D. Hydrophobic silver nanoparticles trapped in lipid bilayers: Size distribution, bilayer phase behavior, and optical properties. *J. Nanobiotechnology* **2008**, *6*, 13 DOI: 10.1186/1477-3155-6-13.

(17) Rasch, M. R.; Rossinyol, E.; Hueso, J. L.; Goodfellow, B. W.; Arbiol, J.; Korgel, B. A. Hydrophobic Gold Nanoparticle Self-Assembly with Phosphatidylcholine Lipid: Membrane-Loaded and Janus Vesicles. *Nano Lett.* **2010**, *10*, 3733–3739 DOI: 10.1021/nl102387n.

(18) Yousefi, N.; Wargenau, A.; Tufenkji, N. Toward More Free-Floating Model Cell Membranes: Method Development and Application to Their Interaction with Nanoparticles. *ACS Appl. Mater. Interfaces* **2016**, *8*, 14339–14348 DOI: 10.1021/acsami.6b00775.

(19) Yousefi, N.; Tufenkji, N. Probing the Interaction between Nanoparticles and Lipid Membranes by Quartz Crystal Microbalance with Dissipation Monitoring. *Front. Chem.* **2016**, *4* DOI: 10.3389/fchem.2016.00046.

(20) Lewinski, N.; Colvin, V.; Drezek, R. Cytotoxicity of Nanoparticles. *Small* **2008**, *4*, 26–49 DOI: 10.1002/smll.200700595.

(21) AshaRani, P. V.; Low Kah Mun, G.; Hande, M. P.; Valiyaveettil, S. Cytotoxicity and Genotoxicity of Silver Nanoparticles in Human Cells. *ACS Nano* **2009**, *3*, 279–290 DOI: 10.1021/nn800596w.

(22) Pekka Sinervo. Small is Different: A Science Perspective on the Regulatory Challenges of the Nanoscale; Council of Canadian Academies: Ottawa, ON, Canada, 2008.

(23) Kessler, R. Engineered Nanoparticles in Consumer Products: Understanding a New Ingredient. *Environ. Health Perspect.* **2011**, *119*, a120–a125 DOI: 10.1289/ehp.119-a120.

(24) Hansen, S. F.; Baun, A. European Regulation Affecting Nanomaterials - Review of Limitations and Future Recommendations. *Dose-Response* **2012**, *10*, dose-response.1 DOI: 10.2203/dose-response.10-029.Hansen.

(25) Chae, Y.; An, Y.-J. Effects of micro- and nanoplastics on aquatic ecosystems: Current research trends and perspectives. *Mar. Pollut. Bull.* **2017** DOI: 10.1016/j.marpolbul.2017.01.070.

(26) Koelmans, A. A.; Besseling, E.; Shim, W. J. Nanoplastics in the Aquatic Environment. Critical Review. In *Marine Anthropogenic Litter*; Bergmann, M., Gutow, L., Klages, M., Eds.; Springer International Publishing: Cham, 2015; pp 325–340.

(27) G. Ames. Mixing, Blending and Size Reduction Handbook.; 2001.

(28) Domingos, R. F.; Baalousha, M. A.; Ju-Nam, Y.; Reid, M. M.; Tufenkji, N.; Lead, J. R.; Leppard, G. G.; Wilkinson, K. J. Characterizing Manufactured Nanoparticles in the Environment: Multimethod Determination of Particle Sizes. *Environ. Sci. Technol.* **2009**, *43*, 7277–7284 DOI: 10.1021/es900249m.

(29) Logan, B. E. *Environmental Transport Processes*, 2nd ed.; Wiley: Hoboken, N.J, 2012.

(30) Gulmine, J. .; Janissek, P. .; Heise, H. .; Akcelrud, L. Polyethylene characterization by FTIR. *Polym. Test.* **2002**, *21*, 557–563 DOI: 10.1016/S0142-9418(01)00124-6.

(31) Foerch, R.; Beamson, G.; Briggs, D. XPS valence band analysis of plasma-treated polymers. *Surf. Interface Anal.* **1991**, *17*, 842–846 DOI: 10.1002/sia.740171204.

(32) Mattsson, K.; Hansson, L.-A.; Cedervall, T. Nano-plastics in the aquatic environment. *Env. Sci Process. Impacts* **2015**, *17*, 1712–1721 DOI: 10.1039/C5EM00227C.

(33) Jahnke, A.; Arp, H. P. H.; Escher, B. I.; Gewert, B.; Gorokhova, E.; Kühnel, D.; Ogonowski, M.; Potthoff, A.; Rummel, C.; Schmitt-Jansen, M.; et al. Reducing Uncertainty and Confronting Ignorance about the Possible Impacts of Weathering Plastic in the Marine Environment. *Environ. Sci. Technol. Lett.* **2017**, *4*, 85–90 DOI: 10.1021/acs.estlett.7b00008.

(34) von Moos, N.; Burkhardt-Holm, P.; Köhler, A. Uptake and Effects of Microplastics on Cells and Tissue of the Blue Mussel *Mytilus edulis* L. after an Experimental Exposure. *Environ. Sci. Technol.* **2012**, *46*, 11327–11335 DOI: 10.1021/es302332w.

(35) Au, S. Y.; Bruce, T. F.; Bridges, W. C.; Klaine, S. J. Responses of *Hyalella azteca* to acute and chronic microplastic exposures: Effects of Microplastic Exposure on *Hyalella azteca*. *Environ. Toxicol. Chem.* **2015**, *34*, 2564–2572 DOI: 10.1002/etc.3093.

(36) Kaposi, K. L.; Mos, B.; Kelaher, B. P.; Dworjanyn, S. A. Ingestion of Microplastic Has Limited Impact on a Marine Larva. *Environ. Sci. Technol.* **2014**, *48*, 1638–1645 DOI: 10.1021/es404295e.

(37) Hüffer, T.; Hofmann, T. Sorption of non-polar organic compounds by micro-sized plastic particles in aqueous solution. *Environ. Pollut.* **2016**, *214*, 194–201 DOI: 10.1016/j.envpol.2016.04.018.

(38) Napper, I. E.; Bakir, A.; Rowland, S. J.; Thompson, R. C. Characterisation, quantity and sorptive properties of microplastics extracted from cosmetics. *Mar. Pollut. Bull.* **2015**, *99*, 178–185 DOI: 10.1016/j.marpolbul.2015.07.029.

(39) Rios*, L. M.; Jones, P. R.; Moore, C.; Narayan, U. V. Quantitation of persistent organic pollutants adsorbed on plastic debris from the Northern Pacific Gyre's "eastern garbage patch." *J. Environ. Monit.* **2010**, *12*, 2226 DOI: 10.1039/c0em00239a.

(40) Eriksson, C.; Burton, H. Origins and biological accumulation of small plastic particles in fur seals from Macquarie Island. *Ambio* **2003**, *32*, 380–384.

(41) Murray, F.; Cowie, P. R. Plastic contamination in the decapod crustacean Nephrops norvegicus (Linnaeus, 1758). *Mar. Pollut. Bull.* **2011**, *62*, 1207–1217 DOI: 10.1016/j.marpolbul.2011.03.032.

(42) Boerger, C. M.; Lattin, G. L.; Moore, S. L.; Moore, C. J. Plastic ingestion by planktivorous fishes in the North Pacific Central Gyre. *Mar. Pollut. Bull.* **2010**, *60*, 2275–2278 DOI: 10.1016/j.marpolbul.2010.08.007.

(43) Rochman, C. M.; Hoh, E.; Kurobe, T.; Teh, S. J. Ingested plastic transfers hazardous chemicals to fish and induces hepatic stress. *Sci. Rep.* **2013**, *3* DOI: 10.1038/srep03263.

(44) Horton, A. A.; Walton, A.; Spurgeon, D. J.; Lahive, E.; Svendsen, C. Microplastics in freshwater and terrestrial environments: Evaluating the current understanding to identify the knowledge gaps and future research priorities. *Sci. Total Environ.* **2017**, *586*, 127–141 DOI: 10.1016/j.scitotenv.2017.01.190.

(45) da Costa, J. P.; Santos, P. S. M.; Duarte, A. C.; Rocha-Santos, T. (Nano)plastics in the environment – Sources, fates and effects. *Sci. Total Environ.* **2016**, *566–567*, 15–26 DOI: 10.1016/j.scitotenv.2016.05.041.

3.7 Supporting information

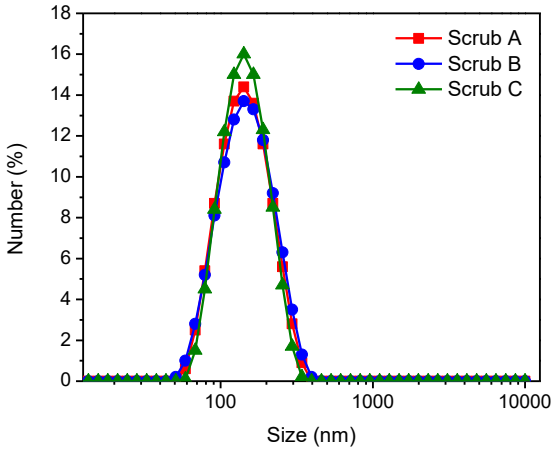

Figure S3.1. Dynamic light scattering number weight distribution for Filtrate 4 of Scrubs A, B and C. The distribution has a significant portion above 100 nm.

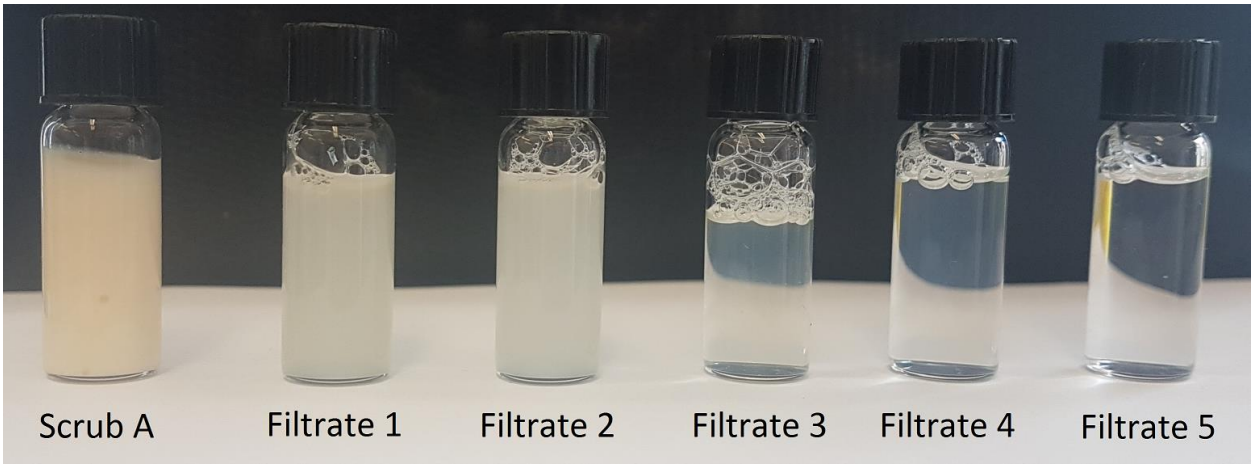

Figure S3.2. Picture of Scrub A and its 5 filtrates.

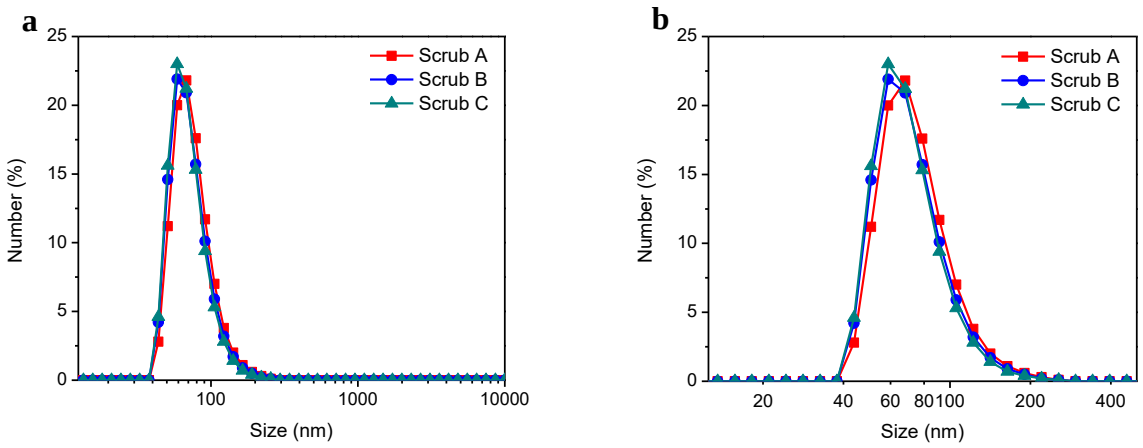

Figure S3.3. (a) Dynamic light scattering number weighted distribution of particles in Filtrate 5 of scrubs A, B and C. (b) Particle size distributions from (a) are shown on a different x-axis scale for improved clarity.

The derived count rates of DLS measurements for scrubs A, B and C were 494878 kcps, 52212 kpcs and 42079 kpcs respectively. The refractive index used for polyethylene was 1.510 and the absorbance for the samples was 0.1. The temperature for the measurements was set to 22°C. The parameters for the medium of dispersion were those of water (viscosity = 0.9540 cP and refractive index = 1.330). The curves were measured using an equilibrium time of 120 seconds, and a measuring angle of 173° with backscattering. The results were automatically calculated by the software using the data processing analysis mode for general purpose measurements with normal resolution.

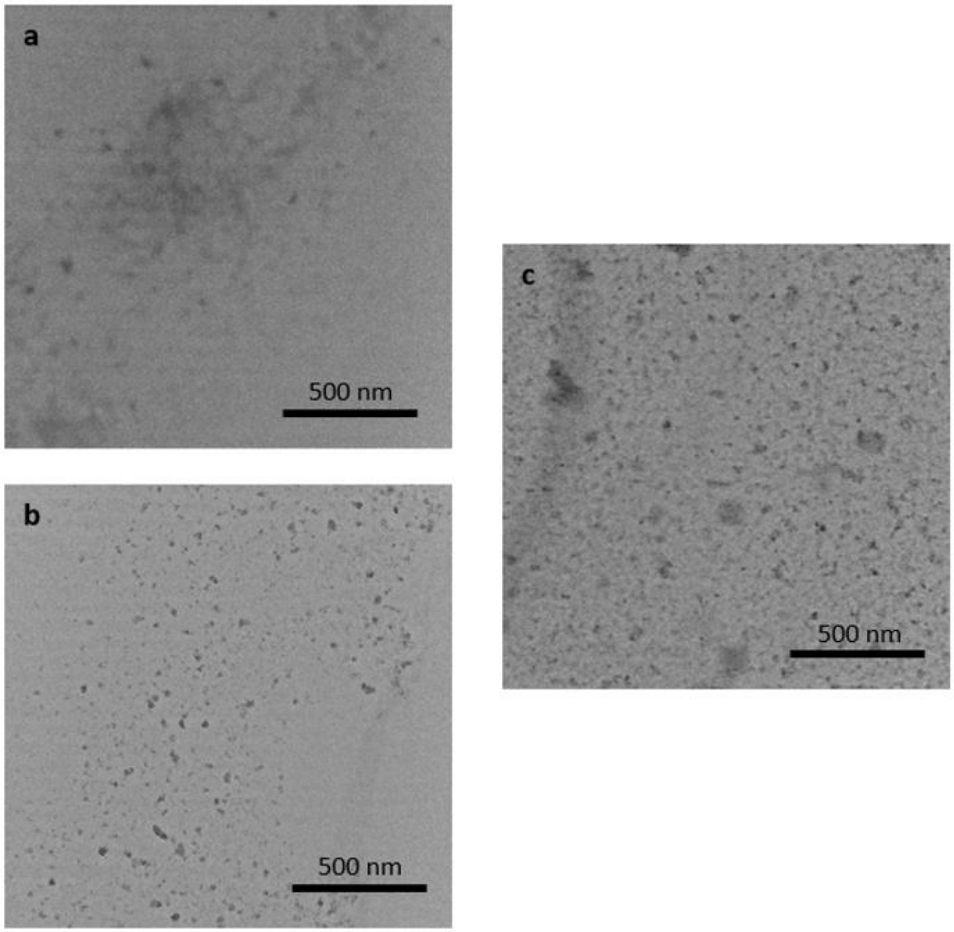

Figure S3.4. TEM images of Filtrate 5 for (a) Scrub A, (b) Scrub B, (c) Scrub C.

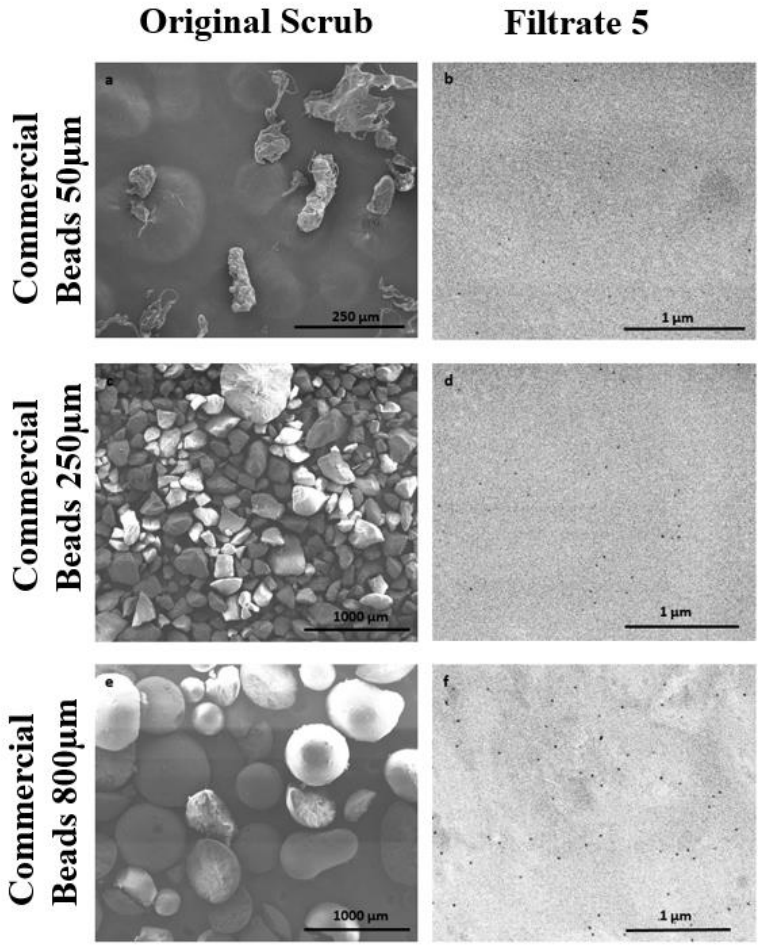

Figure S3.5. SEM images of commercial polyethylene scrub beads and their corresponding Filtrate 5 obtained in the control experiment. (a) Commercial PE beads (50 µm), (b) Filtrate 5 of commercial PE (50 µm), (c) commercial PE beads (250 µm), (d) Filtrate 5 of commercial PE (250 µm), (e) commercial PE beads (800 µm). (f) Filtrate 5 of commercial PE (800 µm).

Figure S5 shows SEM images of Filtrate 5 for the 3 commercial PE beads suspended in soapy water (panels b, d, f). No particles are observed in images b, d and f. The black dots observed are the holes in the 10 nm filtration membrane that is used to fix the samples for observation. The observation was made at 200 kV.

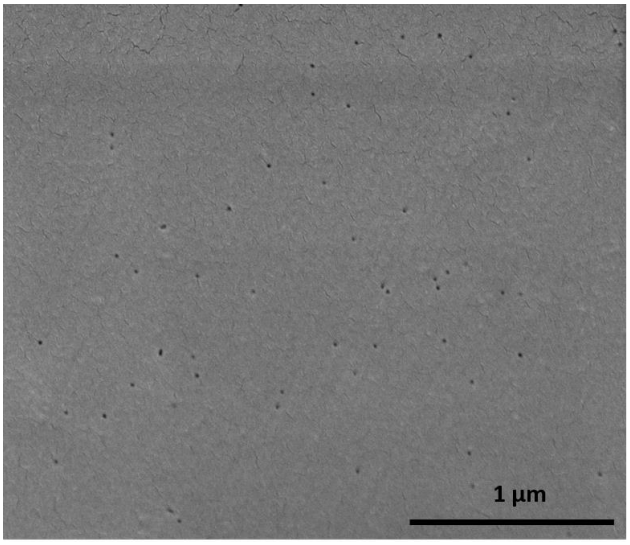

Figure S3.6. SEM image of Filtrate 5 sample when filtering RO water as a negative control. No particles are observed. The black dots are the holes in the 10 nm filtration membrane that is used to fix the sample for observation. The observation was made at 200 kV.

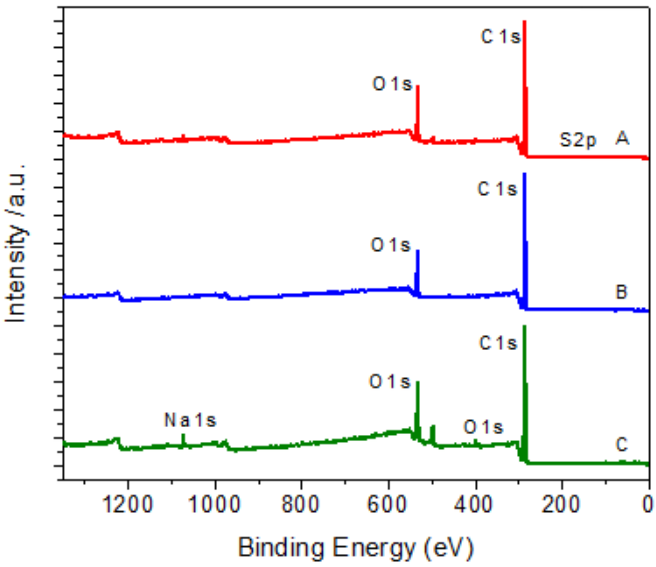

Figure S3.7. XPS survey scan of Filtrate 5 for scrubs A, B and C.

Preface to Chapter 4

Every day we are exposed to plastic particles in the environment, and even the food we eat. While it might not be surprising to find small plastic particles as part of the size distribution in facial scrubs (Chapter 3), we hypothesized that there could be plastic particles released from other plastic products that do not contain plastic but are rather packaged in plastic. In this case, we identified plastic teabags as a potential source of plastic particles. Four brands of teabags were purchased, emptied, and steeping was simulated. The simulated "tea" was later analyzed using electron microscopy, nanoparticle tracking analysis, and spectroscopy techniques. The presence of billions of micro- and nanoplastics was confirmed. This leachate was later used for preliminary toxicity experiments on *Daphnia magna*, results showed dose-dependent behavioral effects. This chapter was published in *Environmental Science and Technology* in 2019.

There was a comment published on this publication. In our response we made clarifications. Mainly that a laminar flow cabinet was used in the preparation of all samples and controls, and that we are only approximating the number of particles released from the plastic teabags. Additionally, we clarified that nanoparticle tracking analysis is done with the "wet" sample, so this technique would be unable to identify dissolved oligomers. The aim of our study was not to quantify the specific number of particles released, but rather to highlight that particles were being released from the teabags.

Chapter 4: Plastic teabags release billions of microparticles and nanoparticles into tea

Abstract

The increasing presence of micro- and nano-sized plastics in the environment and food chain is of growing concern. Although mindful consumers are promoting the reduction of single-use plastics, some manufacturers are creating new plastic packaging to replace traditional paper uses, such as plastic teabags. The objective of this study was to determine whether plastic teabags could release microplastics and/or nanoplastics during a typical steeping process. We show that steeping a single plastic teabag at brewing temperature (95°C) releases approximately 11.6 billion microplastics and 3.1 billion nanoplastics into a single cup of the beverage. The composition of the released particles is matched to the original teabags (nylon and polyethylene terephthalate) using Fourier-transform infrared spectroscopy (FTIR) and X-ray photoelectron spectroscopy (XPS). The levels of nylon and polyethylene terephthalate particles released from the teabag packaging are several orders of magnitude higher than plastic loads previously reported in other foods. An initial acute invertebrate toxicity assessment shows that exposure to only the particles released from the teabags caused dose-dependent behavioral and developmental effects.

4

4.1 Introduction

The widespread use and mismanagement of plastics has led to a significant environmental burden of growing concern.[1] Plastic from consumer goods can break down into microplastics and nanoplastics complicating their detection and quantification.[2–4] The nano-sized fraction of plastic is particularly difficult to identify in complex organic matrices such as soils and foods. Previous studies have used different definitions for the size range of microplastics and nanoplastics,[5–9] but for the purpose of this work, we define microplastics as particles ranging from 100 nm to 5 mm in size and nanoplastics as particles ≤ 100 nm in size. This definition of nanoplastics is in agreement with the definition of nanomaterials by the environmental nanoscience research community.[10–12]

Plastic is commonly used in food packaging and increasingly detected in our food supply.[13] Microplastics identified as poly(ethylene) and poly(ethylene terephthalate) were detected in table salt,[14] at levels up to 681 particles/kg.[15] Several studies report the presence of microplastics in fish (pelagic and demersal),[16–18] with up to a third of the sampled fish containing ingested microplastics at detection levels between 0.2 to 1.9 particles/fish.[17–19] Others have shown that mussels can contain between 0.3-0.5 microplastics/g (wet weight) at the time of consumption. Recent studies reported finding plastic microparticles and fibers in tap waters,[20] and in 240 water bottles sold around the world.[21,22]. A recent study estimates that the annual consumption of microplastics ranges between 39,000 and 52,000 particles depending on sex and age[23].

Attempts are being made to curb the proliferation of plastic pollution by phasing out its use in consumer goods[24,25] such as drinking straws,[26] facial scrubs, and toothpaste; yet, new applications of plastic are being introduced in the food industry. For instance, some tea manufacturers have shifted to using plastic teabags instead of the traditional paper teabags. This raises concern as water

is frequently at or above 95°C when brewing tea, and even "food grade" plastics may degrade or leach toxic substances when heated above 40°C.[27]

The primary objective of this study was to evaluate whether steeping of plastic teabags under conditions that mimic those used when brewing a cup of tea causes release of plastic micro- and nanoparticles into the beverage. Empty plastic teabags were steeped in reverse osmosis (RO) water for 5 minutes at 95°C and the resulting teabag leachate was analyzed for the presence of particles by scanning electron microscopy (SEM). The composition of the particles was confirmed by X-ray photoelectron spectroscopy (XPS) and Fourier-transform infrared spectroscopy (FTIR).

4.2 Materials and Methods

4.2.1 Release of particles from teabags

Four different commercial loose-leaf teas packaged in individual plastic teabags were purchased from grocery stores and coffee shops in Montreal, Canada (January 2016). The plastic teabags were cut with steel scissors and the tea leaves were removed. The teabags were emptied to enable determination of the number and composition of the particles released from the teabag material itself and not from the tea. The empty teabags (referred to as teabags A through D) were thoroughly washed three times using room temperature RO water to remove any tea or plastic debris and subsequently dried under a stream of nitrogen. Glass vials containing 10 mL of RO water were heated to 95°C using a DigiPREP block digestion system. For each of teabags A through D, three empty teabags were inserted into a single heated vial and left to steep for five minutes. After steeping, the water was decanted into an empty clean vial. This decanted water was referred to as the leachate from teabags A through D (Fig. 4.1a). Triplicate samples were prepared for all experiments.

4.2.2 Characterization of debris leached from teabags

Electron microscopy was the method chosen for observation of the leachates, as it provides the possibility of observing nanoparticles which are too small for observation with conventional imaging methods. Samples of the empty teabags (A-D) and tea leachates (A-D) were imaged using a FEI Inspect F50 SEM, as this equipment can observe particles down to 3 nm at 1 kV in SE mode. The plastic empty teabags were imaged before and after steeping by fixing them onto carbon tape. The teabag leachates (100 µL) were carefully drop cast and dried onto silicon wafers for imaging. Silicon wafers were first washed with ethanol to render the surface hydrophilic and only 10 µL of leachate was drop-casted at a time to avoid the so-called coffee ring effect during drying of the leachate (Fig. S4.1). The carbon tape (with the attached teabag sample) and the silicon wafers (coated with tea leachate) were coated with a 2 nm layer of platinum (Leica Microsystems EM ACE600 Sputter Coater) for SEM imaging. Triplicates were analyzed for each teabag and leachate. SEM images of the dried leachates were used to estimate the numbers and sizes of particles released into the leachates. ImageJ analysis software was used to estimate the particle sizes in the leachates of teabags A-D. Because of the polydispersity of the leachates, two average sizes were determined, the first at 1,000× magnification (micro-sized particles) and the second at 100,000× magnification (sub-micron particles). This yields a bimodal size distribution for each leachate. The mean particle diameter in each dried leachate was determined by averaging measured particle sizes from 30 images taken randomly at each magnification for each of three replicates (total of 90 images at each magnification per leachate type).

Nanoparticle Tracking Analysis (NTA) can be used to count the number of sub-micron particles. NTA (LM14 instrument with 532 nm green laser, NanoSight Ltd.) was used to confirm the SEM count of sub-micron particles in leachates diluted at a 1:15 ratio with RO water to fall within the

detection range of the instrument. Results for over 200 tracked sub-micron particles per sample were analyzed to determine the leachate concentration (repeated in triplicate for each teabag type).

The chemical composition of all teabags and leachates was determined by FTIR and XPS. The leachates were first separated into two fractions: micron-sized and sub-micron particles. For this, leachates were filtered through a grade 5 Whatman filter (cellulose filter with 2.5 µm pore size) (Fig. 4.1a). 3 mL of the filtrate containing the sub-micron fraction was dried over aluminum foil in a desiccator yielding a thin powder film. The fraction of particles retained on the Whatman filter was re-suspended in 10 mL RO water. 3 mL of this micron-sized leachate fraction was also dried over aluminum foil. The dried films of leachate and the original teabags were characterized using a Spectrum TWO FTIR instrument with a single-bounce diamond (PerkinElmer) in attenuated total reflection (ATR) mode and a K-Alpha X-ray photoelectron spectrometer (Thermo Scientific, using a monochromatic Al Kα X-ray source and a flood gun in a 10^{-8} mbar vacuum). Additionally, commercial nylon 6,6 and PET (McMaster Carr) were analyzed using FTIR and XPS and used as references to confirm the composition of the teabags and their leachates.

4.2.3 Control experiments with teabags

In this study, all experiments were conducted with cut, emptied, and washed teabags to ensure that the enumerated particles originated from the steeped teabag itself and to avoid interference from tea organics in the SEM, FTIR and XPS analyses. A control experiment with uncut teabags was conducted to confirm that cutting of the teabag did not cause leaching of particles (i.e., to confirm that particles were released even when the plastic teabag was uncut). These leachates contain tea and therefore require two additional steps before analysis, as the organics in tea interfere with SEM, FTIR, and XPS characterization. A 0.45 µm EMD Millipore Millex polyethersulfone sterile syringe filter was used to remove small tea leaves and twigs and a 50 mL Amicon stirred cell

(UFSC05001 model) with a 30 kDa filter was used to remove dissolved organics (Fig. S4.2a). These processed leachates were then characterized by SEM, FTIR and XPS (Fig. S4.2-S4.4).

An experiment was conducted to investigate the effect of heat on the release of particles from the plastic teabags. Briefly, teabags from brands B and D were opened, emptied, rinsed and dried with N_2 as previously described. Subsequently, three empty teabags were inserted into a single glass vial containing 10 mL of RO water at 22 °C. After 5 minutes, the water was decanted into an empty clean vial. This decanted water is referred to as the "unheated leachate" from teabags B and D. The "unheated leachate" was observed by SEM in the same manner as the heated leachate (Fig. S4.2d, e). Moreover, 3 mL of "unheated leachate" were dried over aluminum foil but no film was formed due to the lack of particulate matter in the leachate; therefore; characterization by XPS and FTIR was not possible.

A negative control was performed by processing RO water through the process described in Fig. 4.1a. Briefly, 10 mL of RO water in a vial were heated to 95 °C for 5 minutes and transferred to another vial (decantation step). Subsequently, 100 µL of the negative control were carefully drop-casted onto a silicon wafer for SEM imaging (Fig. S4.2f). To verify that the size separation did not introduce any artefacts to the FTIR and XPS analyses, the remaining leachate of the negative control was filtered through a grade 5 Whatman filter. 3 mL of the micro-sized fraction (retentate resuspended in 10 mL of RO water) and 3 mL of the sub-micron fraction (filtrate) were dried separately over aluminum foil. The chemical analysis on the negative control using FTIR and XPS yielded only background noise due to the absence of particles, indicating the sample processing in Fig. 4.1a did not introduce particles or artefacts into the teabag leachates.

An additional negative control was carried out by repeating the process in Fig. 4.1a using a metallic steeper (IKEA, Canada) with loose tea leaves (from the same supplier as teabag B) to confirm that

plastic particles were not leaching from the tea leaves themselves. The resulting tea was processed to remove twigs and dissolved organics using a 0.45 µm syringe filter and a 50 mL Amicon stirred cell with a 30 kDa filter (Fig. S4.2a). The processed leachate was characterized by SEM (Fig. S4.2g). This control confirms that the tea leaves do not release any particles between 0.45 µm and ~2 nm in size.

Lastly, a control to verify that the system in Fig. S4.2a was not discharging plastic was performed by processing RO water through the Amicon stirred cell and observing the dried retentate for the presence of particles using SEM (Fig. S4.2h). The leachates from all control experiments conducted with RO water were not characterized using XPS or FTIR as it was not possible to drop cast a film of these leachates due to the absence of particulate matter. This control confirms that the apparatus in Fig. S4.2a did not introduce particles into the leachates.

Control experiments with plastic teabags that have never been in contact with tea were not possible, as empty plastic teabags are not commercially available.

4.2.4 Concentrated leachate preparation for preliminary toxicity assays

Teabags B and D were used for toxicity assays as representative nylon and PET teabags, respectively. The number of teabags needed to prepare the concentrated leachates was calculated taking into account the density of each plastic, with the objective of maintaining an equivalent total mass of plastic. Concentrated leachates for toxicity experiments were prepared by using 3.55 teabags/mL of RO water and 2.95 teabags/mL of RO water for teabags B and D, respectively (these concentrations are referred to as “100% leachates”). All teabags were opened with stainless steel scissors, all tea leaves were carefully removed, and the empty teabags were washed three times with RO water and dried with ultrapure N_2. Ten clean teabags at a time were steeped in glass vials

containing RO water at 95°C for 5 minutes, and subsequently removed from the vials. Sequentially, another 10 teabags were steeped in the same water at 95°C for 5 minutes. The process was repeated until the final target number of teabags per mL was achieved. Concentrated leachates mimic the amount of plastic ingested when drinking 1 cup of tea every other day for 1 year. The 100% leachate was sterilized by exposing the suspension to UV light (wavelength 254 nm, 4.6 mW cm^{-2}) for 20 minutes.

Selected toxicity tests with *D. magna* were conducted with dialyzed leachate to isolate the effect of the micro- and nanoplastics. To remove any dissolved metal(loid)s, each concentrated (100%) leachate was dialyzed for 7 days using 3.5 kDa Spectra-Por regenerated cellulose dialysis tubing. RO water for the dialysis process was exchanged every 2 hours for the first 12 hours and every 8 hours for the remaining 7 days. This is referred to as dialyzed 100% leachate.

4.2.5 Characterization of leachates and teabags using ICP-MS

Inductively coupled plasma mass spectrometry (ICP-MS NexION 300, Perkin Elmer) was used to quantify trace levels of Al, As, Cr, and Pb in digested samples of 100% leachates (before and after dialysis), empty plastic teabags (pre-washed with RO water), and full teabags. Three negative control samples and 3 positive control samples (spiked with a known concentration of arsenic) were digested using the same method to account for possible contamination. Finally, because arsenic is a volatile compound and the mixture of organics and acids can cause the release of vapor, the third triplicate of all the samples was spiked with a known concentration of arsenic. Details of sample preparation, digestion and data analysis are provided in the Supporting Information.

4.2.6 Toxicity assays using *D. magna*

Daphnia magna used for this study was provided by Environment and Climate Change Canada (Montreal) and maintained under controlled conditions in the laboratory for more than 1 year in moderately hard reconstituted water (MHRW) at room temperature and a 16 h light, and 8 h dark cycle. They were fed daily with cultured green algae (*Chlamydomonas reinhardtii*) grown in an algae growth incubator (INFORS HT - Multitron Pro). The acute testing procedure was conducted in accordance with the OECD guideline *D. magna* Acute Immobilization Test.[28] Briefly, the 100% leachates B and D as representative of nylon and PET teabag leachate was converted to MHRW by adding calcium chloride (Fisher Scientific, Certified ACS Grade), magnesium sulfate (Fisher Scientific, Certified Grade), sodium bicarbonate (Sigma Aldrich, ACS reagent, ≥99.7%) and potassium chloride (Fisher Scientific, BP/EP/FCC/JP/USP Purity grade), and then diluted to 50%, 5%, and 0.5% with MHRW. Neonates younger than 24 hours were exposed for up to 48 hours to 50%, 5%, and 0.5% non-dialyzed or dialyzed leachate as well as MHRW as a control. Each 50 mL glass beaker contained 10 mL of test solution and five animals. The experiment was done in triplicates for each leachate concentration and the control. All test beakers were placed in a random order at light:dark conditions of 16 hours:8 hours. The temperature (21-22℃), pH (7-8), and dissolved oxygen (9.9-10.6) of the beakers were recorded, which were in accordance with the OECD guideline. The neonates were not fed during the 48 hour exposure, and the immobile neonates were counted and removed at 24 and 48 hours. The swimming behavior of *D. magna* was measured according to the method described by Bownik et al.[29] with some modifications. Experimental details of the assay, analysis of the swimming behavior, and data processing are provided in the Supporting Information. After swimming assessment, a subsample of *D. magna* was randomly selected for X-ray computed tomography scan (CT scan) and optical microscopy.

Experimental details of CT scan and optical microscopy are provided in the Supporting Information.

4.3 Results

4.3.1 Plastic teabags and their leachates contain micro- and nanoparticles

The original teabags (Fig. 4.1b,f,j,n) show changes after steeping at 95℃ (Fig. 4.1c,g,k,o). At 30,000× (insets), small particles can be observed on the teabag before steeping (Fig. 4.1b,f,j,n) whereas after steeping (Fig. 4.1c,g,k,o) these particles disappear, and dents and fractures appear.

SEM was used to determine the shape and size of particles in the dried leachates (Fig. 4.1d-q). Fig. 4.1e and i show similar morphologies of large (~100 nm) and small (~20 nm) spherical nanoparticles in the leachates of teabags A and B. In contrast, irregularly shaped, larger agglomerates (~100-1,000 nm) are observed in the leachates of teabags C and D (Fig. 4.1m,q). Some smaller (~20-30 nm) individual particles are also identified in proximity to the agglomerates. At 1,000×, the particle sizes measured range from 520 nm to 270 µm, whereas at 100,000×, particles show characteristic lengths between ~17 nm and 1,260 nm (large aggregates). The overlap in these ranges suggests that the determined bimodal distribution is representative of the overall leachate sample. The analysis of more than 2,000 particles (and aggregates) in images taken at 1,000× and 100,000×, yields mean particle diameters of 24.3±14.4 µm and 102±22 nm, 52.3±29.3 µm and 171±78 nm, 12.6±6.7 µm and 357±156 nm, and 8.6±5.2 µm and 229±116 nm for leachates A, B, C, and D, respectively. The particle size distributions in Fig. 4.1 clearly show a micro-sized particle population (imaged at 1,000×; particle sizes mostly between ~1-150 µm) and a sub-micron particle population (imaged at 100,000×; particle sizes mostly between 1-1000 nm).

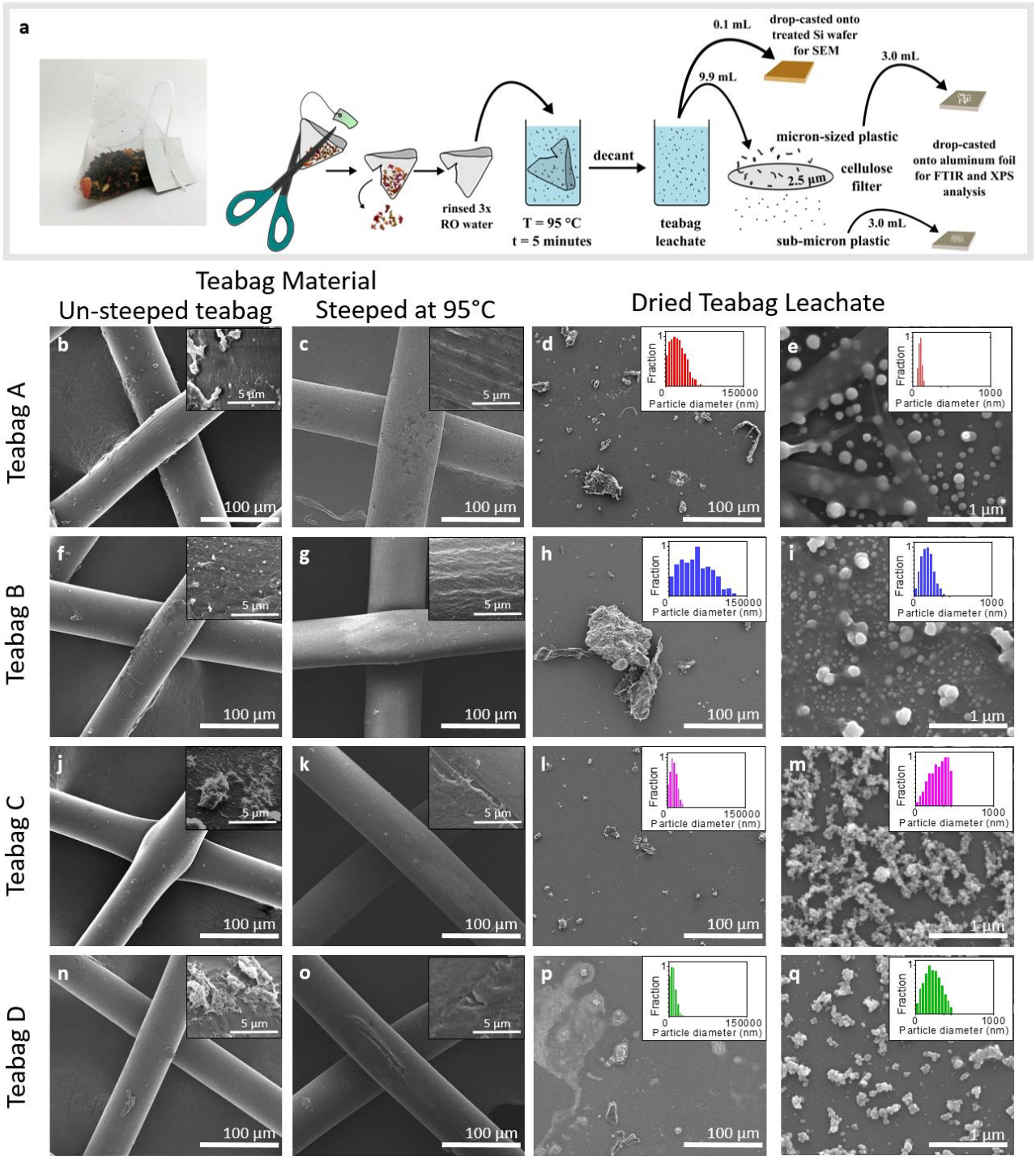

Figure 4.1. Teabag and leachate preparation for analysis with SEM, FTIR and XPS. (a) Schematic showing the preparation of teabag samples. (b-q) SEM images of original teabags and their leachates after steeping. Empty plastic teabags were fixed onto carbon tape and the leachates (100

µL) were drop cast onto silicon wafers. (b, f, j, n) Imaging at 1,000× of the original teabags before steeping shows a net-like structure (~30-70 µm) that appears to have a smooth surface, whereas at higher magnification (30,000× insets) surface roughness and small particles (~200-1,000 nm) are observed. (c, g, k, o) Imaging at 1,000× of the teabags after steeping reveals a rougher surface, at higher magnification (30,000× insets) dents and fractures are observed. (d, h, l, p) Teabag leachates: irregularly shaped microparticles (~1-200 µm) are observed at 1,000×. Micron-sized particle size distribution is shown in the insets. (e, i, m, q) Increasing the magnification to 100,000× confirms the presence of sub-micron and nano-sized particles in the teabag leachates. Sub-micron particle size distribution is shown in the insets.

To estimate the number of particles in each population (imaged at 1,000× and 100,000×), the average number of particles in 90 images was determined for each dried leachate sample (note: each sample consisted of 100 µL of dried leachate). The number of particles per unit area was then calculated using the number of particles per image and the size of the area scanned at each magnification. The surface coverage of the dried leachate at 1,000× yielded an average count of 1,200 micro-sized particles/mm^2, whereas the surface coverage at 100,000× resulted in an average count of 7 million sub-micron particles/mm^2. The overall particle count in 100 µL of leachate was estimated from the total area of the dried droplet (note: no coffee-ring effect was observed in any of the dried leachates indicating a homogeneous distribution of the particles on the imaged surface). These particle counts were used to determine the particle load in the 10 mL of leachate that had been prepared with three teabags. Finally, the result was divided by three to estimate the number of particles released from a single teabag. Hence, we estimate that, when drinking a single cup of tea prepared using one plastic teabag, a person can ingest approximately 2.3 million micro-sized (> 1 µm) and 14.7 billion sub-micron particles (< 1 µm in size). Based on the particle size

distributions for the sub-micron population shown in Fig. 4.1e,i,m,q, we can further determine that, on average, ~21% of this population consists of nano-sized particles (< 100 nm in size). Thus, we estimate that teabags A through D release an average of 3.1 billion nanoparticles per steeped teabag. NTA analysis of over 600 tracked sub-micron particles per leachate sample shows that teabags A-D release 8.9, 7.8, 19.1 and 21.4 billion particles, respectively. The average particle count by NTA (14.3 billion sub-micron particles) is very close to the average determined from SEM image analysis (14.7 billion sub-micron particles), thereby validating the quantitative imaging approach used.

4.3.2 Particles originate from plastic teabags

To verify the composition of the micro-sized and sub-micron particles, filtration was used to separate the micro-sized fraction from the sub-micron fraction in the leachates (Fig. 4.1a). Regardless of the type of teabag tested, the FTIR spectra of the micro-sized and the sub-micron fractions in the leachates are nearly identical to that of the corresponding original teabags, with detection of the same characteristic peaks from 500 to 4,000 cm^{-1} (Fig. 4.2a,b). The FTIR spectra of teabags A and B and their respective leachates are similar to that of a poly(hexamethylene adipamide) (such as nylon 6,6).[30] The FTIR spectra of samples C and D (teabags and their leachates) present the characteristic vibrations of poly(ethylene terephthalate) (PET).[31] Thus, the FTIR results indicate that teabags A and B are composed of nylon 6,6, and teabags C and D are made of PET. To verify the results obtained, commercial PET and nylon 6,6 samples were analyzed and the resulting spectra were in agreement with the characterization of the teabags and their leachates, as seen in Fig. 4.2a,b.

To further confirm the composition of the teabags and their leachates, XPS was used to characterize the elemental composition and electronic configuration of the elements. Fig. 4.2c,e,g

shows C1s, O1s, and N1s XPS spectra of teabags A and B and their corresponding leachates. C1s spectra of samples A and B exhibit two peaks (Fig. 4.2c). A major peak is observed at 285-286 eV which corresponds to three carbon-containing groups of nylon 6,6: C-C, C-N and C-O/C-OH. A minor peak ranging from 287 to 288 eV corresponds to the fourth carbon-containing group, namely CONH, characteristic of nylon 6,6.[32] A monomodal peak, reaching a maximum at ~532 eV, is observed for each O1s spectrum of the teabags and leachates A and B (Fig. 4.2e). CONH/COOH oxygen-containing groups are likely major contributors to this peak. A slight tailing is observed to the left of the peak which is related to C-O/C-OH groups. Lastly, the N1s spectral region was also explored and a peak at 399-400 eV is detected (Fig. 4.2g), revealing the presence of nitrogen-containing groups (N-H). These assignments were corroborated by the XPS analysis of a nylon 6,6 sample, providing very similar spectra. Thus, XPS analysis confirms the presence of nylon 6,6 in teabags A and B and their leachates.[32]

XPS characterization of teabags C and D and their leachates (Fig. 4.2d,f) points to the presence of PET. The C1s spectral region (Fig. 4.2d) is split into three main peaks that are clearly identified on the spectrum: ~284 eV (intense peak) attributed to the C-(CH) bond, ~287 eV (smaller peak at the foot of the intense peak) corresponding to the C-O bond, and ~290 eV attributed to carbon ester groups. Two main components are noted in the O1s spectra of teabags C and D (Fig. 4.2f). A bimodal distribution with peaks at 534 eV (C–O–C groups) and 532 eV (COO groups) is observed, confirming that the two types of oxygen of the ester functional group are present in teabags and leachates C and D.[33] A commercial PET sample was also characterized by XPS and the resulting spectra matched those of the teabags and their leachates. Thus, the XPS data support the FTIR results for all four types of teabags, confirming that the material of the micro-sized and sub-micron particles in the leachate match the parent plastic teabag. Considering the density of

PET and nylon, the average size of the particles observed and the estimated particle count per cup of tea, it was estimated that when drinking a single cup of tea prepared with one plastic teabag, a person might ingest 13-16 μg of plastic micro- and nanoparticles.

SEM images of the leachates from uncut teabags B and D (Fig. S4.2b,c) show that a significant number of particles are released even when teabags are uncut (Fig. 4.1d,h,l,p). FTIR and XPS analyses of the tea leachates from the uncut teabags correspond to those of the original emptied teabags B and D (Figs. S4.3a and S4.4). Thus, plastic micro- and nanoparticles leached out of the teabags even when they were uncut and contained tea, confirming that the plastic particles were not simply formed as a result of cutting the teabag. Since these leachates from uncut teabags required additional processing to remove the tea, it was not deemed appropriate to quantify the number of particles released into these leachates.

SEM imaging of the leachates for the unheated teabags (Fig. S4.2d,e) shows drastically fewer particles than the teabags steeped at 95°C (Fig. 4.1i,q). Analysis of these SEM images shows that the leachates from unheated teabags contain an average of 300 times less particles than leachates prepared at 95 °C. This suggests that the material of the teabag may be fragile such that high temperature can enhance the release of particles from the teabag.

An additional control experiment was performed by processing only RO water through the procedure described in Fig. 4.1a. SEM imaging of the dried sample (Fig. S4.2f) shows that neither the RO water nor the vials were a source of micro- or nanoparticles. An additional experiment was performed using a metallic steeper containing loose-leaf tea to verify whether the detected plastic particles were leaching from the tea. A representative SEM image of the leachate from the tea-filled metallic steeper shows no particles (Fig. S4.2g). A final control experiment conducted by

processing RO water through the system in Fig. S4.2a shows that no particles were released from the filters or stirred cell (Fig. S4.2h).

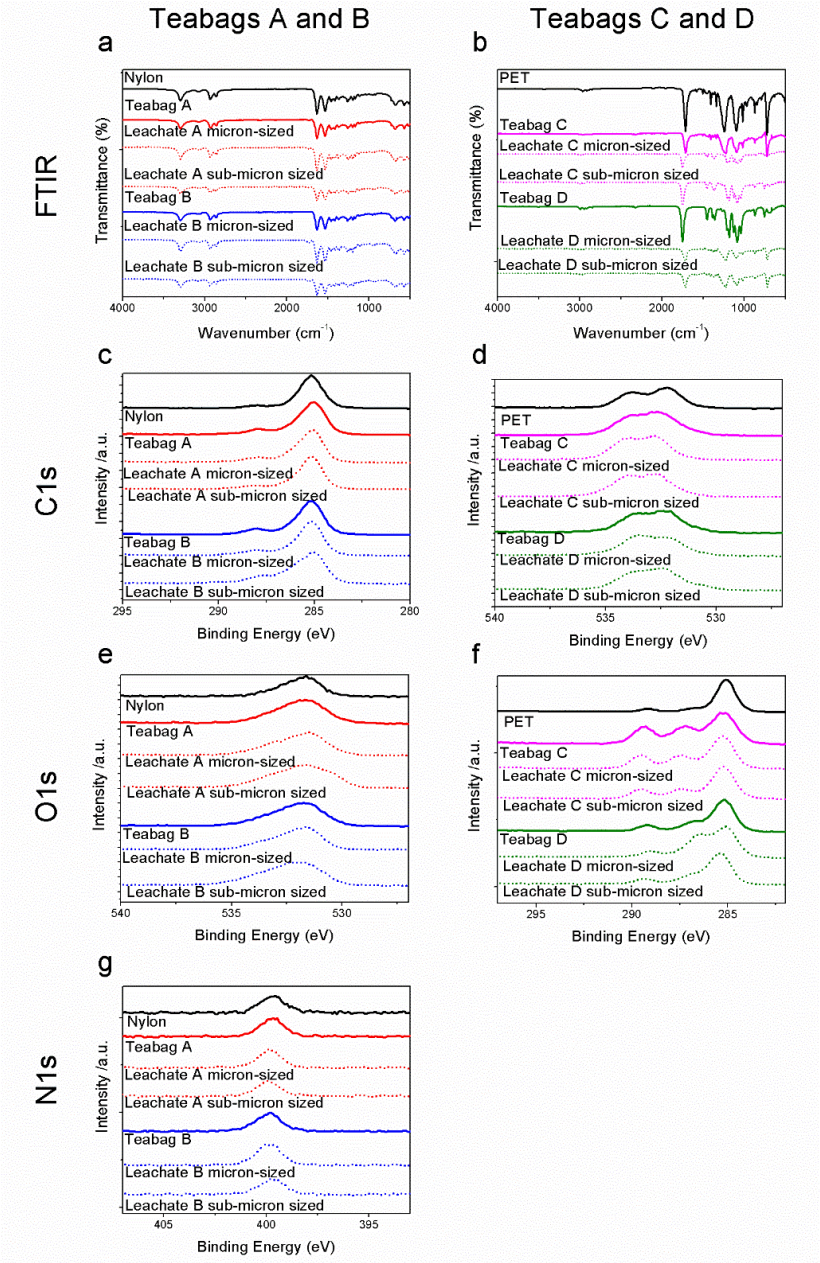

Figure 4.2. FTIR spectra and XPS scans for nylon 6,6, PET, the original teabags and their corresponding leachates. (a) The FTIR peak at 3289 cm^{-1} corresponds to the stretching vibration frequency of N–H groups in nylon 6,6 and the peaks detectable at 2932 cm^{-1} and 2860 cm^{-1} can be

associated to those of the ethylene sequence in nylon 6,6 (CH_2 asymmetric stretching). Teabags A and B, and their leachates, also present characteristic peaks of nylon 6,6 in the fingerprint region of their FTIR spectra (2,000 to 500 cm^{-1}): 1634 cm^{-1} (amide I band, having a main contribution of the C=O stretching), 1535 cm^{-1} (amide II band, bending vibration frequency of N-H), 1371 cm^{-1} (amide III band, CH_2 wagging), and 681 cm^{-1} (bending vibration frequency of N-H). (b) Peaks can be observed at 1748 cm^{-1} (acid ester C=O group), 1375 and 1347 cm^{-1} (CH_2 wagging of glycol, sample D specifically), 1226 and 1089 cm^{-1} (broad bands, asymmetric C-C-O and O-C-C stretching, respectively), 1025 cm^{-1} (in-plane vibration of benzene), and 730 cm^{-1} (C-H wagging vibrations from the aromatic structure, out of plane of benzene group). (c, e, g) C1s, O1s, and N1s XPS spectra of teabags A and B and their corresponding leachates. The peaks observed confirm that the composition of these teabags is nylon. (d, f) C1s and O1s XPS spectra of teabags C and D and their corresponding leachates. The observed peaks confirm that the composition of these teabags is PET.

4.3.3 Adverse biological effects of dialyzed leachates of the plastic teabags

In an effort to isolate the biological impact of the micro- and nanoplastic particles, the concentrated leachates of teabags B and D (as representative nylon and PET teabags, respectively), were dialyzed for 7 days to remove any dissolved species released from the tea or plastic (e.g., metal(loids)). The biological effects of the released micro- and nanoplastics in the aquatic model species, *D. magna*, were assessed using a series of dilutions of the dialyzed leachate (50%, 5%, and 0.5%). No immobility was observed with teabag B or D leachates that had been dialyzed or controls. Nonetheless, a number of micro-sized foreign particles were observed inside the bodies of 5% and 50% leachate-exposed *D. magna* but not in controls, and the shape and size of the particles were similar as observed in the raw leachates (Fig. 4.3a). Some of the *D. magna* also

exhibited anatomical abnormalities that were observed on the third day of development (Fig. 4.3b). The most notable malformation was the failure of the carapace to develop properly into the lateral shields that were present in the controls. For example, in the dialyzed 50% teabag B and D leachates, the carapace shields were fused dorsally and inflated with fluid, producing a large ballooned sack that was suspended over the rest of the animal (Fig. 4.3b).

Sublethal behavioral effects of dialyzed teabag leachate were observed in *D. magna*. Representative images in Fig. 4.3c show a dose-dependent increase of track density for *D. magna* exposed to teabag D leachate. Significantly longer swimming distances were observed at 5% and 50% concentrations of the dialyzed leachates (Fig. 4.3d,e). In addition, the track density was significantly increased in both 5% and 50% teabag B and D leachates (Fig. S4.5c,d).

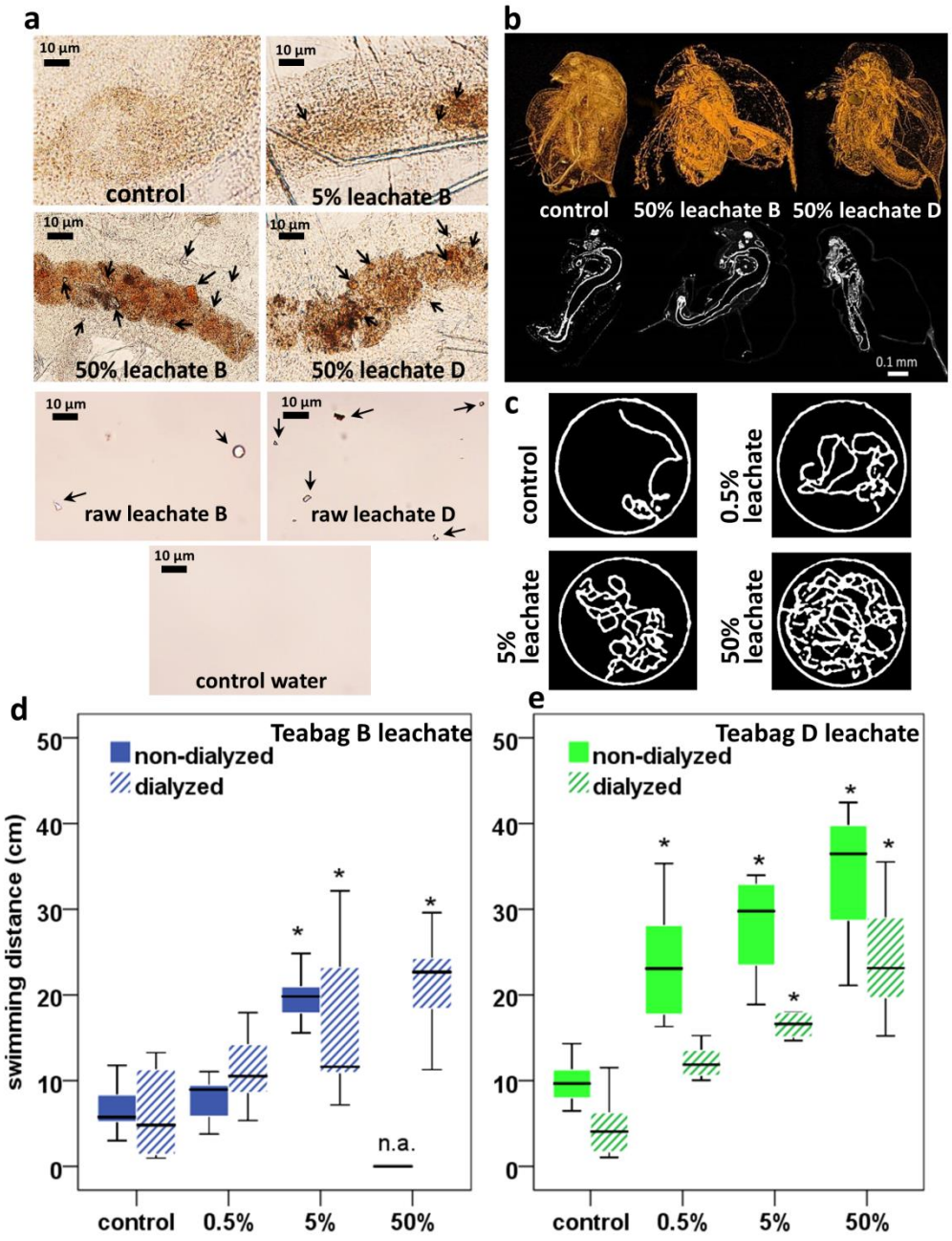

Figure 4.3. Teabag leachates affect the morphology and swimming behavior of *Daphnia magna*. (a) Microparticles identified in *D. magna* exposed to dialyzed teabag B and D leachates, as well as in raw leachates are marked with arrows. Optical images of *D. magna* were taken using an Olympus DP80 microscope digital camera at 60× magnification focusing on the intestine. (b) CT images of *D. magna* exposed to dialyzed teabag B and D leachates. Top images show the 3-D

morphology and bottom images show 2-D internal sections. (c) Representative swimming tracks of *D. magna* exposed to dialyzed teabag D leachate. (d, e) The swimming distance of *D. magna* after exposure to teabag B and teabag D leachates. Asterisk indicates that the measurement is statistically significantly different (p-value<0.05, one-way analysis of variance (ANOVA) followed by the *post-hoc* Tukey's multiple comparison test) from the control; n=9 for dialyzed teabag B, dialyzed leachate D, and non-dialyzed leachate B, and n=6-9 for non-dialyzed teabag D leachate.

4.3.4 Identification of metal(loid)s in the teabag leachate

It is well known that tea can contain several metal(loid)s such as arsenic (As),[34] aluminum (Al),[35] lead (Pb)[35,36] and chromium (Cr).[35] Also, micro- and nanoplastics can sorb a wide variety of contaminants, including heavy metals such as Co, Cr, Cu, Ni, Pb and Zn.[37,38] ICP-MS was used to quantify the levels of selected metal(loid)s (Al, As, Cr, and Pb) in the concentrated (100%) leachates before and after dialysis (Fig. S4.6). The non-dialyzed concentrated leachates generally have higher levels of metal(loid)s than the corresponding dialyzed leachates, with the exception of Cr in teabag D (Fig. S4.6). The residual amount of metal(loids) in the dialyzed leachate may be due to sorption to the plastic particles. Finally, the total amount of metal(loid)s in full teabags (containing tea leaves) is compared to empty teabags (Fig. S4.7). The results suggest that most or all of these metal(loid)s originated from the tea leaves and not the plastic teabags, with the exception of Cr in teabag D.

4.3.5 Biological effects of non-dialyzed leachates

In an effort to begin to evaluate the contribution of the dissolved metal(loids) to the toxicity of teabag leachate, additional experiments were conducted using dilutions of non-dialyzed leachates

(50%, 5%, and 0.5%) of teabags B and D. In contrast to the observations with the dialyzed leachates, during the first 24 hours of *D. magna* exposure, the 50% non-dialyzed teabag B leachate caused significantly higher immobility than the control (Fig. S4.8a). After 48 hours, higher immobility was observed in both non-dialyzed teabag B and D leachates with statistical significance at 50% teabag B leachate and 5% teabag D leachate (Fig. S4.8a,b). The non-dialyzed leachate had a more significant impact on the morphology of *D. magna* than dialyzed leachate, with the tissues and organs in individuals exposed to 50% leachate being poorly defined, especially in the head and intestine (Fig. S4.9). A similar "ballooned" carapace developed, but in leachate concentrations as low as 5%. As noted with the dialyzed leachate, exposure of *D. magna* to the non-dialyzed leachate leaded to uptake of particles (Fig. S4.10) and affected swimming behavior (Figs. 4.3d,e and S4.5), but the body size was not affected (Fig. S4.8c,d).

4.4 Discussion

The mechanism by which nylon and PET degrade to form nanoparticles is yet to be studied. The polymer science literature suggests that these polymers degrade at temperatures higher than 95 °C, at which the polymer undergoes disturbances in the molecular structure.[39] Others have studied the thermal degradation of these polymers under environmental conditions.[40–42] However, none of these studies have considered the possibility of polymers breaking down into nanoparticles. Some studies have shown that polystyrene breaks down to nanoparticles, but no mechanism was suggested[43].

Polymer hydrolysis might be a mechanism by which the degradation is occurring. Hydrolytic degradation is the scission of chemical functional groups by reaction with water.[44] Chain scission is a reduction in the molecular weight of the macromolecules of a polymer, causing the polymer to become more fragile.[45] Nylon is susceptible to hydrolysis, therefore contact with water at high

temperature will produce degradation and fractures.[46] PET is more resistant to hydrolysis; however, studies have shown that in the absence of oxygen and at high temperatures, hydrolytic aging may occur.[47]

Interestingly, the micro and nanoparticles released from teabags A and B have similar shape and size distribution. The microparticles are large (~50-100 μm) irregular pieces, whereas the sub-micron particles are small (~10-400 nm) spheres. Micro and nanoparticles released from teabags C and D are also similar. The microparticles are small (~1-50 μm) and irregular, whereas the sub-micron particles are larger (50-600 nm) and agglomerated. Such high similarities in the shape and size distribution of particles suggest similar materials were used in the manufacture of teabags A and B or teabags C and D. Although the two plastics used in the manufacture of the teabags we tested are considered food grade materials,[48,49] their degradation into micro- and nano-sized particles presents an unknown risk. Several studies detected the presence of microplastics in the food chain at relatively low concentrations.[17,18,50] However, in this study, we report that the level of plastic potentially ingested when drinking tea packaged in plastic teabags is several orders of magnitude higher than levels previously reported in foods. The plastic load per cup of tea prepared with one plastic teabag, is estimated at 16 μg, which is in contrast to the highest level reported in table salt (0.005 μg/g of salt).[14,15] Interestingly, far fewer particles are released when the teabag is steeped at room temperature, showing the impact of packaging utilization conditions on exposure risks. The World Health Organization launched a health review in March 2018 into the potential risks of plastic in drinking water after a study reported that bottled water contained microplastics on the order of only a few tens to a few hundred particles per liter.[21] In contrast, we report here that 2.3 million micron-sized particles (~1–150 μm) and 14.7 billion sub-micron plastic particles (< 1 μm), which is estimated at 16 μg, can be release into 1 cup of tea. The annual load of plastic

particles can be initially predicted as: L × N × P × 365, where L is plastic load per cup of tea (16 µg); N is the number of cups of tea/per day that is suggested to be safe in healthy adults (2-5[51]); P is the population of the tea drinkers in America (159 million[52]). Based on this rough estimation, 1.9 to 4.6 tonnes of micron and sub-micron plastic particles would be generated annually during tea steeping process if only plastic teabags were used. The released plastic particles may not only be ingested/excreted by human,[53] but also enter waterways through domestic drainage systems and via sewage treatment plants, contributing to microplastic pollution in the environment. The discarded single-use plastic teabags themselves further contribute to plastic waste.

D. magna is a common model species in both environmental and pharmaceutical toxicology with the advantage that it has high sensitivity to a wide range of toxic chemicals and its transparency facilitates the imaging of uptaken particles. *D. magna* also contains similar toxin targets (e.g. eyes and heart) or molecular pathways as humans.[54] Moreover, the ease of culture and handling, short life cycle, and low cost of maintenance make *D. magna* a simple, fast, and suitable model for this study.[54–59] We observed no immobility in *D. magna* exposed to the plastic particles (i.e., dialyzed leachate) released from the teabags. In contrast, we noted significant acute toxicity of the non-dialyzed teabag leachate to *D. magna*, likely due to the presence of metal(loid)s (Al, As, Cr, and Pb). However, in both exposure scenarios, *D. magna* swimming behavior was significantly affected in a similar dose-dependent manner (Fig. 4.3d,e), suggesting that the altered behavior can be attributed to the micro- and nanoplastics. The increased swimming distance and track density can lead to an increase in energy expenditure and predation risk which can negatively impact the *D. magna* population.[60–62] Similar results were also noted in previous studies in *D. magna* and fish, showing the disrupted locomotor activity post-exposure to micro- and nanoparticles.[60,63,64] Although the answers to how the micro- and nanoplastics disrupt the swimming behaviors of *D.*

magna remain elusive, some potential mechanisms may be implicated. We hypothesize that the deformed carapace of individuals of 50% dialyzed and 5% and greater non-dialyzed leachate likely alters normal swimming behavior. This malformation might also lead to reproductive failure as eggs and early hatchlings are normally housed in a brooding pouch between the carapace and body. In addition, increases in locomotor activity may correspond to *D. magna* attempting to clean the particles off their appendages (see example of particles on appendages in Fig. S4.10).

Although the *Daphnia* assay cannot be directly related to human ingestion, it has been used as first screening method for assessing the toxic potency of a wide range of chemicals to humans (e.g., pharmaceuticals, heavy metals, pesticides).[65,66] A high correlation between the acute toxicity of chemicals to *Daphnia* and the corresponding toxicity values for mouse and human has been confirmed.[67,68] Furthermore, it has been shown that the predictive screening potential of aquatic invertebrate tests for acute oral toxicity in humans is better than the rat LD50 (median lethal dose) test for some chemicals.[69] Guilhermino et al. also concluded that the *Daphnia* test is more sensitive as an indicator of toxicity to rat.[70] Moreover, the oral reference dose (RfD), a preferred approach by USEPA for characterizing the non-cancer health risks,[71] is significantly correlated with toxicity values for *Daphnia*, suggesting that acute toxicity assays with *Daphnia* can give important and relevant information concerning the possible human oral chronic intoxication.[68]

To date, the health effects of consuming micro- and nanoplastics to humans are still unknown, while the sublethal effects observed in the present study and in other animals (e.g., algae, zooplankton, fish, mice)[64,72–75] give an early warning of both environmental risk and possible human health risk. One of the main potential human exposure pathways of micro- and nanoplastics is likely via ingestion, and particle uptake may occur in the digestive tract.[1] Once inside the digestive tract, cellular uptake and subcellular translocation or localization of the ingested particles

may occur. Translocation of various types of microparticles (particle size 0.03 to 100 μm) across the mammalian gut has been demonstrated in multiple studies involving rodents, rabbits, and dogs.[76] Potential biological responses include genotoxicity, apoptosis, and necrosis, which could lead to tissue damage, fibrosis and carcinogenesis.[1] The only *in vitro* human evidence showed generation of reactive oxygen species in cerebral and epithelial human cell lines after exposure to micro- and nanoplastic particles[77].

The scarce body of data on nanoplastics, both on human exposure and potential toxicity, cannot predict the health risk of consuming nanoplastics. However, experience from nanotoxicological studies on engineered nanoparticles might be extrapolated to advance our current understanding on the uptake kinetics, potential toxicity, and mechanisms of nanoplastic particles.[13] Among different engineered nanoparticles, TiO_2 is one of the most widely studied. Based on the available toxicity data from oral exposures[78–80], nano-TiO_2 seems to have low toxicity following oral exposure. For example, mice exposed to nano-TiO_2 (25 and 80 nm) at a very high dose (5 g/kg) for 2 weeks showed particle translocation from guts to spleen, lungs, kidneys, and injured liver.[81] Lower doses (1-2 mg/kg *in vivo* and < 36 μg/ml *in vitro*) of nano-TiO_2 showed neither cellular toxicity nor oxidative stress in rats, even though they penetrated intestinal cells.[82] Comparing the doses used in these studies with the plastic particles we found here (16 μg/cup of tea), the ingested micro- and nanoplastics are not likely to present acute toxicity risks for human health. However, more subtle or chronic effects are not impossible after long-term exposure. Overall, the knowledge on adverse effects of plastic particles on human is still lacking and there is an urgent need to investigate potential toxic mechanisms in higher vertebrates and human, which is of vital importance when assessing the human health risk of micro- and nanoplastics.[1,77]

4.5 Acknowledgments

The authors thank R. Roy and A. Azimzada for their help in sample digestion and ICP-MS, N. Lin for his help in preparing figures and sample preparation for SEM, and J. Farner and A. Metafiot for helpful discussions. The authors acknowledge the financial support of the Canada Research Chairs program, the Natural Sciences and Engineering Research Council of Canada, and McGill University for a MEDA award to LMH. This research was performed using infrastructure of the Integrated Quantitative Biology Initiative, funded by the Quebec government, McGill University, and Canadian Foundation of Innovation project 33122

4.6 References

(1) Wright, S. L.; Kelly, F. J. Plastic and Human Health: A Micro Issue? *Environ. Sci. Technol.* **2017**, *51* (12), 6634–6647. https://doi.org/10.1021/acs.est.7b00423.

(2) Hernandez, L. M.; Yousefi, N.; Tufenkji, N. Are There Nanoplastics in Your Personal Care Products? *Environ. Sci. Technol. Lett.* **2017**, *4* (7), 280–285. https://doi.org/10.1021/acs.estlett.7b00187.

(3) Eriksen, M.; Lebreton, L. C. M.; Carson, H. S.; Thiel, M.; Moore, C. J.; Borerro, J. C.; Galgani, F.; Ryan, P. G.; Reisser, J. Plastic Pollution in the World's Oceans: More than 5 Trillion Plastic Pieces Weighing over 250,000 Tons Afloat at Sea. *PLoS ONE* **2014**, *9* (12), e111913. https://doi.org/10.1371/journal.pone.0111913.

(4) Nguyen, B.; Claveau-Mallet, D.; Hernandez, L. M.; Xu, E. G.; Farner, J. M.; Tufenkji, N. Separation and Analysis of Microplastics and Nanoplastics in Complex Environmental Samples. *Acc. Chem. Res.* **2019**, *52* (4), 858–866. https://doi.org/10.1021/acs.accounts.8b00602.

(5) Browne, M. A.; Galloway, T.; Thompson, R. Microplastic-an Emerging Contaminant of Potential Concern? *Integr. Environ. Assess. Manag.* **2007**, *3* (4), 559–561. https://doi.org/10.1002/ieam.5630030412.

(6) Hartmann, N. B.; Hüffer, T.; Thompson, R. C.; Hassellöv, M.; Verschoor, A.; Daugaard, A. E.; Rist, S.; Karlsson, T.; Brennholt, N.; Cole, M.; Herrling, M.P.; Hess, M.C.; Ivleva, N.P.; Lusher, A.L.; Wagner, M. Are We Speaking the Same Language? Recommendations for a Definition and Categorization Framework for Plastic Debris. *Environ. Sci. Technol.* **2019**, *53* (3), 1039–1047. https://doi.org/10.1021/acs.est.8b05297.

(7) Wagner, M.; Scherer, C.; Alvarez-Muñoz, D.; Brennholt, N.; Bourrain, X.; Buchinger, S.; Fries, E.; Grosbois, C.; Klasmeier, J.; Marti, T.; Rodriguez-Mozaz, S.; Urbatzka, R.; Vethaak, A.D.; Winther-Nielsen, M.; Reifferscheid, G. Microplastics in Freshwater Ecosystems: What We Know and What We Need to Know. *Environ. Sci. Eur.* **2014**, *26* (1). https://doi.org/10.1186/s12302-014-0012-7.

(8) Andrady, A. L. *Plastics and Environmental Sustainability: Andrady/Plastics and Environmental Sustainability*; John Wiley & Sons, Inc: Hoboken, NJ, 2015. https://doi.org/10.1002/9781119009405.

(9) Koelmans, A. A.; Kooi, M.; Law, K. L.; van Sebille, E. All Is Not Lost: Deriving a Top-down Mass Budget of Plastic at Sea. *Environ. Res. Lett.* **2017**, *12* (11), 114028. https://doi.org/10.1088/1748-9326/aa9500.

(10) European Commission. *Commission Recommendation of 18 October 2011 on the Definition of Nanomaterial*; Official Journal of the European Union; 2011/696/EU; European Commission, 2011; p L 275/38.

(11) Auffan, M.; Rose, J.; Bottero, J.-Y.; Lowry, G. V.; Jolivet, J.-P.; Wiesner, M. R. Towards a Definition of Inorganic Nanoparticles from an Environmental, Health and Safety Perspective. *Nat. Nanotechnol.* **2009**, *4* (10), 634–641. https://doi.org/10.1038/nnano.2009.242.

(12) OECD. *Nanosafety at the OECD: The First Five Years 2006-2010*; Better Policies for Better Lives; France, 2011.

(13) Bouwmeester, H.; Hollman, P. C. H.; Peters, R. J. B. Potential Health Impact of Environmentally Released Micro- and Nanoplastics in the Human Food Production Chain: Experiences from Nanotoxicology. *Environ. Sci. Technol.* **2015**, *49* (15), 8932–8947. https://doi.org/10.1021/acs.est.5b01090.

(14) Karami, A.; Golieskardi, A.; Keong Choo, C.; Larat, V.; Galloway, T. S.; Salamatinia, B. The Presence of Microplastics in Commercial Salts from Different Countries. *Sci. Rep.* **2017**, *7*, 46173. https://doi.org/10.1038/srep46173.

(15) Yang, D.; Shi, H.; Li, L.; Li, J.; Jabeen, K.; Kolandhasamy, P. Microplastic Pollution in Table Salts from China. *Environ. Sci. Technol.* **2015**, *49* (22), 13622–13627. https://doi.org/10.1021/acs.est.5b03163.

(16) Boerger, C. M.; Lattin, G. L.; Moore, S. L.; Moore, C. J. Plastic Ingestion by Planktivorous Fishes in the North Pacific Central Gyre. *Mar. Pollut. Bull.* **2010**, *60* (12), 2275–2278. https://doi.org/10.1016/j.marpolbul.2010.08.007.

(17) Neves, D.; Sobral, P.; Ferreira, J. L.; Pereira, T. Ingestion of Microplastics by Commercial Fish off the Portuguese Coast. *Mar. Pollut. Bull.* **2015**, *101* (1), 119–126. https://doi.org/10.1016/j.marpolbul.2015.11.008.

(18) Lusher, A. L.; McHugh, M.; Thompson, R. C. Occurrence of Microplastics in the Gastrointestinal Tract of Pelagic and Demersal Fish from the English Channel. *Mar. Pollut. Bull.* **2013**, *67* (1–2), 94–99. https://doi.org/10.1016/j.marpolbul.2012.11.028.

(19) Sanchez, W.; Bender, C.; Porcher, J.-M. Wild Gudgeons (*Gobio Gobio*) from French Rivers Are Contaminated by Microplastics: Preliminary Study and First Evidence. *Environ. Res.* **2014**, *128*, 98–100. https://doi.org/10.1016/j.envres.2013.11.004.

(20) Pivokonsky, M.; Cermakova, L.; Novotna, K.; Peer, P.; Cajthaml, T.; Janda, V. Occurrence of Microplastics in Raw and Treated Drinking Water. *Sci. Total Environ.* **2018**, *643*, 1644–1651. https://doi.org/10.1016/j.scitotenv.2018.08.102.

(21) Mason, S. A.; Welch, V. G.; Neratko, J. Synthetic Polymer Contamination in Bottled Water. *Front. Chem.* **2018**, *6*. https://doi.org/10.3389/fchem.2018.00407.

(22) Koelmans, A. A.; Mohamed Nor, N. H.; Hermsen, E.; Kooi, M.; Mintenig, S. M.; De France, J. Microplastics in Freshwaters and Drinking Water: Critical Review and Assessment of Data Quality. *Water Res.* **2019**, *155*, 410–422. https://doi.org/10.1016/j.watres.2019.02.054.

(23) Cox, K. D.; Covernton, G. A.; Davies, H. L.; Dower, J. F.; Juanes, F.; Dudas, S. E. Human Consumption of Microplastics. *Environ. Sci. Technol.* **2019**, *53* (12), 7068–7074. https://doi.org/10.1021/acs.est.9b01517.

(24) Rochman, C. M.; Kross, S. M.; Armstrong, J. B.; Bogan, M. T.; Darling, E. S.; Green, S. J.; Smyth, A. R.; Veríssimo, D. Scientific Evidence Supports a Ban on Microbeads. *Environ. Sci. Technol.* **2015**, *49* (18), 10759–10761. https://doi.org/10.1021/acs.est.5b03909.

(25) United States of America 114th congress (2015-2016). *Microbead-Free Waters Act of 2015*; 2015.

(26) Trevor Nace. UK To Ban All Plastic Straws, Cotton Swabs, And Single-Use Plastics. *Forbes*. April 2018.

(27) Bach, C.; Dauchy, X.; Severin, I.; Munoz, J.-F.; Etienne, S.; Chagnon, M.-C. Effect of Temperature on the Release of Intentionally and Non-Intentionally Added Substances from Polyethylene Terephthalate (PET) Bottles into Water: Chemical Analysis and Potential Toxicity. *Food Chem.* **2013**, *139* (1–4), 672–680. https://doi.org/10.1016/j.foodchem.2013.01.046.

(28) Oecd. *Test No. 202: Daphnia Sp. Acute Immobilisation Test*; 2004; Vol. 1.

(29) Bownik, A.; Sokołowska, N.; Ślaska, B. Effects of Apomorphine, a Dopamine Agonist, on *Daphnia Magna* : Imaging of Swimming Track Density as a Novel Tool in the Assessment of Swimming Activity. *Sci. Total Environ.* **2018**, *635*, 249–258. https://doi.org/10.1016/j.scitotenv.2018.04.157.

(30) Nasr-Esfahani, M.; Mehrabanian, M. HA/Nylon 6,6 Porous Scaffolds Fabricated by Salt-Leaching/Solvent Casting Technique: Effect of Nano-Sized Filler Content on Scaffold Properties. *Int. J. Nanomedicine* **2011**, 1651. https://doi.org/10.2147/IJN.S21203.

(31) Andanson, J.-M.; Kazarian, S. G. In Situ ATR-FTIR Spectroscopy of Poly(Ethylene Terephthalate) Subjected to High-Temperature Methanol. *Macromol. Symp.* **2008**, *265* (1), 195–204. https://doi.org/10.1002/masy.200850521.

(32) Louette, P.; Bodino, F.; Pireaux, J.-J. Nylon 6 (N6) Reference XPS Reference Core Level and Energy Loss Spectra. *Surf. Sci. Spectra* **2005**, *12* (1), 12–17. https://doi.org/10.1116/11.20050903.

(33) Doren, A.; Genet, M. J.; Rouxhet, P. G. Analysis of Poly(Ethylene Terephthalate) (PET) by XPS. *Surf. Sci. Spectra* **1994**, *3* (4), 337–341. https://doi.org/10.1116/1.1247762.

(34) Han, W.-Y.; Shi, Y.-Z.; Ma, L.-F.; Ruan, J.-Y. Arsenic, Cadmium, Chromium, Cobalt, and Copper in Different Types of Chinese Tea. *Bull. Environ. Contam. Toxicol.* **2005**, *75* (2), 272–277. https://doi.org/10.1007/s00128-005-0748-2.

(35) Schunk, P. F. T.; Kalil, I. C.; Pimentel-Schmitt, E. F.; Lenz, D.; de Andrade, T. U.; Ribeiro, J. S.; Endringer, D. C. ICP-OES and Micronucleus Test to Evaluate Heavy Metal Contamination in Commercially Available Brazilian Herbal Teas. *Biol. Trace Elem. Res.* **2016**, *172* (1), 258–265. https://doi.org/10.1007/s12011-015-0566-2.

(36) Han, W.-Y.; Zhao, F.-J.; Shi, Y.-Z.; Ma, L.-F.; Ruan, J.-Y. Scale and Causes of Lead Contamination in Chinese Tea. *Environ. Pollut.* **2006**, *139* (1), 125–132. https://doi.org/10.1016/j.envpol.2005.04.025.

(37) Brennecke, D.; Duarte, B.; Paiva, F.; Caçador, I.; Canning-Clode, J. Microplastics as Vector for Heavy Metal Contamination from the Marine Environment. *Estuar. Coast. Shelf Sci.* **2016**, *178*, 189–195. https://doi.org/10.1016/j.ecss.2015.12.003.

(38) Holmes, L. A.; Turner, A.; Thompson, R. C. Adsorption of Trace Metals to Plastic Resin Pellets in the Marine Environment. *Environ. Pollut.* **2012**, *160*, 42–48. https://doi.org/10.1016/j.envpol.2011.08.052.

(39) J Holland, B.; Hay, J. Thermal Degradation of Nylon Polymers. *Polym. Int.* **2000**, *49*, 943–948. https://doi.org/10.1002/1097-0126(200009)49:9<943::AID-PI400>3.0.CO;2-5.

(40) Biber, N. F. A.; Foggo, A.; Thompson, R. C. Characterising the Deterioration of Different Plastics in Air and Seawater. *Mar. Pollut. Bull.* **2019**, *141*, 595–602. https://doi.org/10.1016/j.marpolbul.2019.02.068.

(41) Pegram, J. E.; Andrady, A. L. Outdoor Weathering of Selected Polymeric Materials under Marine Exposure Conditions. *Polym. Degrad. Stab.* **1989**, *26* (4), 333–345. https://doi.org/10.1016/0141-3910(89)90112-2.

(42) Brandon, J.; Goldstein, M.; Ohman, M. D. Long-Term Aging and Degradation of Microplastic Particles: Comparing in Situ Oceanic and Experimental Weathering Patterns. *Mar. Pollut. Bull.* **2016**, *110* (1), 299–308. https://doi.org/10.1016/j.marpolbul.2016.06.048.

(43) Lambert, S.; Wagner, M. Characterisation of Nanoplastics during the Degradation of Polystyrene. *Chemosphere* **2016**, *145*, 265–268. https://doi.org/10.1016/j.chemosphere.2015.11.078.

(44) Göpferich, A. Mechanisms of Polymer Degradation and Erosion. In *The Biomaterials: Silver Jubilee Compendium*; Elsevier, 1996; pp 117–128. https://doi.org/10.1016/B978-008045154-1.50016-2.

(45) Chapiro, A. Radiation Effects in Polymers. In *Encyclopedia of Materials: Science and Technology*; Elsevier, 2004; pp 1–8. https://doi.org/10.1016/B0-08-043152-6/01918-5.

(46) Tegge, G. Handbook of Adhesives. *Starch - Stärke* **1964**, *16* (1), 38–38. https://doi.org/10.1002/star.19640160117.

(47) Venkatachalam, S.; Shilpa, G.; Jayprakash, V.; Prashant, R.; Krishna, R.; Anil, K. Degradation and Recyclability of Poly (Ethylene Terephthalate). In *Polyester*; Saleh, H. E.-D., Ed.; InTech, 2012. https://doi.org/10.5772/48612.

(48) Bach, C.; Dauchy, X.; Chagnon, M.-C.; Etienne, S. Chemical Compounds and Toxicological Assessments of Drinking Water Stored in Polyethylene Terephthalate (PET) Bottles: A Source of Controversy Reviewed. *Water Res.* **2012**, *46* (3), 571–583. https://doi.org/10.1016/j.watres.2011.11.062.

(49) Muncke, J. Exposure to Endocrine Disrupting Compounds via the Food Chain: Is Packaging a Relevant Source? *Sci. Total Environ.* **2009**, *407* (16), 4549–4559. https://doi.org/10.1016/j.scitotenv.2009.05.006.

(50) Browne, M. A.; Dissanayake, A.; Galloway, T. S.; Lowe, D. M.; Thompson, R. C. Ingested Microscopic Plastic Translocates to the Circulatory System of the Mussel, *Mytilus Edulis* (L). *Environ. Sci. Technol.* **2008**, *42* (13), 5026–5031.

(51) EFSA. EFSA Panel on Dietetic Products, Nutrition & Allergies. *EFSA J.* **2015**, *13* (5).

(52) *Tea Fact Sheet – 2018-2019*; Fact sheet; Tea Association of the USA, 2019.

(53) Liebmann B.; Köppel S.; Königshofer P.; Bucsics T.; Reiberger T.; Schwabl P. Assessment of microplastic concentrations in human stool - final results of a prospective study. **2018**. https://doi.org/10.13140/rg.2.2.16638.02884.

(54) Hartung, T.; Daston, G. Are In Vitro Tests Suitable for Regulatory Use? *Toxicol. Sci.* **2009**, *111* (2), 233–237. https://doi.org/10.1093/toxsci/kfp149.

(55) Colmorgen, M.; Paul, R. J. Imaging of Physiological Functions in Transparent Animals (*Agonus Cataphractus*, *Daphnia Magna*, *Pholcus Phalangioides*) by Video Microscopy and Digital Image Processing. *Comp. Biochem. Physiol. A Physiol.* **1995**, *111* (4), 583–595. https://doi.org/10.1016/0300-9629(95)00059-G.

(56) Corotto, F.; Ceballos, D.; Lee, A.; Vinson, L. Making the Most of the *Daphnia* Heart Rate Lab: Optimizing the Use of Ethanol, Nicotine & Caffeine. *Am. Biol. Teach.* **2010**, *72* (3), 176–179. https://doi.org/10.1525/abt.2010.72.3.9.

(57) Galdiero, E.; Falanga, A.; Siciliano, A.; Maselli, V.; Guida, M.; Carotenuto, R.; Tussellino, M.; Lombardi, L.; Benvenuto, G.; Galdiero, S. *Daphnia Magna* and *Xenopus Laevis* as in Vivo Models to Probe Toxicity and Uptake of Quantum Dots Functionalized with GH625. *Int. J. Nanomedicine* **2017**, *Volume 12*, 2717–2731. https://doi.org/10.2147/IJN.S127226.

(58) Veselá, Š.; Ondruška, V.; Kuča, K.; Patočka, J. Freshwater Microcrustacean *Daphnia Magna Straus* as an Early Screen Model to Compare Toxicity of Acetylcholinesterase Inhibitors. *J. Appl. Biomed.* **2006**, *4* (2), 105–110. https://doi.org/10.32725/jab.2006.010.

(59) Villegas-Navarro, A.; Rosas-L, E.; Reyes, J. L. The Heart of *Daphnia Magna*: Effects of Four Cardioactive Drugs. *Comp. Biochem. Physiol. Toxicol. Pharmacol. CBP* **2003**, *136* (2), 127–134.

(60) Lovern, S. B.; Strickler, J. R.; Klaper, R. Behavioral and Physiological Changes in *Daphnia Magna* When Exposed to Nanoparticle Suspensions (Titanium Dioxide, Nano-C_{60}, and $C_{60}H_xC_{70}H_x$). *Environ. Sci. Technol.* **2007**, *41* (12), 4465–4470.

(61) C.O'Keefe, T.; C.Brewer, M.; Dodson, S. I. Swimming Behavior of *Daphnia* : Its Role in Determining Predation Risk. *J. Plankton Res.* **1998**, *20* (5), 973–984. https://doi.org/10.1093/plankt/20.5.973.

(62) Lovern, S. B.; Klaper, R. *Daphnia Magna* Mortality When Exposed to Titanium Dioxide and Fullerene (C_{60}) Nanoparticles. *Environ. Toxicol. Chem.* **2006**, *25* (4), 1132–1137.

(63) Chen, Q.; Gundlach, M.; Yang, S.; Jiang, J.; Velki, M.; Yin, D.; Hollert, H. Quantitative Investigation of the Mechanisms of Microplastics and Nanoplastics toward Zebrafish Larvae Locomotor Activity. *Sci. Total Environ.* **2017**, *584–585*, 1022–1031. https://doi.org/10.1016/j.scitotenv.2017.01.156.

(64) Pikuda, O.; Xu, E. G.; Berk, D.; Tufenkji, N. Toxicity Assessments of Micro- and Nanoplastics Can Be Confounded by Preservatives in Commercial Formulations. *Environ. Sci. Technol. Lett.* **2018**. https://doi.org/10.1021/acs.estlett.8b00614.

(65) Flaherty, C. M.; Dodson, S. I. Effects of Pharmaceuticals on *Daphnia* Survival, Growth, and Reproduction. *Chemosphere* **2005**, *61* (2), 200–207. https://doi.org/10.1016/j.chemosphere.2005.02.016.

(66) Chevalier, J.; Harscoët, E.; Keller, M.; Pandard, P.; Cachot, J.; Grote, M. Exploration of *Daphnia* Behavioral Effect Profiles Induced by a Broad Range of Toxicants with Different Modes of Action: Effects of Different Toxicants on *Daphnia* Behavior. *Environ. Toxicol. Chem.* **2015**, *34* (8), 1760–1769. https://doi.org/10.1002/etc.2979.

(67) Khangarot, B. S.; Ray, P. K.; Chandr, H. *Daphnia magna* as a Model to Assess Heavy Metal Toxicity: Comparative Assessment with Mouse System. *Acta Hydrochim. Hydrobiol.* **1987**, *15* (4), 427–432. https://doi.org/10.1002/aheh.19870150415.

(68) Martins, J.; Oliva Teles, L.; Vasconcelos, V. Assays with *Daphnia Magna* and *Danio Rerio* as Alert Systems in Aquatic Toxicology. *Environ. Int.* **2007**, *33* (3), 414–425. https://doi.org/10.1016/j.envint.2006.12.006.

(69) Calleja, M. C.; Persoone, G. Cyst-Based Toxicity Tests. IV. The Potential of Ecotoxicological Tests for the Prediction of Acute Toxicity in Man as Evaluated on the First Ten Chemicals of the MEIC Programme. *ATLA* **1992**, *20*, 396–405.

(70) Guilhermino, L.; Diamantino, T.; Carolina Silva, M.; Soares, A. M. V. M. Acute Toxicity Test with *Daphnia Magna*: An Alternative to Mammals in the Prescreening of Chemical Toxicity? *Ecotoxicol. Environ. Saf.* **2000**, *46* (3), 357–362. https://doi.org/10.1006/eesa.2000.1916.

(71) Gibson, M. C.; deMonsabert, S. M.; Orme-Zavaleta, J. Comparison of Noncancer Risk Assessment Approaches for Use in Deriving Drinking Water Criteria. *Regul. Toxicol. Pharmacol.* **1997**, *26* (3), 243–256. https://doi.org/10.1006/rtph.1997.1150.

(72) Deng, Y.; Zhang, Y.; Lemos, B.; Ren, H. Tissue Accumulation of Microplastics in Mice and Biomarker Responses Suggest Widespread Health Risks of Exposure. *Sci. Rep.* **2017**, *7* (1). https://doi.org/10.1038/srep46687.

(73) Besseling, E.; Wang, B.; Lürling, M.; Koelmans, A. A. Nanoplastic Affects Growth of *S. Obliquus* and Reproduction of *D. Magna*. *Environ. Sci. Technol.* **2014**, *48* (20), 12336–12343. https://doi.org/10.1021/es503001d.

(74) Pitt, J. A.; Kozal, J. S.; Jayasundara, N.; Massarsky, A.; Trevisan, R.; Geitner, N.; Wiesner, M.; Levin, E. D.; Di Giulio, R. T. Uptake, Tissue Distribution, and Toxicity of Polystyrene Nanoparticles in Developing Zebrafish (*Danio Rerio*). *Aquat. Toxicol.* **2018**, *194*, 185–194. https://doi.org/10.1016/j.aquatox.2017.11.017.

(75) Mattsson, K.; Johnson, E. V.; Malmendal, A.; Linse, S.; Hansson, L.-A.; Cedervall, T. Brain Damage and Behavioural Disorders in Fish Induced by Plastic Nanoparticles Delivered through the Food Chain. *Sci. Rep.* **2017**, *7* (1). https://doi.org/10.1038/s41598-017-10813-0.

(76) Hussain, N. Recent Advances in the Understanding of Uptake of Microparticulates across the Gastrointestinal Lymphatics. *Adv. Drug Deliv. Rev.* **2001**, *50* (1–2), 107–142. https://doi.org/10.1016/S0169-409X(01)00152-1.

(77) Schirinzi, G. F.; Pérez-Pomeda, I.; Sanchís, J.; Rossini, C.; Farré, M.; Barceló, D. Cytotoxic Effects of Commonly Used Nanomaterials and Microplastics on Cerebral and Epithelial Human Cells. *Environ. Res.* **2017**, *159*, 579–587. https://doi.org/10.1016/j.envres.2017.08.043.

(78) Johnston, H. J.; Hutchison, G. R.; Christensen, F. M.; Peters, S.; Hankin, S.; Stone, V. Identification of the Mechanisms That Drive the Toxicity of TiO2 Particulates: The Contribution of Physicochemical Characteristics. *Part. Fibre Toxicol.* **2009**, *6* (1), 33. https://doi.org/10.1186/1743-8977-6-33.

(79) Christensen, F. M.; Johnston, H. J.; Stone, V.; Aitken, R. J.; Hankin, S.; Peters, S.; Aschberger, K. Nano-TiO_2 – Feasibility and Challenges for Human Health Risk Assessment Based on Open Literature. *Nanotoxicology* **2011**, *5* (2), 110–124. https://doi.org/10.3109/17435390.2010.504899.

(80) Warheit, D. B.; Donner, E. M. Risk Assessment Strategies for Nanoscale and Fine-Sized Titanium Dioxide Particles: Recognizing Hazard and Exposure Issues. *Food Chem. Toxicol.* **2015**, *85*, 138–147. https://doi.org/10.1016/j.fct.2015.07.001.

(81) Wang, J.; Zhou, G.; Chen, C.; Yu, H.; Wang, T.; Ma, Y.; Jia, G.; Gao, Y.; Li, B.; Sun, J. Acute Toxicity and Biodistribution of Different Sized Titanium Dioxide Particles in Mice after

Oral Administration. *Toxicol. Lett.* **2007**, *168* (2), 176–185. https://doi.org/10.1016/j.toxlet.2006.12.001.

(82) Ammendolia, M. G.; Iosi, F.; Maranghi, F.; Tassinari, R.; Cubadda, F.; Aureli, F.; Raggi, A.; Superti, F.; Mantovani, A.; De Berardis, B. Short-Term Oral Exposure to Low Doses of Nano-Sized TiO 2 and Potential Modulatory Effects on Intestinal Cells. *Food Chem. Toxicol.* **2017**, *102*, 63–75. https://doi.org/10.1016/j.fct.2017.01.031.

4.7 Supporting Information

4.7.1 Description of Control Experiments.

Several control experiments were conducted to ensure that: (i) the deposition of particles for SEM imaging and counting was uniform; (ii) particles were not released as a result of cutting the teabags; (iii) particle release was enhanced at high temperature, (iv) the experimental apparatus did not introduce particles into the samples, and (v) the plastic particles identified in the leachates did not originate from the tea leaves.

4.7.1.1 (i) Sample preparation for SEM imaging to avoid coffee ring effect

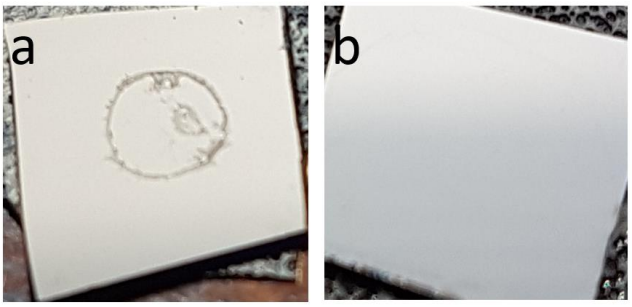

Figure S4.1. Deposition of particles for SEM imaging. (a) Following deposition of 100 µL of leachate as a single droplet onto an untreated silicon wafer, a coffee ring effect can be observed as

a result of the accumulation of particles at the edge of the droplet. (b) Following deposition of 100 µL of leachate in ten successive droplets of 10 µL over a silicon wafer washed with ethanol to increase hydrophilicity of the surface by oxidation. No coffee ring effect is observed as the sample dries uniformly over the silicon wafer.

4.7.1.2 (ii-v) Confirming that particles are not released due to cutting or from the apparatus or from tea leaves, and that particle release is enhanced at high temperature

In this study, all experiments were conducted with cut and emptied teabags to ensure that the enumerated particles originated from the teabag material and not from the tea. Control experiments with uncut teabags were conducted to confirm that cutting of the teabag did not cause leaching of particles (i.e., to confirm that particles were released even when the plastic teabag was uncut) (Fig. S4.2b, c). These samples contain tea and therefore require two additional steps before analysis, as the organics in tea interfere with SEM, FTIR, and XPS characterization. A 0.45 µm EMD Millipore Millex polyethersulfone sterile syringe filter was used to remove small tea leaves and twigs and a 50 mL Amicon stirred cell (UFSC05001 model) with a 30 kDa filter was used to remove dissolved organics (Fig. S4.2a). These processed leachates were then characterized by SEM, FTIR and XPS (Fig. S4.2-S4.4).

Additional controls (Fig. S4.2) were performed to (i) investigate the effect of heat on the degradation of the plastic teabags (Fig. S4.2d, e), (ii) to confirm that the experimental apparatus did not introduce particles into the samples (Fig. S4.2f, h), and (iii) to confirm that the loose leaf tea itself did not release plastic particles into the samples (Fig. S4.2g).

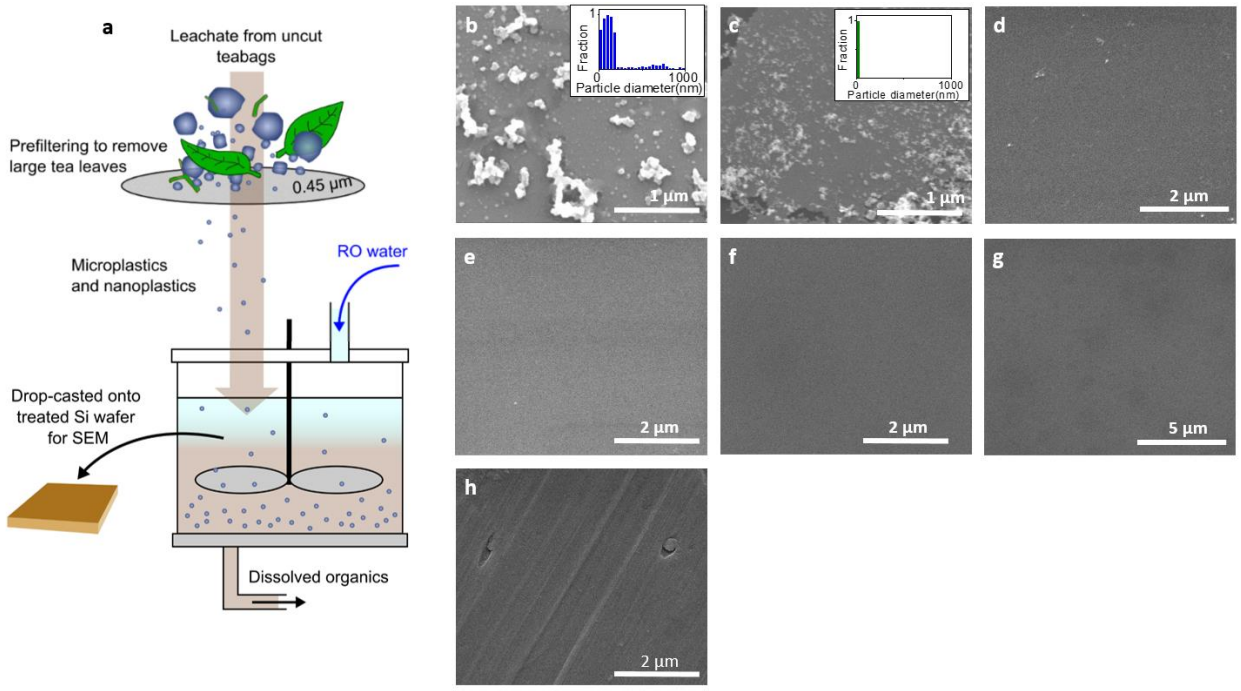

Figure S4.2. Filtration set-up used to process leachate from the unopened teabag (with loose leaf tea inside) and SEM images from control experiments. (a) This process was necessary to remove tea debris and organics; however, it adds steps to the sample processing. Therefore, counts should not be directly compared with those obtained in the main experiment because samples were not processed in the exact same way. First, leaf and twig fragments are removed using a 0.45 µm EMD Millipore Millex sterile syringe filter. Subsequently, dissolved organics are removed using a 50 mL Amicon stirred cell. This procedure is carried out to remove the dissolved organics in order to adequately characterize the leachate. Imaging at 1,000× of dried leachate from (b) control experiment with uncut teabag B and (c) control experiment with uncut teabag D. Both samples were prepared by following the process described in Fig. 4.1a (with the exception of opening and emptying the teabag). Subsequently, the leachates were processed as shown in Fig. S4.2a to remove dissolved organics. Particulate material is observed in both images, supporting the hypothesis that particles are leaching from teabags even when they are unopened. Imaging at

50,000× of (d) unheated leachate B and (e) unheated leachate D. Both samples were prepared by following the process described in Fig. 4.1a with the exception that the temperature of the water in which the teabags were steeped was at 22 °C instead of 95 °C. (f) Imaging at 50,000× of filtrate from the control experiment in which RO water was processed through the system described in Fig. 4.1a. The image shows no micro- or nanoparticles in the filtrate, confirming that the particles are not released from the experimental system (tubing, filters, etc). (g) Imaging at 30,000× of the filtrate from the control experiment conducted using a metallic steeper and loose tea leaves (which were not previously packaged in individual teabags). The image shows no micro- or nanoparticles in the filtrate, confirming that the particles are not released from the tea leaves. (h) SEM image at 50,000× of negative control experiment where RO water was processed through the system described in Figure S4.2a. Results show no micro- or nanoparticles in the filtrate, confirming that there are no particles released by the EMD Millipore Millex sterile syringe filter or the Amicon stirred cell.

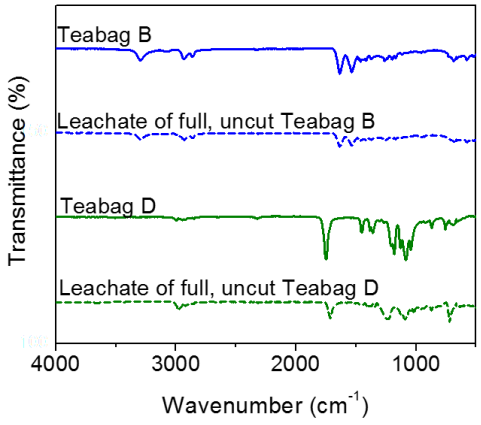

Figure S4.3. FTIR spectra for control experiments. FTIR spectra for the original (cut) teabag and the corresponding leachates prepared without cutting the teabag and removing the tea. FTIR peaks identified for the dried leachates match with those observed for the original teabag material. This

confirms that the particles leaching out of uncut teabags are plastic. This also confirms that teabags leach micro- and nanoplastics even when they are not cut.

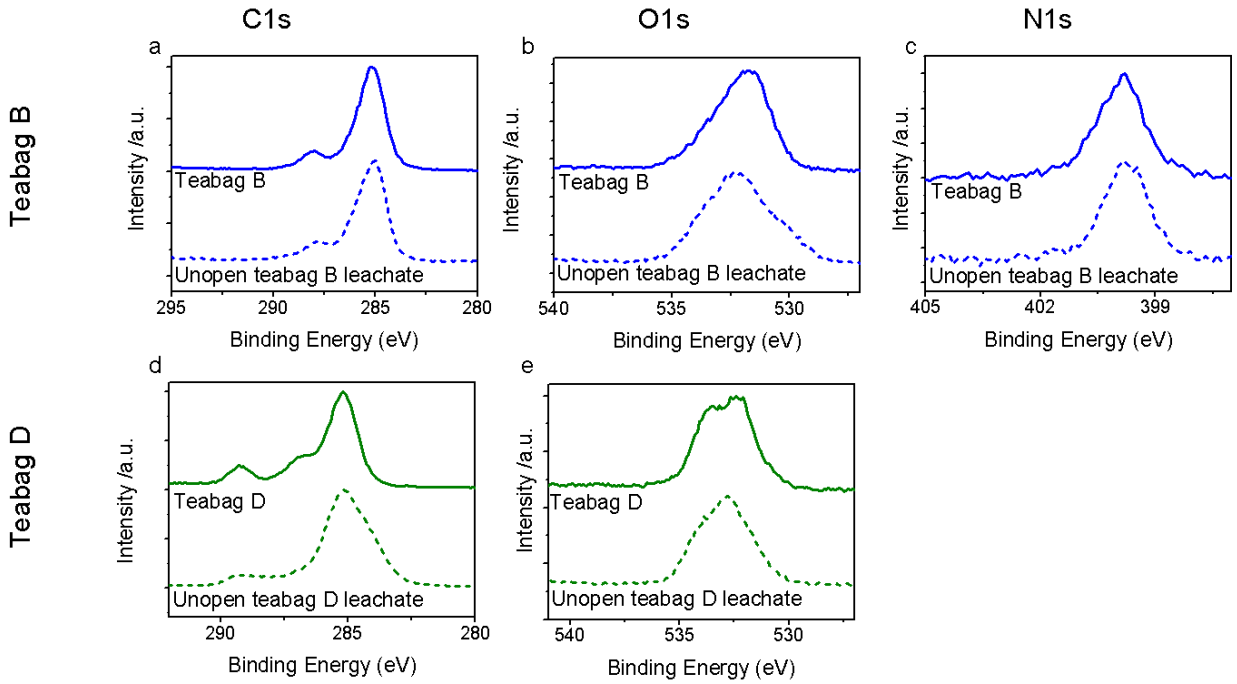

Figure S4.4. XPS analysis of the original (cut and emptied) teabag and leachates prepared without cutting the teabag and removing the tea. (a,b,c) C1s, O1s and N1s spectra of the original teabag B and the leachate obtained by steeping an unopened teabag B (with tea inside) and further processing the leachate as shown in Fig. S4.2a to remove dissolved organics. The measurements confirm that the particles in the leachate are nylon. (d,e) C1s and O1s spectra of the original teabag D and the leachate obtained by steeping an unopened teabag D (with tea inside) and further processing the leachate as shown in Fig. S4.2a to remove dissolved organics. The signals confirm that the particles in the leachate are PET.

4.7.2 Description of *D. magna* Swimming Assay.

At 48 hours, the mobile *Daphnia magna* from each treated group and control group were removed from the beakers and placed in glass bottom culture dishes with 14 mm microwell (MatTek, Ashland, US) filled with 2 mL of MHRW under ambient light conditions. This allowed for lateral movement with restricted vertical movement. The daphnids were allowed 2 minutes to acclimate prior to being recorded. The video was taken from above for 1 minute using a stereomicroscope (Fisher Stereomaster) mounted with a digital camera set at 30 frames per second and a resolution of 1920×1080 pixels. The 14 mm diameter of the microwell was used as the scale in each recording. The swimming movement in each video was identified by Kinovea-0.8.26 (https://www.kinovea.org/) and the swimming track density was determined by the image analysis of the trails left by daphnids during a 1-minute video recording. The tracks in each image were transformed to black pixels and the background to white, and the percentage of black pixels from each image was calculated using ImageJ 1.8.0. Statistical analyses on swimming movement were performed using Prism 5 version 5.01. The normality of data and homogeneity of variances was evaluated by Kolmogorov-Smirnov test and Bartlett's test, respectively. Comparisons between means among the experimental groups were achieved by one-way analysis of variance (ANOVA) followed by the *post-hoc* Tukey's multiple comparison test or Kruskal-Wallis test followed by Dunn’s multiple comparison test when data did not meet the assumptions of ANOVA. The level of significance was set as $p \leq 0.05$.

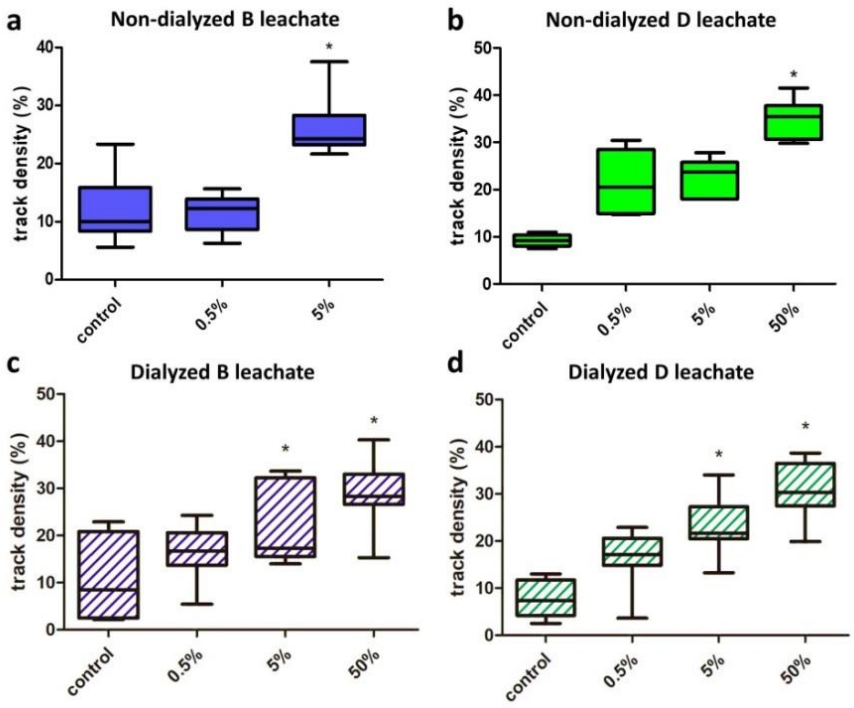

Figure S4.5. Swimming track density of *Daphnia magna* after exposure to different concentrations of (a) non-dialyzed teabag B leachate and (b) teabag D leachate, and (c) dialyzed teabag B leachate and (d) teabag D leachate. Swimming track density was determined by the image analysis of the trails left by *D. magna* during one-minute video recording. The tracks in each image were transformed to black pixels and background as white, and then the percentage of black pixels from each image was calculated using ImageJ 1.8.0. Asterisk indicates that the measurement is significantly different (p-value <0.05) from the control; n=9 for dialyzed teabag B, dialyzed leachate D, and non-dialyzed leachate B, and n=6-9 for non-dialyzed teabag D leachate.

4.7.3 Description of ICP-MS analysis of leachates.

Dialyzed and non-dialyzed leachates as well as the empty and full teabags were digested and analyzed by ICP-MS to determine the concentrations of four metal(loid)s. The closed digestion of all the samples was performed in Teflon tubes that were pre-rinsed five times with RO water. A two-step digestion was performed to reduce the explosion risk due to nitration of organic carbon. The samples to be digested were weighed directly in the Teflon tubes. Subsequently, 5 mL of trace metal grade hydrochloric acid (Fisher) was added to each sample. The Teflon tubes were closed and placed in a Mars 6 OneTouch microwave to complete a cycle that consisted of 20 minutes ramping from 20 °C to 150 °C, 20 minutes holding the temperature at 150 °C, and 20 minutes of cool down. After carefully opening the Teflon tubes, 3 mL of trace metal grade nitric acid (Fisher) was added to each sample. The tubes were closed and placed in the microwave for the same cycle. After the microwave cycle, the tubes were left on the bench to cool overnight. The following day, the digested contents were transferred into DigiPREP tubes. To minimize the loss of metal(loid)s in the Teflon tubes, they were rinsed at least five times with RO water that was added into the DigiPREP tubes. The final volumes of the diluted digested samples were brought to 50 mL with RO water. For the ICP-MS analysis, the samples were further diluted (10 times) to achieve final acid (HNO_3/HCl) concentrations below the 3% v/v level.

To account for solution matrix effects in the ICP-MS measurements, the internal standards of Sc (for Al and Cr), Y (for As), and Bi (for Pb) were used. A calibration curve was done at the beginning of the run and after 20 samples to correct possible signal variations throughout the measurement period. For each metal(loid), NIST standard reference material (Millipore ICP standards, Al #170301, Pb #170328, As #170303, Cr #170312) was used to verify the quality of the measurements at the start of the run, after every 10 samples, and at the end of the run. These

quality control measurements confirmed that the measurements were performed within an acceptable error range (±3%).

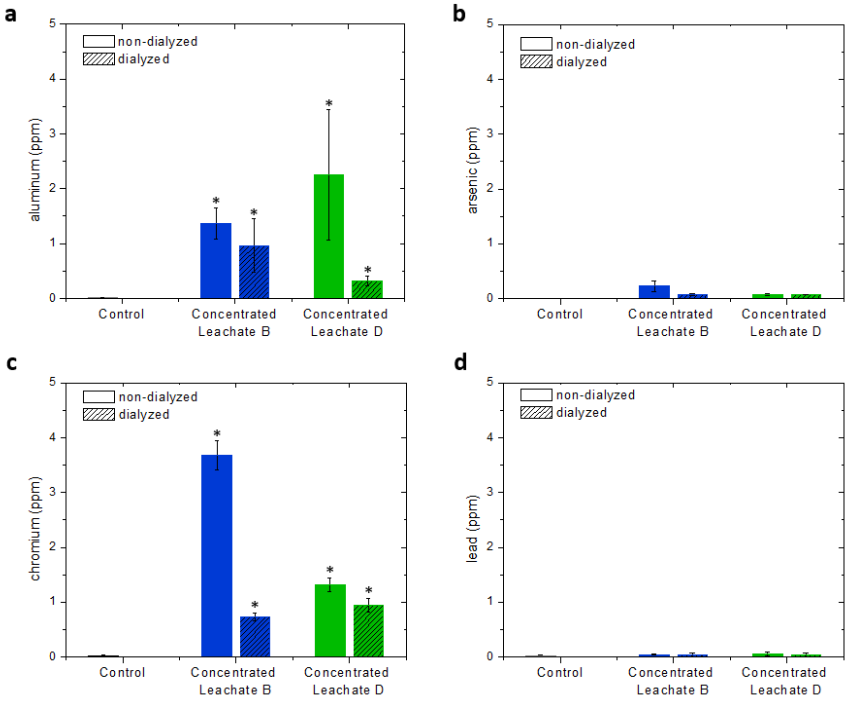

Figure S4.6. ICP-MS measurements of concentrations of (a) aluminum, (b) arsenic, (c) chromium and (d) lead found in the concentrated (100%) leachate before and after dialysis. The negative control was prepared by performing the complete digestion process without any leachate sample (adding acids and performing the temperature ramps). Asterisk indicates that the measurement is significantly (p-value <0.05) different from the control using a t-test. Statistics were not performed on the arsenic measurements as n=2 for those samples. Al and Cr are the most abundant metal(loid)s detected, with concentrations up to 2.3 and 3.7 ppm, respectively. In contrast, the concentrations of As and Pb are more than one order of magnitude lower (0.05-0.3 ppm).

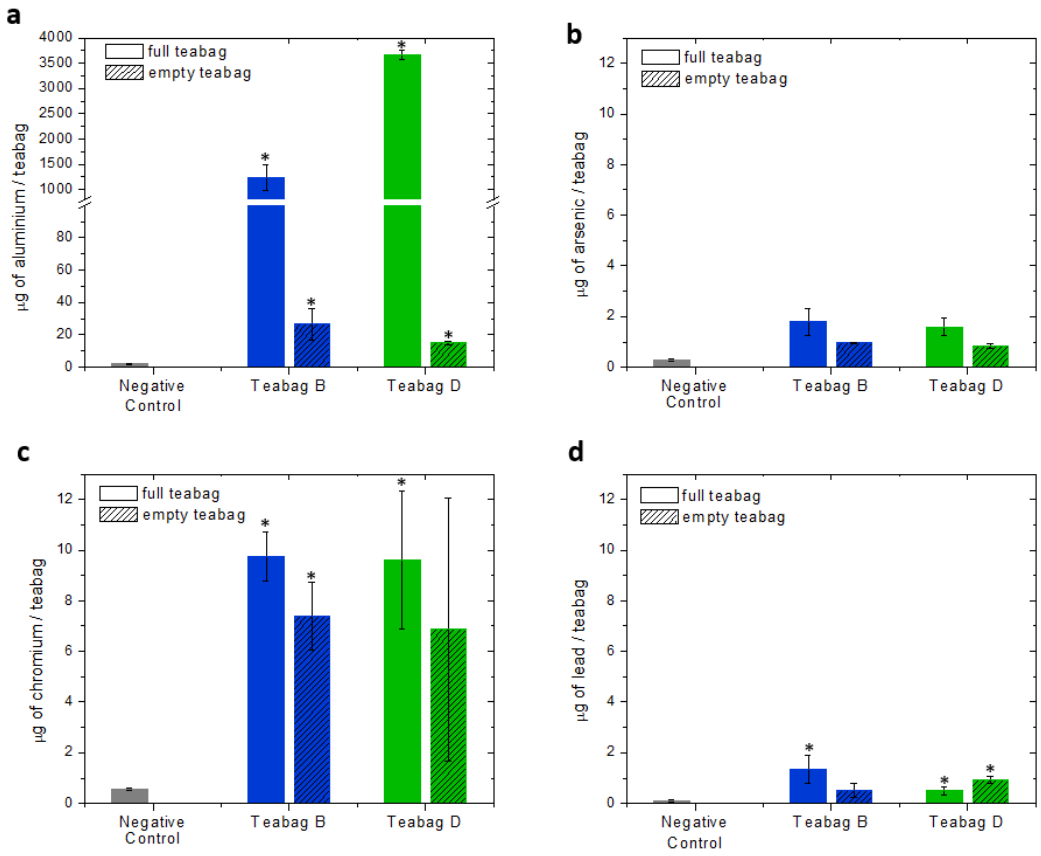

Figure S4.7. ICP-MS measurements of total mass of (a) aluminum, (b) arsenic, (c) chromium and (d) lead detected in a single empty plastic teabag (cleaned with RO water) and one full plastic teabag (containing loose leaf tea) for brands B and D. The negative control was prepared by performing the complete digestion without any leachate sample (i.e., acids were added to empty tubes and temperature ramps were performed). Asterisk indicates that the measurement is significantly (p-value <0.05) different from the control using a t-test. Statistics were not performed on the arsenic measurements as n=2 for those samples. Note that the lead content of full teabag D and empty teabag D are not significantly (p-value <0.05) different from each other using a t-test. The presence of tea leaves significantly increases the levels of Al and As. The concentration of Al is two orders of magnitude higher (18-25 µg per empty teabag compared to 1200-3700 µg per cup of tea), whereas the concentration of As is two-fold greater (from 0.7-1.0 µg per teabag compared

to 1.6-1.7 µg per cup of tea). The levels of Pb and Cr are comparable for the empty and full teabags; therefore, the source of these metal(loid)s could be either the tea leaves or the plastic teabags.

4.7.4 Immobility assessment, body size, X-ray computed tomography scanning, and optical imaging of D. magna exposed to non-dialyzed teabag leachate.

The *D. magna* Acute Immobilization Test was conducted in triplicates for each leachate concentration and the control. All test beakers were placed in a random order at light: dark conditions of 16 hours: 8 hours. The temperature (21-22 ℃), pH (7-8), and dissolved oxygen (9.9-10.6) of the beakers was recorded. The immobile neonates were counted and removed at 24 and 48 hours (Fig. S4.8a,b). At 48 hours, the swimming *D. magna* from each treated group and control group were removed from the beakers and placed in glass bottom culture dishes with 14 mm microwell (MatTek, Ashland, US) filled with 2 mL of MHRW under ambient light conditions. *D. magna* was imaged using a stereomicroscope (Fisher Stereomaster) mounted with a digital camera, and the body size (from head to the base of the tail spine) was measured with ImageJ 1.8.0. (Fig. S4.8c,d).

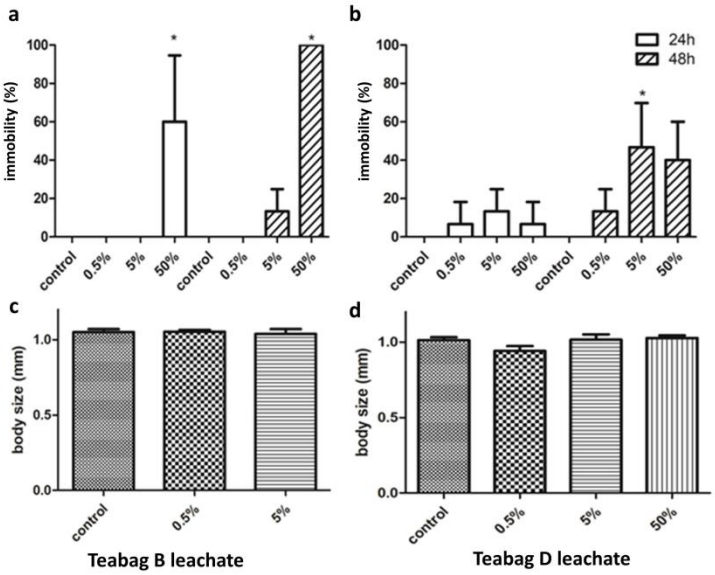

Figure S4.8. Mean immobility and body size of *Daphnia magna*. *D. magna* was exposed to different concentrations (0.5%, 5%, and 50%) of non-dialyzed (a, c) teabag B and (b, d) D leachate for 24 h and 48 h. Asterisk indicates that the measurement is significantly different (p-value <0.05) from the control.

After swimming assessment, a subsample of *D. magna* was randomly selected for X-ray computed tomography scan (CT scan) and optical microscopy. For CT scanning, *D. magna* was stained with 1% phosphotungstic acid dissolved in 70% ethanol for 3 days. Then, samples were quickly washed with 70% ethanol and placed in a pipette tip in 70% ethanol for CT imaging. Samples were scanned at 1.5 µm resolution with phase contrast using a Zeiss Xradia 520 Versa (Carl Zeiss: California, USA). Scan parameters were as follows: 60 kV, 82 uA, 4× objective lens, no filter, 3201 projections over 360-degree scan, 3.4-second exposure, and 2×2 pixel binning yielding 1.5 mm^2 field of view. These parameters resulted in 4.5 hours of scanning per specimen. All raw projection data were reconstructed in Zeiss reconstructor software. The CT images were then analyzed with Dragonfly 3.5 (Object Research System Inc, Montreal, Canada,

http://www.theobjects.com/dragonfly) in order to visualize the 3D reconstructions of daphnids. The sectioned CT images were reproduced in Dragonfly. For optical imaging, a subsample of *D. magna* was randomly selected and fixed in 70% ethanol overnight, and then carefully rinsed 6 times with DI water to remove particles attached externally as much as possible before imaging. Images were taken using an Olympus DP80 microscope digital camera at 60× magnification focusing on the intestine region of *D. magna*.

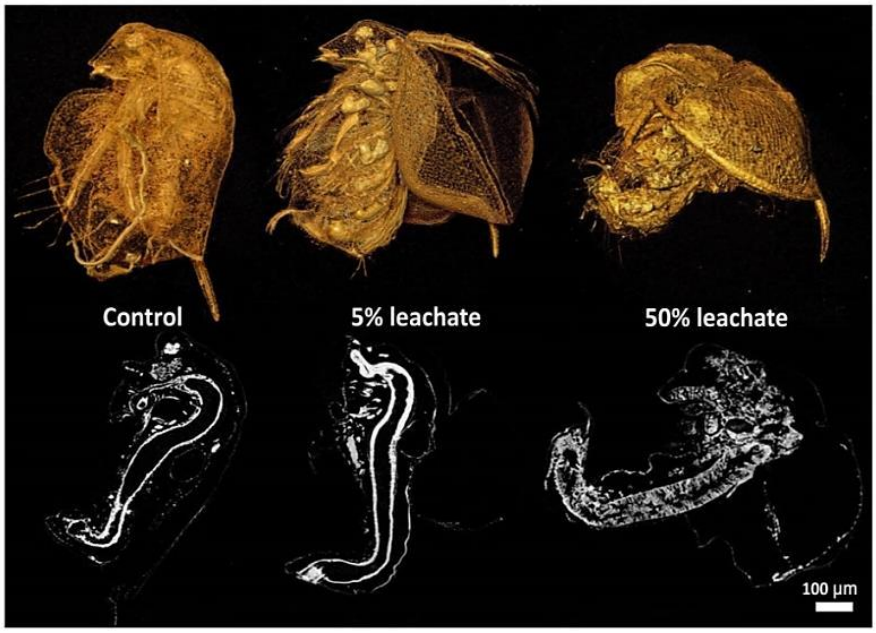

Figure S4.9. CT images of *Daphnia magna* exposed to 5% and 50% non-dialyzed teabag D leachate. Random samples were stained with phosphotungstic acid and scanned using a Zeiss Xradia 520 Versa. Scale bar, 100 µm.

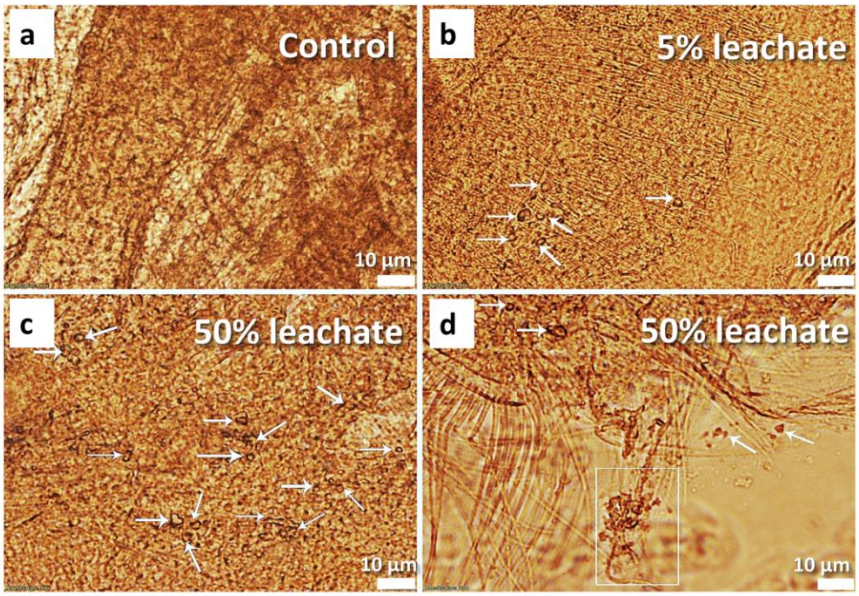

Figure S4.10. The presence of micro-particles in *Daphnia magna* exposed to non-dialyzed teabag D leachate. The particles are indicated with white arrows in intestine (a-c) and abdominal setae (d). Following 48 h of exposure to non-dialyzed leachates, and after the swimming assessment, a subsample of *D. magna* was randomly selected and fixed in 70% ethanol overnight. *D. magna* preserved in ethanol is carefully rinsed 6 times with DI water before imaging. Representative images are taken using an Olympus DP80 microscope digital camera at 60× magnification. Scale bar, 10 µm. Intestine is focused for imaging, as shown in a-c. Foreign microparticles are only found in the leachate-treated *D. magna* (b, c) but not in the control (a). The microparticles are also found on the hair-like abdominal setae close to anus (d). The observed microparticles in (d) may be egested from anus and attach onto the abdominal setae. The size and shape of these microparticles are similar to those of particles we observed in the leachate.

Preface to Chapter 5

While some microplastics are intentionally produced (Chapter 3), others are incidentally produced (Chapter 4). A major source of incidentally produced microplastics is the fragmentation of large bulk plastic that resides in the environment. In this chapter, the weathering of four common plastics was studied. Briefly, these plastics were exposed to either UV or temperature stimuli. We hypothesized that each type of plastic will respond slightly differently to either UV or temperature. To evaluate this response, we monitored the particles released from the bulk plastics and the surface hardness of the bulk plastics. We found that indeed all polymers seem to respond differently when exposed to different weathering. Some differences were observed in the number of particles released. The surface hardness of some plastics was also modified differently with each treatment. The importance of this study was to compare the UV versus temperature weathering effects. This study is in preparation to be submitted to *Environmental Science & Technology*.

Chapter 5: Photolytic and thermal weathering of four commonly used plastics

Abstract

Plastic contamination is ubiquitous in aquatic environments. The breakdown of macroplastics has been observed, and it is dependent on many environmental factors (e.g. sunlight, temperature, mechanical abrasion). However, more studies are needed to understand how the individual components of weathering contribute to the breakdown of plastics resulting in particle release. Here we studied four high volume plastics suspended in water and their response to either UV or temperature weathering. Plastics were analyzed for changes in their surface hardness. The water in which the plastics were suspended was analyzed for the presence of particles. The surface hardness of polypropylene and low-density polyethylene significantly decreased following either treatment. Polystyrene only underwent a significant increase in surface hardness when exposed to UV-weathering. High-density polyethylene had no significant change with either UV or temperature weathering. Analysis of the water in which the original plastics were suspended revealed smaller particles for all four plastic types. Specifically, polystyrene and low-density polyethylene released greater numbers of particles when exposed to temperature weathering. Conversely, high-density polyethylene released more particles when UV-weathering was applied. In the case of polypropylene, there was no significant difference between the UV and temperature weathering. When analyzed with Fourier Transform Infrared Spectroscopy, dried released particles exhibited a plastic signature that corresponded to the parent plastic.

5.1 Introduction

Plastics, especially those used for packaging, are materials with long lifespans but that are often produced for limited expected use. Polystyrene (PS), polypropylene (PP), and polyethylene (PE) represent the bulk of single-use plastics,[1] and their disposal often leads either directly (littering) or indirectly (poor process controls) to environmental release.[2] As a result, roughly 11% of produced plastic waste was estimated to have entered aquatic environments in 2016.[3] The forecast increase in plastic production and subsequent environmental release is such that reducing pollution levels cannot be achieved by improving waste management streams alone.[3] Additionally, the current environmental load represents an embedded toxicity debt that will continue to impact the environment as these plastics age, regardless of any future mass inputs.[4]

The environmental burden of plastic waste poses significant risk to aquatic species. The impact of bulk plastics (e.g., bags, fishing nets, can rings) has been well-documented to cause entanglement, starvation, and mortality in larger wildlife including turtles, birds, and marine mammals.[5] However, most plastics found in the marine environment are smaller than about 5 mm[5] and fall under the generally accepted definition of microplastics. Microplastic accumulation is a rapidly growing global concern. The potential environmental and health impacts of microplastics (or, smaller nanoplastics) are less well known but include effects on aquatic and terrestrial organisms.[6–11] While microplastics have been observed worldwide, comprehensive data on their occurrence are not currently available.[2,12] Current sampling methods include beach combing (which isolates macroscopic marine debris), biological sampling of wildlife (that have ingested plastics) and most commonly, filtration for plastic debris collection from surface water.[12] These sampling techniques are only suitable for the detection of microplastics and larger particles, and as a result, there is precious little information reported on the environmental concentration of nanoplastics.[13,14]

Despite the lack of data on environmental nanoplastic concentrations, the release of nanoplastics is known to occur as a result of bulk plastic degradation. Some examples for this have been observed in laboratory settings following thermal,[15] ultraviolet light (UV),[16] and biological[11] exposures. The release of particles arises as a direct result of the weathering processes, which remain poorly understood phenomena.[4] What is known is that these degradation processes are intrinsically transformative to the polymer matrix itself. UV degradation has been observed to lead to cracking, discoloration, and an increase in brittleness of the bulk polymer which has been primarily attributed to oxidation at the surface.[1,13,17,18] Thermal degradation has been linked to increases in surface roughness and decreased tensile strength in thin films of PE.[19] In combination, weathering processes are likely to work synergistically. For example, exposure to UV light that oxidizes the polymer chains will increase the crystallinity of the material, rendering it more brittle and enhancing the potential for mechanical abrasion.[5] UV coupled to elevated temperatures has been shown to also decrease resistance of the polymer to thermal decomposition.[20] The polymer type has been linked to differences in bulk plastic ageing in some cases, with PS reported to be particularly susceptible.[18,21] Finally, the media in which the plastic exists can influence weathering. Biber *et al.* measured changes in the tensile strength of plastic films, observing that the plastics exposed to sunlight in air medium deteriorated more rapidly and formed carbonyl chain ends in a different manner from those suspended in water.[18]

Despite these studies, there remains large uncertainty in the relative impacts of weathering processes across plastic types. Furthermore, reports generally focus on the initial macro- or microplastic, while there are few studies aimed at characterizing the release of smaller particles as a result of plastic weathering.[22] This study examines the release of nanoparticles resulting from the breakdown of commonly used polymers. Degradation was achieved via laboratory weathering

experiments to expose suspended microplastics of PS, PP, high-density polyethylene (HDPE), and low-density polyethylene (LDPE) to either UV-light or elevated temperature, to understand the relative influence of these environmental factors.

5.2 Materials and Methods

5.2.1 Weathering microplastics with UV radiation or thermal stimulus

All reverse osmosis (RO) water was filtered with a Nalgene® Rapid-Flow™ bottle top filter (PES Membrane, 0.1 µm, VWR #89176-982) attached to pre-washed glass media bottles (06-414-1D, PYREX). Briefly, PS (McMaster Carr #8734k39), PP (McMaster Carr #88742k831), HDPE (McMaster Carr #8619k427) and LDPE (McMaster Carr #8657k811) sheets were cut with clean stainless-steel shears into large microplastics (<5 mm) with dimensions 4.3 mm x 4.3 mm x 1.6 mm (herein termed "prepared microplastics"). The prepared microplastics were washed with filtered RO water and then placed in a desiccator for one week to remove moisture.

For each plastic type, six clean borosilicate glass test tubes were filled with 8 mL of filtered RO water. Five prepared microplastics of the same plastic type were weighed and placed in each test tube. The tubes were covered with borosilicate glass plates to reduce contamination from atmospheric deposition. Additionally, for each plastic type, two procedural blanks containing only RO water were prepared and placed in the same conditions as the samples, to account for any contamination arising from sample preparation or processing.

UV-light and thermal weathering conditions were tested individually to determine their relative impact on the plastics. For UV treatment, half of the prepared samples and procedural blanks (three samples and one procedural blank for each of the 4 plastics) were placed into a UV-light chamber illuminated by ten 8 W fluorescent lamps: 5 visible light (6500 K-daylight bulbs, Eiko Global,

Kansas, USA) and 5 UV light (Hikari Lamps, California, USA, peak output 365 ± 15 nm). The irradiance from the UV bulbs at the air-water interface of the test tubes was 23.0 ± 1.3 W m^{-2}, as measured with a UV-radiometer (MU-200, Apogee Instruments, spectral range 295 – 400 nm). For comparison, this is similar to the observed average UV irradiance (UVA + UVB) in August from 10 AM – 2 PM over Edmonton, Canada (22.5 W m^{-2}),[23] while a UV irradiance of 32.4 W m^{-2} over similar wavelengths used here (340–390 nm) has been reported at 38 °N on a clear summer day.[24] The total UV radiant exposure was 2.50 × 10^8 J m^{-2}. The visible light lamps yielded an intensity of 118 ± 5 μmol m^{-2} s^{-1}, measured with a MQ-200 light meter (Apogee Instruments, spectral range 370 – 650 nm). The chamber was covered with drapes to prevent external light from entering, and the setup was held at room temperature (21 ℃). The other half of the prepared samples were subjected to thermal treatment (T) and were placed in an incubator (Labnet, 311 DS Digital Shaking Incubator) set to 37 ℃, the door of which was covered with aluminum foil to maintain a dark environment. Exposures were maintained for 18 weeks, after which the prepared microplastics were removed and placed in a desiccator until further analysis. The remaining liquid from each test tube (hereafter termed UV-leachate and T-leachate) was characterized for the presence of small micro- and nanoparticles.

A control was set up at 4 ℃ and with no light, herein termed fridge-control. For each plastic, three test tubes with filtered RO water each containing five prepared microplastics were placed in a refrigerator and covered with aluminum foil. For each plastic type, one procedural control was prepared containing only filtered RO water, herein termed fridge-procedural blank. Leachates and prepared microplastics were analyzed after 18 weeks of fridge treatment.

5.2.2 Analysis of particles in leachates using SEM and NTA

Leachates, controls, and blanks were analyzed in triplicate for the presence of released micro-sized and nano-sized particles by scanning electron microscopy (SEM) and nanoparticle tracking analysis (NTA). For SEM, samples were prepared by attaching a hydrophilic polycarbonate membrane filter shiny side up (Sterlitech # PCT00147100, pore size 10 nm) to an SEM stud (Ted Pella # 16084-1) using carbon tape (Ted Pella # 16111). In a biosafety cabinet with laminar flow (BSC), two thousand µL of leachate were drop-cast onto the membrane 10 µL at a time (the hydrophilic nature of the membrane reduces the coffee-ring effect). In between 10 µL additions, the samples were placed in glass Petri dishes and allowed to dry. After the total volume was deposited, the membrane was then coated with a 2 nm layer of platinum (Leica Microsystems EM ACE600 Sputter Coater) for SEM imaging (FEI Quanta 450 environmental SEM, 5 kV, spot size: 3.0). ImageJ analysis software was used to measure the diameter of all the particles in the SEM images of the dried leachates. To capture the polydispersity of the sample, two magnifications were used (low magnification: 1,200× and high magnification: 25,000×). The particle diameter distribution for each magnification was determined by measuring the particles in 15 images taken randomly in each of the three replicates (45 images total for each sample type, for each magnification). ImageJ analysis was performed by subtracting the background, adjusting the threshold, and then using the automatic particle counting function. The diameter was assigned to be the maximum Ferret diameter, as this is the largest distance between two boundary points of the particles. This assures we are not over-interpreting the "nano"-size of particles.

The number of particles smaller than ~1 µm was determined using nanoparticle tracking analysis (NTA, LM14 instrument with 532 nm green laser, NanoSight Ltd.) by introducing 1 mL of leachate into the NTA chamber. A 60 s video was taken (335 shutter aperture, 0-5 gain) and over 200 particles/run were tracked with the NanoSight software. The run was repeated three times per

triplicate (9 times for each leachate), between which the chamber was cleaned, and a fresh sample was used for each replicate.

5.2.3 Characterization of the chemical composition of leachates and prepared microplastics

Approximately 3 mL of the remaining leachate for each plastic and treatment was drop-cast onto aluminum foil. Briefly, a droplet was added to the aluminum foil, the droplet was left to dry, and this process was repeated approximately 40 times until a film developed on the aluminum foil. Pristine prepared microplastics, weathered prepared microplastics (UV and temperature), and dried films were characterized using a Spectrum TWO Fourier Transform Infrared Spectrometer (FTIR) instrument with a single-bounce diamond (PerkinElmer) in attenuated total reflection mode (ATR). The spectra were taken from 500 to 4,000 cm^{-1}, and 16 scans were performed.

5.2.4 Vickers microhardness (H_v, kg mm^{-2}) of pristine and weathered prepared microplastics

Microhardness of pristine, weathered, and fridge-control prepared microplastics was tested using a Clark CM100 AT Vickers microhardness instrument. Briefly, the surface of each prepared microplastic was indented using a pyramid-shaped diamond head. The indentation load was set to 10 gram-force over 10 s. Five indentations were conducted per weathered plastic, whereas 10 indentations were conducted on the pristine plastics. Indentation images were processed using the built-in camera and computer software (Clemex CMT), performed at an optical threshold of 500× with the CM 100 AT M50/0.68 magnification setting.

5.3 Results and discussion

5.3.1 Size and number of particles in the leachate

Figure 5.1 shows SEM images of dried leachates taken at low and high magnifications. Observations from these two magnifications overlap as at low magnification, the minimum diameter measured was 72 nm, whereas at high magnification, the maximum diameter measured was 1980 nm. The results of particle sizing measurements (using ImageJ) show that all the leachates are mainly composed of nanoparticles. The particles appear to have irregular morphologies and a high degree of polydispersity.

Size distributions for the diameters of the particles observed are shown in Figure 5.1. Polydispersity indices of the particles, calculated as the square of the ratio of standard deviation divided by the average maximum ferret diameter,[25] were between 0.82 - 3.58 at low magnification, and 0.90 - 3.30 at high magnification. At both magnifications, the polydispersity of released particle sizes is high, however, the average diameters confirm that observed particles were mainly in the < 1 μm range. As such, the number concentration of particles can be approximated using NTA (Figure 5.2). To better illustrate the particle size distributions, histograms for each leachate are presented in the insets of Figure 5.1.

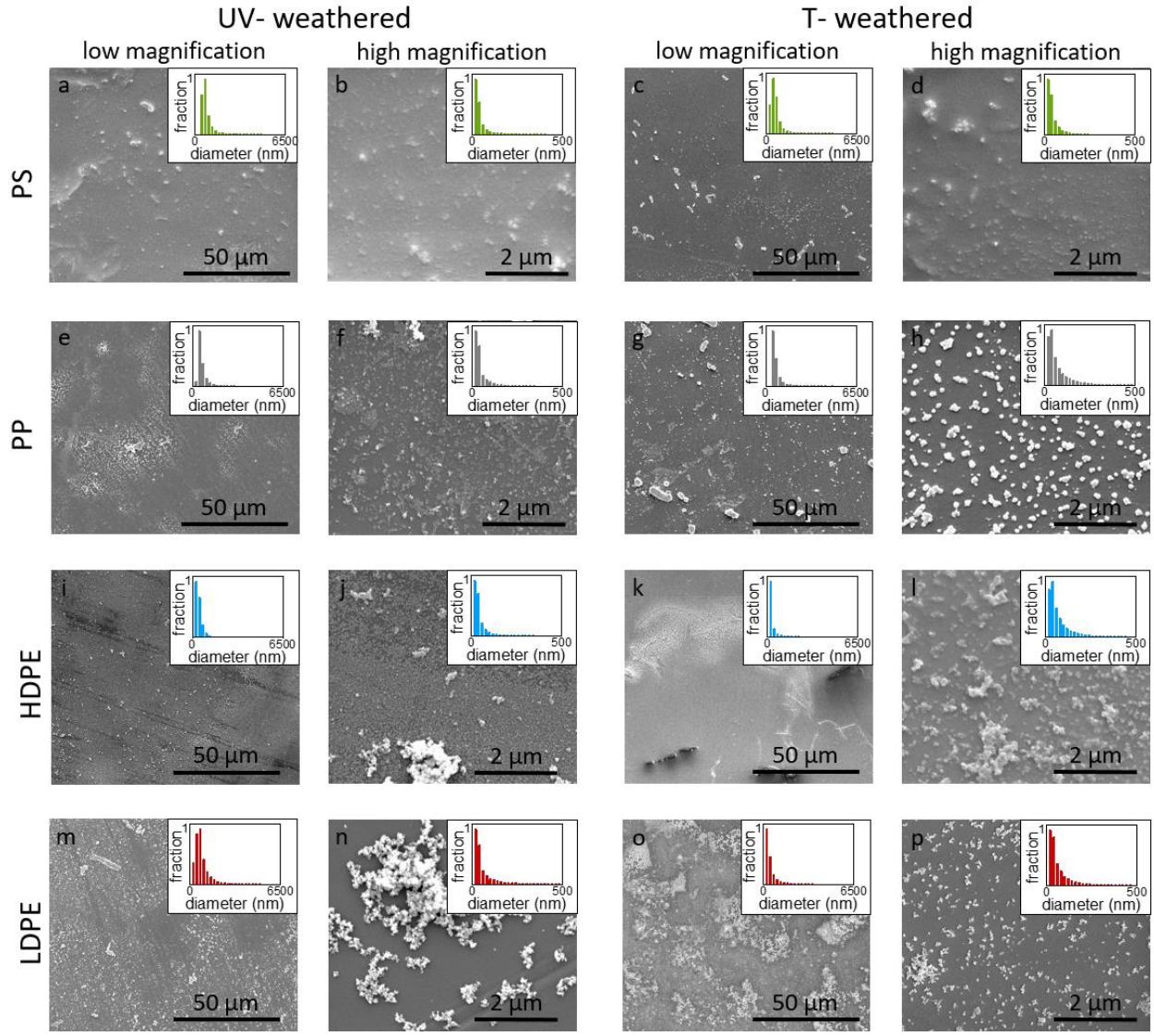

Figure 5.1. SEM images of the leachates of plastics exposed to UV or high temperature weathering. (a, e, i, m) Imaging at low magnification of leachates of UV-weathered plastics. Particle size distributions shown in insets. (b, f, j, n) Imaging at high magnification of leachates of UV-weathered plastics. Nanoparticle size distribution shown in insets. (c, g, k, o) Imaging at low magnification of leachates of plastics weathered at high temperature. Microparticle distribution shown in insets. (d, h, l, p) Imaging at high magnification of leachates of plastics weathered at high temperature. Nanoparticle size distribution shown in insets.

The number of particles in the leachates was determined using NTA, which measures particles in suspension that are approximately 10 nm to 1 μm in size. For the results to be significant, more than 200 particles were tracked for each measurement. NTA is useful to obtain an order of magnitude estimate of the particle number concentration for submicron particles. From these data (Figure 5.2), all plastic leachates were observed to contain approximately 10^8-10^9 particles mL^{-1}. By performing a Student t-test on the averages of the 9 measurements taken (3 for each triplicate), it was determined that HDPE released significantly more particles when degraded by UV. In contrast, PS and LDPE released significantly more particles when exposed to high temperature. PP (both weathering approaches) released the least number of particles, and there were no significant differences between the weathering approaches. These results generally agree with the reported stability of PP.[26] All fridge controls and procedural blanks measured by NTA did not yield more than 200 tracks, suggesting that they contain < 10^8 particles mL^{-1}. This is supported by SEM images of the fridge-controls (Figure 5.3) and procedural blanks (Figure 5.4) in which few particles are observed. While the SEM images of fridge-controls (Figure 5.3) and procedural blanks (Figure 5.4) show very few contamination particles, for further experiments, it would be most appropriate to use a laminar flow cabinet to reduce the likelihood of contamination.

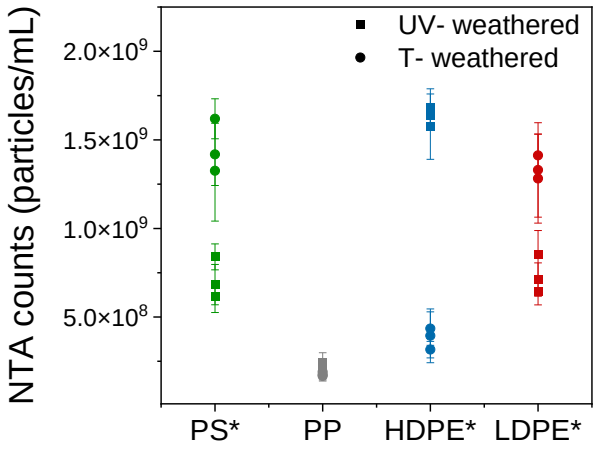

Figure 5.2. NTA measurements of the leachates for each UV and T weathering. Results were obtained by tracking > 200 particles. The tracks were processed using the NanoSight software. Three samples were measured three times, for a total of 9 measurements per leachate. Asterisk indicates that the average of the 9 measurements for UV-weathered and T-weathered were statistically significantly different (p-value < 0.05, Student t-test, n=9).

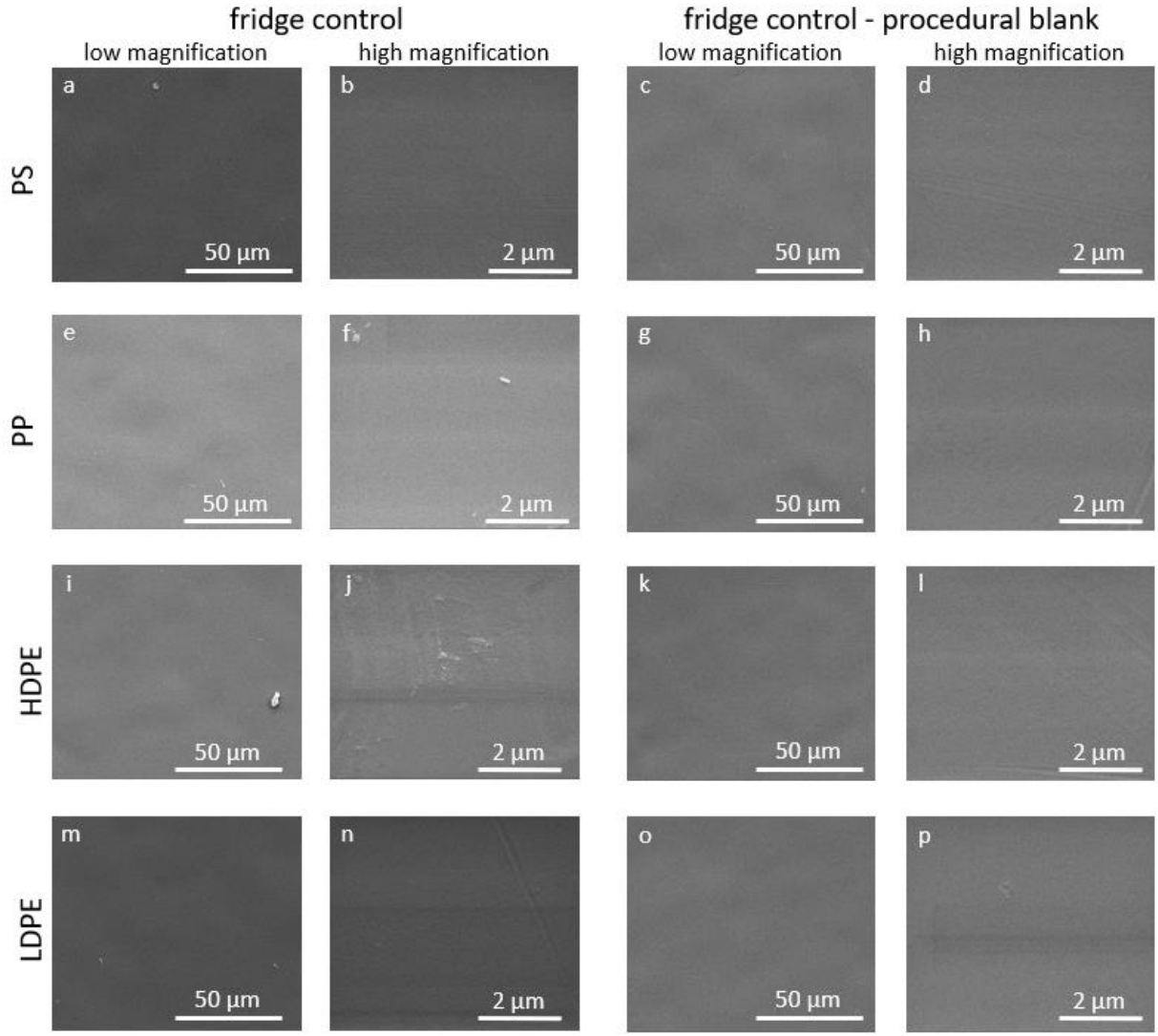

Figure 5.3. SEM images of fridge-controls and fridge-procedural blanks. (a, e, i, m) Imaging at 1,200× of leachate of fridge-controls of plastics. (b, f, j, n) Imaging at 25,000× of leachate of fridge-controls for plastics. (c, g, k, o) Imaging at 1,200× of leachate of fridge-procedural blanks of plastics. (d, h, l, p) Imaging at 25,000× of leachate of fridge-procedural blanks of plastics.

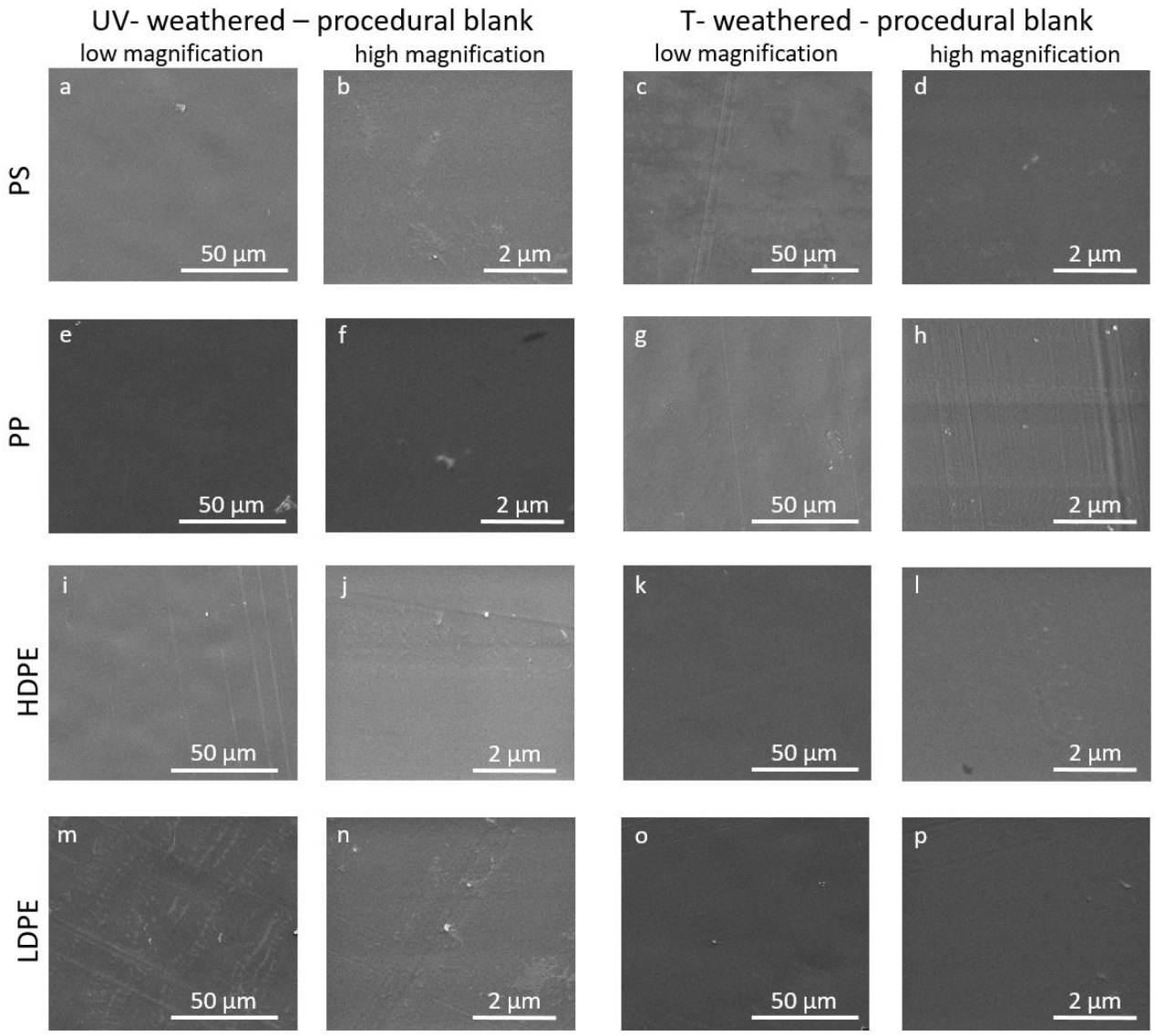

Figure 5.4. SEM images of procedural blanks. (a, e, i, m) Imaging at 1,200× of leachate of procedural blank for UV-weathering of plastics. (b, f, j, n) Imaging at 25,000× of leachate of procedural blank for UV-weathering of plastics. (c, g, k, o) Imaging at 1,200× of leachate of procedural blank for T-weathering of plastics. (d, h, l, p) Imaging at 25,000× of leachate of procedural blank for T-weathering of plastics.

5.3.2 FTIR analysis of the prepared microplastics and their leachates

FTIR analysis was performed on thin films prepared from the leachates to confirm that the chemical structures of the released particles match those of the parent bulk materials. For PS (Figure 5.5a and b), the films obtained resulted in low transmittance signals, which can be attributed to a relatively small amount of particles deposited compared to the bulk material. However, characteristic PS reference bands were detected for both films at 2825-3100 cm^{-1} (-CH_2 and aromatic -CH stretches, multiple peaks), 1450-1500 cm^{-1} (-CH_2 bend and aromatic ring stretch, two peaks), 750-760 cm^{-1} (ring in-phase H wag, one peak), 695-700 cm^{-1} (aromatic CH out-of-plane bend, one peak) and 535-540 cm^{-1} (aromatic ring out-of-plane bend, one peak).[27] It can thus be concluded that the PS samples, after being exposed to UV or heated for 18 weeks, released PS particles into the leachate.

Differences between weathered and pristine prepared PS microplastics can be observed in the carbonyl groups (-C=O) (1600-1800 cm^{-1}). Specifically, this peak increases in both UV-weathered and T-weathered prepared microplastics (Figure 5.5a and b) with a more pronounced change in the UV-weathered prepared microplastic. This peak confirms the oxidation of the surface when the prepared microplastics are weathered.[28] However, there was no notable difference in both the hydroxyl (-OH) (3600-3100 cm^{-1}) and the double bond (=C-H) (1000-880 cm^{-1}) regions.

Likewise, particles observed in the PP leachate were confirmed to be PP (Figure 5.5c and d). The FTIR spectrum of PP is recognized by its main absorption bands at 2825-2975 cm^{-1} (-CH_2 and -CH_3 stretches, multiple peaks), 1450-1460 cm^{-1} (-CH_2 scissors, one peak), 1375-1380 cm^{-1} (-CH_3 bend and -CH_2 wag, one peak) and 1160-1170 cm^{-1} (CH bend, CH_3 rock and C-C stretch, one peak).[27] These characteristic peaks can be clearly observed for the PP pristine prepared microplastic and after UV or thermal weathering as well as for the films obtained from the leachate

(Figure 5.5), confirming that there is PP in the leachates. When observing the pristine prepared microplastic we find that there is a slight peak in the carbonyl region (-C=O) (1600-1800 cm^{-1}). This peak grows slightly in the UV-weathered and T-weathered prepared microplastics, and this may be a sign of oxidative stress on the surface (Figure 5.5c and d).

Even though HDPE is a linear polyethylene with minimal branching while LDPE has long PE branches, their differentiation by FTIR is particularly tedious since they share the same major structural units. Jung *et al.* recently developed a method to differentiate these two plastics, relying on the small LDPE peak at 1377 cm^{-1}, which corresponds to the methyl bending deformation of the branched chain ends.[29,30] In our study, this band was not clearly detectable due to the relatively low intensity of the films' signals. Nonetheless, FTIR analysis performed here ascertained that the dried leachates from LDPE (Figure 5.5e and f) and HDPE particles (Figure 5.5g and h), whether after UV- or T-weathering, corresponded to polyethylene. Indeed, the two broad bands at 2825-2950 cm^{-1} represent C-H stretch of ethylene repeating unit whereas the peaks at 1450-1475 cm^{-1} and 715-730 cm^{-1} correspond respectively to $-CH_2$ bending and CH_2 rocking deformations of PE. [31] Thus, this proves that there is HDPE and LDPE in the respective leachates.

When comparing the weathered and pristine prepared polyethylene microplastics, there is no observable differences in the hydroxyl groups (-OH) (3000-3600 cm^{-1}) in either HDPE or LDPE (Figure 5.5e, f, g and h). In the carbonyl groups (-C=O) (1600-1800) no difference can be observed in HDPE for both weathering treatments (Figure 5.5e and f). However, for LDPE, a slight increase in the carbonyl groups was observed in both the UV-weathered and T-weathered prepared plastics when compared to the pristine prepared plastic (Figure 5.5g and h). This increase in the carbonyl groups is an indicator of oxidative stress. All HDPE and LDPE weathered leachate films were too thin, and thus the signal too low, to reveal such slight differences in the FTIR spectra.

Drop-casting of ~3 mL from the fridge-controls and procedural blanks yielded no film for analysis, further confirming that there was not substantial particulate contamination in this study.

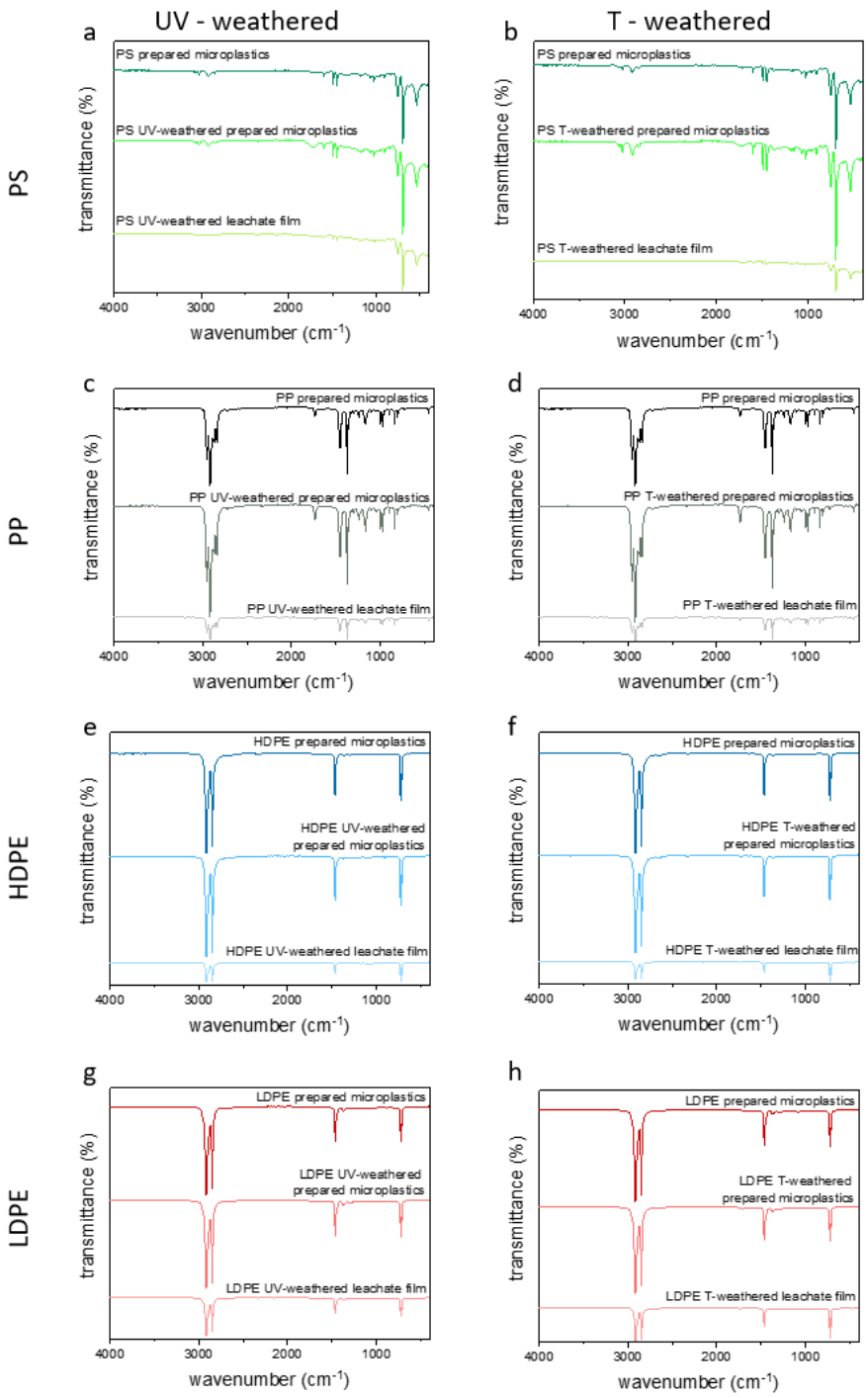

Figure 5.5. FTIR spectra for bulk plastics (before and after weathering) and their corresponding films for (a,b) PS, (c,d) PP, (e,f) HDPE, and (g,h) LDPE. It can be observed that the signal for each film corresponds to that of their parent plastic.

5.3.3 Microhardness changes in prepared microplastics after weathering

Figure 5.6 shows the microhardness values for the four different plastics in pristine condition (prior to weathering),after 18 weeks of either UV or thermal treatment, and after 18 weeks of fridge treatment (dark control). The microhardness of the pristine samples decreased as follows: PS > PP > HDPE > LDPE. This can be directly correlated to the different chemical structures of the polyolefins. PS, bearing phenyl groups, is for instance much more rigid (glass transition temperature $T_{g,PS}$ ~ 100 ^{o}C) than LDPE, consisting solely of branched and aliphatic chains ($T_{g,LDPE}$ typically lower than -100 ^{o}C).[2]

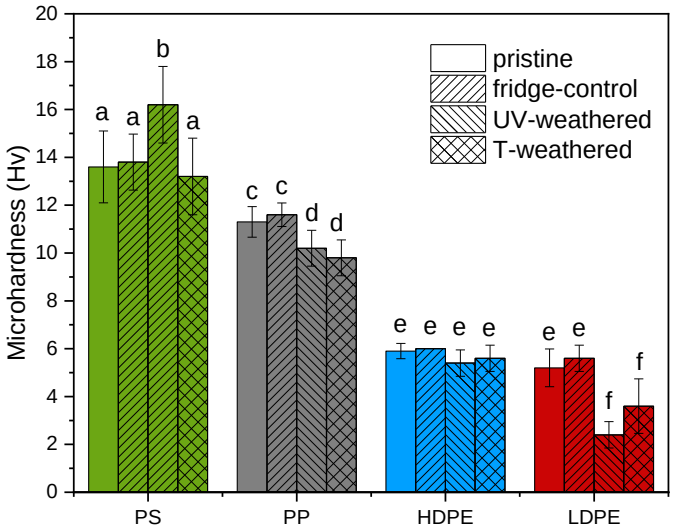

Figure 5.6. Vickers microhardness measurements for PS, PP, LDPE and HDPE microplastics. Each prepared microplastic sample, exposed to UV irradiation, heated or fridge-control, was compared to its pristine form, except HDPE and LDPE which were also compared to each other. Five UV-weathered, T-weathered, and fridge-control samples were analyzed (N=5). Ten pristine

samples were analyzed (N=10). Error bars represent the standard deviation. Letters denote results of a 1-way ANOVA test performed with post hoc Tukey's HSD $\alpha = 0.05$.

Microhardness is the measurement of the localized surface hardening. This localized hardness is particularly interesting when comparing pristine and weathered prepared microplastics, as degradation is expected to occur mostly on the surface. For all four plastics, there was no significant difference between the pristine prepared microplastics and the fridge-control prepared microplastics. For PP, and LDPE samples, UV-weathering resulted in a softening of the materials' surface, which can be explained by oxidative degradation processes via the formation of hydroperoxides.[32] Indeed, auto-oxidative and photo-oxidative mechanisms generated in polyolefins via free-radical chain reactions have been exhaustively reported and provoke a decrease in the average chain length of the plastics by direct scission of the covalent bonds.[32] There was no significant change in microhardness for HDPE. The microhardness for LDPE decreased more significantly compared to PP samples after UV-weathering. This may be explained by the larger amorphous fraction in pristine LDPE versus HDPE which did not undergo any change in microhardness.[33] In the amorphous state, the rate of degradation likely increases due to the higher chain mobility, promoting radical propagation reactions and thus chain scissions.[26]

A marked increase in microhardness from about 13.5 to 16.0 Hv was measured at the surface of PS after being irradiated with UV for 18 weeks. This result may be explained by a higher degree of crystallinity of UV-exposed PS, as recently reported by Monsores *et al.*[34] Polystyrene plates exhibited both higher microhardness and higher degrees of crystallinity after being exposed to UV-B (280-320 nm) for 14 days or more. This latter structural change was attributed to crystalline rearrangement after cleavage of the chains. Similar impacts of UV exposure were observed for PS over short time-frames by Meides *et al.*, who also observed an increase in elongation at break for

PS tensile bars. This was attributed to a temporary increase in polymer degree of crosslinking, although extensibility decreased as weathering continued.[1]

PP and LDPE microplastics exhibited a decrease in microhardness after being exposed to 37 °C for 18 weeks. Thermolysis and thermo-oxidative degradation at the surface of the plastics can be highlighted as likely causes of the materials' softening. As temperature increases, the formation of radicals is accelerated, and the mobility of the chains increases, which favors depolymerization.[35]In principle, HDPE and PS should exhibit a decrease in microhardness as well, however, in this experiment the results were not significantly different possibly because of the number of replicates and the precision of the instrument.

It must be mentioned that, even though the prepared microplastics tested were floating in the test water, the degradation of those samples by hydrolysis or swelling was not visually observed. This can be explained as polyolefins are very hydrophobic and particularly resistant to hydrolysis, and all four microplastics used are of this nature.

5.4 Environmental implications

The presence of vast amounts of plastic waste in the environment is well known and documented.[2] While the incorporation of primary microplastics in certain commercial goods is increasingly regulated, the break-down and fragmentation of plastic that is already in the environment is an issue that raises many questions. The release of microplastics from bulk plastics has been reported; however, more research is needed to understand the relative importance of environmental factors on the breakdown of microplastics into smaller particles. To study this, we chose PS, PP, LDPE, and HDPE for our experiments. PS is commonly used in food packaging as well as in walls and roofs of housing. PP is used in packaging of commercial products, and plastic furniture. HDPE

and LDPE have a variety of uses, such as containers, grocery bags, and agricultural mulch. Although not all these applications are directly exposed to the environment when used, the mismanagement of plastic waste assures a large fraction of these will end up in the environment.[2]

In this study, we exposed microplastics of commonly used plastics to individual weathering stimuli for 18 weeks. For UV-weathering, we used 23 W m^{-2} of UV and 118 μmol m^{-2} s^{-1} of visible light, however, the visible light portion of this weathering is less significant as the intensity of full sunlight is ~2,000 μmol m^{-2} s^{-1}. The UV exposure is significant, and we estimate that 18 weeks at 23 W m^{-2} is equivalent to 17 months in environmental conditions (assuming 49000 Wh m^{-2} yearly radiant exposure).[23] For the thermal weathering, we chose a temperature of 37 °C which is equivalent to a hot summer day. We estimate that if this temperature is held during 6 hours in a day, 18 weeks at 37 °C is equivalent to 504 hot summer days. For locations on the equator (where the temperature is stable throughout the year), 504 days is the equivalent of 17 months. In locations where seasonal changes of temperature occur, it would take longer to reach 504 days. The temperature of 37 °C is hot for many locations, but it is still relevant, because several locations worldwide frequently experience similar temperatures. It is not straight forward to establish which of the weathering treatments has a higher impact in polymer degradation or release of particles. T-weathering seemed to produce more particles of LDPE and PS, whereas UV-weathering produced more particles of HDPE. However, these results do not necessarily correspond to the measured surface hardness. Both UV- and T-weathered HDPE did not exhibit any significant difference when compared to the pristine prepared microplastic. Similarly, the microhardness of PS increased significantly when exposed to UV-weathering but had no significant change when exposed to T-weathering. The incongruencies are likely linked to microhardness being directly related to the structure of the polymer chains. In contrast, formation of particles can be related to the breakage

of polymer chains and thus the generation of micro-cracks in the bulk material (which can lead to an increased rate of particle formation).[1] However, the fridge-control exhibited no significant release of particles nor a significant change in the surface hardness of the prepared microplastics. Thus, there is a significant role of temperature and UV in the degradation of all four plastics.

While it is difficult to compare between studies due to differences in experimental design, similar degradation of microplastics has been observed that agree with our findings. Biber *et al.* observed that degradation, measured as carbonyl content by FTIR, was greater for PS than PE.[18] Furthermore, Meides *et al.* observed a multi-stage degradation which initially proceeded slowly as photooxidation proceeds at the surface.[1] Eventually, the formation of microcracks and changes to the bulk structure led to an increase in the rate of degradation, measured as changes in the average microparticle size.[1] They indeed observed a decrease in the polymer number-average molecular weight of PS after 2000 h of UV radiation (from 125,000 g mol^{-1} to 3,300 g mol^{-1}).[1] This highlighted the occurrence, at the surface of the samples, of PS chain scissions that result in the polymer chain disentanglement and defects; causing embrittlement of the PS.[1]

Although PS degradation is commonly studied because of this material's sensitivity to UV irradiation (related to the presence of the carbonyl ring), most plastics can degrade in the environment and fragment. Overall, this study shows that all four plastics tested release or break-down into nanoparticles, regardless of changes to the surface hardness of the bulk material. Technology to simultaneously observe and characterize nanoplastics is rapidly being developed, which will allow a more in-depth understanding of the formation dynamics of these small particles. Still, the concern is that these nanoplastics already exist in the environment, where they can be bioavailable and their short- and long-term effects on organisms remain poorly defined.

5.5 Acknowledgements

The authors thank Dr. Kevin Wilkinson for providing access to the NTA, and Dr A. Metafiot for helpful discussions. The authors acknowledge the financial support of the Canada Research Chairs program, a Killam Research Fellowship to NT, the Natural Sciences and Engineering Research Council of Canada, McGill University for a MEDA award to LMH and Rathlyn Fellowship for JG, the Inspired Award for JG, the American Indian Science and Engineering Society scholarship for JG, and the NIB trust for JG. This project was supported partially by a financial contribution from Fisheries and Oceans Canada.

5.6 References

(1) Meides, N.; Menzel, T.; Poetzschner, B.; Löder, M. G. J.; Mansfeld, U.; Strohriegl, P.; Altstaedt, V.; Senker, J. Reconstructing the Environmental Degradation of Polystyrene by Accelerated Weathering. *Environ. Sci. Technol.* **2021**, *55* (12), 7930–7938. https://doi.org/10.1021/acs.est.0c07718.

(2) Alimi, O. S.; Farner Budarz, J.; Hernandez, L. M.; Tufenkji, N. Microplastics and Nanoplastics in Aquatic Environments: Aggregation, Deposition, and Enhanced Contaminant Transport. *Environmental Science & Technology* **2018**. https://doi.org/10.1021/acs.est.7b05559.

(3) Borrelle, S. B.; Ringma, J.; Law, K. L.; Monnahan, C. C.; Lebreton, L.; McGivern, A.; Murphy, E.; Jambeck, J.; Leonard, G. H.; Hilleary, M. A.; Eriksen, M.; Possingham, H. P.; De Frond, H.; Gerber, L. R.; Polidoro, B.; Tahir, A.; Bernard, M.; Mallos, N.; Barnes, M.; Rochman, C. M. Predicted Growth in Plastic Waste Exceeds Efforts to Mitigate Plastic Pollution. *Science* **2020**, *369* (6510), 1515–1518. https://doi.org/10.1126/science.aba3656.

(4) Rillig, M. C.; Kim, S. W.; Kim, T.-Y.; Waldman, W. R. The Global Plastic Toxicity Debt. *Environ. Sci. Technol.* **2021**, *55* (5), 2717–2719. https://doi.org/10.1021/acs.est.0c07781.

(5) Mattsson, K.; Hansson, L.-A.; Cedervall, T. Nano-Plastics in the Aquatic Environment. *Environ. Sci.: Processes Impacts* **2015**, *17* (10), 1712–1721. https://doi.org/10.1039/C5EM00227C.

(6) Bergin, I. L.; Witzmann, F. A. Nanoparticle Toxicity by the Gastrointestinal Route: Evidence and Knowledge Gaps. *International Journal of Biomedical Nanoscience and Nanotechnology* **2013**, *3* (1/2), 163. https://doi.org/10.1504/IJBNN.2013.054515.

(7) Bouldin, J. L.; Ingle, T. M.; Sengupta, A.; Alexander, R.; Hannigan, R. E.; Buchanan, R. A. Aqueous Toxicity and Food Chain Transfer of Quantum DOTs in Freshwater Algae and *Ceriodaphnia Dubia*. *Environ. Toxicol. Chem.* **2008**, *27* (9), 1958–1963.

(8) Lithner, D.; Damberg, J.; Dave, G.; Larsson, Å. Leachates from Plastic Consumer Products – Screening for Toxicity with *Daphnia Magna*. *Chemosphere* **2009**, *74* (9), 1195–1200. https://doi.org/10.1016/j.chemosphere.2008.11.022.

(9) Capolupo, M.; Sørensen, L.; Jayasena, K. D. R.; Booth, A. M.; Fabbri, E. Chemical Composition and Ecotoxicity of Plastic and Car Tire Rubber Leachates to Aquatic Organisms. *Water Research* **2020**, *169*, 115270. https://doi.org/10.1016/j.watres.2019.115270.

(10) Van Cauwenberghe, L.; Claessens, M.; Vandegehuchte, M. B.; Janssen, C. R. Microplastics Are Taken up by Mussels (*Mytilus Edulis*) and Lugworms (*Arenicola Marina*) Living in Natural Habitats. *Environmental Pollution* **2015**, *199*, 10–17. https://doi.org/10.1016/j.envpol.2015.01.008.

(11) Kwak, J. I.; An, Y.-J. Microplastic Digestion Generates Fragmented Nanoplastics in Soils and Damages Earthworm Spermatogenesis and Coelomocyte Viability. *Journal of Hazardous Materials* **2021**, *402*, 124034. https://doi.org/10.1016/j.jhazmat.2020.124034.

(12) Nguyen, B.; Claveau-Mallet, D.; Hernandez, L. M.; Xu, E. G.; Farner, J. M.; Tufenkji, N. Separation and Analysis of Microplastics and Nanoplastics in Complex Environmental Samples. *Accounts of Chemical Research* **2019**, *52* (4), 858–866. https://doi.org/10.1021/acs.accounts.8b00602.

(13) Jakubowicz, I.; Enebro, J.; Yarahmadi, N. Challenges in the Search for Nanoplastics in the Environment—A Critical Review from the Polymer Science Perspective. *Polymer Testing* **2021**, *93*, 106953. https://doi.org/10.1016/j.polymertesting.2020.106953.

(14) Gigault, J.; El Hadri, H.; Nguyen, B.; Grassl, B.; Rowenczyk, L.; Tufenkji, N.; Feng, S.; Wiesner, M. Nanoplastics Are Neither Microplastics nor Engineered Nanoparticles. *Nat. Nanotechnol.* **2021**, *16* (5), 501–507. https://doi.org/10.1038/s41565-021-00886-4.

(15) Hernandez, L. M.; Xu, E. G.; Larsson, H. C. E.; Tahara, R.; Maisuria, V. B.; Tufenkji, N. Plastic Teabags Release Billions of Microparticles and Nanoparticles into Tea. *Environ. Sci. Technol.* **2019**, *53* (21), 12300–12310. https://doi.org/10.1021/acs.est.9b02540.

(16) Lambert, S.; Wagner, M. Characterisation of Nanoplastics during the Degradation of Polystyrene. *Chemosphere* **2016**, *145*, 265–268. https://doi.org/10.1016/j.chemosphere.2015.11.078.

(17) Sait, S. T. L.; Sørensen, L.; Kubowicz, S.; Vike-Jonas, K.; Gonzalez, S. V.; Asimakopoulos, A. G.; Booth, A. M. Microplastic Fibres from Synthetic Textiles: Environmental Degradation and Additive Chemical Content. *Environmental Pollution* **2021**, *268*, 115745. https://doi.org/10.1016/j.envpol.2020.115745.

(18) Biber, N. F. A.; Foggo, A.; Thompson, R. C. Characterising the Deterioration of Different Plastics in Air and Seawater. *Marine Pollution Bulletin* **2019**, *141*, 595–602. https://doi.org/10.1016/j.marpolbul.2019.02.068.

(19) Ranjan, V. P.; Joseph, A.; Goel, S. Microplastics and Other Harmful Substances Released from Disposable Paper Cups into Hot Water. *Journal of Hazardous Materials* **2021**, *404*, 124118. https://doi.org/10.1016/j.jhazmat.2020.124118.

(20) Luo, H.; Zhao, Y.; Li, Y.; Xiang, Y.; He, D.; Pan, X. Aging of Microplastics Affects Their Surface Properties, Thermal Decomposition, Additives Leaching and Interactions in Simulated Fluids. *Science of The Total Environment* **2020**, *714*, 136862. https://doi.org/10.1016/j.scitotenv.2020.136862.

(21) Zhu, L.; Zhao, S.; Bittar, T. B.; Stubbins, A.; Li, D. Photochemical Dissolution of Buoyant Microplastics to Dissolved Organic Carbon: Rates and Microbial Impacts. *Journal of Hazardous Materials* **2020**, *383*, 121065. https://doi.org/10.1016/j.jhazmat.2019.121065.

(22) Alimi, O. S.; Claveau-Mallet, D.; Kurusu, R. S.; Lapointe, M.; Bayen, S.; Tufenkji, N. Weathering Pathways and Protocols for Environmentally Relevant Microplastics and Nanoplastics: What Are We Missing?, 2021.

(23) Sadler, G. W. Ultraviolet Radiation at Edmonton, Alberta, Canada. *Solar Energy* **1992**, *49* (1), 13–17. https://doi.org/10.1016/0038-092X(92)90121-P.

(24) Diffey, B. L. Sources and Measurement of Ultraviolet Radiation. *Methods* **2002**, *28* (1), 4–13. https://doi.org/10.1016/S1046-2023(02)00204-9.

(25) Raval, N.; Maheshwari, R.; Kalyane, D.; Youngren-Ortiz, S. R.; Chougule, M. B.; Tekade, R. K. Importance of Physicochemical Characterization of Nanoparticles in Pharmaceutical Product Development. In *Basic Fundamentals of Drug Delivery*; Elsevier, 2019; pp 369–400. https://doi.org/10.1016/B978-0-12-817909-3.00010-8.

(26) Chamas, A.; Moon, H.; Zheng, J.; Qiu, Y.; Tabassum, T.; Jang, J. H.; Abu-Omar, M.; Scott, S. L.; Suh, S. Degradation Rates of Plastics in the Environment. *ACS Sustainable Chem. Eng.* **2020**, *8* (9), 3494–3511. https://doi.org/10.1021/acssuschemeng.9b06635.

(27) Noda, I.; Dowrey, A. E.; Haynes, J. L.; Marcott, C. Group Frequency Assignments for Major Infrared Bands Observed in Common Synthetic Polymers. In *Physical Properties of Polymers Handbook*; Mark, J. E., Ed.; Springer New York: New York, NY, 2007; pp 395–406. https://doi.org/10.1007/978-0-387-69002-5_22.

(28) Vilaplana, F.; Ribes-Greus, A.; Karlsson, S. Degradation of Recycled High-Impact Polystyrene. Simulation by Reprocessing and Thermo-Oxidation. *Polymer Degradation and Stability* **2006**, *91* (9), 2163–2170. https://doi.org/10.1016/j.polymdegradstab.2006.01.007.

(29) Jung, M. R.; Horgen, F. D.; Orski, S. V.; Rodriguez C., V.; Beers, K. L.; Balazs, G. H.; Jones, T. T.; Work, T. M.; Brignac, K. C.; Royer, S.-J.; Hyrenbach, K. D.; Jensen, B. A.; Lynch, J. M. Validation of ATR FT-IR to Identify Polymers of Plastic Marine Debris, Including Those Ingested by Marine Organisms. *Marine Pollution Bulletin* **2018**, *127*, 704–716. https://doi.org/10.1016/j.marpolbul.2017.12.061.

(30) Chércoles Asensio, R.; San Andrés Moya, M.; de la Roja, J. M.; Gómez, M. Analytical Characterization of Polymers Used in Conservation and Restoration by ATR-FTIR Spectroscopy. *Anal Bioanal Chem* **2009**, *395* (7), 2081–2096. https://doi.org/10.1007/s00216-009-3201-2.

(31) Gulmine, J. V.; Janissek, P. R.; Heise, H. M.; Akcelrud, L. Polyethylene Characterization by FTIR. *Polymer Testing* **2002**, *21* (5), 557–563. https://doi.org/10.1016/S0142-9418(01)00124-6.

(32) Gijsman, P. P. The Long-Term Stability of Polyolefins. **1994**. https://doi.org/10.6100/IR427216.

(33) Jordan, A. M.; Kim, K.; Soetrisno, D.; Hannah, J.; Bates, F. S.; Jaffer, S. A.; Lhost, O.; Macosko, C. W. Role of Crystallization on Polyolefin Interfaces: An Improved Outlook for Polyolefin Blends. *Macromolecules* **2018**, *51* (7), 2506–2516. https://doi.org/10.1021/acs.macromol.8b00206.

(34) Castro Monsores, K. G. de; Silva, A. O. da; Sant' Ana Oliveira, S. de; Weber, R. P.; Filho, P. F.; Monteiro, S. N. Influence of Ultraviolet Radiation on Polystyrene. *Journal of Materials Research and Technology* **2021**, *13*, 359–365. https://doi.org/10.1016/j.jmrt.2021.04.035.

(35) McKeen, L. W. Introduction to the Effect of Heat Aging on Plastics. In *The Effect of Long Term Thermal Exposure on Plastics and Elastomers*; Elsevier, 2014; pp 17–42. https://doi.org/10.1016/B978-0-323-22108-5.00002-3.

Preface to Chapter 6

There are several limitations when identifying and characterizing microplastics. Samples are simpler to characterize when the particles released are of one specific polymer nature (Chapters 3, 4, and 5). However, most environmental samples will have particles composed of a wide variety of polymers. the research field has developed quickly, and new techniques to simultaneously characterize several plastic particles are emerging. One of the most commonly used techniques is pyrolysis coupled with gas chromatography and mass spectroscopy (Py-GC-MS). This technique allows for the simultaneous identification of plastics in environmental samples with low organic contamination. However, the literature has no uniformity in the analysis of samples with Py-GC-MS. While some authors chose to confirm a polymer is present with one identifying ion, others use two or more. This results in a lack of standardization of the data analysis.

In this project, we propose a rigorous scoring system that allows the assignment of a numerical value to the match between the environmental sample and the polymer library. We tested this system with drinking water and Arctic water samples. Results show that various polymers were identified, while others could not be confirmed because the match was below the set threshold. This study is in preparation to be submitted to the *Journal of Hazardous Materials* for publication.

Chapter 6: Detection of widespread microplastics using pyrolysis gas chromatography-mass spectrometry

Abstract

Identification and quantification of microplastics in the environment have become a technology challenge. Fourier Transform microscopy and Raman microscopy are most often used for identifying microplastics, however, these techniques pose certain limitations with regards to throughput and the need to select a sub-sample for analysis. Thermal methods have been explored more recently as they present the possibility to analyze for multiple microplastics simultaneously. In this work, pyrolysis coupled with gas chromatography and mass spectroscopy with single ion monitoring is used to search for twelve polymer microplastics in drinking water samples and Arctic waters. Both types of samples present a low organic matter content which allows for simplification of sample preparation (i.e. filtration only). Polymers were identified in the samples by using a point system to match their characteristic pyrolysis products with bulk plastics. On-site blanks, procedural blanks, and negative controls were performed and showed no detectable presence of any of the polymers. The limit of detection for the Py-GC-MS used was found to be between 0.005-0.05 ng under ideal conditions (no organic matrix or other contaminants).

6.1 Introduction

The world's plastic production has reached 348 million tons in 2017.[1,2] In most of the world, the mismanagement of plastic has led to an environmental worldwide contamination of plastic. Literature has been flooded with studies that identify microplastics in the environment, attempt to quantify them, and evaluate the impact these are having on individual species and ecosystems.

There is strong evidence that supports that macro-sized plastics in the environment will eventually break down into microplastics.[3,4] The further degradation of these microplastics is likely to result in small microplastics and nanoplastics.

Fourier transform infrared microspectroscopy (μ-FTIR) and Raman microscopy (μ-Raman) are the most common analytical techniques used to identify microplastics in the environment. [5–8] μ-FTIR uses the molecular vibrations induced by absorption of infrared light, whereas μ-Raman is based on inelastic scattering of photons. The main advantage of these techniques is that the number of particles, shape, and chemical composition can be identified. Both techniques can detect particles down to a couple of micrometers; however, these detection limits are only achieved under ideal conditions and are difficult to obtain with environmental samples. Multi-step sample processing that may include digestions, depositions on substrates, multiple filtrations, etc. is often needed. With each processing step, the probability of contamination of the sample increases. Therefore, these methods are not ideal for the characterization of small microplastics. Additionally, these techniques can only be applied to pre-selected particles or by performing a scan on a filter after multiple steps of treatment[9]. There is a need for equipment that would be able to both quantify and characterize small micro- and nanoplastics. However, the perfect technique is not available in the market at present.

The ability of Pyrolysis-gas chromatography-mass spectrometry (Py-GC-MS) to characterize the chemical composition of small microplastics in environmental samples has been less explored. This technique has been used to identify pre-selected particles (as is the case for μ-FTIR and μ-Raman),[10,11] but it has the advantage that it can also identify multiple polymers in a single sample.[9,12,13] This technique is highly sensitive and therefore can be used to identify microplastics

in relatively clean matrices with simple sample processing. In more complex matrices with higher organic content, additional sample preparation steps such as digestions might be needed.[14,15]

There are three common pyrolyzers used to identify polymers: Curie-Point, micro furnace, and coil. They differ in the way a sample is introduced and pyrolyzed. In Curie-Point pyrolysis, the sample is placed in a ferromagnetic foil which is placed in an induction pyrolyzer. The disadvantage of this technique is the restricted sample capacity and the risk of sample loss during transfer[9]. In micro furnace pyrolysis, the sample is placed in a stainless-steel cup and later inserted into a preheated furnace. Lastly, in coil pyrolysis, the sample is inserted into a quartz tube which is later placed inside a coil that will perform the pyrolysis. Quantification with Py-GC-MS is highly dependent on the type of pyrolyzer. Fischer *et al.* studied the reliability of microplastic quantification using a Curie-Point pyrolyzer and a micro furnace pyrolyzer.[9] Their findings showed that micro furnace pyrolysis results were reproducible and reliable, with the additional advantage of having a larger sample chamber.[9] However, in the present study, a coil pyrolyzer was the available technique to process samples. First steps for quantification were made, however, more experiments are needed to confirm reproducibility.

Various techniques can be used to increase the signal detected in the MS. For instance, decreasing the split ratio allows for more pyrolysis products to enter the GC-MS. However, a low split ratio (lower split ratio means higher volume of sample entering the GC-MS), is likely to cause deposition on the MS and increase the frequency of reparations of the equipment. Another method to increase the signal is cryogenic focusing. In this method, the pyrolysis products are cooled in a chamber, narrowing the chromatographic band and improving the detection limit. This technique is not always convenient as it requires additional accessories for the Py-GC-MS and the use of liquid nitrogen or CO_2 gas. A more convenient alternative is the use of single ion monitoring (SIM)

in which only certain ions (selected by the user) are recorded in the MS, subtracting significant background noise and hence enhancing the signal. The drawback of using SIM is that the user will determine what polymers are of interest and information about other polymers may be lost.

The final step of Py-GC-MS is data processing. Data processing is not trivial, as there is no uniform method in literature for the analysis of polymers. Pyrolysis of a polymer produces characteristic products that can be confirmed by the presence of indicator ions in the MS results at specific retention times. The metrics for confirming and identifying polymers are not well agreed upon. Reports have used one indicator ion, or multiples. Some authors propose that with one matched indicator ion a characteristic pyrolysis product can be confirmed.[14,15] Other authors necessitate the presence of at least two indicator ions to confirm the identity of a characteristic pyrolysis product.[9] To complicate things further, some authors identify the presence/absence of a polymer by monitoring only one characteristic pyrolysis product[14,15], while others select two (or more) characteristic pyrolysis products[9,16]. On the other hand, some only confirm the presence/absence of a polymer when all characteristic pyrolysis products are present. The rigidity or flexibility of the analysis is highly dependent on the type of sample analyzed, however, there is a need for standardization. This work presents a technique in which a score is assigned to each pyrolysis product depending on the presence and intensity of its identifying ions. Then a percentage match is calculated by comparing the sample score to the perfect score (from a commercial bulk plastic). The presence of a polymer is confirmed when the percentage match is ≥83.3%. We chose 83.3% as it is the maximum score that allows for a three characteristic pyrolysis product of a polymer to have one partial match (0.5 points) and 2 full matches (1 point each). Therefore, giving it a score of 2.5 out of 3 possible points, which gives a percentage match of 83.3%.

In this work, we used a coil pyrolyzer coupled to a GC-MS to characterize the small microplastic (1-106 µm) content of drinking waters and Arctic waters. These two types of samples are relatively clean matrices, which simplified sample preparation. We also characterized commercial polystyrene nanoplastics to evaluate the sensitivity of the Py-GC-MS and attempt quantification.

6.2 Materials and Methods

6.2.1 Commercial bulk plastics to create polymer library and evaluate the sensitivity of the equipment

Commercial samples of bulk plastics and nanoplastics were pyrolyzed to produce a polymer library (Table 6.1). Although commercial libraries exist, the results will vary due to instrumental variations of different Py-GC-MS systems. The NIST library was used to verify the results and to match ions with pyrolysis products, however, the retention times were taken from the library we built. The characteristic pyrolysis products for each polymer were obtained from the literature (Table 6.2). Additionally, different masses of PS nanoparticles were pyrolyzed to determine the sensitivity of the equipment. This was also the first attempt to evaluate the possibility to relate the signal to the mass for quantification purposes.

6.2.1.1 Bulk plastics

Samples of common plastics (Table 6.1) were pyrolyzed at 500 °C to determine the characteristic mass spectrum of each plastic. Briefly, 0.1-0.2 mg of plastic (Table 6.1) was placed in a quartz pyrolysis tube (dimensions: 25 mm length, 1.9 mm internal diameter, CDS Analytical) using stainless steel tweezers. A small quantity of quartz wool (Chromatographic Specialties) was also inserted into both ends of the tube to ensure the plastic did not fall out of the tube. The tube was then pyrolyzed at 500 °C for 20 s using a ¼ inch probe (GERSTEL Twister automatic pyrolysis

unit). The pyrolysis products were introduced with a 1:25 split ratio into a Thermo TRACE 1300 series gas chromatographer (GC) at 200 °C with a fused silica column of length 50 m (internal diameter 0.2 mm, UNSPSC code: 41115710) using helium as the carrier gas. This was coupled to a Thermo ITQ-MS 1100 GC programmed with a constant temperature ramp from 50 °C to 350 °C over 32 minutes. Each pyrogram was analyzed using the XCalibur software to find the characteristic pyrolysis products and determine their retention time. It was not possible to find a sample for Kraton, however, the work of Klee and Chang was taken as a reference for the characteristic pyrolysis products, indicator ions, and retention time.[17]

Table 6.1. Common plastics were chosen to generate a small library of bulk plastics. These standards served as references when analyzing environmental samples. The plastics chosen were determined based on other studies where larger plastics were identified in drinking water using FTIR (Chapter 7).

Bulk plastic	Mass inserted in quartz tube (mg)	Source
Polystyrene (PS)	0.1246	Polystyrene sheet- McMaster Carr (8734k39)
High density polyethylene (HDPE)	0.1542	High density polystyrene sheet- McMaster Carr (8619k427)
Low density polyethylene (LDPE)	0.1341	Low density polystyrene sheet- McMaster Carr (8657k811)
Polyvinyl chloride (PVC)	0.1774	PVC sheet- McMaster Carr (87545K73)
Polycarbonate (PC)	0.1414	Polycarbonate sheet- McMaster Carr (8574K281)
Polyethylene terephthalate (PET)	0.1901	Polyester Film- McMaster Carr (8567K102)
Rayon	0.1102	Rayon cotton from tipped applicators- Fisher (22-025-205)
Cellulose acetate	0.1749	Cellulose acetate spheres- Cospheric (CAS-ALA-1.3 1.41+/-0.05mm-100)
Kraton	N/A	N/A
Cellulose	0.1461	Softwood kraft pulp sheets (Domtar, Canada)
Polypropylene (PP)	0.1213	Polypropylene sheet- McMaster Carr (8742k831)
Nylon	0.1341	Nylon 6 pellet- Sigma Aldrich (181110)
Polymethyl methacrylate (PMMA)	0.1210	PMMA powder (average M_W ~350,000)-Sigma Aldrich (445746)

The resulting spectra of the bulk plastics were used to determine the retention time of each characteristic pyrolysis product (Table 6.2). A full mass scan was collected as well as three single ion monitoring (SIM) scans (Table 6.3). The SIM scans were used to enhance the signal of ions of interest and were chosen based on the most common plastics and fibers. SIM scans were especially useful to identify the signal of polymers present in environmental samples. The indicator ions and retention times obtained from the bulk plastic samples were compared to the environmental samples to evaluate the presence or absence of plastics.

Table 6.2. Common plastics and fibers and their characteristic pyrolysis products. Each characteristic pyrolysis product is identified by its indicator ions at the retention time. Only indicator ions with mass above 50 were considered to preserve the integrity of the MS detector (the instrument was tuned between 50-250 amu). We did not observe notable differences between the pyrograms of HDPE and LDPE, therefore we consolidated these two materials into simply polyethylene (PE).

Plastic	Characteristic pyrolysis product(s)	Indicator ions (m/z)	Approximate retention time (± 1 min)
Polystyrene [(1)] **(PS)**	styrene	78, 104	9
	3-butene-1,3-diyldibenzene	91, 208	21
	5-hexene-1,3,5-triyltribenzene	91, 207	23
Polyethylene [(1)] **(PE)**	alkenes	85, 99	20
	α-alkenes	83, 97	19
	α,ω-alkenes	82, 95	23
Polyvinyl chloride [(1)] **(PVC)**	benzene	78	4
	chlorobenzene	77, 112	8
Polycarbonate [(1)] **(PC)**	p-methoxy-tert-butylbenzene	149, 164	16
	2,2-bis(4′-methoxy-phenyl)propane	241, 256	26
Polyethylene terephthalate [(1)] **(PET)**	dimethyl terephthalate	163, 194	21
Rayon [(2)]	furfural	95/96	7
	2-furanmethanol	53, 69, 81, 97/98	8
	2-furancarboxaldehyde, 5-methyl-	53, 109/110	10
	5-hydroxymethylfurfural	69, 97, 126	20
Cellulose acetate [(3)]	acetic acid	60	4
	2-hydroxyethyl acetate	73	6
	4,6-dimethyl-2H-pyran-2-one	53, 81, 96	10
	unidentified	114	16
	unidentified	82	17
Kraton [(4)]	isoprene	53, 67/68	4
	styrene	78, 104	9
	limonene	68, 93, 107, 136	11
Cellulose [(3)]	hydroxyacetaldehyde	60	5
	5-(hydroxymethyl)dihydro-2(3H)-furanone	58, 114	13
	5-(hydroxymethyl)-2-furfural	97, 126	15
Polypropylene [(1)] **(PP)**	2,4-dimethylhept-1-ene	70, 126	8
	2,4,6,8-tetramethyl-1-undecene	69, 111	16
	2,4,6,8-tetramethyl-1-undecene	69, 111	19
	2,4,6,8-tetramethyl-1-undecene	69, 111	22
Nylon [(1)]	ε-Caprolactam	85/84, 113	15
	N-methyl ε-caprolactam	70, 127	18
Polymethyl methacrylate [(1)] **(PMMA)**	methyl acrylate	55, 85	5
	methyl methacrylate	69, 100	7

(1) [18]
(2) [19]
(3) [20]
(4) [17]

Table 6.3. Single ion monitoring (SIM) groups used in this study.

SIM Group	Plastics and fibers	Mass of ions (ranges) for each SIM
SIM 1	Polystyrene (PS)	75.50 – 92.50
	Polyethylene (PE)	94.00 – 114.00
	Polyvinyl chloride (PVC)	204.50 – 209.50
SIM 2	Polyethylene terephthalate (PET)	147.00 – 167.00
	Polycarbonate (PC)	192.50 – 195.50
		238.00 – 256.00
SIM 3	Rayon	50.50 – 75.50
	Cellulose acetate	76.00 – 96.00
	Kraton	92.50 – 117.50
	Cellulose	123.50 – 138.50
	Polypropylene (PP)	
	Nylon	
	Polymethyl methacrylate (PMMA)	

6.2.1.2 Commercial micro and nanobeads

Polystyrene commercial nanobeads were analyzed to evaluate the Py-GC-MS sensitivity as well as to correlate the peak signal (intensity) with the mass analyzed. 25 µL of several dilutions of 20 nm PS beads were deposited into a quartz tube. The volume and concentrations were used to calculate the mass of nanoparticles deposited. The tube was then left to dry and later injected into the Py-GC-MS. The area under the peak for the styrene pyrolysis product (retention time: ~9 minutes) was recorded (Figure 6.1).

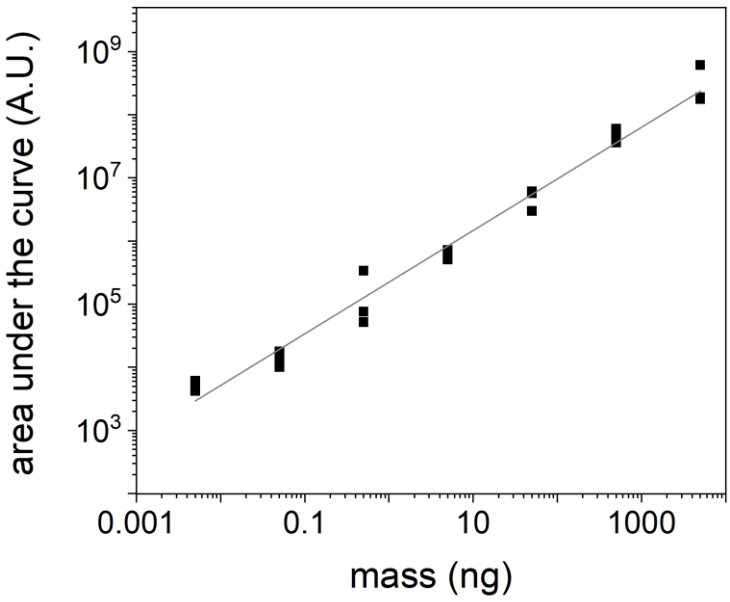

Figure 6.1. 0.005 ng to 5000 ng of 20 nm commercial PS nanobeads were analyzed using Py-GC-MS. Using the XCalibur software the area under the curve for the styrene peak was calculated with an ICIS integration algorithm. The area under the curve was plotted in a log-log scale to show the correlation with the mass of plastic. Samples were analyzed in triplicate.

The results in Figure 6.1 show that the GC/MS can detect down to 0.005-0.05 ng of commercial PS beads. However, it is important to note that this detection was achieved under ideal conditions, as the PS beads were diluted with reverse osmosis (RO) water. In environmental samples, the conditions will surely not be ideal. Therefore, the limit of detection obtained represents a best-case scenario. Future experiments should use matrices that more closely simulate environmental water samples such as water containing NOM, moderately hard reconstituted water, or other alternatives that would be more environmentally relevant.

Figure 6.1 shows a high correlation between signal (area under the curve) and mass of nanoparticles. However, because in this work we attempt to analyze environmental samples, more experiments are required before we can reliably quantify. These further experiments should include the addition of organic matter, salts, simulated seawater, and other possible contaminants which might be present in trace amounts.

6.2.2 Environmental samples

Two types of environmental samples were analyzed with Py-GC-MS. The first included effluent and distribution line waters that had been previously processed by a drinking water treatment plant (DWTP). The second was surface Arctic waters. Both samples are relatively clean in terms of organic matter and anthropogenic contamination when compared to other environmental samples and thus digestion was not needed.

6.2.2.1 Sampling campaign at drinking water treatment plants (DWTPs)

Five locations of DWTPs across eastern Canada were sampled between May and October 2019. Cotton lab coats and cotton sleeves (during sampling) were used throughout the project to avoid plastic fiber contamination from clothing. Water was sampled in 1 L glass bottles with PTFE lined polypropylene caps (1L Fisherbrand™ Certified Cleaned Straight Sided Bottles, 02-912-313, Fisher). Before use, beakers and bottles were washed with soap (sodium carbonate 10 to 25% and sodium dodecylbenzenesulfonate 1 to 10% and nonionic detergent 1 to 10%, Fisherbrand™ Sparkleen™ 1 Detergent, Fisher) and tap water, triple rinsed with DI water, and lastly, rinsed with acetone in a laminar flow biosafety cabinet (BSC) to avoid contaminant carryover. All instruments (e.g., tweezers, glassware, funnels) were rinsed with acetone (A18-4,

glass bottles, Fisher) in the BSC between samples. Moreover, all filtration steps were conducted in the BSC which was previously cleaned with acetone.

Five drinking water treatment plants (DWTPs) in Canada were sampled between May and October 2019.

- Location 1 (L1): Sampled on May 23rd, 2019.
- Location 2 (L2): Sampled on June 26, 2019.
- Location 3 (L3): Sampled on May 3rd, 2019.
- Location 4 (L4): Sampled on September 16, 2019.
- Location 5 (L5): Sampled on October 3rd, 2019.

The water tap was left open for at least ten minutes before sampling. A sampling bottle was carefully opened, paying attention to not touch the inside of the bottle, and placed directly below the tap. The bottle was filled to overflowing and then emptied. This step was performed twice. The third time, before the bottle was full (approximately 800 mL), it was removed from under the tap and sealed carefully. This procedure was done for two waters at different points of the DWTP process. The effluent water (E) is the outlet of the DWTP after water has been treated, whereas the distribution line water (D) was sampled at a water outlet in a nearby location downstream of the DWTP. Three bottles were sampled for each location. All samples were kept at 4°C until they were prepared for Py-GC-MS.

6.2.2.1.1 Preparation of blanks for DWTP

Two field blanks were performed for each condition (named respectively E-BLK and D-BLK) to account for the contamination in the air during the sampling. These blanks were used to measure

the background levels of particles present in the air which could potentially deposit in the bottles during the sampling. The caps of three BLK bottles were opened and the bottles were placed on a counter near the sampling tap, but not directly below it (no water was introduced into the BLK bottles). The open bottles were left open for the duration of one sample collection (30 seconds to 1 min depending on the water flow rate) and then sealed. Inside a BSC, the field blanks were filled with 800 mL of ultra-pure LC-MS water. After filling the bottles, the field blanks are processed for Py-GC-MS (same procedure as the samples). Therefore, the field blanks account for both the field contamination as well as the processing contamination. All blanks were kept at 4°C until they were prepared for Py-GC-MS.

Contamination from the LC-MS/bottle blanks was also evaluated (herein termed Py-BLK). 800 mL of LC-MS water was poured into a clean virgin glass bottle following the same procedure as with the samples to assess the contamination that could occur during sample processing in the laboratory. This blank was performed in duplicate. The Py-BLK was kept at 4°C until it was prepared for Py-GC-MS.

Additionally, two empty quartz tubes (herein termed “empty tube”) and two tubes with unused glass fiber filters (herein termed “clean filter”) were pyrolyzed to account for possible contamination coming from the quartz tubes or the glass fiber filters. Both the empty tube and clean filter controls were assembled when performing the Py-GC-MS, therefore no storage was required.

6.2.2.2 Arctic water sampling

The samples were collected from the Amundsen expedition ship in the summer of 2017 (Table 6.4). Replicates of these samples was used by Huntington *et al.* in their work, where particles >~100 µm were identified.[21] In the present work, we chemically analyzed particles < 106 µm.

The location (coordinates and name of the station), any extraordinary circumstances, and the type of clothes worn while sampling was recorded for each sample. A mustang neoprene suit was worn to sample unless otherwise specified in the notes (Table 6.4). Approximately 25 L (exact volume recorded per sample) of surface water was collected using stainless steel buckets. The water was then filtered on a 140 mm diameter polycarbonate filter (EMD Millipore Isopore™ TCTP14250, Fisher) with a 10 µm pore size. All samples were kept at 4°C until processing was performed.

A field blank was taken (AR-BLK), in this case, 25 L of filtered water was re-filtered through the setup (on the ship) simulating a real sample. The blank was later processed using the same procedure as for the samples.

In the laboratory, particles were detached from the original filters by placing half of the filter into a clean 500 mL glass beaker (previously cleaned by triple rinsing with RO and acetone) containing 300 mL LC-MS water. This process was performed in a BSC with laminar flow, the beaker was then covered with aluminum foil to prevent contamination, sonicated for 120 minutes, and allowed to settle for 5 minutes. Following this, the filter was carefully removed with clean steel tweezers in the BSC, and the resulting sample was stored in a clean glass jar with a PTFE lined lid at 4°C until it was prepared for Py-GC-MS.

Table 6.4. Information regarding section of the Amundsen cruise, station ID where samples were taken, exact location (latitude and longitude), and the volume filtered. Samples were taken wearing only a neoprene suit unless otherwise specified in the notes. Samples 2B-5 and 2B-11 are missing due to procedural or processing mistakes on the ship and/or laboratory.

SAMPLE ID	LEG OF AMUNDSEN	STATION ID	LATITUDE LONGITUDE	VOLUME OF SAMPLE (L)	NOTES TAKEN AT CRUISE
AR-BLK	2A	684	61º 47.35N 71º 55.01W	8	done with filtered freshwater
2A-1	2A	736	58º 25.77 N 78º 18.00W	38	n/a
2A-2	2A	720	60º 41.89N 78º 33.56W	38	filter clogged
2A-3	2A	694	61º 24.0982N 78º 42.6972W	20	leaks
2A-4	2A	688	62º 22.0237N 74º 39.6997W	28	n/a
2A-5	2A	682	61º 02.56N 69º 42.87W	25.5	filter clogged
2A-6	2A	676	60º 07.56N 69º 03.45W	33	n/a
2A-7	2A	670	58º 59.36N 67º 56.25W	36.6	n/a
2B-1	2B	OFB14	62º 23.0085N 66º 1.6396W	38.5	clothes were leaky black cotton
2B-2	2B	180	67º 25.1888N 61º 22.2734W	37.25	n/a
2B-3	2B	Disko fan	67º 58.052N 59º 30.199W	35.5	purple cotton and Nylon
2B-4	2B	BB2	72º 46.108N 67º 0.271W	37	black cotton and polyester
2B-6	2B	129	78º 19.560 N 74º 8.156W	38.5	n/a

2B-7	2B	323	74º 9.6905N 80º 27.0193W	37	black cotton
2B-8	2B	Pond inlet	72º 49.6795N 77º 36.5908W	30	filter clogged
2B-9	2B	Resolute	74º 43.6815N 95º 7.6835W	37	helicopter operations
2B-10	2B	QMG-M	68º 18.1649N 101º 44.589W	37.5	n/a
2B-12	2B	312	69º 10.227N 100º 42.252W	37.5	n/a
2B-13	2B	3.7	72º 05.764N 96º 02.645 W	37	white/purple fleece
2B-14	2B	3.5	70º 26.197N 91º 14.179W	37.5	n/a
2B-15	2B	1.1	65º 09.304N 81º 21.269W	38	red cotton, purple fleece

Figure 6.2. Map showing the pinned locations where surface water was sampled on the Amundsen expedition ship.

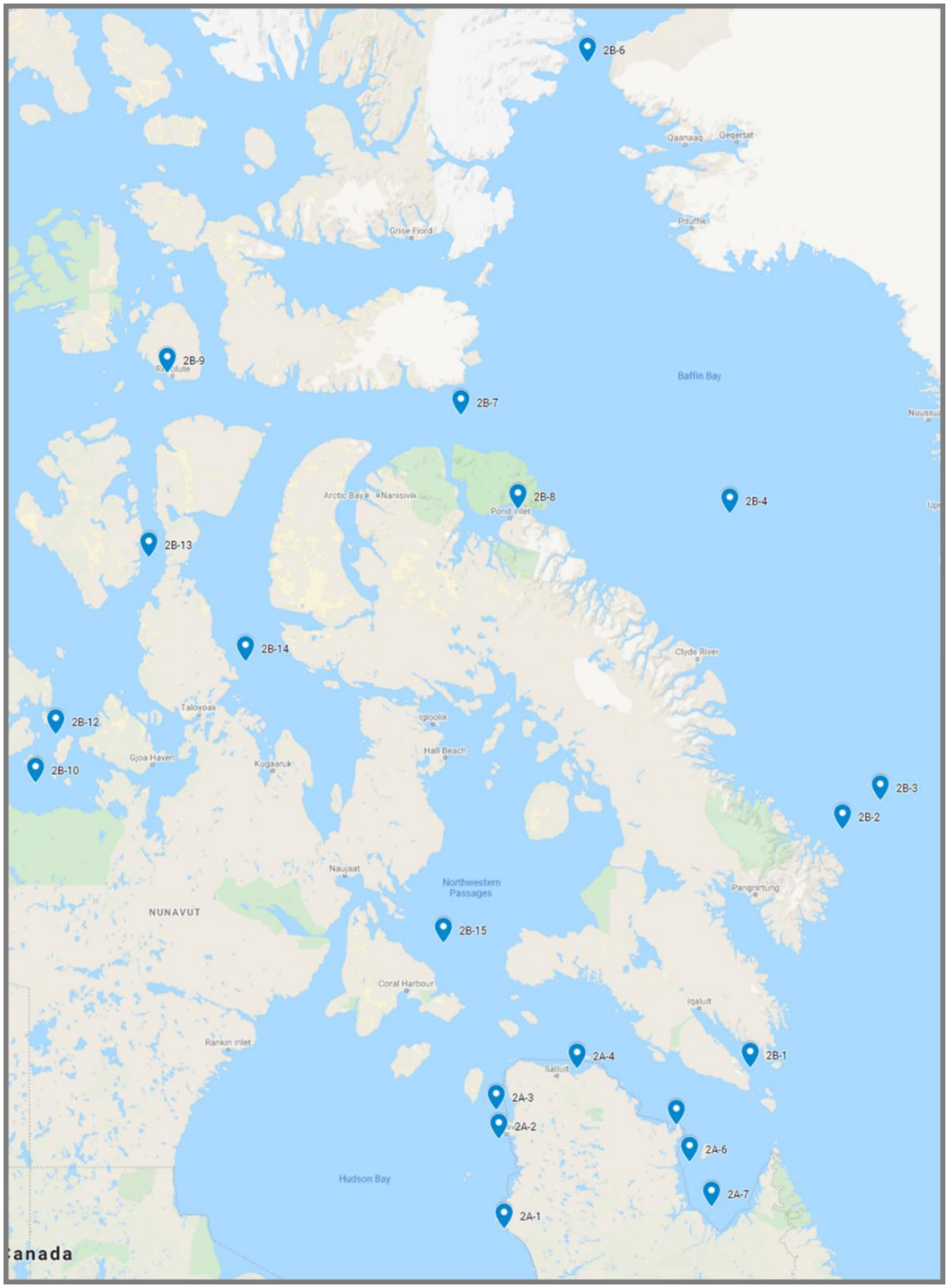

6.2.2.3 Preparation of samples for Py-GC-MS analysis and injection

The preparation procedure was performed in a BSC with laminar flow. DWTP samples, Arctic samples, and their respective controls were processed for Py-GC-MS in the same way. Each sample was sieved using a 106 µm size mesh (Fisherbrand™ U.S. Standard Stainless Steel Sieves, 8 in. dia. x 2 in. diameter, 106 um pore size, 04-881-10Z, Fisher) to remove particles >106 µm. The sieved water was then vacuum filtered through a 21 mm diameter Whatman glass microfiber filter (pore size = 1.5 µm) on a ceramic Büchner funnel using a glass separation funnel which slowly introduced the sample onto the glass fiber filter to prevent accumulation of liquid on the filter or sides of the funnel during filtration, which could result in particle losses. After filtering the sample, the filter was left to dry in a glass Petri dish for 48 hours in a BSC.

For some Arctic samples, the filter would clog before the volume of the whole sample could be filtered. When this occurred, the filter was removed and replaced by a new filter. This filter replacement was repeated until all liquid was filtered. Filters of the same sample (sub-sample filters) were labelled with the sample ID and an increasing numeral (e.g. 2A-1-1, 2A-1-2, etc.). A maximum of two filters per sample were analyzed by Py-GC-MS.

Dried filters were inserted into a quartz pyrolysis tube (dimensions: 25 mm length, 1.9 mm internal diameter, CDS Analytical) using clean stainless-steel tweezers. The samples were pyrolyzed in the same condition as the bulk plastics were pyrolyzed. The Py-GC-MS was programmed to collect a total mass scan followed by the three SIM scans (Table 6.3).

6.2.2.4 Analysis of Py-GC-MS data

Each pyrogram was analyzed using the XCalibur deconvolution software for mass spectra. The indicator ions which confirm the presence of the bulk plastic standards injected were found in the

literature (Table 6.2). The pyrograms of the bulk plastics were analyzed for the indicator ion retention times (Table 6.2). Note that retention time is highly dependent on the system, thus this highlights the need for reference materials. Each sample's spectra were compared to the bulk plastic injected using the same instrument conditions.

Each sample was analyzed for the indicator ions and retention times of the bulk plastics. Pyrolysis products were assigned a score depending on the level of coincidence for their indicator ions. A perfect match (green = 1 point) was given when all indicator ions were present at the correct retention time (see Table 6.2) and with a m/z signal at least 15% above the baseline. A partial match (yellow = 0.5 points) was given when the retention time of one of the pyrolysis products was shifted (within one minute of the target time).. Another partial match (yellow = 0.5 points) was given when the m/z signal was weak (only 5-15% above the baseline). No match (orange = 0 point) was given in any other scenario. The presence of a certain polymer was confirmed when at least one of the triplicates (DWTP samples) or sub-sample filters (Arctic water samples) had a percentage match ≥83.3% when compared with the bulk plastics. Note that the bulk plastics had a perfect match (1 point) for all indicator ions.

6.3 Results

6.3.1 DWTP waters can contain plastics

The chemical composition of particles 1.5-106 μm were analyzed for the effluent and distribution line samples for all locations using Py-GC-MS to identify their chemical nature. Detailed results of each characteristic pyrolysis product found can be seen in Tables 6.5-6.9. Each pyrolysis product was assigned a score: green= 1 (perfect match), yellow= 0.5 (partial match), and orange= 0 points (no match).

Table 6.5. Detailed Py-GC-MS results of SIM 1 for each replicate of DWTP samples.

polymers		polystyrene			polyethylene		polyvinyl chloride		
pyrolysis products		styrene	3-butene-1,3-diyldibenzene	5-hexene-1,3,5-triyltribenzene	alkenes	α-alkenes	α,ω-alkenes	benzene	chlorobenzene
L1-E	1								
	2								
	3								
L1-E-BLK	1								
	2								
L1-D	1								
	2								
	3								
L1-D-BLK	1								
	2								
L2-E	1								
	2								
	3								
L2-E-BLK	1								
	2								
L2-D	1								
	2								
	3								
L2-D-BLK	1								
	2								
L3-E	1								
	2								
	3								
L3-E-BLK	1								
	2								
L3-D	1								
	2								
	3								
L3-D-BLK	1								
	2								
L4-E	1								
	2								
	3								
L4-E-BLK	1								
	2								
L4-D	1								
	2								
	3								
L4-D-BLK	1								
	2								
L5-E	1								
	2								
	3								
L5-E-BLK	1								
	2								
L5-D	1								
	2								
	3								
L5-D-BLK	1								
	2								
Py-BLK	1								
	2								
CLEAN FILTER	1								
	2								
EMPTY TUBE	1								
	2								

Table 6.6. Detailed Py-GC-MS results of SIM 2 for each replicate of DWTP samples.

polymers		polycarbonate		polyethylene terephthalate
pyrolysis products		p-methoxy-tert-butylbenzene	2,2-bis(4′-methoxy-phenyl)propane	dimethyl terephthalate
L1-E	1			
	2			
	3			
L1-E-BLK	1			
	2			
L1-D	1			
	2			
	3			
L1-D-BLK	1			
	2			
L2-E	1			
	2			
	3			
L2-E-BLK	1			
	2			
L2-D	1			
	2			
	3			
L2-D-BLK	1			
	2			
L3-E	1			
	2			
	3			
L3-E-BLK	1			
	2			
L3-D	1			
	2			
	3			
L3-D-BLK	1			
	2			
L4-E	1			
	2			
	3			
L4-E-BLK	1			
	2			
L4-D	1			
	2			
	3			
L4-D-BLK	1			
	2			
L5-E	1			
	2			
	3			
L5-E-BLK	1			
	2			
L5-D	1			
	2			
	3			
L5-D-BLK	1			
	2			
Py-BLK	1			
	2			
CLEAN FILTER	1			
	2			
EMPTY TUBE	1			
	2			

Table 6.7. Detailed Py-GC-MS results of SIM 3 for each replicate of DWTP samples (rayon and cellulose acetate).

polymers		rayon				cellulose acetate				
pyrolysis products		furfural	2-furanmethanol	2-furancarboxaldehyde, 5-methyl-	5-hydroxymethylfurfural	acetic acid	2-hydroxyethyl acetate	4,6-dimethyl-2H-pyran-2-one	unknown peak 1	unknown peak 2
L1-E	1									
	2									
	3									
L1-E-BLK	1									
	2									
L1-D	1									
	2									
	3									
L1-D-BLK	1									
	2									
L2-E	1									
	2									
	3									
L2-E-BLK	1									
	2									
L2-D	1									
	2									
	3									
L2-D-BLK	1									
	2									
L3-E	1									
	2									
	3									
L3-E-BLK	1									
	2									
L3-D	1									
	2									
	3									
L3-D-BLK	1									
	2									
L4-E	1									
	2									
	3									
L4-E-BLK	1									
	2									
L4-D	1									
	2									
	3									
L4-D-BLK	1									
	2									
L5-E	1									
	2									
	3									
L5-E-BLK	1									
	2									
L5-D	1									
	2									
	3									
L5-D-BLK	1									
	2									
Py-BLK	1									
	2									
CLEAN FILTER	1									
	2									
EMPTY TUBE	1									
	2									

Table 6.8. Detailed Py-GC-MS results of SIM 3 for each replicate of DWTP samples (kraton and cellulose).

polymers		**kraton**			**cellulose**		
pyrolysis products		isoprene	styrene	limonene	hydroxyacetaldehyde	5-(hydroxymethyl)dihydro-2(3H)-furanone	5-(hydroxymethyl)-2-furfural
L1-E	1						
	2						
	3						
L1-E-BLK	1						
	2						
L1-D	1						
	2						
	3						
L1-D-BLK	1						
	2						
L2-E	1						
	2						
	3						
L2-E-BLK	1						
	2						
L2-D	1						
	2						
	3						
L2-D-BLK	1						
	2						
L3-E	1						
	2						
	3						
L3-E-BLK	1						
	2						
L3-D	1						
	2						
	3						
L3-D-BLK	1						
	2						
L4-E	1						
	2						
	3						
L4-E-BLK	1						
	2						
L4-D	1						
	2						
	3						
L4-D-BLK	1						
	2						
L5-E	1						
	2						
	3						
L5-E-BLK	1						
	2						
L5-D	1						
	2						
	3						
L5-D-BLK	1						
	2						
Py-BLK	1						
	2						
CLEAN FILTER	1						
	2						
EMPTY TUBE	1						
	2						

Table 6.9. Detailed Py-GC-MS results of SIM 3 for each replicate of DWTP samples (polypropylene, Nylon and poly(methylmethacrylate)).

polymers		polypropylene				Nylon		poly(methyl methacrylate)	
pyrolysis products		2,4-dimethylhept-1-ene	2,4,6,8-tetramethyl-1-undecene	2,4,6,8-tetramethyl-1-undecene	2,4,6,8-tetramethyl-1-undecene	ε-caprolactam	N-methyl ε-caprolactam	methyl acrylate	methyl methacrylate
L1-E	1								
	2								
	3								
L1-E-BLK	1								
	2								
L1-D	1								
	2								
	3								
L1-D-BLK	1								
	2								
L2-E	1								
	2								
	3								
L2-E-BLK	1								
	2								
L2-D	1								
	2								
	3								
L2-D-BLK	1								
	2								
L3-E	1								
	2								
	3								
L3-E-BLK	1								
	2								
L3-D	1								
	2								
	3								
L3-D-BLK	1								
	2								
L4-E	1								
	2								
	3								
L4-E-BLK	1								
	2								
L4-D	1								
	2								
	3								
L4-D-BLK	1								
	2								
L5-E	1								
	2								
	3								
L5-E-BLK	1								
	2								
L5-D	1								
	2								
	3								
L5-D-BLK	1								
	2								
Py-BLK	1								
	2								
CLEAN FILTER	1								
	2								
EMPTY TUBE	1								
	2								

Results shown in Table 6.10 summarize the presence or absence of selected polymers in DWTP samples and blanks. No polymers were identified in the controls (Py-BLK, Clean filter, and empty tube). It is important to note that the null results for the blanks do not necessarily translate to a complete absence of particles, but rather that the amount of material present is below the detection limit of the Py-GC-MS technique.

In the case of the field blanks, a few pyrolysis products were sometimes present (Tables 6.5-6.9). For instance, the styrene molecule (pyrolysis product of polystyrene, Table 6.5, and Kraton, Table 6.8) was found in the L1-E-BLK and the L3-D-BLK. The presence of indicator ions and therefore pyrolysis products could be evidence of field contamination; however, it is not possible to determine its origin because such contamination was below the detection threshold and therefore yielded a match below the 83.3% threshold level. It is also possible that these identifier ions came from other sources such as dust or other debris and these happen to produce decomposition products that overlap with pyrolysis products of plastics.

Table 6.10. Chemical identification via Py-GC-MS of particles between 1.5 and 106 µm present in DWTP samples collected from the effluent and distribution lines for 5 locations.

The presence of a certain polymer is confirmed (✓) when at least one of the triplicates had a percentage match ≥83.3%. If the percentage match was below 83.3% it is marked with ×.

	PS	PE	PVC	PC	PET	Rayon	Cellulose Acetate	Kraton	Cellulose	PP	Nylon	PMMA
L1-E	✓	✓	✓	✓	✓	✓	×	✓	✓	×	✓	×
L1-E-BLK	×	×	×	×	×	×	×	×	×	×	×	×
L1-D	✓	✓	✓	✓	✓	✓	✓	✓	✓	✓	✓	×
L1-D-BLK	×	×	×	×	×	×	×	×	×	×	×	×
L2-E	✓	×	×	×	✓	×	×	✓	×	×	×	×
L2-E-BLK	×	×	×	×	×	×	×	×	×	×	×	×
L2-D	×	✓	×	×	✓	✓	×	✓	×	×	✓	×
L2-D-BLK	×	×	×	×	×	×	×	×	×	×	×	×
L3-E	✓	✓	✓	×	✓	✓	×	✓	×	✓	✓	✓
L3-E-BLK	×	×	×	×	×	×	×	×	×	×	×	×
L3-D	✓	✓	✓	×	×	✓	✓	✓	✓	✓	✓	✓
L3-D-BLK	×	×	×	×	×	×	×	×	×	×	×	×
L4-E	✓	✓	✓	×	✓	✓	×	✓	×	✓	✓	✓
L4-E-BLK	×	×	×	×	×	×	×	×	×	×	×	×
L4-D	✓	✓	✓	×	✓	✓	✓	✓	×	✓	✓	✓
L4-D-BLK	×	×	×	×	×	×	×	×	×	×	×	×
L5-E	✓	✓	✓	×	✓	✓	×	✓	×	✓	×	×
L5-E-BLK	×	×	×	×	×	×	×	×	×	×	×	×
L5-D	✓	✓	✓	×	✓	✓	✓	✓	×	✓	✓	×
L5-D-BLK	×	×	×	×	×	×	×	×	×	×	×	×
Py-BLK	×	×	×	×	×	×	×	×	×	×	×	×
CLEAN FILTER	×	×	×	×	×	×	×	×	×	×	×	×
EMPTY TUBE	×	×	×	×	×	×	×	×	×	×	×	×

At L1, PS, PE, PVC, PC, PET, Rayon, Kraton, cellulose, and Nylon were found in both effluent and distribution line waters. Interestingly, PP and cellulose acetate were only found in the distribution line.

At L2, only PET and Kraton were found in both the effluent and the distribution line. PS was also found in the effluent, whereas, PE, Rayon, and Nylon were found in the distribution line. At L3, both the effluent and the distribution line samples contained PS, PE, PVC, Rayon, Kraton, PP, Nylon, and PMMA. Additionally, the effluent contained PET and the distribution line contained cellulose. At the L4, both the effluent and the distribution line samples contained PS, PE, PVC, PET, Rayon, Kraton, PP, Nylon, and PMMA. The distribution line also contained cellulose acetate. At L5, both the effluent and the distribution line samples contained PS, PE, PVC, PET, Rayon, Kraton, and PP. Additionally, the distribution line contained cellulose acetate and Nylon.

Kraton was detected in all locations by Py-GC-MS. This is a high-performance elastomer which is a synthetic replacement for rubber.[22] This product is commonly used in both infrastructure (e.g., pavement (highly modified asphalt), telecommunication cables) and consumer products (e.g., cars (coatings, interiors, carpets, and seals), adhesives, diapers, toys). Due to the wide variety of uses, it is not possible to determine the origin. However, as it is commonly used in pavement, one possible source may be particles released from roadways and carried by surface runoff.

Almost all locations contained Rayon in both the effluent and the distribution line, except for L2-E where this material was not detected. Rayon is one of the most common water contaminants due to its wide use in clothing.[23–25] Other microplastics (1.5-106 μm) that were detected in almost all samples were PS (all except L2-D), PE (all except L2-E), PVC (all except both samples collected at L2), and PET (all except L3-D). All these plastics are commonly found in the environment. PE, in particular, has been widely found in rivers [26,27]. PP is also commonly found in the environment, but here it was not found in either L2 or L1-E. The case of PVC is especially interesting, as PVC is commonly used in pipes, valves, and junctions. It would be interesting to determine the material of the water distribution system in each location to draw further conclusions.

Anecdotally, cellulose particles were only found in L1 (both effluent and distribution line) and the distribution line of L3. Polycarbonate, which was only observed in L1 (Table 6.10), was the least common plastic observed.

6.3.2 Analysis of Arctic water samples

Particles 1-106 µm were analyzed with Py-GC-MS and the presence of each characteristic pyrolysis product was determined. Detailed results of each characteristic pyrolysis product can be seen in Tables 6.11-6.15. Each pyrolysis product was assigned a score: green= 1 (perfect match), yellow= 0.5 (partial match), and orange= 0 points (no match).

Table 6.11. Detailed Py-GC-MS results of SIM 1 for all filters with Arctic samples.

polymers	**polystyrene**			**polyethylene**		**polyvinyl chloride**		
pyrolysis products	styrene	3-butene-1,3-diyldibenzene	5-hexene-1,3,5-triyltribenzene	alkenes	α-alkenes	α,ω-alkenes	benzene	chlorobenzene
AR-BLK								
2A-1A-1								
2A-1A-2								
2A-2A-1								
2A-2A-2								
2A-3A								
2A-4A								
2A-5A								
2A-6A-1								
2A-6A-2								
2A-7A-1								
2A-7A-2								
2B-1A-1								
2B-1A-2								
2B-2A								
2B-3A								
2B-4A								
2B-6A-1								
2B-6A-2								
2B-7A								
2B-8A								
2B-9A-1								
2B-9A-2								
2B-10A								
2B-12A								
2B-13A								
2B-14A								
2B-15A								

Table 6.12. Detailed Py-GC-MS results of SIM 2 for all filters with Arctic samples.

polymers	**polycarbonate**		**polyethylene terephthalate**
pyrolysis products	p-methoxy-tert-butylbenzene	2,2-bis(4′-methoxy-phenyl)propane	dimethyl terephthalate
AR-BLK			
2A-1A-1			
2A-1A-2			
2A-2A-1			
2A-2A-2			
2A-3A			
2A-4A			
2A-5A			
2A-6A-1			
2A-6A-2			
2A-7A-1			
2A-7A-2			
2B-1A-1			
2B-1A-2			
2B-2A			
2B-3A			
2B-4A			
2B-6A-1			
2B-6A-2			
2B-7A			
2B-8A			
2B-9A-1			
2B-9A-2			
2B-10A			
2B-12A			
2B-13A			
2B-14A			
2B-15A			

Table 6.13. Detailed Py-GC-MS results of SIM 3 for all filters with Arctic samples (rayon and cellulose acetate).

polymers	**rayon**				**cellulose acetate**				
pyrolysis products	furfural	2-furanmethanol	2-furancarboxaldehyde, 5-methyl-	5-hydroxymethylfurfural	acetic acid	2-hydroxyethyl acetate	4,6-dimethyl-2H-pyran-2-one	unknown peak 1	unknown peak 2
AR-BLK									
2A-1A-1									
2A-1A-2									
2A-2A-1									
2A-2A-2									
2A-3A									
2A-4A									
2A-5A									
2A-6A-1									
2A-6A-2									
2A-7A-1									
2A-7A-2									
2B-1A-1									
2B-1A-2									
2B-2A									
2B-3A									
2B-4A									
2B-6A-1									
2B-6A-2									
2B-7A									
2B-8A									
2B-9A-1									
2B-9A-2									
2B-10A									
2B-12A									
2B-13A									
2B-14A									
2B-15A									

Table 6.14. Detailed Py-GC-MS results of SIM 3 for all filters with Arctic samples (kraton and cellulose).

polymers	**kraton**			**cellulose**		
pyrolysis products	Isoprene	styrene	Limonene	hydroxyacetaldehyde	5-(hydroxymethyl)dihydro-2(3H)-furanone	5-(hydroxymethyl)-2-furfural
AR-BLK						
2A-1A-1						
2A-1A-2						
2A-2A-1						
2A-2A-2						
2A-3A						
2A-4A						
2A-5A						
2A-6A-1						
2A-6A-2						
2A-7A-1						
2A-7A-2						
2B-1A-1						
2B-1A-2						
2B-2A						
2B-3A						
2B-4A						
2B-6A-1						
2B-6A-2						
2B-7A						
2B-8A						
2B-9A-1						
2B-9A-2						
2B-10A						
2B-12A						
2B-13A						
2B-14A						
2B-15A						

Table 6.15. Detailed Py-GC-MS results of SIM 3 for all filters with Arctic samples (polypropylene, Nylon and poly(methylmethacrylate)).

polymers	**polypropylene**				**Nylon**		**poly(methyl methacrylate)**	
pyrolysis products	2,4-dimethylhept-1-ene	2,4,6,8-tetramethyl-1-undecene	2,4,6,8-tetramethyl-1-undecene	2,4,6,8-tetramethyl-1-undecene	ε-caprolactam	N-methyl ε-caprolactam	methyl acrylate	methyl methacrylate
AR-BLK								
2A-1A-1								
2A-1A-2								
2A-2A-1								
2A-2A-2								
2A-3A								
2A-4A								
2A-5A								
2A-6A-1								
2A-6A-2								
2A-7A-1								
2A-7A-2								
2B-1A-1								
2B-1A-2								
2B-2A								
2B-3A								
2B-4A								
2B-6A-1								
2B-6A-2								
2B-7A								
2B-8A								
2B-9A-1								
2B-9A-2								
2B-10A								
2B-12A								
2B-13A								
2B-14A								
2B-15A								

Results in Table 6.16 summarize the presence or absence of selected polymers in samples and the blank. Even though no polymers were confirmed in the AR-BLK, several characteristic pyrolysis

products were identified either with a perfect match or a partial match (Tables 6.11-6.15). This highlights the importance of having a more thorough analysis of the data, and not identifying plastics with just one pyrolysis product.

Table 6.16. Chemical identification via Py-GC-MC of particles between 1.5 and 106 μm present in Arctic samples. The presence of a certain polymer is confirmed (✓) when at least one of the triplicates had a percentage match ≥83.3%. If the percentage match was below 83.3%, it is marked with ×.

	PS	PE	PVC	PC	PET	Rayon	Cellulose Acetate	Kraton	Cellulose	PP	Nylon	PMMA
AR-BLK	×	×	×	×	×	×	×	×	×	×	×	×
2A-1A	✓	✓	✓	×	✓	✓	×	×	×	✓	✓	×
2A-2A	✓	✓	✓	×	✓	×	×	×	×	✓	✓	×
2A-3A	✓	✓	✓	×	✓	×	✓	✓	×	✓	×	✓
2A-4A	✓	×	✓	×	✓	×	×	✓	×	✓	✓	×
2A-5A	✓	×	×	×	✓	✓	×	×	×	✓	✓	×
2A-6A	✓	✓	✓	×	✓	✓	×	✓	×	×	✓	×
2A-7A	✓	✓	×	×	✓	×	×	✓	×	✓	✓	×
2B-1A	✓	✓	×	×	✓	×	×	✓	×	✓	✓	×
2B-2A	✓	✓	×	×	✓	✓	×	×	×	✓	×	×
2B-3A	×	✓	×	×	✓	×	×	×	×	×	✓	×
2B-4A	✓	✓	✓	×	✓	✓	×	✓	×	×	✓	×
2B-6A	✓	✓	✓	×	✓	✓	×	×	×	✓	×	×
2B-7A	✓	✓	✓	×	✓	✓	×	×	×	×	✓	×
2B-8A	✓	✓	×	×	✓	×	×	×	×	×	×	✓
2B-9A	✓	✓	✓	×	✓	✓	×	×	×	✓	✓	×
2B-10A	×	×	✓	×	✓	×	✓	×	×	✓	×	×
2B-12A	✓	✓	×	×	✓	✓	×	✓	×	×	✓	×
2B-13A	✓	✓	×	×	✓	×	×	×	×	×	✓	×
2B-14A	✓	×	✓	×	✓	×	✓	✓	×	✓	✓	×
2B-15A	✓	✓	✓	×	✓	×	×	✓	×	✓	×	×

It is important to note that, despite the samples being filtered onto PC, this polymer was not detected in any of the samples or controls. Thus the sample preparation method, including the

sonication process did not introduce detectable contamination to the samples. Cellulose was also not detected in any of the samples, however this is not surprising as cellulose is water-soluble and biodegradable. Interestingly, Cellulose Acetate was detected in 15% of the samples, suggesting that this synthetic biopolymer fiber may not be as degradable as its natural counterpart (cellulose). In contrast, PET was found in all Arctic samples. This is not surprising, as PET bottle contamination in the ocean is well documented.[28,29] This is in agreement with the results obtained in the DWTPs, where almost all samples also contained PET. Similarly, PS, PE, PP and Nylon were present in 90%, 80%, 65%, and 70% of DWTP samples respectively. PVC and Kraton were only found in 60% and 45% respectively of the Arctic samples, whereas they were found in 80% and 100%, respectively of the DWTP samples. PVC in DWTP samples was possibly coming from the piping, whereas Kraton could be from road wear, therefore it makes sense that these materials would be less prevalent in remote locations such as Arctic waters. PMMA was not very common in either DWTP samples or Arctic waters.

When comparing the results obtained in the two legs of the Amundsen expedition, there is no significant difference in the number of plastics identified. Out of the 12 plastics we assessed, in leg 2A we identified on average 6 ± 1 plastics, while in leg 2B the average was 5 ± 1. This agrees with the literature which identifies the Arctic as a sink for microplastic contamination that reaches these remote locations via deposition or marine currents[21,30–33].

Interestingly, our findings show that microplastics in Arctic surface waters were not consistently buoyant and ranged from lower to higher density plastics. These findings are in agreement with the results of Huntington *et al.* [21]

6.4 Limitations of the technique and future work

One of the limitations of sample analysis using Py-GC-MS is that it is a bulk analysis, and thus organic content in the matrix will cause interferences when identifying polymers. In the case of the samples analyzed in this work, the low organic content facilitated the sample processing. However, even with low organic content, the MS exhibited significant performance loss, requiring maintenance to clean the instrument, and delaying the acquisition of results. In samples with higher organic content, two main approaches can be used to remove the organic matrix: separation and digestion. Separation methods usually target large microplastics and deal with liquid matrices such as water, sand, or sludge.[2,34] To remove microplastics from the matrix, sample filtration or density fractionation can be used as separation methods.[34] Sample digestion is more complex, as it uses chemical[14] or enzymatic[15] methods to remove (degradation, oxidization, etc.) the organic matter from samples. Digestions are commonly used when identifying microplastics in organisms[18] or solid media such as soil,[35] and are useful when performing analyses by reducing background noise and interference. However, these digestions are not without drawbacks. For example, digestions using KOH may lead to loss of mass of some plastics.[36] This highlights the importance of separate digestion studies that focus on understanding the effects of digestion techniques on different microplastics according to their sizes, types, and degradation potential.

As described above, there is a need to standardize the analysis of Py-GC-MS data. In this study, we presented a scoring system in which each pyrolysis product is rated based on the presence/absence of its identifying ions. Then, this score is compared to the perfect score that a bulk plastic would have and a percentage match with the bulk plastic is calculated. We confirm the presence of a plastic if the percentage match is ≥83.3%. This chosen threshold allowed us to confidently confirm the presence of plastics in the DWTP and Arctic samples, using all identifying ions and pyrolysis products for each plastic. Equally important, it allowed us to discard the

detectable presence of plastics in the controls, which in some cases contained some pyrolysis product but never a ≥83.3% match. However, it is important to note that both DWTP samples and Arctic samples are very similar in nature. It would be interesting to test this threshold in other types of samples such as soil, food, or animal tissue. Other samples might contain pyrolysis products that directly interfere with the plastic's pyrolysis products.

Another limitation was the use of single ion monitoring (SIM) scans to enhance the m/z signal of the indicator ions. The main limitation of using SIM scans is that the user must select the ions to be monitored prior to analysis. In this study, the most common plastics were monitored. While other plastics may have been present, since they were not monitored, they could not be identified. Py-GC-MS libraries are available (e.g. the NIST library), however, sample cleanliness is a concern. Here, the samples studied contained elevated levels of background noise, the signal was not high enough for a library search to yield positive matches.

Py-GC-MS was used to identify plastics between 106 and 1.5 µm. While this technique has been previously reported in the literature, we proposed a new metrics to assess the goodness of a match for polymer identification. We applied this metrics to samples with low organic content and without further digestion. It was determined that both DWTP samples and Arctic samples contain a wide array of polymers which highlights the necessity for further research on the topic to be performed. Ideally, Py-GC-MS could be combined with a technique that allows for quantification such as µ-FTIR or Raman microscopy. Alternatively, more experiments to determine the possibility of quantification with a coil-pyrolyzer are required.

We would like to extend this work by analyzing the particles < 1.5 µm using Py-GC-MS. This would be achieved by direct deposition of the concentrated sample into the quartz tube. However,

it was not possible to perform these experiments before the submission of this manuscript due to issues with the equipment.

6.5 Acknowledgements

The authors acknowledge the financial support of the Canada Research Chairs program, the Natural Sciences and Engineering Research Council of Canada, the Killam Research Fellowship, and the Canada Foundation for Innovation. LMH was supported by a McGill Engineering Doctoral Award, a Eugenie Ulmer-Lamothe Award and an NSERC CREATE PURE award. This project was supported partially by a financial contribution from Fisheries and Oceans Canada. The authors thank Dr. Sarah Bernstein and Dr. Rachelle Robitaille for sample collection during the Amundsen cruise.

6.6 References

(1) He, P.; Chen, L.; Shao, L.; Zhang, H.; Lü, F. Municipal Solid Waste (MSW) Landfill: A Source of Microplastics? -Evidence of Microplastics in Landfill Leachate. *Water Research* **2019**, *159*, 38–45. https://doi.org/10.1016/j.watres.2019.04.060.

(2) El Hayany, B.; El Fels, L.; Quénéa, K.; Dignac, M.-F.; Rumpel, C.; Gupta, V. K.; Hafidi, M. Microplastics from Lagooning Sludge to Composts as Revealed by Fluorescent Staining-Image Analysis, Raman Spectroscopy and Pyrolysis-GC/MS. *Journal of Environmental Management* **2020**, *275*, 111249. https://doi.org/10.1016/j.jenvman.2020.111249.

(3) Li, X.; Chen, L.; Mei, Q.; Dong, B.; Dai, X.; Ding, G.; Zeng, E. Y. Microplastics in Sewage Sludge from the Wastewater Treatment Plants in China. *Water Research* **2018**, *142*, 75–85. https://doi.org/10.1016/j.watres.2018.05.034.

(4) da Costa, J. P.; Duarte, A. C.; Rocha-Santos, T. A. P. Microplastics – Occurrence, Fate and Behaviour in the Environment. In *Comprehensive Analytical Chemistry*; Elsevier, 2017; Vol. 75, pp 1–24. https://doi.org/10.1016/bs.coac.2016.10.004.

(5) Cabernard, L.; Roscher, L.; Lorenz, C.; Gerdts, G.; Primpke, S. Comparison of Raman and Fourier Transform Infrared Spectroscopy for the Quantification of Microplastics in the Aquatic Environment. *Environ. Sci. Technol.* **2018**, *52* (22), 13279–13288. https://doi.org/10.1021/acs.est.8b03438.

(6) Müller, Y. K.; Wernicke, T.; Pittroff, M.; Witzig, C. S.; Storck, F. R.; Klinger, J.; Zumbülte, N. Microplastic Analysis—Are We Measuring the Same? Results on the First Global Comparative Study for Microplastic Analysis in a Water Sample. *Anal Bioanal Chem* **2020**, *412* (3), 555–560. https://doi.org/10.1007/s00216-019-02311-1.

(7) Shim, W. J.; Hong, S. H.; Eo, S. E. Identification Methods in Microplastic Analysis: A Review. *Anal. Methods* **2017**, *9* (9), 1384–1391. https://doi.org/10.1039/C6AY02558G.

(8) Witzig, C. S.; Földi, C.; Wörle, K.; Habermehl, P.; Pittroff, M.; Müller, Y. K.; Lauschke, T.; Fiener, P.; Dierkes, G.; Freier, K. P.; Zumbülte, N. When Good Intentions Go Bad—False Positive Microplastic Detection Caused by Disposable Gloves. *Environ. Sci. Technol.* **2020**, *54* (19), 12164–12172. https://doi.org/10.1021/acs.est.0c03742.

(9) Fischer, M.; Scholz-Böttcher, B. M. Microplastics Analysis in Environmental Samples – Recent Pyrolysis-Gas Chromatography-Mass Spectrometry Method Improvements to Increase the Reliability of Mass-Related Data. *Anal. Methods* **2019**, *11* (18), 2489–2497. https://doi.org/10.1039/C9AY00600A.

(10) Käppler, A.; Fischer, M.; Scholz-Böttcher, B. M.; Oberbeckmann, S.; Labrenz, M.; Fischer, D.; Eichhorn, K.-J.; Voit, B. Comparison of μ-ATR-FTIR Spectroscopy and Py-GCMS as Identification Tools for Microplastic Particles and Fibers Isolated from River Sediments. *Anal Bioanal Chem* **2018**, *410* (21), 5313–5327. https://doi.org/10.1007/s00216-018-1185-5.

(11) Hermabessiere, L.; Himber, C.; Boricaud, B.; Kazour, M.; Amara, R.; Cassone, A.-L.; Laurentie, M.; Paul-Pont, I.; Soudant, P.; Dehaut, A.; Duflos, G. Optimization, Performance, and Application of a Pyrolysis-GC/MS Method for the Identification of Microplastics. *Anal Bioanal Chem* **2018**, *410* (25), 6663–6676. https://doi.org/10.1007/s00216-018-1279-0.

(12) Eisentraut, P.; Dümichen, E.; Ruhl, A. S.; Jekel, M.; Albrecht, M.; Gehde, M.; Braun, U. Two Birds with One Stone—Fast and Simultaneous Analysis of Microplastics: Microparticles Derived from Thermoplastics and Tire Wear. *Environ. Sci. Technol. Lett.* **2018**, *5* (10), 608–613. https://doi.org/10.1021/acs.estlett.8b00446.

(13) Dümichen, E.; Eisentraut, P.; Bannick, C. G.; Barthel, A.-K.; Senz, R.; Braun, U. Fast Identification of Microplastics in Complex Environmental Samples by a Thermal Degradation Method. *Chemosphere* **2017**, *174*, 572–584. https://doi.org/10.1016/j.chemosphere.2017.02.010.

(14) Fabbri, D.; Rombolà, A. G.; Vassura, I.; Torri, C.; Franzellitti, S.; Capolupo, M.; Fabbri, E. Off-Line Analytical Pyrolysis GC–MS to Study the Accumulation of Polystyrene Microparticles in Exposed Mussels. *Journal of Analytical and Applied Pyrolysis* **2020**, *149*, 104836. https://doi.org/10.1016/j.jaap.2020.104836.

(15) Gomiero, A.; Øysæd, K. B.; Agustsson, T.; van Hoytema, N.; van Thiel, T.; Grati, F. First Record of Characterization, Concentration and Distribution of Microplastics in Coastal Sediments

of an Urban Fjord in South West Norway Using a Thermal Degradation Method. *Chemosphere* **2019**, *227*, 705–714. https://doi.org/10.1016/j.chemosphere.2019.04.096.

(16) O'Brien, S.; Okoffo, E. D.; O'Brien, J. W.; Ribeiro, F.; Wang, X.; Wright, S. L.; Samanipour, S.; Rauert, C.; Toapanta, T. Y. A.; Albarracin, R.; Thomas, K. V. Airborne Emissions of Microplastic Fibres from Domestic Laundry Dryers. *Science of The Total Environment* **2020**, *747*, 141175. https://doi.org/10.1016/j.scitotenv.2020.141175.

(17) Klee, M.; Chang, I. *Pyrolysis-GC/MS/IR Analysis of Kraton*; Hewlett Packard; 1989.

(18) Fischer, M.; Scholz-Böttcher, B. M. Simultaneous Trace Identification and Quantification of Common Types of Microplastics in Environmental Samples by Pyrolysis-Gas Chromatography–Mass Spectrometry. *Environ. Sci. Technol.* **2017**, *51* (9), 5052–5060. https://doi.org/10.1021/acs.est.6b06362.

(19) Acevedo, B.; Fernández, A. M.; Barriocanal, C. Identification of Polymers in Waste Tyre Reinforcing Fibre by Thermal Analysis and Pyrolysis. *Journal of Analytical and Applied Pyrolysis* **2015**, *111*, 224–232. https://doi.org/10.1016/j.jaap.2014.11.005.

(20) Tsuge, S.; Ohtani, H.; Watanabe, C. *Pyrolysis - GC/MS Data Book of Synthetic Polymers: Pyrograms, Thermograms and MS of Pyrolyzates*; Elsevier, 2011.

(21) Huntington, A.; Corcoran, P. L.; Jantunen, L.; Thaysen, C.; Bernstein, S.; Stern, G. A.; Rochman, C. M. A First Assessment of Microplastics and Other Anthropogenic Particles in Hudson Bay and the Surrounding Eastern Canadian Arctic Waters of Nunavut. *FACETS* **2020**, *5* (1), 432–454. https://doi.org/10.1139/facets-2019-0042.

(22) Kraton Corporation https://kraton.com/ (accessed 2020 -04 -16).

(23) Comnea-Stancu, I. R.; Wieland, K.; Ramer, G.; Schwaighofer, A.; Lendl, B. On the Identification of Rayon/Viscose as a Major Fraction of Microplastics in the Marine Environment: Discrimination between Natural and Manmade Cellulosic Fibers Using Fourier Transform Infrared Spectroscopy. *Appl Spectrosc* **2017**, *71* (5), 939–950. https://doi.org/10.1177/0003702816660725.

(24) Ross, P. S.; Chastain, S.; Vassilenko, E.; Etemadifar, A.; Zimmermann, S.; Quesnel, S.-A.; Eert, J.; Solomon, E.; Patankar, S.; Posacka, A. M.; Williams, B. Pervasive Distribution of Polyester Fibres in the Arctic Ocean Is Driven by Atlantic Inputs. *Nat Commun* **2021**, *12* (1), 106. https://doi.org/10.1038/s41467-020-20347-1.

(25) De Falco, F.; Di Pace, E.; Cocca, M.; Avella, M. The Contribution of Washing Processes of Synthetic Clothes to Microplastic Pollution. *Sci Rep* **2019**, *9* (1), 6633. https://doi.org/10.1038/s41598-019-43023-x.

(26) Klein, S.; Worch, E.; Knepper, T. P. Occurrence and Spatial Distribution of Microplastics in River Shore Sediments of the Rhine-Main Area in Germany. *Environ. Sci. Technol.* **2015**, *49* (10), 6070–6076. https://doi.org/10.1021/acs.est.5b00492.

(27) Ng, K. L.; Obbard, J. P. Prevalence of Microplastics in Singapore's Coastal Marine Environment. *Marine Pollution Bulletin* **2006**, *52* (7), 761–767. https://doi.org/10.1016/j.marpolbul.2005.11.017.

(28) Dris, R.; Imhof, H.; Sanchez, W.; Gasperi, J.; Galgani, F.; Tassin, B.; Laforsch, C. Beyond the Ocean: Contamination of Freshwater Ecosystems with (Micro-)Plastic Particles. *Environ. Chem.* **2015**, *12* (5), 539. https://doi.org/10.1071/EN14172.

(29) Castelvetro, V.; Corti, A.; Bianchi, S.; Giacomelli, G.; Manariti, A.; Vinciguerra, V. Microplastics in Fish Meal: Contamination Level Analyzed by Polymer Type, Including Polyester

(PET), Polyolefins, and Polystyrene. *Environmental Pollution* **2021**, *273*, 115792. https://doi.org/10.1016/j.envpol.2020.115792.

(30) Bergmann, M.; Mützel, S.; Primpke, S.; Tekman, M. B.; Trachsel, J.; Gerdts, G. White and Wonderful? Microplastics Prevail in Snow from the Alps to the Arctic. *Sci Adv* **2019**, *5* (8), eaax1157. https://doi.org/10.1126/sciadv.aax1157.

(31) Bergmann, M.; Lutz, B.; Tekman, M. B.; Gutow, L. Citizen Scientists Reveal: Marine Litter Pollutes Arctic Beaches and Affects Wild Life. *Marine Pollution Bulletin* **2017**, *125* (1–2), 535–540. https://doi.org/10.1016/j.marpolbul.2017.09.055.

(32) Kanhai, L. D. K.; Gårdfeldt, K.; Lyashevska, O.; Hassellöv, M.; Thompson, R. C.; O'Connor, I. Microplastics in Sub-Surface Waters of the Arctic Central Basin. *Marine Pollution Bulletin* **2018**, *130*, 8–18. https://doi.org/10.1016/j.marpolbul.2018.03.011.

(33) Lusher, A. L.; Tirelli, V.; O'Connor, I.; Officer, R. Microplastics in Arctic Polar Waters: The First Reported Values of Particles in Surface and Sub-Surface Samples. *Sci Rep* **2015**, *5* (1), 14947. https://doi.org/10.1038/srep14947.

(34) Minor, E. C.; Lin, R.; Burrows, A.; Cooney, E. M.; Grosshuesch, S.; Lafrancois, B. An Analysis of Microlitter and Microplastics from Lake Superior Beach Sand and Surface-Water. *Science of The Total Environment* **2020**, *744*, 140824. https://doi.org/10.1016/j.scitotenv.2020.140824.

(35) Nizzetto, L.; Futter, M.; Langaas, S. Are Agricultural Soils Dumps for Microplastics of Urban Origin? *Environmental Science & Technology* **2016**, *50* (20), 10777–10779. https://doi.org/10.1021/acs.est.6b04140.

(36) Kühn, S.; van Werven, B.; van Oyen, A.; Meijboom, A.; Bravo Rebolledo, E. L.; van Franeker, J. A. The Use of Potassium Hydroxide (KOH) Solution as a Suitable Approach to Isolate Plastics Ingested by Marine Organisms. *Marine Pollution Bulletin* **2017**, *115* (1–2), 86–90. https://doi.org/10.1016/j.marpolbul.2016.11.034.

Preface to Chapter 7

The release of micro- and nanoplastics into the environment is unquestionable (Chapter 3). So is the breakdown of larger plastics into smaller particles (Chapter 4 and 5). Thus, governments are considering microplastic screening for drinking water. Some advanced techniques could be useful for this (Chapter 6), however, there is a need for quick and low-cost methods to screen for microplastics. By using a common dye, we were able to identify organic particles. Particles larger than 100 μm were later chemically identified as plastics using spectroscopy. Our study highlights that for each type of environmental sample, an optimization of the dye concentration should be performed. Such optimization should aim to reduce false positives (caused by excess dye), while preventing false negatives due to lack of dye. Additionally, we used pyrolysis coupled with gas chromatography and mass spectroscopy to chemically analyze the smaller particles in the sample. This study will be submitted to *Environmental Science & Technology*.

Chapter 7: Optimizing the concentration of Nile red for screening of microplastics in bottled water

Abstract

Increasing concern regarding the presence of microplastics in drinking water has led to a growing number of studies aimed at quantifying microplastics in water. In this work, we present an optimized procedure for the use of Nile red (NR) as a fluorescent staining agent for pre-screening of microplastics in bottled water. Positive and negative control experiments with NR concentrations ranging from 0.001 to 10 mg/L showed that non-optimized staining concentrations led to underestimation or overestimation of the particle count. The optimized NR staining concentration was found to be 0.1 mg/L. This method was successfully used to screen particles in seven different brands of bottled water consisting of both still and carbonated water, in both plastic and glass bottles. Particles larger than 100 µm were chemically characterized using attenuated total reflection-Fourier transform infrared spectroscopy (ATR-FTIR), and, overall, 67 % of particles identified with NR were confirmed to be polymers. Particles smaller than 100 µm were qualitatively analyzed using pyrolysis coupled with gas chromatography and mass spectroscopy (Py-GC-MS). Analysis of polymers between 5-100 µm using Py-GC-MS confirmed that this smaller fraction generally mirrors the FTIR results for particles > l00 µm.

7.1 Introduction

Plastics are introduced into the environment through direct application (e.g., plastic mulch in agriculture, construction materials) or mishandling, and have been detected in nearly every environmental compartment, from air to soil to remote lakes[1–6]. Currently, the lack of comprehensive and robust data obscures our understanding of the extent of the issue[7,8]. Addressing

the methodological limitations to microplastic detection and quantification is necessary to reduce uncertainties associated with current estimates of microplastic contaminant concentrations[9,10]. This is particularly relevant for smaller sized particles, which often dominate particle counts[11]. There are multiple reports of microplastics occurrence in the food chain[7,12–19], specifically in drinking water[10,20–25]. The state of California passed a bill in 2018 which requires the on-site continuous screening of microplastics in drinking water[26]. The results of these screenings will be used to set a guideline on microplastic limits in drinking water. However, currently there are few fast, effective, and low-cost methods to screen for microplastics.

Surface waters are common sources for water treatment plants, and a fraction of the plastics present in these rivers and lakes will make it through treatment processes [6,21,22,27–29]. At the same time, the presence of microplastics has been reported for bottled waters and other beverages[23,30]. While these microplastics are suggested to come from the packaging material, plastic types different from those that make up the bottle or cap were also detected, pointing to external sources of contamination[31].

One approach that has been used to detect and quantify microplastics in drinking water involves staining polymer particles using hydrophobic dyes. The few existing studies on this subject have been conducted using fluorescent dyes with varying degrees of success.[24,32,33] Nile red (9-diethylamino-5H-benzo[α]phenoxazine-5-one) (NR) is a non-specific lipophilic dye that has been applied to plastic detection [23,24,32–44]. While the lack of specificity and the potential for staining organic matter means secondary confirmation is required, the initial screening of particles by fluorescence microscopy does not have the same size limitations inherent to Fourier transform infrared spectroscopy (FTIR) and Raman spectroscopy[45]. Previous reports of staining with NR tend to use high dye concentrations (1 – 1000 mg/L)[23,32,33,36,38–42], which may lead to detection issues: *e.g.* dye aggregation, quenching, or autofluorescence from precipitated dye. To date, there

has been little optimization or agreement in methods for the use of NR in freshwaters such as drinking water. Maes *et al*. highlighted the importance of NR concentration when balancing plastic detection and background fluorescence for detection of microplastics in marine sediments.[34] Similarly, Prata *et al*. highlighted the importance of camera settings, staining conditions, and analysis of digital images.[42] The optimal NR concentration is anticipated to be dependent on sample matrix, and there remains a need to further examine the appropriateness of this approach and to optimize the dye concentration to reduce the likelihood of false positives for plastics occurring in freshwater samples.

Comparisons of reported microplastics concentrations are further complicated by differences in the lower size limit of detection from one study to another. These differences arise from the methods used during sample collection, processing, and analysis, and the difficulty of microplastic detection increases with decreasing particle size[45]. For water samples, filtration is a common technique to isolate particles, however the selection of filters with relatively large pore sizes often means that smaller microplastics are lost during this initial step and remain unanalyzed[20]. When smaller pore-size filters are employed, detection limits of available analytical techniques present a second challenge. The two most commonly used techniques for plastic identification are Raman spectroscopy and FTIR[9,46–48]. Both techniques have advantages and drawbacks, depending on the size of plastic particles and potential interferents[45]. Additionally, both techniques are time intensive, and attempts to automate identification by rastering with Raman or FTIR microscopes report analysis times on the order of tens of hours per sample[9,31]. An alternative for these small particles is pyrolysis coupled to gas chromatography and mass spectroscopy (Py-GC-MS), which can confirm the presence low masses of micro and nanoplastics,[49,50] but may not yield reliable particle counts[45].

In this study, we present a low-cost, reproducible, and rapid method to pre-screen for microplastics in drinking water. We optimized the concentration of NR to label and count particles present in water. We then applied the optimized NR method to study the presence of microplastics in bottled drinking water purchased in Canadian supermarkets. We examined seven products, including both carbonated and still water, packaged in either plastic or glass bottles. In developing the method, we show improvements in detection of spiked particles (positive controls) as well as a reduction in the occurrence of false positives in negative controls. Particles were counted via fluorescence microscopy. The composition of particles larger than ~100 µm was determined with FTIR while smaller particles were qualitatively identified using Py-GC-MS. This work demonstrates the applicability of the optimized NR method for analysis of microplastics > 100 µm and confirms the presence of small microplastics (> 1.5 µm and < 100 µm) in commercial bottled drinking water.

7.2 Materials and methods

The experimental work involved two different sample processing approaches with each using independent samples (Figure 7.1a). In the first approach, focusing on particles > 100 µm, samples were processed through NR staining, filtration, imaging, particle counting and FTIR analyses. In the second approach, focusing on particles > 1.5 µm and < 100 µm, samples were filtered prior to NR staining and then analyzed using Py-GC-MS.

7.2.1 Bottled water samples

Seven types of bottled water (herein referred to as bottled water 1 to 7) were purchased from grocery or convenience stores in Montreal, Quebec (bottle characteristics are listed in Table 7.1). Of these, four were bottled in Canada, and three were bottled outside of Canada. These were chosen to include two variables: bottle material (polyethylene terephthalate (PET) or glass) and

water type/processing (e.g., still, carbonated, reverse osmosis filtration). The bottle caps were either made of polypropylene (PP) or polyethylene (PE). Each bottled water was stained with NR as determined by the method developed below. All seven types of bottled waters were analyzed seven times each to ensure reproducibility of the method.

7.2.1.1 Approach 1 - imaging and FTIR analysis

7.2.1.1.1 Staining and filtration

Stock Nile red (99%, Arcos, CAS: 7385-67-3) solutions were prepared in acetone (Certified ACS grade, Fisher) at concentrations of 1 to 1000 mg/L, and water samples were spiked with stock NR solutions to achieve final concentrations ranging from 0.001 - 10 mg/L NR in water. For all tests, an acetone/water ratio of 1 % v/v was maintained to ensure uniform testing conditions.

For NR staining, half of each water sample was transferred to an 800 mL clean glass beaker. This was done prior to staining to prevent uncontrolled loss of NR by partitioning to the walls of plastic bottles. The glass beaker was then spiked with NR from the appropriate stock solution after which the second half of the sample was introduced into the beaker to thoroughly mix the NR. Samples were left to rest for 30 min to allow time for staining and were then vacuum filtered through a 1.5 μm filter (110 mm, Whatman Binder-Free glass microfiber filters Grade 934-AH), previously cut to a diameter of 9 cm (using clean stainless steel scissors) and placed in a Buchner funnel in a coffee-filter conformation (Figure S7.1). This configuration was used to ensure that all water and particles being filtered only came in contact with the filter itself, rather than with the walls of the funnel, which could lead to the loss of particles. Following filtration, filters were dried overnight in a covered Petri dish before imaging. For bottled waters with larger volumes (> 700 mL), two

clean beakers were used to stain the contents of a single bottle and the entire volume was filtered through a single filter (Figure 7.1a).

All filtration and staining steps were conducted in a laminar flow biosafety cabinet (BSC), which was previously cleaned with acetone to limit contamination. All lab equipment (e.g., scissors, tweezers, beakers, glass pipets, and Buchner funnel) was rinsed with acetone inside the BSC before processing new samples. Separate, dedicated beakers were used for negative controls, positive controls, and bottled water samples to avoid cross-contamination. Before each use, glass beakers were washed with soap and water, triple rinsed with reverse osmosis (RO) water, and then rinsed with acetone in the BSC to avoid contaminant carryover. Filters were kept in the BSC after filtering and prior to imaging. Cotton lab coats were used throughout the project to avoid plastic microfiber contamination from clothing.

7.2.1.1.2 Method development (positive and negative controls)

Negative and positive controls were performed using LC/MS grade water (considered high purity water in this study) delivered in 4 L amber glass bottles (Fisher Scientific, CAS:7732-18-5), and a range of NR concentrations with the goal of determining a concentration that minimized false positives while maintaining effective microplastic staining. Control samples consisted of 500 mL of LC/MS water in a clean 800 mL glass beaker. The NR staining and incubation procedure was the same as that used for commercial bottled samples. Negative controls were designed to evaluate the impact of NR concentration on the background level of counts in a clean system. Five concentrations ranging from 0.001 to 10 mg NR/L were tested. Negative control samples were processed through the imaging and counting steps (described below) but were not analyzed by FTIR as no large particles (> 100 µm) were identified.

Positive controls were performed to evaluate the effect of NR concentration on the recovery of spiked microplastics. Two thousand particles (±20 particles) (1.00 mL ±0.01 mL) of a 2000 particle/mL stock suspension) of 20 μm polystyrene latex beads (Polybead® Carboxylate Microspheres, Polysciences) were added to 500 mL of LC/MS water and gently mixed before staining. The spike concentration (2000 particles per replicate) was chosen to be on the same order of magnitude as the results of preliminary screening tests using bottled waters. Based on the results of the negative control tests, three NR concentrations, ranging from 0.01 to 1 mg NR/L, were used for the positive controls. Positive control samples were processed through imaging and counting steps (described below) but were not analyzed by FTIR as no large particles (> 100 μm) were identified. Details for negative controls, positive controls, and bottled water samples are presented in Table 7.1.

Table 7.1. Preparation of negative controls, positive controls and bottled water samples used in imaging, counting and FTIR analysis

Water Sample Description				NR Staining Description		
Type	**Brand**	**Bottle**	**Cap**	**Sample volume (mL)**	**NR (mg/L)**	**Number of Replicates**
Negative Controls						
LC/MS grade water	Fisher	glass	PTFE	500	10	10
LC/MS grade water	Fisher	glass	PTFE	500	1	10
LC/MS grade water	Fisher	glass	PTFE	500	0.1	10
LC/MS grade water	Fisher	glass	PTFE	500	0.01	10
LC/MS grade water	Fisher	glass	PTFE	500	0.001	10
Positive Controls						
Spiked LC/MS grade water*	Fisher	glass	PTFE	500	1	5
Spiked LC/MS grade water*	Fisher	glass	PTFE	500	0.1	5
Spiked LC/MS grade water*	Fisher	glass	PTFE	500	0.01	5
Bottled Water Samples						
Bottled water 1	A	PET	PE	500	0.1	7
Bottled water 2**	A	glass	PE	750	0.1	7
Bottled water 3	B	PET	PE	500	0.1	7
Bottled water 4	C	PET	PE	500	0.1	7
Bottled water 5	D	glass	PP	800	0.1	7
Bottled water 6	D	PET	PP	500	0.1	7
Bottled water 7**	D	glass	PP	800	0.1	7

*: Spiked with 2000 particles of 20 μm polystyrene latex beads
**: Carbonated water
Polytetrafluoroethylene (PTFE)
Polyethylene terephthalate (PET)
Polyethylene (PE)
Polypropylene (PP)

7.2.1.1.3 Imaging

Following filtration, dry filters were imaged via fluorescence microscopy. An Olympus SZX16 stereoscope equipped with an anti-glare longpass optical filter (OG 550 nm, Schott Inc.) and an external blue/green (450-510 nm) light source (Crime-Lite 2, Foster and Freeman Inc.) were used

to visualize the stained particles on the filters. Images were collected with a Canon digital single-lens reflex (DSLR) camera (Model DS12607) mounted on the stereomicroscope. The camera was set to Automatic Depth of Field mode to ensure that the objects in the image were in focus and that the exposure was sufficiently long to capture fluorescence from the particles (exposure time of 30 to 40 s). This setup enabled the detection of particles invisible to the naked eye. The filters were initially brought into focus using the 10× objective and 2× zoom; however, images were acquired at 4× zoom following further adjustment of the focal plane. To ensure that the entire area of each filter was collected, the imaging was divided into three sequences: the outer edge, the inner edge, and the central circle (Figure S7.2). The outer and inner edges were each within the 2× zoomed-in areas, while the central circle was flat with distinguishable dark circles as a result of the filtration step (Figure S7.1). These dark circles were used as points of reference during imaging.

7.2.1.1.4 Particle counts

Image files were processed with ImageJ (Fiji 1.50g). Images were processed using the subtract background function and then converted to 8-bit; a threshold between 23-28 A.U. was chosen, depending on the lighting of the original image. Then, processed images were compared to the original image to ensure the particles identified in the processed image existed in the original image. Finally, all particles were counted using a 0 - 1 circularity and a 50 - ∞ (pixel^2) area. The 50 pixel^2 lower limit was chosen as this is the area of the smallest particle that can be observed at this magnification, corresponding to a 5.1 µm diameter. The particle counts for each image were then summed to obtain the total number of particles per sample. Statistical analysis of mean particle counts between brands was carried out by one-way ANOVA ($\alpha = 0.05$) followed by *post-hoc* Tukey's HSD using Matlab.

7.2.1.1.5 FTIR analysis

For each filtered bottled water sample, the composition of particles and fibers larger than 100 µm was determined using a Spectrum TWO FTIR (PerkinElmer) with a single-bounce diamond in attenuated total reflection (ATR) mode. Potential polymeric particles were identified by NR fluorescence which was excited using the external blue/green (450 - 510 nm) light source and observed through a 550 nm longpass filter without magnification. Up to 20 randomly selected particles were analyzed per sample. Using a fine-tip antistatic tweezer, large fluorescent particles and fibers (> 100 µm) were carefully picked up, placed on the prism, and compressed with the FTIR rod. For each particle, a spectrum (averaging 16 scans taken between 450-4000 cm^{-1} with resolution of 1 cm^{-1}) was collected and compared against the Perkin Elmer Spectrum- polymer library, which includes common polymers, to identify the particles and fibers. All FTIR spectra were later analyzed manually to confirm the match to a specific polymer, this was done by comparing the FTIR peaks to those reported in literature.

7.2.1.2 Approach 2 - Py-GC-MS

During analysis by Py-GC-MS, a sample is decomposed at high temperature (pyrolysis), the characteristic products are then separated in a gas chromatography column (GC), and finally detected using a mass spectrometer (MS). Py-GC-MS offers high sensitivity and is capable of detecting ~50 µg of plastic[45]. The presence of a specific type of polymer was confirmed when a ≥ 83.3% match was made with the characteristic pyrolysis products (see SI for a detailed explanation).

7.2.1.2.1 Filtration and staining for sample preparation

The samples analyzed by Py-GC-MS were prepared in a BSC. To prepare each sample for Py-GC-MS analysis, several bottles totaling a volume of 2.5 L of water were vacuum filtered through a 21-mm diameter Whatman glass microfiber filter (934-AH, 1.5 µm pore size) placed in the coffee filter configuration on a ceramic Bucher funnel, using a 500 mL glass separation funnel to make dropwise additions. This coffee filter configuration was used to prevent particles from sticking along the inside of the ceramic Bucher funnel. The last approximately 80-100 mL of bottled water was added in 2-3 small volumes of water to rinse the glass separation funnel and dislodge any potentially deposited particles from the stopcock. Finally, 20 mL of bottled water was transferred into a glass beaker, stained to a final concentration of 0.1 mg NR/L, and pipetted with a glass Pasteur pipette onto the filter. The filter was wetted with the NR-containing water which was allowed to sit on the filter for 30 min to stain the deposited particles. In this way, only a small amount of NR was used to stain and detect the largest particles. This prevented the NR signal from masking the signal from other materials of interest (i.e., polymers) in the MS. After filtration and staining, particles > ~100 µm were carefully removed from the filter with tweezers, mirroring the procedure used for FTIR analysis (described above), leaving particles between 1.5 and 100 µm on the filter for analysis by Py-GC-MS (Figure 7.1a). Two negative controls were prepared by filtering 2.5 L of LC/MS grade water following the same protocol and conditions mentioned previously. These controls were used to determine if there was any polymer contamination that arose from the sample preparation protocol.

7.2.1.2.2 Py-GC-MS analysis

The filters for Py-GC-MS samples were left to dry in a Petri dish for over 48 hours. Once dry, these were inserted using stainless steel tweezers into a quartz tube (dimensions: 25 mm length, 1.9 mm internal diameter, CDS Analytical). Samples were pyrolyzed at 500 °C for 20 s using a ¼

inch probe (GERSTEL Twister automatic pyrolysis unit). The pyrolysis products were subsequently introduced into a Thermo TRACE 1300 series gas chromatographer (GC) with a fused silica column-DB-5ms of length 50 m (internal diameter 0.2 mm, Agilent 128-5552) coupled to a Thermo ITQ-MS 1100 (external ion trap). A full mass scan was taken as well as four single ion monitoring (SIM) scans (Tables S7.1 & S7.2). The main limitation of Py-GC-MS is that full scans are often not sensitive enough given the heterogeneity of the samples. Thus, the SIM scans were used to enhance the signal of ions of interest and were chosen based on the polymers that were most commonly found using FTIR in the > 100 µm size range. Standards for the most common polymers were injected to determine the retention time of the characteristic pyrolysis products (details in Table S7.3). A Kraton standard could not be sourced, so the retention time was obtained from literature[51]. The two negative control filters were pyrolyzed using the same conditions.

7.3 Results and discussion

7.3.1 Nile red staining optimization

Negative controls consisting of LC/MS water spiked with a range of concentrations from 0.001 to 10 mg NR/L were used to evaluate the impact of NR concentration on imaging and particle counts, and results are shown in Figure 7.1b. No statistically significant difference was observed in the average counts for 10 mg NR/L (778 ± 948), 1 mg NR/L (371 ± 131), 0.1 mg NR/L (274 ± 92) and 0.01 mg NR/L (260 ± 151) ($p > 0.05$). Nile red has a low solubility in water[52], and a thick NR coating was observed on the filters for 10 mg NR/L (Figure S7.3). The elevated average count and large uncertainty of the 10 mg NR/L negative controls could be due to excess NR precipitating, resulting in false positives. Furthermore, the thick NR coating on the filter suggests the potential for masking actual particles that may be deposited and subsequently covered. The thickness of the

NR coating on the filter appeared to decrease with NR concentration. At the lowest concentration (0.001 mg NR/L), significantly lower particle counts were observed in LC/MS water (10 ± 13), with four samples having 0 counts. While this concentration would limit false positives, fluorescence signals were generally weak which could increase the possibility of incomplete staining in samples, leading to false negatives and under-reporting. Regardless of the concentration used, all conditions tested yielded some false positives. It is well known that NR can aggregate and auto-fluoresce resulting in the observation of a few particles[53].

Given the higher average and large standard deviation of the 10 mg NR/L negative control and the likelihood of incomplete staining at 0.001 mg NR/L, these concentrations were not further evaluated in the positive control tests. Particles observed in the positive controls were uniformly small and round, owing to the use of commercial 20 µm PS particles for the spikes. Raw and corrected (negative control subtracted) results of LC/MS water spiked with 2000 PS beads are shown in Figure 7.1c. We hypothesize that part of the background counts seen in the negative controls are due to excess NR. In the high purity water, where there are few particles for the dye to bind to, the NR is more likely to self-aggregate and yield false positives. In contrast, in samples that contain particles (i.e., the spiked positive control or the bottled water), where there is available surface for the NR to adhere, we do not expect to have the same number of false positives due to excess NR. It is very challenging to know how many of the particles observed in the negative controls are NR aggregates. Thus, for the positive controls, we present both the corrected counts and the raw counts and expect the true recovery to be somewhere in between. Good recovery was observed for 0.1 mg NR/L (between 84.6 ± 10.8% and 98.3 ± 9.8%). Recoveries were lower for both 1 mg NR/L (between 29.8 ± 40.1% and 48.4 ± 39.4%) and 0.01 mg NR/L (between 9.2 ± 8.0% and 22.2 ± 2.8%). The data for the 0.01 mg NR/L condition appears to confirm the hypothesis

that insufficient NR is available for staining of all particles in the sample. Conversely, the 1 mg NR/L positive controls exhibited large variability which is likely due to masking of particles arising from the presence of the NR film that, while less than what was observed for 10 mg NR/L, is still present on the filter (Figure S7.3). The filters for positive controls stained with 0.1 mg NR/L exhibited a faint pink coloration. This suggests that while an excess of NR was still present, the concentration was not so high as to mask considerable particles during imaging. NR attached to the glass filter itself exhibited clearly different fluorescence compared to stained particles (Figure S7.3). A slight excess of NR is desirable when dealing with samples of unknown particle concentrations, to ensure adequate staining of all particles. While more NR would be appealing to ensure full staining in unknown samples, the hydrophobic nature of the dye and the deposition that occurs during filtration suggests that overshooting the concentration can easily confound particle detection. As a result, for this study, 0.1 mg NR/L was chosen for staining bottled water samples due to the high recovery and low variability as well as the fact that particles were easily observed both at the filter edges and center during imaging.

Results from the negative and positive controls highlight the importance of selecting the appropriate NR concentration in the staining step. The second key aspect of the NR method optimization is that all bottled water samples, regardless of plastic or glass containers, were transferred into glass beakers. This ensured uniformity across brands as well as control samples because the walls of plastic bottles represent significant sinks for NR. Preliminary tests adding NR directly to plastic bottles or glass bottles (not shown) yielded inconsistent results which were attributed at least partially to a decrease in NR concentration in the water. While digestion is commonly employed to aid in the identification of polymers, the cleanliness of samples in this study did not require digestion, which is itself associated with plastic degradation[45].

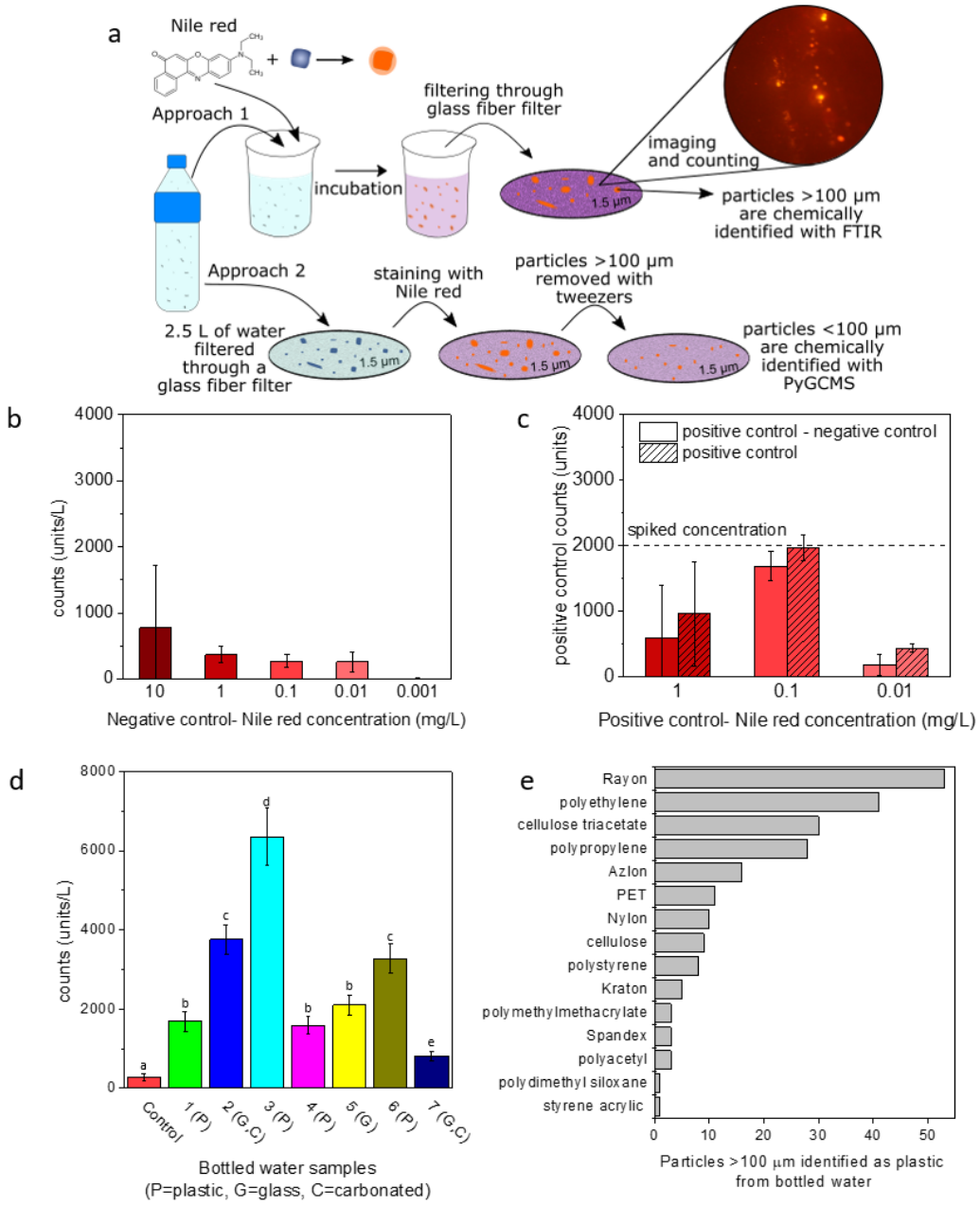

Figure 7.1. (a) Schematic showing the process followed to analyze bottled water. Approach 1 for counting and identification of particles > 100 µm with FTIR, and Approach 2 for identification of particles < 100 µm with Py-GC-MS. (b) Average particle counts observed in LC/MS water negative controls versus NR concentration. No statistically significant difference is observed

between NR concentrations ($p > 0.05$, $n = 10$). (c) Effect of NR concentration on the average recovery from positive controls spiked with 20 µm PS particles in LC/MS water at 2000 particles/L ($n = 5$). The solid bar has been corrected by subtracting the counts from the negative control, the hatched bar represents the raw positive control counts. (d) Average total number of particles (>5 µm) observed in each type of bottled water using a NR concentration of 0.1 mg L^{-1}. Letters indicate that the measurement is statistically significantly different ($p > 0.05$, $n = 7$) from the other letter groups. Counts are not corrected with the negative control, however, the values for the negative controls are shown in red. Raw data shown in Table S7.4. (e) Polymers identified using FTIR and total number of particles identified of each type (for all bottled water samples combined $n = 49$). A maximum of 20 particles per sample were analyzed by FTIR. Raw data shown in Table S7.5. All error bars represent standard deviation.

7.3.2 Particles in bottled water samples

Whereas particles in the positive controls were uniformly distributed over the filter, particles found in bottled water samples were generally observed in the inner and outer edge of the filter rather than the central circle (Figure S7.2). Discrepancies in the distribution of particles on the filter itself highlight the importance of scanning the whole filter when imaging. The fact that the particles were located in the filter folds (at the edge of the filter) might be an indication that they were floating in the bottled water and drawn into the folds through capillary action. While particles in the positive controls were observed to be uniformly fluorescent, in the bottled water samples, the fluorescence intensity between particles appeared more variable. Identification of the polymer based on the intensity of the fluorescence after staining has been attempted by others although an effective method has not yet been established[24,34,40].

Particles identified from the filter images were counted, and the results are shown in Figure 7.1d and Table S7.4. Due to the non-specificity of the NR method, it is possible that some of these particles are not polymers; however drinking water is a clean matrix containing low levels of organic contamination which reduces the likelihood of false positives. While some background counts and false positives were observed in the negative controls (274 ± 92 particles at 0.1 mg NR/L), the particle counts for all seven bottled waters were significantly different. Bottled water 7 contained the fewest particles (813 ± 123), but still significantly more than the negative controls. Bottled waters 2, 3, and 6 contained significantly more particles than bottled waters 1, 4, and 5. Bottled water 3 contained the most particles (6355 ± 726), with counts significantly higher than all the others. The morphology of the observed particles varied widely; fibers, small particles (< 100 µm) and larger particles (> 100 µm) were present in all samples of bottled water. However, bottled water 2 contained a surprising amount of large fiber-like material compared to the others (Figure S7.4). Some of this material was identified by FTIR as wood (i.e., cellulose). Interestingly, no correlation was observed between the total particle counts and either bottle type (plastic versus glass) or water type (carbonated versus still).

Particles > 100 µm were identified using FTIR. Interestingly, no particles >100 µm could be picked up for FTIR in the controls. This corroborates that the smaller particles observed with the NR method could have been false positives due to agglomeration of NR. Results for the bottles in Figure 7.1e show a wide variety of polymeric materials. 67% of all particles characterized by FTIR (n = 222) were identified as polymers. Both the diversity and frequency of the identified polymers is notable, as the vast majority do not match with the packaging. Rayon, a fiber frequently used in clothing, was the most frequently identified polymer (Figure 7.1e) and was observed in the majority of samples (Figure 7.2, yellow color). Cotton lab coats were worn exclusively when

preparing and handling samples, and neither Rayon, cotton, or cellulose were identified in any of the negative controls. As such, this contamination is unlikely to come from sample preparation, which suggests other sources (potentially during processing or bottling). Additionally, all bottled water samples contain Azlon, a synthetic textile fabric, while 42% of the particles analyzed in bottled water 6 consist of cellulose triacetate (Table S7.6).

Interestingly, the material of the plastic water bottles (PET) was identified as only the tenth most prevalent polymer, and no trend was observed between the presence of PET particles and the packaging (glass versus plastic). In comparison, the materials of the caps (PE and PP) were identified as the second and fourth most prevalent polymers, respectively. While some PE and PP particles were found in nearly every bottled water type, bottled waters 1, 2, 3, and 4 had caps made of PE and contained higher counts of PE (39 counts total) than bottles 5, 6, or 7 (2 counts total). Bottled waters 5, 6 and 7 had caps made of PP and contained the three highest counts of PP particles (24 of 28 total counts). It has been hypothesized that the action of opening and closing a water bottle causes abrasion of the lid which could lead to the release of particles.[24] Given the limited number of replicates in the material of the bottles and caps, it is hard to draw generalized conclusions, however, some observations can be noted. Bottles 1-4 (PE cap) contained a higher percentage of PE than bottles 5-7 (PP cap). On the other hand, bottles 5 and 7 (PP cap, glass bottles) contain a higher percentage of PP than the rest. Interestingly, even though bottle 6 had a PP cap, we hypothesize that because the bottle is PET (instead of glass) the abrasion of the cap was lower. Thus, our results agree with the hypothesis that abrasion of the cap when the bottle is opened leads to the release of particles. In the case of PP caps, this abrasion may be more pronounced for the harder glass bottles.

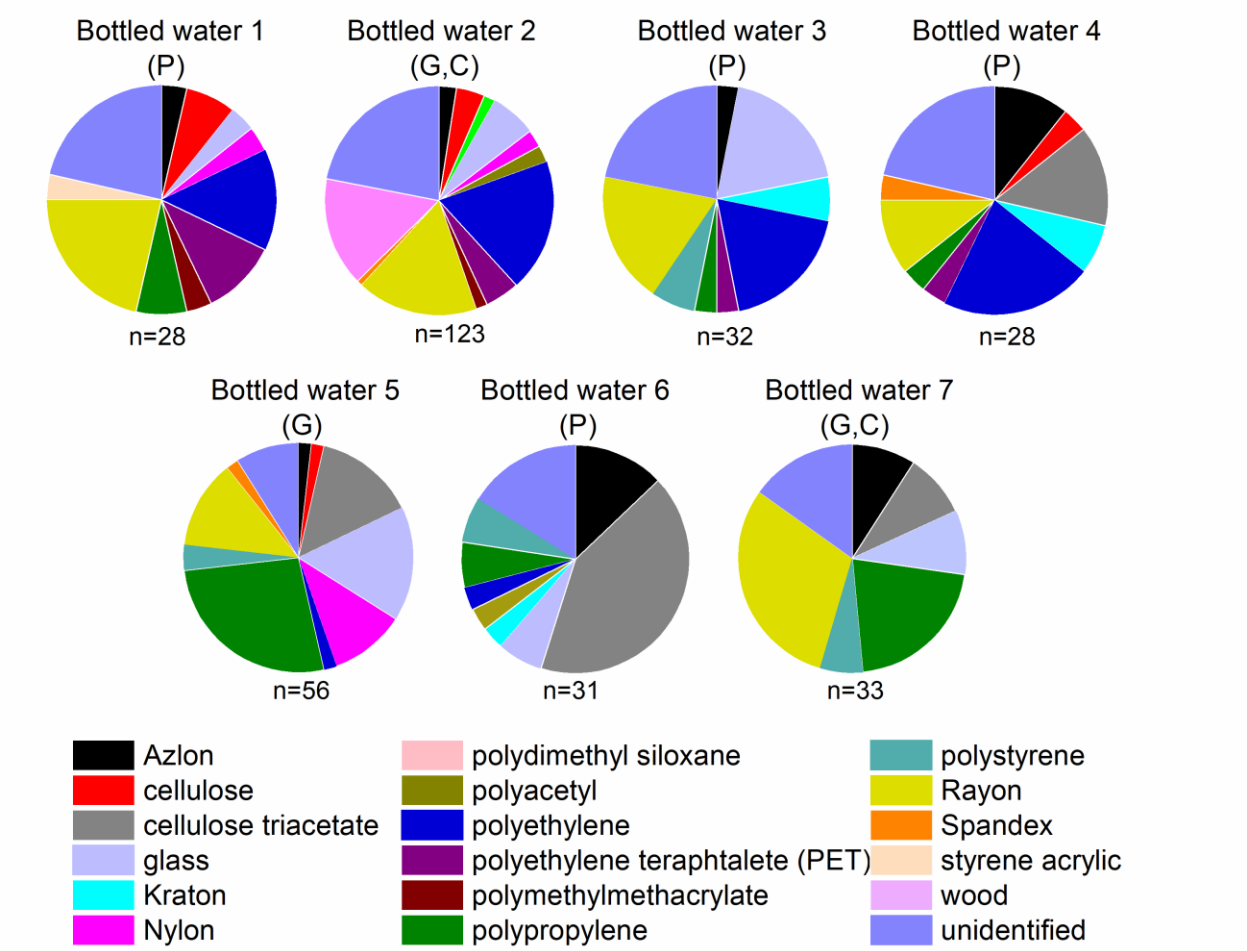

Figure 7.2. FTIR identification of particles and fibers >100 µm found in each bottled water sample. n refers to the number of particles analyzed for each bottled water. Raw data shown in Table S7.6. P=plastic bottle, G=glass bottle, C=carbonated water.

7.3.3 Analysis of particles > 1.5 µm and < 100 µm using Py-GC-MS

Polymers in the > 1.5 µm and < 100 µm size range in bottled water samples were qualitatively identified using Py-GC-MS (Table 7.1). While FTIR is a faster and more quantitative analysis, this smaller fraction of particles falls below the lower size limit of the technique. No polymers were positively identified by Py-GC-MS in the negative controls, which suggests that the particles observed were agglomerated Nile red. Some potential polymer degradation products were

identified in the negative controls; however, in all cases, the match with any polymer in the spectral library was below the 83.3% threshold, and no positive identifications were made. In general, similar profiles are observed in terms of the types of polymers identified across the bottled waters. All bottled water brands contained polystyrene (PS), polyvinyl carbonate (PVC), PET, Kraton, PP and nylon. Polycarbonate (PC), cellulose acetate, and polymethyl methacrylate (PMMA) were the most variable between waters. Kraton is a synthetic rubber replacement used in, e.g., modified asphalt; automotive interiors, carpets, and seals; adhesives; diapers; and telecommunication cables[54]. Azlon, which was detected in nearly all bottled waters in the larger fraction by FTIR, was not included in the MS analysis of the smaller size fraction of particles as neither a standard reference material nor a reference pyrogram could be located. This highlights one of the limitations of Py-GC-MS as an analysis technique: polymers could not be identified by the full scan alone and required *a priori* selection when programming the SIM scans. As a result, polymers that were not specifically targeted could not be positively identified.

Generally, each type of polymer is observed more consistently across the different bottled waters at the smaller size range than at the larger (> 100 µm), regardless of the packaging, origin, or treatment process. In a few cases, polymers identified by FTIR (> 100 µm) and Py-GC-MS (> 1.5 µm and < 100 µm) are not the same. PC was observed in half the bottled waters, and PVC was found in all bottled waters, at the smaller size classification with Py-GC-MS, while neither were observed above 100 µm with FTIR. Additionally, while PET was only observed in four of the seven bottled waters in the larger fraction (FTIR), it was present in all bottled waters in the smaller fraction. This includes bottled water 2, 5, and 7 which are made of glass and do not contain PET in their packaging. Similar to FTIR results, PE and PP were observed in most bottled waters, and a positive match was always made with the material of the cap.

Several types of polymers are identified in the particles > 1.5 µm and < 100 µm that do not match with the packaging material. Similar results are observed for the particles > 100 µm, which suggests that contamination is coming either from the water itself, the bottling process, or pre-existing in the bottle. Airborne plastics are more likely to be composed of small particles and fibers which could directly deposit during the bottling process or at the water source[55]. Given that some waters are filtered groundwater, some are treated tap water, and some are untreated ground water, these findings suggest that further research should be undertaken to identify the origin of these particles.

Table 7.2. Polymers <100 µm identified by Py-GC-MS for each bottled water sample and negative controls. Polymers were positively identified when a sample resulted in ≥83.3% match with the characteristic pyrolysis products (see SI for detailed explanation). A ✓ indicates a positive match, while the × means either the polymer was not observed, or the match was below the threshold. Raw data in Tables S7.7 to S7.11.

Bottled water	PS	PE	PVC	PC	PET	Rayon	Cellulose Triacetate	Kraton	Cellulose	PP	Nylon	PMMA
1 (P)	✓	✓	✓	✓	✓	✓	✓	✓	✓	✓	✓	✓
2 (G,C)	✓	✓	✓	×	✓	✓	×	✓	✓	✓	✓	×
3 (P)	✓	✓	✓	✓	✓	✓	×	✓	✓	✓	✓	✓
4 (P)	✓	✓	✓	×	✓	✓	×	✓	✓	✓	✓	×
5 (G)	✓	✓	✓	×	✓	✓	×	✓	✓	✓	✓	×
6 (P)	✓	✓	✓	×	✓	✓	✓	✓	✓	✓	✓	✓
7 (G,C)	✓	×	✓	✓	✓	×	✓	✓	×	✓	✓	✓
Negative control	×	×	×	×	×	×	×	×	×	×	×	×

7.4 Environmental implications

Microplastic particles have been observed in the food chain[13,18,19]. In the case of bottled water, several studies have been published attempting to quantify the number of microplastics and their

type. Schymanski *et al*. found only about 1-2% of particles were larger than 100 µm, highlighting the importance of analyzing the smaller fraction. Our results are comparable, as total counts were on average 2800 particles per liter, whereas, particles > 100 µm analyzed by FTIR were on average 6.7 particles per bottle (approximately 2% of the total particles)[31]. Using Raman microspectroscopy, that study found that the particles consisted of various polymers (PP, PE, polyester, polyamide and PET), not uniquely those polymers related to the packaging (bottle and cap).[31] A similar study by Oßmann *et al*. found up to 6292 particles per liter in mineral water (> 1 µm), 90% of which were confirmed to be polymeric (mainly PP, PE, PET and styrene-based polymers) by Raman microspectroscopy.[25] This study also found that up to 99.6% of particles were smaller than 10 µm. However, large variability was observed between samples, thus the results were not significantly different from the controls[25]. Indeed, studies that have used dyes to identify microplastics often present high variability between samples of the same brand of water bottle[23,25]. We hypothesize this might be due to the concentration of dye used, as our results show that using high or low concentrations of dye will increase the variability of particle counts. This study highlights the importance of performing an initial NR optimization that will assure the reliability of the results obtained. As observed, high NR concentrations can lead to false positives, whereas low NR concentrations can lead to an underestimation as not all particles will be stained. Additionally, while most studies choose to discard natural polymers (e.g. cellulose) or synthetic cellulosic polymers (e.g. Rayon) from their analysis, recent discussion on the topic had led to believe that the environmental impact of natural polymers might be as important as the impact of synthetic polymers[56]. The method developed in this study has been demonstrated to perform successfully in clean matrices with very low organic content such as bottled water. However, the use of the NR method would have to be tuned and accompanied by digestions when

analyzing more complex matrices such as environmental samples. We believe this cost-efficient and simple method can be used on-site in drinking water plants as a screening method for microplastics, as the minimum required equipment consists of a stereomicroscope and a laminar flow cabinet.

The non-specificity of NR also requires secondary confirmation of plastics, rather than relying solely on fluorescence. Here, we confirmed the presence of microplastics in all samples at both size classifications. Results from Py-GC-MS largely mirror the plastics identified by FTIR. This is unsurprising as the size cutoff between the two detection methods was functionally determined by what was able to be picked up and placed on the FTIR prism. This highlights that microplastics exist at a continuum of sizes[57] and suggests the breakdown of macro sized plastic particles into microplastics, and, most likely, nanoplastics due to weathering in the environment or the water bottling process.

7.5 Acknowledgements

The authors acknowledge the financial support of the Canada Research Chairs program, the Natural Sciences and Engineering Research Council of Canada, the Killam Research Fellowship, and the Canada Foundation for Innovation. LMH was supported by a McGill Engineering Doctoral Award, a Eugenie Ulmer-Lamothe Award and an NSERC CREATE PURE award, DCM was supported by an NSERC Banting Fellowship, HJ was supported by an NSERC Alexander Graham Bell Canada Graduate Scholarship, and SM was supported by an NSERC CGSM scholarship and an NSERC CREATE PURE award. The authors would like to thank P. Shakeri for her contribution in the preliminary stages of the project, B. Nguyen for helpful discussions, and S. Mason of the State University of New York for sharing the original NR protocol.

7.6 References

(1) Alimi, O. S.; Farner Budarz, J.; Hernandez, L. M.; Tufenkji, N. Microplastics and Nanoplastics in Aquatic Environments: Aggregation, Deposition, and Enhanced Contaminant Transport. *Environmental Science & Technology* **2018**. https://doi.org/10.1021/acs.est.7b05559.

(2) Panko, J. M.; Chu, J.; Kreider, M. L.; Unice, K. M. Measurement of Airborne Concentrations of Tire and Road Wear Particles in Urban and Rural Areas of France, Japan, and the United States. *Atmospheric Environment* **2013**, *72*, 192–199. https://doi.org/10.1016/j.atmosenv.2013.01.040.

(3) Dris, R.; Gasperi, J.; Mirande, C.; Mandin, C.; Guerrouache, M.; Langlois, V.; Tassin, B. A First Overview of Textile Fibers, Including Microplastics, in Indoor and Outdoor Environments. *Environmental Pollution* **2017**, *221*, 453–458. https://doi.org/10.1016/j.envpol.2016.12.013.

(4) Zalasiewicz, J.; Waters, C. N.; Ivar do Sul, J. A.; Corcoran, P. L.; Barnosky, A. D.; Cearreta, A.; Edgeworth, M.; Gałuszka, A.; Jeandel, C.; Leinfelder, R.; McNeill, J. R.; Steffen, W.; Summerhayes, C.; Wagreich, M.; Williams, M.; Wolfe, A. P.; Yonan, Y. The Geological Cycle of Plastics and Their Use as a Stratigraphic Indicator of the Anthropocene. *Anthropocene* **2016**, *13*, 4–17. https://doi.org/10.1016/j.ancene.2016.01.002.

(5) Zubris, K. A. V.; Richards, B. K. Synthetic Fibers as an Indicator of Land Application of Sludge. *Environmental Pollution* **2005**, *138* (2), 201–211. https://doi.org/10.1016/j.envpol.2005.04.013.

(6) Horton, A. A.; Walton, A.; Spurgeon, D. J.; Lahive, E.; Svendsen, C. Microplastics in Freshwater and Terrestrial Environments: Evaluating the Current Understanding to Identify the

Knowledge Gaps and Future Research Priorities. *Science of The Total Environment* **2017**, *586*, 127–141. https://doi.org/10.1016/j.scitotenv.2017.01.190.

(7) Wright, S. L.; Kelly, F. J. Plastic and Human Health: A Micro Issue? *Environmental Science & Technology* **2017**, *51* (12), 6634–6647. https://doi.org/10.1021/acs.est.7b00423.

(8) Eerkes-Medrano, D.; Thompson, R. C.; Aldridge, D. C. Microplastics in Freshwater Systems: A Review of the Emerging Threats, Identification of Knowledge Gaps and Prioritisation of Research Needs. *Water Research* **2015**, *75*, 63–82. https://doi.org/10.1016/j.watres.2015.02.012.

(9) Cabernard, L.; Roscher, L.; Lorenz, C.; Gerdts, G.; Primpke, S. Comparison of Raman and Fourier Transform Infrared Spectroscopy for the Quantification of Microplastics in the Aquatic Environment. *Environ. Sci. Technol.* **2018**, *52* (22), 13279–13288. https://doi.org/10.1021/acs.est.8b03438.

(10) World Health Organization. *Microplastics in Drinking Water*; Switzerland, 2019.

(11) Klein, S.; Worch, E.; Knepper, T. P. Occurrence and Spatial Distribution of Microplastics in River Shore Sediments of the Rhine-Main Area in Germany. *Environ. Sci. Technol.* **2015**, *49* (10), 6070–6076. https://doi.org/10.1021/acs.est.5b00492.

(12) Hernandez, L. M.; Xu, E. G.; Larsson, H. C. E.; Tahara, R.; Maisuria, V. B.; Tufenkji, N. Plastic Teabags Release Billions of Microparticles and Nanoparticles into Tea. *Environ. Sci. Technol.* **2019**, *53* (21), 12300–12310. https://doi.org/10.1021/acs.est.9b02540.

(13) Rochman, C. M.; Tahir, A.; Williams, S. L.; Baxa, D. V.; Lam, R.; Miller, J. T.; Teh, F.-C.; Werorilangi, S.; Teh, S. J. Anthropogenic Debris in Seafood: Plastic Debris and Fibers from

Textiles in Fish and Bivalves Sold for Human Consumption. *Sci Rep* **2015**, *5* (1), 14340. https://doi.org/10.1038/srep14340.

(14) Bouwmeester, H.; Hollman, P. C. H.; Peters, R. J. B. Potential Health Impact of Environmentally Released Micro- and Nanoplastics in the Human Food Production Chain: Experiences from Nanotoxicology. *Environmental Science & Technology* **2015**, *49* (15), 8932–8947. https://doi.org/10.1021/acs.est.5b01090.

(15) Castelvetro, V.; Corti, A.; Bianchi, S.; Giacomelli, G.; Manariti, A.; Vinciguerra, V. Microplastics in Fish Meal: Contamination Level Analyzed by Polymer Type, Including Polyester (PET), Polyolefins, and Polystyrene. *Environmental Pollution* **2021**, *273*, 115792. https://doi.org/10.1016/j.envpol.2020.115792.

(16) Browne, M. A.; Dissanayake, A.; Galloway, T. S.; Lowe, D. M.; Thompson, R. C. Ingested Microscopic Plastic Translocates to the Circulatory System of the Mussel, *Mytilus Edulis* (L). *Environ. Sci. Technol.* **2008**, *42* (13), 5026–5031.

(17) Van Cauwenberghe, L.; Claessens, M.; Vandegehuchte, M. B.; Janssen, C. R. Microplastics Are Taken up by Mussels (*Mytilus Edulis*) and Lugworms (*Arenicola Marina*) Living in Natural Habitats. *Environmental Pollution* **2015**, *199*, 10–17. https://doi.org/10.1016/j.envpol.2015.01.008.

(18) Schwabl, P.; Köppel, S.; Königshofer, P.; Bucsics, T.; Trauner, M.; Reiberger, T.; Liebmann, B. Detection of Various Microplastics in Human Stool: A Prospective Case Series. *Ann Intern Med* **2019**, *171* (7), 453. https://doi.org/10.7326/M19-0618.

(19) Peixoto, D.; Pinheiro, C.; Amorim, J.; Oliva-Teles, L.; Guilhermino, L.; Vieira, M. N. Microplastic Pollution in Commercial Salt for Human Consumption: A Review. *Estuarine, Coastal and Shelf Science* **2019**, *219*, 161–168. https://doi.org/10.1016/j.ecss.2019.02.018.

(20) Novotna, K.; Cermakova, L.; Pivokonska, L.; Cajthaml, T.; Pivokonsky, M. Microplastics in Drinking Water Treatment – Current Knowledge and Research Needs. *Science of The Total Environment* **2019**, *667*, 730–740. https://doi.org/10.1016/j.scitotenv.2019.02.431.

(21) Pivokonsky, M.; Cermakova, L.; Novotna, K.; Peer, P.; Cajthaml, T.; Janda, V. Occurrence of Microplastics in Raw and Treated Drinking Water. *Science of The Total Environment* **2018**, *643*, 1644–1651. https://doi.org/10.1016/j.scitotenv.2018.08.102.

(22) Mintenig, S. M.; Löder, M. G. J.; Primpke, S.; Gerdts, G. Low Numbers of Microplastics Detected in Drinking Water from Ground Water Sources. *Science of The Total Environment* **2019**, *648*, 631–635. https://doi.org/10.1016/j.scitotenv.2018.08.178.

(23) Mason, S. A.; Welch, V. G.; Neratko, J. Synthetic Polymer Contamination in Bottled Water. *Frontiers in Chemistry* **2018**, *6*. https://doi.org/10.3389/fchem.2018.00407.

(24) Singh, T. Generation of Microplastics from the Opening and Closing of Disposable Plastic Water Bottles. *Journal of Water and Health* **2021**, *19* (3), 488–498. https://doi.org/10.2166/wh.2021.025.

(25) Oßmann, B. E.; Sarau, G.; Holtmannspötter, H.; Pischetsrieder, M.; Christiansen, S. H.; Dicke, W. Small-Sized Microplastics and Pigmented Particles in Bottled Mineral Water. *Water Research* **2018**, *141*, 307–316. https://doi.org/10.1016/j.watres.2018.05.027.

(26) *SB-1422 California Safe Drinking Water Act: Microplastics*.

(27) Browne, M. A.; Crump, P.; Niven, S. J.; Teuten, E.; Tonkin, A.; Galloway, T.; Thompson, R. Accumulation of Microplastic on Shorelines Woldwide: Sources and Sinks. *Environ. Sci. Technol.* **2011**, *45* (21), 9175–9179. https://doi.org/10.1021/es201811s.

(28) McCormick, A.; Hoellein, T. J.; Mason, S. A.; Schluep, J.; Kelly, J. J. Microplastic Is an Abundant and Distinct Microbial Habitat in an Urban River. *Environ. Sci. Technol.* **2014**, *48* (20), 11863–11871. https://doi.org/10.1021/es503610r.

(29) Morritt, D.; Stefanoudis, P. V.; Pearce, D.; Crimmen, O. A.; Clark, P. F. Plastic in the Thames: A River Runs through It. *Marine Pollution Bulletin* **2014**, *78* (1–2), 196–200. https://doi.org/10.1016/j.marpolbul.2013.10.035.

(30) Kosuth, M.; Mason, S. A.; Wattenberg, E. V. Anthropogenic Contamination of Tap Water, Beer, and Sea Salt. *PLoS ONE* **2018**, *13* (4), e0194970. https://doi.org/10.1371/journal.pone.0194970.

(31) Schymanski, D.; Goldbeck, C.; Humpf, H.-U.; Fürst, P. Analysis of Microplastics in Water by Micro-Raman Spectroscopy: Release of Plastic Particles from Different Packaging into Mineral Water. *Water Research* **2018**, *129*, 154–162. https://doi.org/10.1016/j.watres.2017.11.011.

(32) Ranjan, V. P.; Joseph, A.; Goel, S. Microplastics and Other Harmful Substances Released from Disposable Paper Cups into Hot Water. *Journal of Hazardous Materials* **2021**, *404*, 124118. https://doi.org/10.1016/j.jhazmat.2020.124118.

(33) Kankanige, D.; Babel, S. Contamination by ≥6.5 Mm-Sized Microplastics and Their Removability in a Conventional Water Treatment Plant (WTP) in Thailand. *Journal of Water Process Engineering* **2021**, *40*, 101765. https://doi.org/10.1016/j.jwpe.2020.101765.

(34) Maes, T.; Jessop, R.; Wellner, N.; Haupt, K.; Mayes, A. G. A Rapid-Screening Approach to Detect and Quantify Microplastics Based on Fluorescent Tagging with Nile Red. *Sci Rep* **2017**, *7* (1), 44501. https://doi.org/10.1038/srep44501.

(35) Shim, W. J.; Song, Y. K.; Hong, S. H.; Jang, M. Identification and Quantification of Microplastics Using Nile Red Staining. *Marine Pollution Bulletin* **2016**, *113* (1–2), 469–476. https://doi.org/10.1016/j.marpolbul.2016.10.049.

(36) Erni-Cassola, G.; Gibson, M. I.; Thompson, R. C.; Christie-Oleza, J. A. Lost, but Found with Nile Red: A Novel Method for Detecting and Quantifying Small Microplastics (1 Mm to 20 Mm) in Environmental Samples. *Environ. Sci. Technol.* **2017**, *51* (23), 13641–13648. https://doi.org/10.1021/acs.est.7b04512.

(37) Ji, X.; Ma, Y.; Zeng, G.; Xu, X.; Mei, K.; Wang, Z.; Chen, Z.; Dahlgren, R.; Zhang, M.; Shang, X. Transport and Fate of Microplastics from Riverine Sediment Dredge Piles: Implications for Disposal. *Journal of Hazardous Materials* **2021**, *404*, 124132. https://doi.org/10.1016/j.jhazmat.2020.124132.

(38) El Hayany, B.; El Fels, L.; Quénéa, K.; Dignac, M.-F.; Rumpel, C.; Gupta, V. K.; Hafidi, M. Microplastics from Lagooning Sludge to Composts as Revealed by Fluorescent Staining-Image Analysis, Raman Spectroscopy and Pyrolysis-GC/MS. *Journal of Environmental Management* **2020**, *275*, 111249. https://doi.org/10.1016/j.jenvman.2020.111249.

(39) Nel, H. A.; Chetwynd, A. J.; Kelleher, L.; Lynch, I.; Mansfield, I.; Margenat, H.; Onoja, S.; Goldberg Oppenheimer, P.; Sambrook Smith, G. H.; Krause, S. Detection Limits Are Central to Improve Reporting Standards When Using Nile Red for Microplastic Quantification. *Chemosphere* **2021**, *263*, 127953. https://doi.org/10.1016/j.chemosphere.2020.127953.

(40) Labbe, A. B.; Bagshaw, C. R.; Uttal, L. Inexpensive Adaptations of Basic Microscopes for the Identification of Microplastic Contamination Using Polarization and Nile Red Fluorescence Detection. *J. Chem. Educ.* **2020**, *97* (11), 4026–4032. https://doi.org/10.1021/acs.jchemed.0c00518.

(41) Kang, H.; Park, S.; Lee, B.; Ahn, J.; Kim, S. Modification of a Nile Red Staining Method for Microplastics Analysis: A Nile Red Plate Method. *Water* **2020**, *12* (11), 3251. https://doi.org/10.3390/w12113251.

(42) Prata, J. C.; Alves, J. R.; da Costa, J. P.; Duarte, A. C.; Rocha-Santos, T. Major Factors Influencing the Quantification of Nile Red Stained Microplastics and Improved Automatic Quantification (MP-VAT 2.0). *Science of The Total Environment* **2020**, *719*, 137498. https://doi.org/10.1016/j.scitotenv.2020.137498.

(43) Costa, C. Q. V.; Cruz, J.; Martins, J.; Teodósio, M. A. A.; Jockusch, S.; Ramamurthy, V.; Da Silva, J. P. Fluorescence Sensing of Microplastics on Surfaces. *Environ Chem Lett* **2021**, *19* (2), 1797–1802. https://doi.org/10.1007/s10311-020-01136-0.

(44) Sturm, M. T.; Horn, H.; Schuhen, K. The Potential of Fluorescent Dyes—Comparative Study of Nile Red and Three Derivatives for the Detection of Microplastics. *Anal Bioanal Chem* **2021**, *413* (4), 1059–1071. https://doi.org/10.1007/s00216-020-03066-w.

(45) Nguyen, B.; Claveau-Mallet, D.; Hernandez, L. M.; Xu, E. G.; Farner, J. M.; Tufenkji, N. Separation and Analysis of Microplastics and Nanoplastics in Complex Environmental Samples. *Accounts of Chemical Research* **2019**, *52* (4), 858–866. https://doi.org/10.1021/acs.accounts.8b00602.

(46) Elert, A. M.; Becker, R.; Duemichen, E.; Eisentraut, P.; Falkenhagen, J.; Sturm, H.; Braun, U. Comparison of Different Methods for MP Detection: What Can We Learn from Them, and Why Asking the Right Question before Measurements Matters? *Environmental Pollution* **2017**, *231*, 1256–1264. https://doi.org/10.1016/j.envpol.2017.08.074.

(47) Mallikarjunachari, G.; Ghosh, P. Analysis of Strength and Response of Polymer Nano Thin Film Interfaces Applying Nanoindentation and Nanoscratch Techniques. *Polymer* **2016**, *90*, 53–66. https://doi.org/10.1016/j.polymer.2016.02.042.

(48) Löder, M. G. J.; Gerdts, G. Methodology Used for the Detection and Identification of Microplastics—A Critical Appraisal. In *Marine Anthropogenic Litter*; Bergmann, M., Gutow, L., Klages, M., Eds.; Springer International Publishing: Cham, 2015; pp 201–227. https://doi.org/10.1007/978-3-319-16510-3_8.

(49) Fabbri, D.; Rombolà, A. G.; Vassura, I.; Torri, C.; Franzellitti, S.; Capolupo, M.; Fabbri, E. Off-Line Analytical Pyrolysis GC–MS to Study the Accumulation of Polystyrene Microparticles in Exposed Mussels. *Journal of Analytical and Applied Pyrolysis* **2020**, *149*, 104836. https://doi.org/10.1016/j.jaap.2020.104836.

(50) Fischer, M.; Scholz-Böttcher, B. M. Simultaneous Trace Identification and Quantification of Common Types of Microplastics in Environmental Samples by Pyrolysis-Gas Chromatography–Mass Spectrometry. *Environ. Sci. Technol.* **2017**, *51* (9), 5052–5060. https://doi.org/10.1021/acs.est.6b06362.

(51) Klee, M. S.; Chang, I. Pyrolysis-GC/MS/IR Analysis of Kraton 1107. Hewlett Packard July 1989.

(52) Greenspan, P.; Fowler, S. D. Spectrofluorometric Studies of the Lipid Probe, Nile Red. *J Lipid Res* **1985**, *26* (7), 781–789.

(53) Ray, A.; Das, S.; Chattopadhyay, N. Aggregation of Nile Red in Water: Prevention through Encapsulation in β-Cyclodextrin. *ACS Omega* **2019**, *4* (1), 15–24. https://doi.org/10.1021/acsomega.8b02503.

(54) Kraton Corporation.

(55) Dris, R.; Gasperi, J.; Saad, M.; Mirande, C.; Tassin, B. Synthetic Fibers in Atmospheric Fallout: A Source of Microplastics in the Environment? *Marine Pollution Bulletin* **2016**, *104* (1–2), 290–293. https://doi.org/10.1016/j.marpolbul.2016.01.006.

(56) Felismino, M. E. L.; Helm, P. A.; Rochman, C. M. Microplastic and Other Anthropogenic Microparticles in Water and Sediments of Lake Simcoe. *Journal of Great Lakes Research* **2021**, *47* (1), 180–189. https://doi.org/10.1016/j.jglr.2020.10.007.

(57) Gigault, J.; El Hadri, H.; Nguyen, B.; Grassl, B.; Rowenczyk, L.; Tufenkji, N.; Feng, S.; Wiesner, M. Nanoplastics Are Neither Microplastics nor Engineered Nanoparticles. *Nat. Nanotechnol.* **2021**, *16* (5), 501–507. https://doi.org/10.1038/s41565-021-00886-4.

7.7 Supporting information

Table S7.1. Most common plastics and fibers found with FTIR and their characteristic pyrolysis products. Each characteristic pyrolysis product is identified in the MS by finding the indicator ions at the retention time. References indicate pyrolysis product information taken from literature.

Plastic	Characteristic pyrolysis product(s)	Indicator ions	Approximate retention time (± 1 min)
polystyrene (PS)[1]	styrene	104, 78	9
	3-butene-1,3-diyldibenzene	208, 91	21
	5-hexene-1,3,5-triyltribenzene	207, 91	23
polyethylene	alkenes	99, 85	20
(PE)[1]	α-alkenes	97, 83	19
	α,ω-alkenes	95, 82	23
polyvinyl chloride	benzene	78	4
(PVC)[1]	chlorobenzene	112, 77	8
polycarbonate	p-methoxy-tert-butylbenzene	164, 149	16
(PC)[1]	2,2-bis(4′-methoxy-phenyl)propane	256, 241	26
polyethylene terephthalate (PET)[1]	dimethyl terephthalate	194,163	21
rayon[2]	furfural	39, 95/96	7
	2-furanmethanol	41, 53, 69, 81, 97/98	8
	2-furancarboxaldehyde, 5-methyl-	53, 109/110	10
	5-hydroxymethylfurfural	41, 69, 97, 126	20
cellulose acetate[3]	acetic acid	45, 60	4
	2-hydroxyethyl acetate	43, 73	6
	4,6-dimethyl-2H-pyran-2-one	43, 53, 81, 96	10
	unidentified	43, 114	16
	unidentified	43, 82	17
Kraton[4]	isoprene	39, 53, 67/68	4
	styrene	78, 104	9
	limonene	68, 93, 107, 136	11

cellulose[3]	pyruvic aldehyde	29, 43	4
	hydroxyacetaldehyde	31, 60	5
	5-(hydroxymethyl)dihydro-2(3H)-furanone	29, 58, 114	13
	5-(hydroxymethyl)-2-furfural	41, 97, 126	15
polypropylene (PP)[1]	2,4-dimethylhept-1-ene	126, 70	8
	2,4,6,8-tetramethyl-1-undecene	111, 69	16
	2,4,6,8-tetramethyl-1-undecene	111, 69	19
	2,4,6,8-tetramethyl-1-undecene	111, 69	22
nylon[1]	ε-Caprolactam	113, 85/84	15
	N-methyl ε-caprolactam	127, 70	18
polymethyl methacrylate (PMMA)[1]	methyl acrylate	85, 55	5
	methyl methacrylate	100, 69	7

Table S7.2. Plastics and fibers were placed into single ion monitoring (SIM) groups according to similar mass of ion ranges for their characteristic pyrolysis products.

SIM Group	Plastics and fibers	Mass of ions (ranges) for each SIM
SIM 1	Polystyrene (PS)	75.50 – 92.50
	Polyethylene (PE)	94.00 – 114.00
	Polyvinyl chloride (PVC)	204.50 – 209.50
SIM 2	Polyethylene terephthalate (PET)	147.00 – 167.00
	Polycarbonate (PC)	192.50 – 195.50
		238.00 – 256.00
SIM 3	Rayon	37.00 – 47.00
	Cellulose acetate	50.50 – 75.50
	Kraton	76.00 – 96.00
	Cellulose	92.50 – 117.50
		123.50 – 138.50
SIM 4	Polypropylene	53.00 – 73.00
	Nylon	81.50 – 86.50
	Polymethyl methacrylate (PMMA)	98.50 – 115.50
		123.50 – 128.50

Table S7.3. Specifications for the standards used for each polymer.

Material	Description of the standard used
polystyrene (PS)	McMaster Carr polystyrene sheet (product number: 8734K39)
polyethylene (PE)* *both low and high density PE were tested. The pyrolysis result was the same.	McMaster Carr high density polyethylene sheet (product number: 8619K427) McMaster Carr low density polyethylene sheet (product number: 8657K811)
polyvinyl chloride (PVC)	McMaster Carr Clear Chemical-Resistant PVC film (product number: 8562K11)
polycarbonate (PC)	McMaster Carr Clear polycarbonate sheet (product number: 8574K281)
polyethylene terephthalate (PET)	McMaster Carr PET polyester film (product number: 8567K102)
rayon	Piece of fabric purchased at Winners (Montreal, Canada). Labelled as 100% rayon
cellulose acetate	Cospheric Cellulose Acetate Spheres (product number: CAS-ALA-1.3 1.41+/-0.05mm-100)
Kraton	N/A. Values taken from literature [4]
cellulose	Domtar Softwood kraft pulp sheets
polypropylene (PP)	McMaster Carr polypropylene sheet (product number: 8742K831)
nylon	McMaster Carr nylon mesh (product number: 9318T41)
polymethyl methacrylate (PMMA)	ACROS Organics Poly(methyl methacrylate), sec. stand., M.W. 94600, M.N. 52300 (product number: AC178780250)

Individual pyrolysis product (Table S7.1) matches were categorized into three levels: perfect match (1 point), partial match (0.5 points), no match (0 points). These levels were dependent on the strength of the ion signal and the retention time from the SIM scans (Tables S7.7-7.11). A perfect match meant all ions were present at the correct retention time and the signal in the MS spectra was at least 15% above the baseline. A partial match was given either when the retention time of one of the ions was shifted a few seconds, or when the MS signal was weak (peak only 5-

15% above the baseline). No match was given in any other scenario. The percent match for each polymer in a specific sample was determined by adding the scores obtained in each pyrolysis product and diving this by the score of the standard (perfect match (1 point) in all pyrolysis products- Table S7.3). Positive identification of a polymer was assigned for samples with ≥83.3% match of the pyrolysis products.

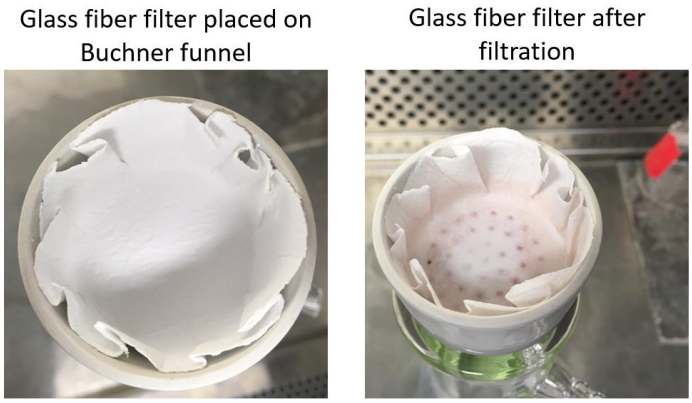

Figure S7.1. Whatman binder-free glass microfiber filter placed on Buchner funnel in a coffee-filter formation before and after filtration of the samples.

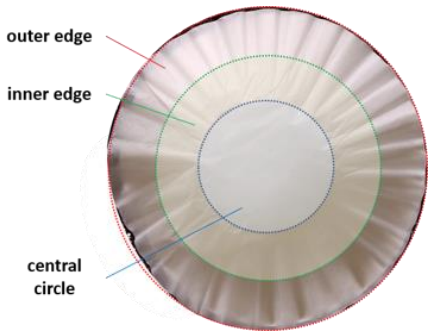

Figure S7.2. Schematic that shows the division in which the imaging was divided. This approach ensured that the entire area of the filter was imaged.

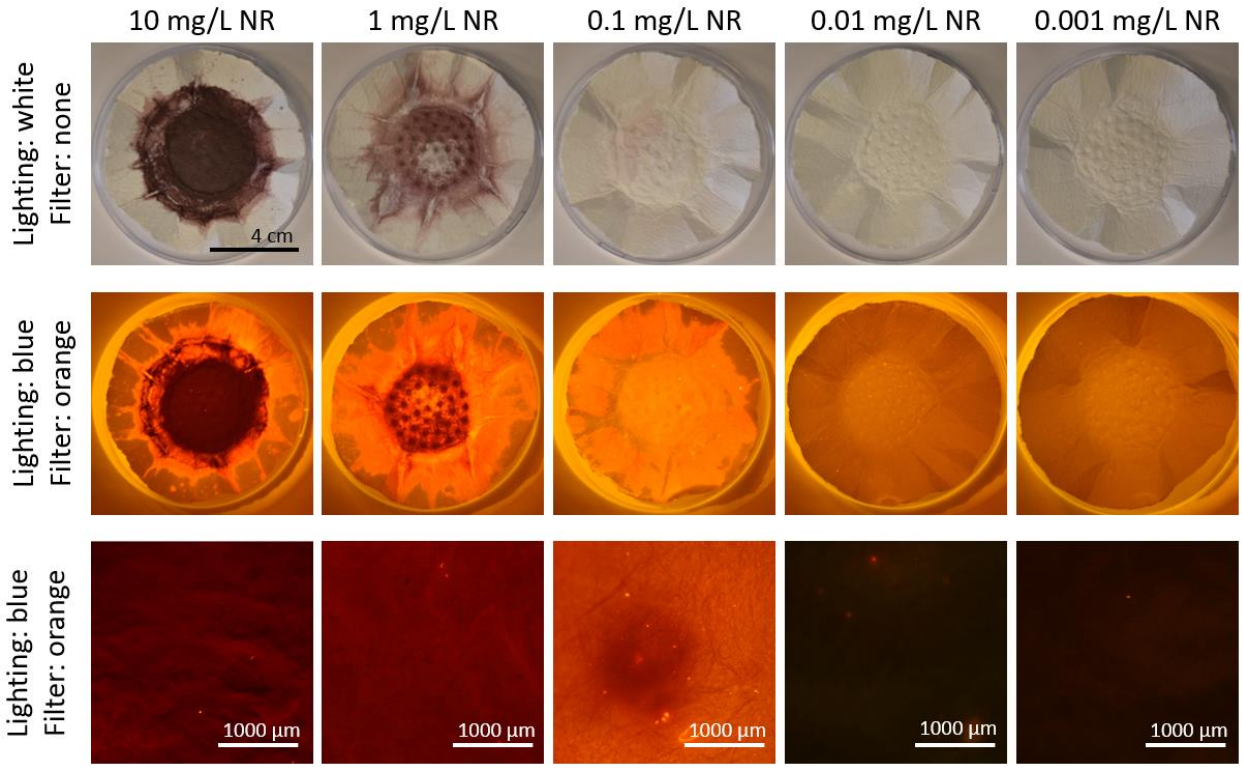

Figure S7.3. Representative filters of negative controls at varying NR concentrations. Row 1 - filters under ambient light with no emission filter. Row 2 - filters under blue light with an orange emission filter. Row 3 - filters under blue light with an orange emission filter taken at 40× total magnification.

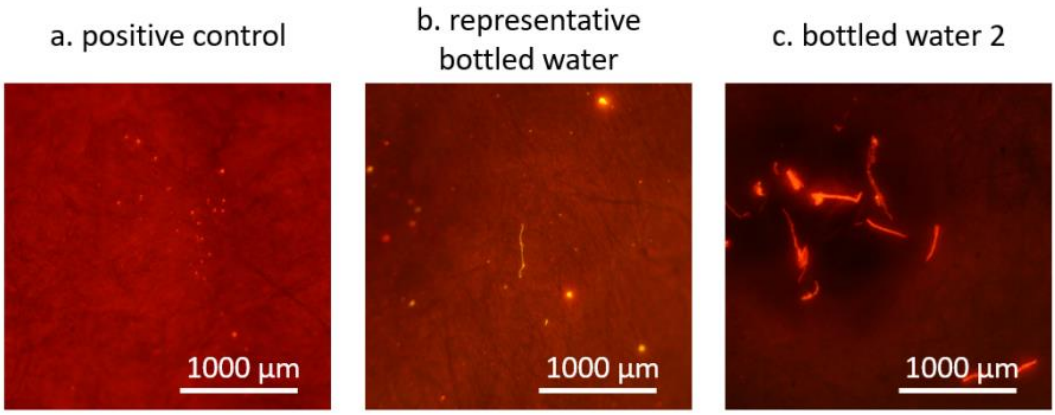

Figure S7.4. Representative images of the particles observed in (a) the positive control (which was spiked with 20 µm PS), (b) bottled water samples, and (c) bottled water sample 2, which contained an unusually large amount of fibers. All samples shown were spiked with 0.1 mg NR/L.

Table S7.4. Total particle counts from bottled water samples. Data plotted in Figure 7.1c.

Bottled Water	Average	STD
Control	274	92
1 (P)	1693	246
2 (G, C)	3765	362
3 (P)	6355	726
4 (P)	1595	225
5 (G)	2110	255
6 (P)	3275	366
7 (G, C)	813	123

Table S7.5. Plastics and fibers identified using FTIR and total number of particles identified of each type (for all bottled water samples combined n = 49). A maximum of 20 particles per sample were analyzed by FTIR. Data plotted in Figure 7.1d.

Material	Count
Rayon	53
Polyethylene	41
Cellulose Triacetate	30
Polypropylene	28
Azlon	16
Polyethylene Teraphtalete (PET)	11
Nylon	10
Cellulose	9
Polystyrene	8
Kraton	5
Polyacetyl	3
Spandex	3
Polymethylmethacrylate	3
Styrene Acrylic	1
Polydimethyl siloxane	1

Table S7.6. Plastic particle counts from FTIR identification of particles >100 µm found in each bottled water sample. Data plotted in Figure 7.4.

	Bottled Water						
Material	**1 (P)**	**2 (G, C)**	**3 (P)**	**4 (P)**	**5 (G)**	**6 (P)**	**7 (G, C)**
Azlon	1	3	1	3	1	4	3
Cellulose	2	5	0	1	1	0	0
Cellulose Triacetate	0	2	0	4	8	13	3
Glass	1	8	6	0	9	2	3
Kraton	0	0	2	2	0	1	0
Nylon	1	3	0	0	6	0	0
Polydimethyl Siloxane	0	0	0	0	0	1	0
Polyacetyl	0	3	0	0	0	0	0
Polyethylene	4	23	6	6	1	1	0
Polyethylene Terephthalate (PET)	3	6	1	1	0	0	0
Polymethylmethacrylate	1	2	0	0	0	0	0
Polypropylene	2	0	1	1	15	2	7
Polystyrene	0	0	2	0	2	2	2
Rayon	6	21	6	3	7	0	10
Spandex	0	1	0	1	1	0	0
Styrene Acrylic	1	0	0	0	0	0	0
Wood	0	19	0	0	0	0	0
Unidentified	6	27	7	6	5	5	5

Table S7.7. Detailed Py-GC-MS results from SIM 1 plastics and fibers. Each characteristic pyrolysis product is given a match score: perfect match (green = 1 point), partial match (yellow = 0.5 points), no match (red = 0 points).

	polymers		polystyrene			polyethylene			polyvinyl chloride	
	pyrolysis products		styrene	3-butene-1,3-diyldibenzene	5-hexene-1,3,5-triyltribenzene	alkenes	α-alkenes	α,ω-alkenes	benzene	chlorobenzene
bottled water samples (1 to 7) (replicates a and b)	1	a								
	1	b								
	2	a								
	2	b								
	3	a								
	3	b								
	4	a								
	4	b								
	5	a								
	5	b								
	6	a								
	6	b								
	7	a								
	7	b								
	negative control	a								
		b								

Table S7.8. Detailed Py-GC-MS results from SIM 2 plastics and fibers. Each characteristic pyrolysis product is given a match score: perfect match (green = 1 point), partial match (yellow = 0.5 points), no match (red = 0 points).

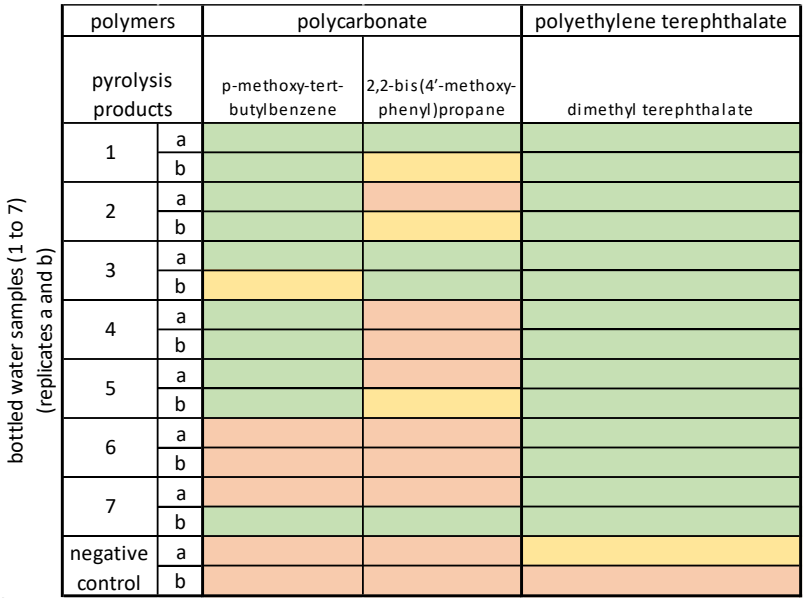

Table S7.9. Detailed Py-GC-MS results from SIM 3 plastics and fibers. See also Table S7.10. Each characteristic pyrolysis product is given a match score: perfect match (green = 1 point), partial match (yellow = 0.5 points), no match (red = 0 points).

bottled water samples (1 to 7) (replicates a and b)	polymers		rayon				cellulose acetate				
	pyrolysis products		furfural	2-furanmethanol	2-furancarboxaldehyde, 5-methyl-	5-hydroxymethylfurfural	acetic acid	2-hydroxyethyl acetate	4,6-dimethyl-2H-pyran-2-one	unidentified	unidentified
	1	a									
		b									
	2	a									
		b									
	3	a									
		b									
	4	a									
		b									
	5	a									
		b									
	6	a									
		b									
	7	a									
		b									
	negative control	a									
		b									

Table S7.10. Detailed Py-GC-MS results from SIM 3 plastics and fibers. Each characteristic pyrolysis product is given a match score: perfect match (green = 1 point), partial match (yellow = 0.5 points), no match (red = 0 points).

bottled water samples (1 to 7) (replicates a and b)		polymers	kraton			cellulose			
		pyrolysis products	Isoprene	styrene	Limonene	pyruvic aldehyde	hydroxyacetaldehyde	5-(hydroxymethyl)dihydro-2(3H)-furanone	5-(hydroxymethyl)-2-furfural
	1	a							
		b							
	2	a							
		b							
	3	a							
		b							
	4	a							
		b							
	5	a							
		b							
	6	a							
		b							
	7	a							
		b							
	negative control	a							
		b							

Table S7.11. Detailed Py-GC-MS results from SIM 4 plastics and fibers. Each characteristic pyrolysis product is given a match score: perfect match (green = 1 point), partial match (yellow = 0.5 points), no match (red = 0 points).

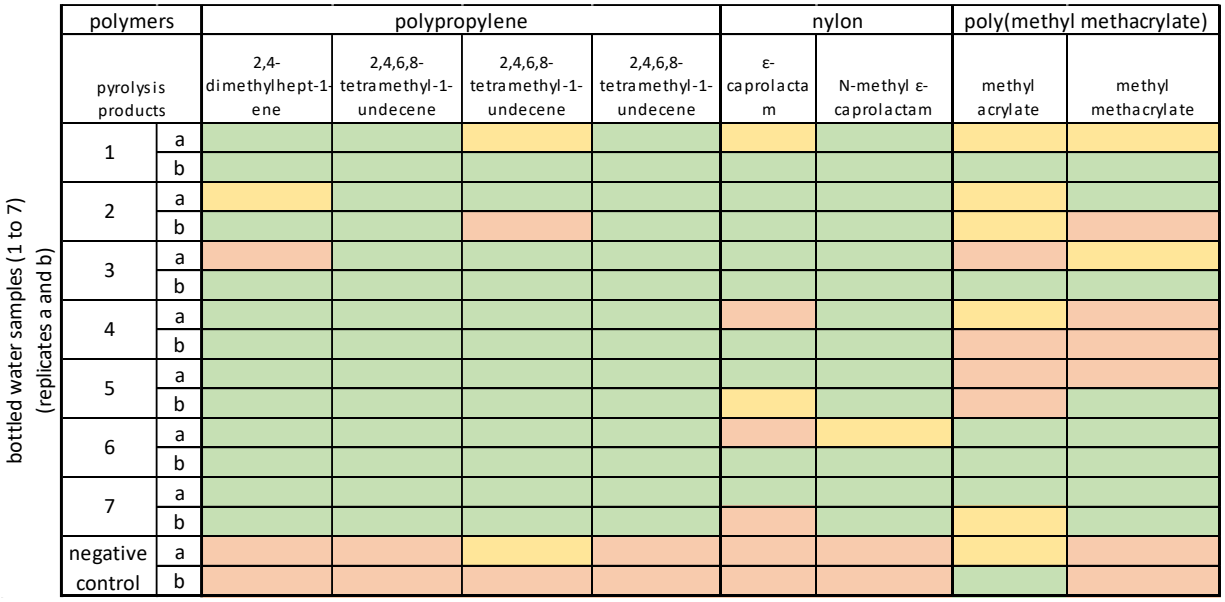

7.7.1 References

(1) Fischer, M.; Scholz-Böttcher, B. M. Simultaneous Trace Identification and Quantification of Common Types of Microplastics in Environmental Samples by Pyrolysis-Gas Chromatography–Mass Spectrometry. *Environ. Sci. Technol.* **2017**, *51* (9), 5052–5060. https://doi.org/10.1021/acs.est.6b06362.

(2) Acevedo, B.; Fernández, A. M.; Barriocanal, C. Identification of Polymers in Waste Tyre Reinforcing Fibre by Thermal Analysis and Pyrolysis. *Journal of Analytical and Applied Pyrolysis* **2015**, *111*, 224–232. https://doi.org/10.1016/j.jaap.2014.11.005.

(3) Tsuge, S.; Ohtani, H.; Watanabe, C. *Pyrolysis-GC/MS Data Book of Synthetic Polymers: Pyrograms, Thermograms and MS of Pyrolyzates*, 1st ed.; Elsevier: Amsterdam ; Boston, 2011.

(4) Klee, M. S.; Chang, I. Pyrolysis-GC/MS/IR Analysis of Kraton 1107. Hewlett Packard July 1989.

Chapter 8: Conclusions and future work

8.1 Conclusions

The presence of micro- and nanoplastics in consumer products and environmental samples was studied. In this work, traditional characterization techniques were used and their capacities were pushed to their limits to identify small plastics.

In Chapter 3, the presence of plastic particles smaller than 100 nm was confirmed in facial scrubs. This was the first report of the detection of plastic particles of this size in consumer products. Due to the nature of these commercial products, their waste is directly introduced into wastewater. We estimate that when consumers use one gram of these commercial products, they are releasing approximately 300 billion plastic particles having a diameter lower than 100 nm. While the retention of microplastics (1 μm to 5 mm) in wastewater treatment plants has been reported by others, the retention rates of plastics < 100 nm is largely unknown. It can be thus hypothesized that those plastic particles likely contribute to the number of plastics in the environment. These plastics in the environment present several risks, one of them being their introduction into the human food chain.

In Chapter 4, we confirmed that plastic teabags release micro- and nanoplastics directly into the human food chain. Thus, highlighting that food packaging might lead to the release of anthropogenic substances into food. These are secondary micro- and nanoplastics that are breaking down from the packaging. We approximate that a person can consume billions micro- and nanoplastics when drinking a cup of tea prepared with a plastic teabag. There is an immediate need to evaluate the effects of the ingestion of these plastic particles to human health. This is just one source of the multiple direct pathways of plastics into the human food chain.

It is well known that tons of plastics are floating in the ocean. These plastics are of different compositions and arise from different sources. There is a need to understand how plastics are degraded when floating in water for years. In Chapter 5, we evaluated the effects of UV-weathering and thermal weathering on four common plastics, namely PS, PP, HDPE and LDPE. We found that all four types of plastic release particulate material (mostly < 1 μm sized), in concentrations approximately of 10^8-10^9 particles per mL. This particulate material had a plastic signature that matched the plastic being degraded. We also found that the degraded microplastic had changed in its surface roughness, which suggested its degradation. This work contributes to the knowledge on plastic weathering under simulated environmental conditions.

One of the main limitations when evaluating environmental samples is the lack of detection methods. Even when detection methods exist, such as pyrolysis coupled with gas chromatography-mass spectroscopy (Py-GC-MS), there is no uniformity in the analysis of data in the literature. An objective of this thesis was to contribute to the uniformity of methods to analyze environmental samples. In Chapter 6, we proposed a systematic method to evaluate Py-GC-MS data. We propose a method that evaluates the presence of pyrolysis products using a scoring system that compares each sample to a standard. The nature of the polymer is confirmed when the score is higher than 83.3%. We applied this method in drinking water and Arctic water samples looking for the presence of 12 common plastics. We were able to confirm the presence of some of these plastics in the samples, as well as validating the method with the appropriate controls. The minimum matching score was set to 83.3% for these low-organic content samples. However, this percentage can be tuned to allow more flexibility for samples with higher contamination.

To tackle the emerging issue of microplastics in drinking water, governments are exploring the possibility of requiring water to be screened for microplastics at the drinking water treatment plant.

Although methods to screen exist, we believe that most of them are complex and requite state-of-the-art equipment. In Chapter 7, we used a common dye (Nile red) to pre-screen for micro- and nanoplastics in low-organic content samples. We found that it is extremely important to tune the concentration of Nile red to match the organic content of the sample that is being analyzed. A high concentration of Nile red will cause excess to accumulate and mask particles, auto-fluorescence, and agglomeration of the dye. On the other hand, concentrations of Nile red that are too low will cause an underestimation of the number of particles. In this work, we demonstrated a reproducible and low-cost approach to optimize the concentration of Nile red for pre-screening of microplastics in potable water. The minimum requirements for quantification (particles between 5-100 μm) and chemical characterization (particles > 100 μm) are a laminar flow cabinet, a stereo-microscope, a fluorescent light, and a benchtop FTIR. We also used Py-GC-MS to chemically identify plastics between 1.5 - 100 μm. Applying the optimized method to bottled water samples, we found an average of 2800 particles per liter, and a wide variety of plastic types.

8.2 Perspectives

Although the presence and detection of microplastics have been thoroughly studied, there is a need for more research in nanoplastics. Both primary and secondary sources of nanoplastics need further attention. Specifically, there is a need to determine the nanoplastics concentrations in the environment, and if these concentrations have any significant effect on the ecosystems. Techniques and equipment that allow for the individual identification of nanoplastics are desired. Currently, the lowest detection achieved is approximately 1 μm. This is missing the smallest fraction which is likely the most harmful to cells and tissues.

The effects of “real” micro- and nanoplastics must be further studied. To date, most studies use prepared micro- and nanoparticles, which can be quite different from a “real particle” that resides

in the environment. When a micro- or nanoplastic is in the environment, it is likely to be degraded, coated with contaminants or organic matter, functionalized with chemicals, have sorbed contaminants, and have an irregular size and shape. More studies using “real” environmental plastic particles to assess fate and toxicity are necessary. However, it is not as simple, due to the nature of “real” environmental plastic particles. Two “real” samples will likely not behave the same as each sample has its own history in the environment.

It is now known that macroplastics will degrade to form microplastics, and these will degrade further to form nanoplastics. However, an important area of study should be the degradation of nanoplastics. It is important to determine if nanoplastics persist in the environment in particulate form, or if the process of weathering causes further degradation into oligomers and monomers. Additionally, the timeline in which this degradation happens is crucial, as it will help predict the environmental loads of nanoplastics. The further degradation of nanoplastics will also bring other questions such as the effects of oligomers and monomers in the environment. What would be more harmful: a nanoplastic or an oligomer?

Finally, there is a need for the widespread communication of this topic to the general population. If we want to achieve a decrease on plastic proliferation, science divulgation is of the essence. Consumers should realize what happens to their products when they reach the environment. Large plastic breaks down into smaller plastics. These smaller plastics exist and persist in the environment. Even if we were able to remove macroplastic from the environment, it will be extremely challenging to remove micro- and nanoplastics. There is a need to communicate the toxicity that these small plastics will have in bacteria, plants, and animals. The possibility that these small plastic particles will come back to us in our food is real, while their effects on human health are unknown.

References

Abbasi, S.; Keshavarzi, B.; Moore, F.; Turner, A.; Kelly, F. J.; Dominguez, A. O.; Jaafarzadeh, N. Distribution and Potential Health Impacts of Microplastics and Microrubbers in Air and Street Dusts from Asaluyeh County, Iran. Environmental Pollution 2019, 244, 153–164. https://doi.org/10.1016/j.envpol.2018.10.039.

Acevedo, B.; Fernández, A. M.; Barriocanal, C. Identification of Polymers in Waste Tyre Reinforcing Fibre by Thermal Analysis and Pyrolysis. Journal of Analytical and Applied Pyrolysis 2015, 111, 224–232. https://doi.org/10.1016/j.jaap.2014.11.005.

Alexeeva, K. V.; Khramova, L. P. Comparison of Various Pyrolyzers in the Study of Polymer Compositions. Journal of Chromatography A 1972, 69 (1), 65–70. https://doi.org/10.1016/S0021-9673(00)83084-8.

Alimi, O. S.; Claveau-Mallet, D.; Kurusu, R. S.; Lapointe, M.; Bayen, S.; Tufenkji, N. Weathering Pathways and Protocols for Environmentally Relevant Microplastics and Nanoplastics: What Are We Missing?, 2021.

Alimi, O. S.; Farner Budarz, J.; Hernandez, L. M.; Tufenkji, N. Microplastics and Nanoplastics in Aquatic Environments: Aggregation, Deposition, and Enhanced Contaminant Transport. Environmental Science & Technology 2018. https://doi.org/10.1021/acs.est.7b05559.

Ammendolia, M. G.; Iosi, F.; Maranghi, F.; Tassinari, R.; Cubadda, F.; Aureli, F.; Raggi, A.; Superti, F.; Mantovani, A.; De Berardis, B. Short-Term Oral Exposure to Low Doses of Nano-Sized TiO 2 and Potential Modulatory Effects on Intestinal Cells. Food Chem. Toxicol. 2017, 102, 63–75. https://doi.org/10.1016/j.fct.2017.01.031.

Analysis of Nanoplastics and Microplastics in Food, First edition.; Nollet, L. M. L., Siddiqi, K. S., Eds.; Food analysis & properties; CRC Press / Taylor & Francis Group: Boca Raton, 2021.

Andanson, J.-M.; Kazarian, S. G. In Situ ATR-FTIR Spectroscopy of Poly(Ethylene Terephthalate) Subjected to High-Temperature Methanol. Macromol. Symp. 2008, 265 (1), 195–204. https://doi.org/10.1002/masy.200850521.

Andrady, A. L. Microplastics in the marine environment. Mar. Pollut. Bull. 2011, 62, 1596–1605.

Andrady, A. L. Plastics and Environmental Sustainability: Andrady/Plastics and Environmental Sustainability; John Wiley & Sons, Inc: Hoboken, NJ, 2015. https://doi.org/10.1002/9781119009405.

AshaRani, P. V.; Low Kah Mun, G.; Hande, M. P.; Valiyaveettil, S. Cytotoxicity and Genotoxicity of Silver Nanoparticles in Human Cells. ACS Nano 2009, 3, 279–290 DOI: 10.1021/nn800596w.

Au, S. Y.; Bruce, T. F.; Bridges, W. C.; Klaine, S. J. Responses of Hyalella azteca to acute and chronic microplastic exposures: Effects of Microplastic Exposure on Hyalella azteca. Environ. Toxicol. Chem. 2015, 34, 2564–2572 DOI: 10.1002/etc.3093.

Auffan, M.; Rose, J.; Bottero, J.-Y.; Lowry, G. V.; Jolivet, J.-P.; Wiesner, M. R. Towards a Definition of Inorganic Nanoparticles from an Environmental, Health and Safety Perspective. Nat. Nanotechnol. 2009, 4 (10), 634–641. https://doi.org/10.1038/nnano.2009.242.

Bach, C.; Dauchy, X.; Chagnon, M.-C.; Etienne, S. Chemical Compounds and Toxicological Assessments of Drinking Water Stored in Polyethylene Terephthalate (PET) Bottles: A Source of Controversy Reviewed. Water Res. 2012, 46 (3), 571–583. https://doi.org/10.1016/j.watres.2011.11.062.

Bach, C.; Dauchy, X.; Severin, I.; Munoz, J.-F.; Etienne, S.; Chagnon, M.-C. Effect of Temperature on the Release of Intentionally and Non-Intentionally Added Substances from Polyethylene Terephthalate (PET) Bottles into Water: Chemical Analysis and Potential Toxicity. Food Chem. 2013, 139 (1–4), 672–680. https://doi.org/10.1016/j.foodchem.2013.01.046.

Baden, N.; Kobayashi, H.; Urayama, N. Submicron-Resolution Polymer Orientation Mapping by Optical Photothermal Infrared Spectroscopy. International Journal of Polymer Analysis and Characterization 2020, 25 (1), 1–7. https://doi.org/10.1080/1023666X.2020.1735851.

Barnes, D. K. A.; Galgani, F.; Thompson, R. C.; Barlaz, M. Accumulation and fragmentation of plastic debris in global environments. Philos. Trans. R. Soc. B Biol. Sci. 2009, 364, 1985–1998 DOI: 10.1098/rstb.2008.0205.

Bayo, J.; Olmos, S.; López-Castellanos, J.; Alcolea, A. Microplastics and Microfibers in the Sludge of a Municipal Wastewater Treatment Plant. Int. J. SDP 2016, 11 (5), 812–821. https://doi.org/10.2495/SDP-V11-N5-812-821.

Bergin, I. L.; Witzmann, F. A. Nanoparticle Toxicity by the Gastrointestinal Route: Evidence and Knowledge Gaps. International Journal of Biomedical Nanoscience and Nanotechnology 2013, 3 (1/2), 163. https://doi.org/10.1504/IJBNN.2013.054515.

Bergmann, M.; Lutz, B.; Tekman, M. B.; Gutow, L. Citizen Scientists Reveal: Marine Litter Pollutes Arctic Beaches and Affects Wild Life. Marine Pollution Bulletin 2017, 125 (1–2), 535–540. https://doi.org/10.1016/j.marpolbul.2017.09.055.

Bergmann, M.; Mützel, S.; Primpke, S.; Tekman, M. B.; Trachsel, J.; Gerdts, G. White and Wonderful? Microplastics Prevail in Snow from the Alps to the Arctic. Sci Adv 2019, 5 (8), eaax1157. https://doi.org/10.1126/sciadv.aax1157.

Besseling, E.; Wang, B.; Lürling, M.; Koelmans, A. A. Nanoplastic Affects Growth of S. Obliquus and Reproduction of D. Magna. Environ. Sci. Technol. 2014, 48 (20), 12336–12343. https://doi.org/10.1021/es503001d.

Betzig, E.; Patterson, G. H.; Sougrat, R.; Lindwasser, O. W.; Olenych, S.; Bonifacino, J. S.; Davidson, M. W.; Lippincott-Schwartz, J.; Hess, H. F. Imaging Intracellular Fluorescent Proteins at Nanometer Resolution. Science 2006, 313 (5793), 1642–1645. https://doi.org/10.1126/science.1127344.

Biber, N. F. A.; Foggo, A.; Thompson, R. C. Characterising the Deterioration of Different Plastics in Air and Seawater. Marine Pollution Bulletin 2019, 141, 595–602. https://doi.org/10.1016/j.marpolbul.2019.02.068.

Boerger, C. M.; Lattin, G. L.; Moore, S. L.; Moore, C. J. Plastic Ingestion by Planktivorous Fishes in the North Pacific Central Gyre. Mar. Pollut. Bull. 2010, 60 (12), 2275–2278. https://doi.org/10.1016/j.marpolbul.2010.08.007.

Borrelle, S. B.; Ringma, J.; Law, K. L.; Monnahan, C. C.; Lebreton, L.; McGivern, A.; Murphy, E.; Jambeck, J.; Leonard, G. H.; Hilleary, M. A.; Eriksen, M.; Possingham, H. P.; De Frond, H.; Gerber, L. R.; Polidoro, B.; Tahir, A.; Bernard, M.; Mallos, N.; Barnes, M.; Rochman, C. M. Predicted Growth in Plastic Waste Exceeds Efforts to Mitigate Plastic Pollution. Science 2020, 369 (6510), 1515–1518. https://doi.org/10.1126/science.aba3656.

Bothun, G. D. Hydrophobic silver nanoparticles trapped in lipid bilayers: Size distribution, bilayer phase behavior, and optical properties. J. Nanobiotechnology 2008, 6, 13 DOI: 10.1186/1477-3155-6-13.

Bouldin, J. L.; Ingle, T. M.; Sengupta, A.; Alexander, R.; Hannigan, R. E.; Buchanan, R. A. Aqueous Toxicity and Food Chain Transfer of Quantum DOTs in Freshwater Algae and *Ceriodaphnia Dubia*. Environ. Toxicol. Chem. 2008, 27 (9), 1958–1963.

Bouwmeester, H.; Hollman, P. C. H.; Peters, R. J. B. Potential Health Impact of Environmentally Released Micro- and Nanoplastics in the Human Food Production Chain: Experiences from Nanotoxicology. Environ. Sci. Technol. 2015, 49 (15), 8932–8947. https://doi.org/10.1021/acs.est.5b01090.

Bownik, A.; Sokołowska, N.; Ślaska, B. Effects of Apomorphine, a Dopamine Agonist, on *Daphnia Magna* : Imaging of Swimming Track Density as a Novel Tool in the Assessment of Swimming Activity. Sci. Total Environ. 2018, 635, 249–258. https://doi.org/10.1016/j.scitotenv.2018.04.157.

Brandon, J.; Goldstein, M.; Ohman, M. D. Long-Term Aging and Degradation of Microplastic Particles: Comparing in Situ Oceanic and Experimental Weathering Patterns. Mar. Pollut. Bull. 2016, 110 (1), 299–308. https://doi.org/10.1016/j.marpolbul.2016.06.048.

Brennecke, D.; Duarte, B.; Paiva, F.; Caçador, I.; Canning-Clode, J. Microplastics as Vector for Heavy Metal Contamination from the Marine Environment. Estuar. Coast. Shelf Sci. 2016, 178, 189–195. https://doi.org/10.1016/j.ecss.2015.12.003.

Browne, M. A.; Crump, P.; Niven, S. J.; Teuten, E.; Tonkin, A.; Galloway, T.; Thompson, R. Accumulation of Microplastic on Shorelines Woldwide: Sources and Sinks. Environ. Sci. Technol. 2011, 45 (21), 9175–9179. https://doi.org/10.1021/es201811s.

Browne, M. A.; Dissanayake, A.; Galloway, T. S.; Lowe, D. M.; Thompson, R. C. Ingested Microscopic Plastic Translocates to the Circulatory System of the Mussel, Mytilus Edulis (L). Environ. Sci. Technol. 2008, 42 (13), 5026–5031.

Browne, M. A.; Galloway, T.; Thompson, R. Microplastic-an Emerging Contaminant of Potential Concern? Integr. Environ. Assess. Manag. 2007, 3 (4), 559–561. https://doi.org/10.1002/ieam.5630030412.

Burton, G. A. Losing sight of science in the regulatory push to ban microbeads from consumer products and industrial use. Integr. Environ. Assess. Manag. 2015, 11, 346–347 DOI: 10.1002/ieam.1645.

C.O'Keefe, T.; C.Brewer, M.; Dodson, S. I. Swimming Behavior of *Daphnia* : Its Role in Determining Predation Risk. J. Plankton Res. 1998, 20 (5), 973–984. https://doi.org/10.1093/plankt/20.5.973.

Cabernard, L.; Roscher, L.; Lorenz, C.; Gerdts, G.; Primpke, S. Comparison of Raman and Fourier Transform Infrared Spectroscopy for the Quantification of Microplastics in the Aquatic Environment. Environ. Sci. Technol. 2018, 52 (22), 13279–13288. https://doi.org/10.1021/acs.est.8b03438.

Calleja, M. C.; Persoone, G. Cyst-Based Toxicity Tests. IV. The Potential of Ecotoxicological Tests for the Prediction of Acute Toxicity in Man as Evaluated on the First Ten Chemicals of the MEIC Programme. ATLA 1992, 20, 396–405.

Capolupo, M.; Sørensen, L.; Jayasena, K. D. R.; Booth, A. M.; Fabbri, E. Chemical Composition and Ecotoxicity of Plastic and Car Tire Rubber Leachates to Aquatic Organisms. Water Research 2020, 169, 115270. https://doi.org/10.1016/j.watres.2019.115270.

Carr, S. A.; Liu, J.; Tesoro, A. G. Transport and Fate of Microplastic Particles in Wastewater Treatment Plants. Water Research 2016, 91, 174–182. https://doi.org/10.1016/j.watres.2016.01.002.

Castelvetro, V.; Corti, A.; Bianchi, S.; Giacomelli, G.; Manariti, A.; Vinciguerra, V. Microplastics in Fish Meal: Contamination Level Analyzed by Polymer Type, Including Polyester (PET), Polyolefins, and Polystyrene. Environmental Pollution 2021, 273, 115792. https://doi.org/10.1016/j.envpol.2020.115792.

Castro Monsores, K. G. de; Silva, A. O. da; Sant' Ana Oliveira, S. de; Weber, R. P.; Filho, P. F.; Monteiro, S. N. Influence of Ultraviolet Radiation on Polystyrene. Journal of Materials Research and Technology 2021, 13, 359–365. https://doi.org/10.1016/j.jmrt.2021.04.035.

Chae, Y.; An, Y.-J. Effects of micro- and nanoplastics on aquatic ecosystems: Current research trends and perspectives. Mar. Pollut. Bull. 2017 DOI: 10.1016/j.marpolbul.2017.01.070.

Chamas, A.; Moon, H.; Zheng, J.; Qiu, Y.; Tabassum, T.; Jang, J. H.; Abu-Omar, M.; Scott, S. L.; Suh, S. Degradation Rates of Plastics in the Environment. ACS Sustainable Chem. Eng. 2020, 8 (9), 3494–3511. https://doi.org/10.1021/acssuschemeng.9b06635.

Chapiro, A. Radiation Effects in Polymers. In Encyclopedia of Materials: Science and Technology; Elsevier, 2004; pp 1–8. https://doi.org/10.1016/B0-08-043152-6/01918-5.

Chen, Q.; Gundlach, M.; Yang, S.; Jiang, J.; Velki, M.; Yin, D.; Hollert, H. Quantitative Investigation of the Mechanisms of Microplastics and Nanoplastics toward Zebrafish Larvae Locomotor Activity. Sci. Total Environ. 2017, 584–585, 1022–1031. https://doi.org/10.1016/j.scitotenv.2017.01.156.

Chércoles Asensio, R.; San Andrés Moya, M.; de la Roja, J. M.; Gómez, M. Analytical Characterization of Polymers Used in Conservation and Restoration by ATR-FTIR Spectroscopy. Anal Bioanal Chem 2009, 395 (7), 2081–2096. https://doi.org/10.1007/s00216-009-3201-2.

Chevalier, J.; Harscoët, E.; Keller, M.; Pandard, P.; Cachot, J.; Grote, M. Exploration of *Daphnia* Behavioral Effect Profiles Induced by a Broad Range of Toxicants with Different Modes of Action: Effects of Different Toxicants on *Daphnia* Behavior. Environ. Toxicol. Chem. 2015, 34 (8), 1760–1769. https://doi.org/10.1002/etc.2979.

Christensen, F. M.; Johnston, H. J.; Stone, V.; Aitken, R. J.; Hankin, S.; Peters, S.; Aschberger, K. Nano-TiO 2 – Feasibility and Challenges for Human Health Risk Assessment Based on Open Literature. Nanotoxicology 2011, 5 (2), 110–124. https://doi.org/10.3109/17435390.2010.504899.

Colmorgen, M.; Paul, R. J. Imaging of Physiological Functions in Transparent Animals (Agonus Cataphractus, *Daphnia Magna*, Pholcus Phalangioides) by Video Microscopy and Digital Image Processing. Comp. Biochem. Physiol. A Physiol. 1995, 111 (4), 583–595. https://doi.org/10.1016/0300-9629(95)00059-G.

Comnea-Stancu, I. R.; Wieland, K.; Ramer, G.; Schwaighofer, A.; Lendl, B. On the Identification of Rayon/Viscose as a Major Fraction of Microplastics in the Marine Environment: Discrimination between Natural and Manmade Cellulosic Fibers Using Fourier Transform Infrared Spectroscopy. Appl Spectrosc 2017, 71 (5), 939–950. https://doi.org/10.1177/0003702816660725.

Corotto, F.; Ceballos, D.; Lee, A.; Vinson, L. Making the Most of the *Daphnia* Heart Rate Lab: Optimizing the Use of Ethanol, Nicotine & Caffeine. Am. Biol. Teach. 2010, 72 (3), 176–179. https://doi.org/10.1525/abt.2010.72.3.9.

Costa, C. Q. V.; Cruz, J.; Martins, J.; Teodósio, M. A. A.; Jockusch, S.; Ramamurthy, V.; Da Silva, J. P. Fluorescence Sensing of Microplastics on Surfaces. Environ Chem Lett 2021, 19 (2), 1797–1802. https://doi.org/10.1007/s10311-020-01136-0.

Costa, M. F.; Barletta, M. Microplastics in Coastal and Marine Environments of the Western Tropical and Sub-Tropical Atlantic Ocean. Environ. Sci.: Processes Impacts 2015, 17 (11), 1868–1879. https://doi.org/10.1039/C5EM00158G.

Cox, K. D.; Covernton, G. A.; Davies, H. L.; Dower, J. F.; Juanes, F.; Dudas, S. E. Human Consumption of Microplastics. Environ. Sci. Technol. 2019, 53 (12), 7068–7074. https://doi.org/10.1021/acs.est.9b01517.

Cozar, A.; Echevarria, F.; Gonzalez-Gordillo, J. I.; Irigoien, X.; Ubeda, B.; Hernandez-Leon, S.; Palma, A. T.; Navarro, S.; Garcia-de-Lomas, J.; Ruiz, A.; et al. Plastic debris in the open ocean. Proc. Natl. Acad. Sci. 2014, 111, 10239–10244 DOI: 10.1073/pnas.1314705111.

Cózar, A.; Martí, E.; Duarte, C. M.; García-de-Lomas, J.; van Sebille, E.; Ballatore, T. J.; Eguíluz, V. M.; González-Gordillo, J. I.; Pedrotti, M. L.; Echevarría, F.; Troublè, R.; Irigoien, X. The Arctic Ocean as a Dead End for Floating Plastics in the North Atlantic Branch of the Thermohaline Circulation. Sci. Adv. 2017, 3 (4), e1600582. https://doi.org/10.1126/sciadv.1600582.

da Costa, J. P.; Duarte, A. C.; Rocha-Santos, T. A. P. Microplastics – Occurrence, Fate and Behaviour in the Environment. In Comprehensive Analytical Chemistry; Elsevier, 2017; Vol. 75, pp 1–24. https://doi.org/10.1016/bs.coac.2016.10.004.

da Costa, J. P.; Santos, P. S. M.; Duarte, A. C.; Rocha-Santos, T. (Nano)plastics in the environment – Sources, fates and effects. Sci. Total Environ. 2016, 566–567, 15–26 DOI: 10.1016/j.scitotenv.2016.05.041.

De Falco, F.; Di Pace, E.; Cocca, M.; Avella, M. The Contribution of Washing Processes of Synthetic Clothes to Microplastic Pollution. Sci Rep 2019, 9 (1), 6633. https://doi.org/10.1038/s41598-019-43023-x.

Deng, Y.; Zhang, Y.; Lemos, B.; Ren, H. Tissue Accumulation of Microplastics in Mice and Biomarker Responses Suggest Widespread Health Risks of Exposure. Sci. Rep. 2017, 7 (1). https://doi.org/10.1038/srep46687.

Diaz-Basantes, M. F.; Conesa, J. A.; Fullana, A. Microplastics in Honey, Beer, Milk and Refreshments in Ecuador as Emerging Contaminants. Sustainability 2020, 12 (14), 5514. https://doi.org/10.3390/su12145514.

Diffey, B. L. Sources and Measurement of Ultraviolet Radiation. Methods 2002, 28 (1), 4–13. https://doi.org/10.1016/S1046-2023(02)00204-9.

Domingos, R. F.; Baalousha, M. A.; Ju-Nam, Y.; Reid, M. M.; Tufenkji, N.; Lead, J. R.; Leppard, G. G.; Wilkinson, K. J. Characterizing Manufactured Nanoparticles in the Environment: Multimethod Determination of Particle Sizes. Environ. Sci. Technol. 2009, 43, 7277–7284 DOI: 10.1021/es900249m.

Doren, A.; Genet, M. J.; Rouxhet, P. G. Analysis of Poly(Ethylene Terephthalate) (PET) by XPS. Surf. Sci. Spectra 1994, 3 (4), 337–341. https://doi.org/10.1116/1.1247762.

Dris, R.; Gasperi, J.; Mirande, C.; Mandin, C.; Guerrouache, M.; Langlois, V.; Tassin, B. A First Overview of Textile Fibers, Including Microplastics, in Indoor and Outdoor Environments. Environmental Pollution 2017, 221, 453–458. https://doi.org/10.1016/j.envpol.2016.12.013.

Dris, R.; Imhof, H.; Sanchez, W.; Gasperi, J.; Galgani, F.; Tassin, B.; Laforsch, C. Beyond the Ocean: Contamination of Freshwater Ecosystems with (Micro-)Plastic Particles. Environ. Chem. 2015, 12 (5), 539. https://doi.org/10.1071/EN14172.

Duemichen, E.; Braun, U.; Senz, R.; Fabian, G.; Sturm, H. Assessment of a New Method for the Analysis of Decomposition Gases of Polymers by a Combining Thermogravimetric Solid-Phase Extraction and Thermal Desorption Gas Chromatography Mass Spectrometry. Journal of Chromatography A 2014, 1354, 117–128. https://doi.org/10.1016/j.chroma.2014.05.057.

Duemichen, E.; Javdanitehran, M.; Erdmann, M.; Trappe, V.; Sturm, H.; Braun, U.; Ziegmann, G. Analyzing the Network Formation and Curing Kinetics of Epoxy Resins by in Situ Near-Infrared Measurements with Variable Heating Rates. Thermochimica Acta 2015, 616, 49–60. https://doi.org/10.1016/j.tca.2015.08.008.

Dümichen, E.; Barthel, A.-K.; Braun, U.; Bannick, C. G.; Brand, K.; Jekel, M.; Senz, R. Analysis of Polyethylene Microplastics in Environmental Samples, Using a Thermal Decomposition Method. Water Research 2015, 85, 451–457. https://doi.org/10.1016/j.watres.2015.09.002.

Dümichen, E.; Eisentraut, P.; Bannick, C. G.; Barthel, A.-K.; Senz, R.; Braun, U. Fast Identification of Microplastics in Complex Environmental Samples by a Thermal Degradation Method. Chemosphere 2017, 174, 572–584. https://doi.org/10.1016/j.chemosphere.2017.02.010.

Dyachenko, A.; Mitchell, J.; Arsem, N. Extraction and Identification of Microplastic Particles from Secondary Wastewater Treatment Plant (WWTP) Effluent. Anal. Methods 2017, 9 (9), 1412–1418. https://doi.org/10.1039/C6AY02397E.

Eerkes-Medrano, D.; Thompson, R. C.; Aldridge, D. C. Microplastics in freshwater systems: A review of the emerging threats, identification of knowledge gaps and prioritisation of research needs. Water Res. 2015, 75, 63–82 DOI: 10.1016/j.watres.2015.02.012.

EFSA. EFSA Panel on Dietetic Products, Nutrition & Allergies. EFSA J. 2015, 13 (5).

Eisentraut, P.; Dümichen, E.; Ruhl, A. S.; Jekel, M.; Albrecht, M.; Gehde, M.; Braun, U. Two Birds with One Stone—Fast and Simultaneous Analysis of Microplastics: Microparticles Derived from Thermoplastics and Tire Wear. Environ. Sci. Technol. Lett. 2018, 5 (10), 608–613. https://doi.org/10.1021/acs.estlett.8b00446.

Ekvall, M. T.; Lundqvist, M.; Kelpsiene, E.; Šileikis, E.; Gunnarsson, S. B.; Cedervall, T. Nanoplastics Formed during the Mechanical Breakdown of Daily-Use Polystyrene Products. Nanoscale Adv. 2019, 1 (3), 1055–1061. https://doi.org/10.1039/C8NA00210J.

El Hayany, B.; El Fels, L.; Quénéa, K.; Dignac, M.-F.; Rumpel, C.; Gupta, V. K.; Hafidi, M. Microplastics from Lagooning Sludge to Composts as Revealed by Fluorescent Staining- Image Analysis, Raman Spectroscopy and Pyrolysis-GC/MS. Journal of Environmental Management 2020, 275, 111249. https://doi.org/10.1016/j.jenvman.2020.111249.

Elert, A. M.; Becker, R.; Duemichen, E.; Eisentraut, P.; Falkenhagen, J.; Sturm, H.; Braun, U. Comparison of Different Methods for MP Detection: What Can We Learn from Them, and Why Asking the Right Question before Measurements Matters? Environmental Pollution 2017, 231, 1256–1264. https://doi.org/10.1016/j.envpol.2017.08.074.

Encyclopedia of Spectroscopy and Spectrometry; Lindon, J. C., Ed.; Academic Press: San Diego, 20.

Eriksen, M.; Lebreton, L. C. M.; Carson, H. S.; Thiel, M.; Moore, C. J.; Borerro, J. C.; Galgani, F.; Ryan, P. G.; Reisser, J. Plastic Pollution in the World's Oceans: More than 5 Trillion Plastic Pieces Weighing over 250,000 Tons Afloat at Sea. PLoS ONE 2014, 9 (12), e111913. https://doi.org/10.1371/journal.pone.0111913.

Eriksson, C.; Burton, H. Origins and Biological Accumulation of Small Plastic Particles in Fur Seals from Macquarie Island. Ambio 2003, 32 (6), 380–384.

Erni-Cassola, G.; Gibson, M. I.; Thompson, R. C.; Christie-Oleza, J. A. Lost, but Found with Nile Red: A Novel Method for Detecting and Quantifying Small Microplastics (1 Mm to 20 Mm) in Environmental Samples. Environ. Sci. Technol. 2017, 51 (23), 13641–13648. https://doi.org/10.1021/acs.est.7b04512.

European Chemical Agency. Microplastics; 2017.

European Commission. Commission Recommendation of 18 October 2011 on the Definition of Nanomaterial; Official Journal of the European Union; 2011/696/EU; European Commission, 2011; p L 275/38.

European Commission. Joint Research Centre. Institute for Environment and Sustainability.; MSFD Technical Subgroup on Marine Litter. Guidance on Monitoring of Marine Litter in European Seas.; Publications Office: LU, 2013.

Evandri, M. G.; Tucci, P.; Bolle, P. Toxicological Evaluation of Commercial Mineral Water Bottled in Polyethylene Terephthalate: A Cytogenetic Approach with Allium Cepa. Food Additives and Contaminants 2000, 17 (12), 1037–1045. https://doi.org/10.1080/02652030010014411.

Fabbri, D.; Rombolà, A. G.; Vassura, I.; Torri, C.; Franzellitti, S.; Capolupo, M.; Fabbri, E. Off-Line Analytical Pyrolysis GC–MS to Study the Accumulation of Polystyrene Microparticles in Exposed Mussels. Journal of Analytical and Applied Pyrolysis 2020, 149, 104836. https://doi.org/10.1016/j.jaap.2020.104836.

Felismino, M. E. L.; Helm, P. A.; Rochman, C. M. Microplastic and Other Anthropogenic Microparticles in Water and Sediments of Lake Simcoe. Journal of Great Lakes Research 2021, 47 (1), 180–189. https://doi.org/10.1016/j.jglr.2020.10.007.

Filipe, V.; Hawe, A.; Jiskoot, W. Critical Evaluation of Nanoparticle Tracking Analysis (NTA) by NanoSight for the Measurement of Nanoparticles and Protein Aggregates. Pharm Res 2010, 27 (5), 796–810. https://doi.org/10.1007/s11095-010-0073-2.

Fischer, M.; Scholz-Böttcher, B. M. Microplastics Analysis in Environmental Samples – Recent Pyrolysis-Gas Chromatography-Mass Spectrometry Method Improvements to Increase the Reliability of Mass-Related Data. Anal. Methods 2019, 11 (18), 2489–2497. https://doi.org/10.1039/C9AY00600A.

Fischer, M.; Scholz-Böttcher, B. M. Simultaneous Trace Identification and Quantification of Common Types of Microplastics in Environmental Samples by Pyrolysis-Gas Chromatography–Mass Spectrometry. Environ. Sci. Technol. 2017, 51 (9), 5052–5060. https://doi.org/10.1021/acs.est.6b06362.

Flaherty, C. M.; Dodson, S. I. Effects of Pharmaceuticals on *Daphnia* Survival, Growth, and Reproduction. Chemosphere 2005, 61 (2), 200–207. https://doi.org/10.1016/j.chemosphere.2005.02.016.

Foerch, R.; Beamson, G.; Briggs, D. XPS valence band analysis of plasma-treated polymers. Surf. Interface Anal. 1991, 17, 842–846 DOI: 10.1002/sia.740171204.

G. Ames. Mixing, Blending and Size Reduction Handbook.; 2001.

Galdiero, E.; Falanga, A.; Siciliano, A.; Maselli, V.; Guida, M.; Carotenuto, R.; Tussellino, M.; Lombardi, L.; Benvenuto, G.; Galdiero, S. *Daphnia Magna* and *Xenopus Laevis* as *in Vivo* Models to Probe Toxicity and Uptake of Quantum Dots Functionalized with GH625. Int. J. Nanomedicine 2017, Volume 12, 2717–2731. https://doi.org/10.2147/IJN.S127226.

Galgani, F.; Hanke, G.; Werner, S.; De Vrees, L. Marine Litter within the European Marine Strategy Framework Directive. ICES Journal of Marine Science 2013, 70 (6), 1055–1064. https://doi.org/10.1093/icesjms/fst122.

Gasperi, J.; Wright, S. L.; Dris, R.; Collard, F.; Mandin, C.; Guerrouache, M.; Langlois, V.; Kelly, F. J.; Tassin, B. Microplastics in Air: Are We Breathing It In? Current Opinion in Environmental Science & Health 2018, 1, 1–5. https://doi.org/10.1016/j.coesh.2017.10.002.

Gibson, M. C.; deMonsabert, S. M.; Orme-Zavaleta, J. Comparison of Noncancer Risk Assessment Approaches for Use in Deriving Drinking Water Criteria. Regul. Toxicol. Pharmacol. 1997, 26 (3), 243–256. https://doi.org/10.1006/rtph.1997.1150.

Gies, E. A.; LeNoble, J. L.; Noël, M.; Etemadifar, A.; Bishay, F.; Hall, E. R.; Ross, P. S. Retention of Microplastics in a Major Secondary Wastewater Treatment Plant in Vancouver, Canada. Marine Pollution Bulletin 2018, 133, 553–561. https://doi.org/10.1016/j.marpolbul.2018.06.006.

Gigault, J.; El Hadri, H.; Nguyen, B.; Grassl, B.; Rowenczyk, L.; Tufenkji, N.; Feng, S.; Wiesner, M. Nanoplastics Are Neither Microplastics nor Engineered Nanoparticles. Nat. Nanotechnol. 2021, 16 (5), 501–507. https://doi.org/10.1038/s41565-021-00886-4.

Gigault, J.; Pedrono, B.; Maxit, B.; Ter Halle, A. Marine Plastic Litter: The Unanalyzed Nano-Fraction. Environ. Sci.: Nano 2016, 3 (2), 346–350. https://doi.org/10.1039/C6EN00008H.

Gijsman, P. P. The Long-Term Stability of Polyolefins. 1994. https://doi.org/10.6100/IR427216.

Gomiero, A.; Øysæd, K. B.; Agustsson, T.; van Hoytema, N.; van Thiel, T.; Grati, F. First Record of Characterization, Concentration and Distribution of Microplastics in Coastal Sediments of an Urban Fjord in South West Norway Using a Thermal Degradation Method. Chemosphere 2019, 227, 705–714. https://doi.org/10.1016/j.chemosphere.2019.04.096.

Göpferich, A. Mechanisms of Polymer Degradation and Erosion. In The Biomaterials: Silver Jubilee Compendium; Elsevier, 1996; pp 117–128. https://doi.org/10.1016/B978-008045154-1.50016-2.

Greenspan, P.; Fowler, S. D. Spectrofluorometric Studies of the Lipid Probe, Nile Red. J Lipid Res 1985, 26 (7), 781–789.

Greven, A.-C.; Merk, T.; Karagöz, F.; Mohr, K.; Klapper, M.; Jovanović, B.; Palić, D. Polycarbonate and Polystyrene Nanoplastic Particles Act as Stressors to the Innate Immune System of Fathead Minnow (Pimephales Promelas): Nanoplastics' Effect on the Immune System of Fish. Environ Toxicol Chem 2016, 35 (12), 3093–3100. https://doi.org/10.1002/etc.3501.

Guilhermino, L.; Diamantino, T.; Carolina Silva, M.; Soares, A. M. V. M. Acute Toxicity Test with *Daphnia Magna*: An Alternative to Mammals in the Prescreening of Chemical Toxicity? Ecotoxicol. Environ. Saf. 2000, 46 (3), 357–362. https://doi.org/10.1006/eesa.2000.1916.

Gulmine, J. .; Janissek, P. .; Heise, H. .; Akcelrud, L. Polyethylene characterization by FTIR. Polym. Test. 2002, 21, 557–563 DOI: 10.1016/S0142-9418(01)00124-6.

Hammond, T.; Lehrle, R. S. Pyrolysis GLC. In Comprehensive Polymer Science and Supplements; Elsevier, 1989; pp 589–612. https://doi.org/10.1016/B978-0-08-096701-1.00027-6.

Han, W.-Y.; Shi, Y.-Z.; Ma, L.-F.; Ruan, J.-Y. Arsenic, Cadmium, Chromium, Cobalt, and Copper in Different Types of Chinese Tea. Bull. Environ. Contam. Toxicol. 2005, 75 (2), 272–277. https://doi.org/10.1007/s00128-005-0748-2.

Han, W.-Y.; Zhao, F.-J.; Shi, Y.-Z.; Ma, L.-F.; Ruan, J.-Y. Scale and Causes of Lead Contamination in Chinese Tea. Environ. Pollut. 2006, 139 (1), 125–132. https://doi.org/10.1016/j.envpol.2005.04.025.

Hansen, S. F.; Baun, A. European Regulation Affecting Nanomaterials - Review of Limitations and Future Recommendations. Dose-Response 2012, 10, dose-response.1 DOI: 10.2203/dose-response.10-029.Hansen.

Hartmann, N. B.; Hüffer, T.; Thompson, R. C.; Hassellöv, M.; Verschoor, A.; Daugaard, A. E.; Rist, S.; Karlsson, T.; Brennholt, N.; Cole, M.; Herrling, M.P.; Hess, M.C.; Ivleva, N.P.; Lusher, A.L.; Wagner, M. Are We Speaking the Same Language? Recommendations for a Definition and Categorization Framework for Plastic Debris. Environ. Sci. Technol. 2019, 53 (3), 1039–1047. https://doi.org/10.1021/acs.est.8b05297.

Hartung, T.; Daston, G. Are In Vitro Tests Suitable for Regulatory Use? Toxicol. Sci. 2009, 111 (2), 233–237. https://doi.org/10.1093/toxsci/kfp149.

He, P.; Chen, L.; Shao, L.; Zhang, H.; Lü, F. Municipal Solid Waste (MSW) Landfill: A Source of Microplastics? -Evidence of Microplastics in Landfill Leachate. Water Research 2019, 159, 38–45. https://doi.org/10.1016/j.watres.2019.04.060.

Hermabessiere, L.; Himber, C.; Boricaud, B.; Kazour, M.; Amara, R.; Cassone, A.-L.; Laurentie, M.; Paul-Pont, I.; Soudant, P.; Dehaut, A.; Duflos, G. Optimization, Performance, and Application of a Pyrolysis-GC/MS Method for the Identification of Microplastics. Anal Bioanal Chem 2018, 410 (25), 6663–6676. https://doi.org/10.1007/s00216-018-1279-0.

Hermsen, E.; Mintenig, S. M.; Besseling, E.; Koelmans, A. A. Quality Criteria for the Analysis of Microplastic in Biota Samples: A Critical Review. Environ. Sci. Technol. 2018, 52 (18), 10230–10240. https://doi.org/10.1021/acs.est.8b01611.

Hernandez, E.; Nowack, B.; Mitrano, D. M. Polyester Textiles as a Source of Microplastics from Households: A Mechanistic Study to Understand Microfiber Release During Washing. Environ. Sci. Technol. 2017, 51 (12), 7036–7046. https://doi.org/10.1021/acs.est.7b01750.

Hernandez, L. M.; Xu, E. G.; Larsson, H. C. E.; Tahara, R.; Maisuria, V. B.; Tufenkji, N. Plastic Teabags Release Billions of Microparticles and Nanoparticles into Tea. Environ. Sci. Technol. 2019, 53 (21), 12300–12310. https://doi.org/10.1021/acs.est.9b02540.

Hernandez, L. M.; Yousefi, N.; Tufenkji, N. Are There Nanoplastics in Your Personal Care Products? Environ. Sci. Technol. Lett. 2017, 4 (7), 280–285. https://doi.org/10.1021/acs.estlett.7b00187.

Hidalgo-Ruz, V.; Gutow, L.; Thompson, R. C.; Thiel, M. Microplastics in the Marine Environment: A Review of the Methods Used for Identification and Quantification. Environ. Sci. Technol. 2012, 46, 3060–3075 DOI: 10.1021/es2031505.

Hirai, H.; Takada, H.; Ogata, Y.; Yamashita, R.; Mizukawa, K.; Saha, M.; Kwan, C.; Moore, C.; Gray, H.; Laursen, D.; Zettler, E. R.; Farrington, J. W.; Reddy, C. M.; Peacock, E. E.; Ward, M. W. Organic Micropollutants in Marine Plastics Debris from the Open Ocean and Remote and Urban Beaches. Marine Pollution Bulletin 2011, 62 (8), 1683–1692. https://doi.org/10.1016/j.marpolbul.2011.06.004.

Hoet, P. H. M.; Nemmar, A.; Nemery, B. Health impact of nanomaterials? Nat. Biotechnol. 2004, 22, 19–19 DOI: 10.1038/nbt0104-19.

Holmes, L. A.; Turner, A.; Thompson, R. C. Adsorption of Trace Metals to Plastic Resin Pellets in the Marine Environment. Environ. Pollut. 2012, 160, 42–48. https://doi.org/10.1016/j.envpol.2011.08.052.

Horton, A. A.; Walton, A.; Spurgeon, D. J.; Lahive, E.; Svendsen, C. Microplastics in freshwater and terrestrial environments: Evaluating the current understanding to identify the knowledge gaps and future research priorities. Sci. Total Environ. 2017, 586, 127–141 DOI: 10.1016/j.scitotenv.2017.01.190.

Hüffer, T.; Hofmann, T. Sorption of non-polar organic compounds by micro-sized plastic particles in aqueous solution. Environ. Pollut. 2016, 214, 194–201 DOI: 10.1016/j.envpol.2016.04.018.

Huntington, A.; Corcoran, P. L.; Jantunen, L.; Thaysen, C.; Bernstein, S.; Stern, G. A.; Rochman, C. M. A First Assessment of Microplastics and Other Anthropogenic Particles in Hudson Bay and

the Surrounding Eastern Canadian Arctic Waters of Nunavut. FACETS 2020, 5 (1), 432–454. https://doi.org/10.1139/facets-2019-0042.

Hussain, N. Recent Advances in the Understanding of Uptake of Microparticulates across the Gastrointestinal Lymphatics. Adv. Drug Deliv. Rev. 2001, 50 (1–2), 107–142. https://doi.org/10.1016/S0169-409X(01)00152-1.

J Holland, B.; Hay, J. Thermal Degradation of Nylon Polymers. Polym. Int. 2000, 49, 943–948. https://doi.org/10.1002/1097-0126(200009)49:9<943::AID-PI400>3.0.CO;2-5.

Jahnke, A.; Arp, H. P. H.; Escher, B. I.; Gewert, B.; Gorokhova, E.; Kühnel, D.; Ogonowski, M.; Potthoff, A.; Rummel, C.; Schmitt-Jansen, M.; et al. Reducing Uncertainty and Confronting Ignorance about the Possible Impacts of Weathering Plastic in the Marine Environment. Environ. Sci. Technol. Lett. 2017, 4, 85–90 DOI: 10.1021/acs.estlett.7b00008.

Jakubowicz, I.; Enebro, J.; Yarahmadi, N. Challenges in the Search for Nanoplastics in the Environment—A Critical Review from the Polymer Science Perspective. Polymer Testing 2021, 93, 106953. https://doi.org/10.1016/j.polymertesting.2020.106953.

Jambeck, J. R.; Geyer, R.; Wilcox, C.; Siegler, T. R.; Perryman, M.; Andrady, A.; Narayan, R.; Law, K. L. Plastic Waste Inputs from Land into the Ocean. Science 2015, 347 (6223), 768–771. https://doi.org/10.1126/science.1260352.

Ji, X.; Ma, Y.; Zeng, G.; Xu, X.; Mei, K.; Wang, Z.; Chen, Z.; Dahlgren, R.; Zhang, M.; Shang, X. Transport and Fate of Microplastics from Riverine Sediment Dredge Piles: Implications for Disposal. Journal of Hazardous Materials 2021, 404, 124132. https://doi.org/10.1016/j.jhazmat.2020.124132.

Johnston, H. J.; Hutchison, G. R.; Christensen, F. M.; Peters, S.; Hankin, S.; Stone, V. Identification of the Mechanisms That Drive the Toxicity of TiO2 Particulates: The Contribution of Physicochemical Characteristics. Part. Fibre Toxicol. 2009, 6 (1), 33. https://doi.org/10.1186/1743-8977-6-33.

Jordan, A. M.; Kim, K.; Soetrisno, D.; Hannah, J.; Bates, F. S.; Jaffer, S. A.; Lhost, O.; Macosko, C. W. Role of Crystallization on Polyolefin Interfaces: An Improved Outlook for Polyolefin Blends. Macromolecules 2018, 51 (7), 2506–2516. https://doi.org/10.1021/acs.macromol.8b00206.

Jung, M. R.; Horgen, F. D.; Orski, S. V.; Rodriguez C., V.; Beers, K. L.; Balazs, G. H.; Jones, T. T.; Work, T. M.; Brignac, K. C.; Royer, S.-J.; Hyrenbach, K. D.; Jensen, B. A.; Lynch, J. M. Validation of ATR FT-IR to Identify Polymers of Plastic Marine Debris, Including Those Ingested by Marine Organisms. Marine Pollution Bulletin 2018, 127, 704–716. https://doi.org/10.1016/j.marpolbul.2017.12.061.

Kaiser, J. The Dirt on Ocean Garbage Patches. Science 2010, 328 (5985), 1506–1506. https://doi.org/10.1126/science.328.5985.1506.

Kang, H.; Park, S.; Lee, B.; Ahn, J.; Kim, S. Modification of a Nile Red Staining Method for Microplastics Analysis: A Nile Red Plate Method. Water 2020, 12 (11), 3251. https://doi.org/10.3390/w12113251.

Kanhai, L. D. K.; Gårdfeldt, K.; Lyashevska, O.; Hassellöv, M.; Thompson, R. C.; O'Connor, I. Microplastics in Sub-Surface Waters of the Arctic Central Basin. Marine Pollution Bulletin 2018, 130, 8–18. https://doi.org/10.1016/j.marpolbul.2018.03.011.

Kankanige, D.; Babel, S. Contamination by ≥6.5 Mm-Sized Microplastics and Their Removability in a Conventional Water Treatment Plant (WTP) in Thailand. Journal of Water Process Engineering 2021, 40, 101765. https://doi.org/10.1016/j.jwpe.2020.101765.

Kaposi, K. L.; Mos, B.; Kelaher, B. P.; Dworjanyn, S. A. Ingestion of Microplastic Has Limited Impact on a Marine Larva. Environ. Sci. Technol. 2014, 48, 1638–1645 DOI: 10.1021/es404295e.

Käppler, A.; Fischer, D.; Oberbeckmann, S.; Schernewski, G.; Labrenz, M.; Eichhorn, K.-J.; Voit, B. Analysis of Environmental Microplastics by Vibrational Microspectroscopy: FTIR, Raman or Both? Anal Bioanal Chem 2016, 408 (29), 8377–8391. https://doi.org/10.1007/s00216-016-9956-3.

Käppler, A.; Fischer, M.; Scholz-Böttcher, B. M.; Oberbeckmann, S.; Labrenz, M.; Fischer, D.; Eichhorn, K.-J.; Voit, B. Comparison of μ-ATR-FTIR Spectroscopy and Py-GCMS as Identification Tools for Microplastic Particles and Fibers Isolated from River Sediments. Anal Bioanal Chem 2018, 410 (21), 5313–5327. https://doi.org/10.1007/s00216-018-1185-5.

Karami, A.; Golieskardi, A.; Keong Choo, C.; Larat, V.; Galloway, T. S.; Salamatinia, B. The Presence of Microplastics in Commercial Salts from Different Countries. Sci. Rep. 2017, 7, 46173. https://doi.org/10.1038/srep46173.

Kessler, R. Engineered Nanoparticles in Consumer Products: Understanding a New Ingredient. Environ. Health Perspect. 2011, 119, a120–a125 DOI: 10.1289/ehp.119-a120.

Khangarot, B. S.; Ray, P. K.; Chandr, H. *Daphnia magna* as a Model to Assess Heavy Metal Toxicity: Comparative Assessment with Mouse System. Acta Hydrochim. Hydrobiol. 1987, 15 (4), 427–432. https://doi.org/10.1002/aheh.19870150415.

Klee, M. S.; Chang, I. Pyrolysis-GC/MS/IR Analysis of Kraton 1107. Hewlett Packard July 1989.

Klein, S.; Worch, E.; Knepper, T. P. Occurrence and Spatial Distribution of Microplastics in River Shore Sediments of the Rhine-Main Area in Germany. Environ. Sci. Technol. 2015, 49 (10), 6070–6076. https://doi.org/10.1021/acs.est.5b00492.

Koehler, A.; Anderson, A.; Andrady, A.; Arthur, C.; Baker, J.; Bouwman, H.; Gall, S.; Hidalgo-Ruz, V.; Köhler, A.; Law, K. L.; Leslie, H.; Kershaw, P.; Pahl, S.; Potemra, J.; Ryan, P.; Shim, W. J.; Thompson, R.; Hideshige Takada; Turra, A.; Vethaak, D.; Wyles, K. SOURCES, FATE AND EFFECTS OF MICROPLASTICS IN THE MARINE ENVIRONMENT: A GLOBAL ASSESSMENT. 2015. https://doi.org/10.13140/RG.2.1.3803.7925.

Koelmans, A. A.; Besseling, E.; Shim, W. J. Nanoplastics in the Aquatic Environment. Critical Review. In Marine Anthropogenic Litter; Bergmann, M., Gutow, L., Klages, M., Eds.; Springer International Publishing: Cham, 2015; pp 325–340.

Koelmans, A. A.; Kooi, M.; Law, K. L.; van Sebille, E. All Is Not Lost: Deriving a Top-down Mass Budget of Plastic at Sea. Environ. Res. Lett. 2017, 12 (11), 114028. https://doi.org/10.1088/1748-9326/aa9500.

Koelmans, A. A.; Mohamed Nor, N. H.; Hermsen, E.; Kooi, M.; Mintenig, S. M.; De France, J. Microplastics in Freshwaters and Drinking Water: Critical Review and Assessment of Data Quality. Water Res. 2019, 155, 410–422. https://doi.org/10.1016/j.watres.2019.02.054.

Kosuth, M.; Mason, S. A.; Wattenberg, E. V. Anthropogenic Contamination of Tap Water, Beer, and Sea Salt. PLoS ONE 2018, 13 (4), e0194970. https://doi.org/10.1371/journal.pone.0194970.

Kraton Corporation https://kraton.com/ (accessed 2020 -04 -16).

Kühn, S.; van Werven, B.; van Oyen, A.; Meijboom, A.; Bravo Rebolledo, E. L.; van Franeker, J. A. The Use of Potassium Hydroxide (KOH) Solution as a Suitable Approach to Isolate Plastics Ingested by Marine Organisms. Marine Pollution Bulletin 2017, 115 (1–2), 86–90. https://doi.org/10.1016/j.marpolbul.2016.11.034.

Kwak, J. I.; An, Y.-J. Microplastic Digestion Generates Fragmented Nanoplastics in Soils and Damages Earthworm Spermatogenesis and Coelomocyte Viability. Journal of Hazardous Materials 2021, 402, 124034. https://doi.org/10.1016/j.jhazmat.2020.124034.

Labbe, A. B.; Bagshaw, C. R.; Uttal, L. Inexpensive Adaptations of Basic Microscopes for the Identification of Microplastic Contamination Using Polarization and Nile Red Fluorescence Detection. J. Chem. Educ. 2020, 97 (11), 4026–4032. https://doi.org/10.1021/acs.jchemed.0c00518.

Lambert, S.; Wagner, M. Characterisation of Nanoplastics during the Degradation of Polystyrene. Chemosphere 2016, 145, 265–268. https://doi.org/10.1016/j.chemosphere.2015.11.078.

Law, K. L.; Thompson, R. C. Microplastics in the Seas. Science 2014, 345 (6193), 144–145. https://doi.org/10.1126/science.1254065.

Lee, J.; Hong, S.; Song, Y. K.; Hong, S. H.; Jang, Y. C.; Jang, M.; Heo, N. W.; Han, G. M.; Lee, M. J.; Kang, D.; et al. Relationships among the abundances of plastic debris in different size classes on beaches in South Korea. Mar. Pollut. Bull. 2013, 77, 349–354 DOI: 10.1016/j.marpolbul.2013.08.013.

Lenz, R.; Enders, K.; Stedmon, C. A.; Mackenzie, D. M. A.; Nielsen, T. G. A Critical Assessment of Visual Identification of Marine Microplastic Using Raman Spectroscopy for Analysis

Improvement. Marine Pollution Bulletin 2015, 100 (1), 82–91. https://doi.org/10.1016/j.marpolbul.2015.09.026.

Lewinski, N.; Colvin, V.; Drezek, R. Cytotoxicity of Nanoparticles. Small 2008, 4, 26–49 DOI: 10.1002/smll.200700595.

Li, X.; Chen, L.; Mei, Q.; Dong, B.; Dai, X.; Ding, G.; Zeng, E. Y. Microplastics in Sewage Sludge from the Wastewater Treatment Plants in China. Water Research 2018, 142, 75–85. https://doi.org/10.1016/j.watres.2018.05.034.

Liebmann B.; Köppel S.; Königshofer P.; Bucsics T.; Reiberger T.; Schwabl P. Assessment of microplastic concentrations in human stool - final results of a prospective study. 2018. https://doi.org/10.13140/rg.2.2.16638.02884.

Lithner, D.; Damberg, J.; Dave, G.; Larsson, Å. Leachates from Plastic Consumer Products – Screening for Toxicity with *Daphnia Magna*. Chemosphere 2009, 74 (9), 1195–1200. https://doi.org/10.1016/j.chemosphere.2008.11.022.

Löder, M. G. J.; Gerdts, G. Methodology Used for the Detection and Identification of Microplastics—A Critical Appraisal. In Marine Anthropogenic Litter; Bergmann, M., Gutow, L., Klages, M., Eds.; Springer International Publishing: Cham, 2015; pp 201–227. https://doi.org/10.1007/978-3-319-16510-3_8.

Löder, M. G. J.; Kuczera, M.; Mintenig, S.; Lorenz, C.; Gerdts, G. Focal Plane Array Detector-Based Micro-Fourier-Transform Infrared Imaging for the Analysis of Microplastics in Environmental Samples. Environ. Chem. 2015, 12 (5), 563. https://doi.org/10.1071/EN14205.

Logan, B. E. Environmental Transport Processes, 2nd ed.; Wiley: Hoboken, N.J, 2012.

Louette, P.; Bodino, F.; Pireaux, J.-J. Nylon 6 (N6) Reference XPS Reference Core Level and Energy Loss Spectra. Surf. Sci. Spectra 2005, 12 (1), 12–17. https://doi.org/10.1116/11.20050903.

Lovern, S. B.; Klaper, R. *Daphnia Magna* Mortality When Exposed to Titanium Dioxide and Fullerene (C60) Nanoparticles. Environ. Toxicol. Chem. 2006, 25 (4), 1132–1137.

Lovern, S. B.; Strickler, J. R.; Klaper, R. Behavioral and Physiological Changes in *Daphnia Magna* When Exposed to Nanoparticle Suspensions (Titanium Dioxide, Nano-C60, and C60HxC70Hx). Environ. Sci. Technol. 2007, 41 (12), 4465–4470.

Lu, Y.; Zhang, Y.; Deng, Y.; Jiang, W.; Zhao, Y.; Geng, J.; Ding, L.; Ren, H. Uptake and Accumulation of Polystyrene Microplastics in Zebrafish (Danio Rerio) and Toxic Effects in Liver. Environ. Sci. Technol. 2016, 50 (7), 4054–4060. https://doi.org/10.1021/acs.est.6b00183.

Luo, H.; Zhao, Y.; Li, Y.; Xiang, Y.; He, D.; Pan, X. Aging of Microplastics Affects Their Surface Properties, Thermal Decomposition, Additives Leaching and Interactions in Simulated Fluids. Science of The Total Environment 2020, 714, 136862. https://doi.org/10.1016/j.scitotenv.2020.136862.

Lusher, A. L.; McHugh, M.; Thompson, R. C. Occurrence of Microplastics in the Gastrointestinal Tract of Pelagic and Demersal Fish from the English Channel. Mar. Pollut. Bull. 2013, 67 (1–2), 94–99. https://doi.org/10.1016/j.marpolbul.2012.11.028.

Lusher, A. L.; Tirelli, V.; O'Connor, I.; Officer, R. Microplastics in Arctic Polar Waters: The First Reported Values of Particles in Surface and Sub-Surface Samples. Sci Rep 2015, 5 (1), 14947. https://doi.org/10.1038/srep14947.

Maes, T.; Jessop, R.; Wellner, N.; Haupt, K.; Mayes, A. G. A Rapid-Screening Approach to Detect and Quantify Microplastics Based on Fluorescent Tagging with Nile Red. Sci Rep 2017, 7 (1), 44501. https://doi.org/10.1038/srep44501.

Mahon, A. M.; O'Connell, B.; Healy, M. G.; O'Connor, I.; Officer, R.; Nash, R.; Morrison, L. Microplastics in Sewage Sludge: Effects of Treatment. Environ. Sci. Technol. 2017, 51 (2), 810–818. https://doi.org/10.1021/acs.est.6b04048.

Makhdoumi, P.; Amin, A. A.; Karimi, H.; Pirsaheb, M.; Kim, H.; Hossini, H. Occurrence of Microplastic Particles in the Most Popular Iranian Bottled Mineral Water Brands and an Assessment of Human Exposure. Journal of Water Process Engineering 2021, 39, 101708. https://doi.org/10.1016/j.jwpe.2020.101708.

Mallikarjunachari, G.; Ghosh, P. Analysis of Strength and Response of Polymer Nano Thin Film Interfaces Applying Nanoindentation and Nanoscratch Techniques. Polymer 2016, 90, 53–66. https://doi.org/10.1016/j.polymer.2016.02.042.

Martins, J.; Oliva Teles, L.; Vasconcelos, V. Assays with *Daphnia Magna* and *Danio Rerio* as Alert Systems in Aquatic Toxicology. Environ. Int. 2007, 33 (3), 414–425. https://doi.org/10.1016/j.envint.2006.12.006.

Mason, S. A.; Welch, V. G.; Neratko, J. Synthetic Polymer Contamination in Bottled Water. Front. Chem. 2018, 6. https://doi.org/10.3389/fchem.2018.00407.

Mattsson, K.; Ekvall, M. T.; Hansson, L.-A.; Linse, S.; Malmendal, A.; Cedervall, T. Altered Behavior, Physiology, and Metabolism in Fish Exposed to Polystyrene Nanoparticles. Environ. Sci. Technol. 2015, 49 (1), 553–561. https://doi.org/10.1021/es5053655.

Mattsson, K.; Hansson, L.-A.; Cedervall, T. Nano-plastics in the aquatic environment. Env. Sci Process. Impacts 2015, 17, 1712–1721 DOI: 10.1039/C5EM00227C.

Mattsson, K.; Johnson, E. V.; Malmendal, A.; Linse, S.; Hansson, L.-A.; Cedervall, T. Brain Damage and Behavioural Disorders in Fish Induced by Plastic Nanoparticles Delivered through the Food Chain. Sci. Rep. 2017, 7 (1). https://doi.org/10.1038/s41598-017-10813-0.

McCormick, A.; Hoellein, T. J.; Mason, S. A.; Schluep, J.; Kelly, J. J. Microplastic Is an Abundant and Distinct Microbial Habitat in an Urban River. Environ. Sci. Technol. 2014, 48 (20), 11863–11871. https://doi.org/10.1021/es503610r.

McDevitt, J. P.; Criddle, C. S.; Morse, M.; Hale, R. C.; Bott, C. B.; Rochman, C. M. Addressing the Issue of Microplastics in the Wake of the Microbead-Free Waters Act—A New Standard Can Facilitate Improved Policy. Environ. Sci. Technol. 2017, 51 (12), 6611–6617. https://doi.org/10.1021/acs.est.6b05812.

McIlwraith, H. K.; Lin, J.; Erdle, L. M.; Mallos, N.; Diamond, M. L.; Rochman, C. M. Capturing Microfibers – Marketed Technologies Reduce Microfiber Emissions from Washing Machines. Marine Pollution Bulletin 2019, 139, 40–45. https://doi.org/10.1016/j.marpolbul.2018.12.012.

McKeen, L. W. Introduction to the Effect of Heat Aging on Plastics. In The Effect of Long Term Thermal Exposure on Plastics and Elastomers; Elsevier, 2014; pp 17–42. https://doi.org/10.1016/B978-0-323-22108-5.00002-3.

Meides, N.; Menzel, T.; Poetzschner, B.; Löder, M. G. J.; Mansfeld, U.; Strohriegl, P.; Altstaedt, V.; Senker, J. Reconstructing the Environmental Degradation of Polystyrene by Accelerated Weathering. Environ. Sci. Technol. 2021, 55 (12), 7930–7938. https://doi.org/10.1021/acs.est.0c07718.

Minor, E. C.; Lin, R.; Burrows, A.; Cooney, E. M.; Grosshuesch, S.; Lafrancois, B. An Analysis of Microlitter and Microplastics from Lake Superior Beach Sand and Surface-Water. Science of The Total Environment 2020, 744, 140824. https://doi.org/10.1016/j.scitotenv.2020.140824.

Mintenig, S. M.; Löder, M. G. J.; Primpke, S.; Gerdts, G. Low Numbers of Microplastics Detected in Drinking Water from Ground Water Sources. Science of The Total Environment 2019, 648, 631–635. https://doi.org/10.1016/j.scitotenv.2018.08.178.

Mitrano, D. M.; Beltzung, A.; Frehland, S.; Schmiedgruber, M.; Cingolani, A.; Schmidt, F. Synthesis of Metal-Doped Nanoplastics and Their Utility to Investigate Fate and Behaviour in Complex Environmental Systems. Nat. Nanotechnol. 2019, 14 (4), 362–368. https://doi.org/10.1038/s41565-018-0360-3.

Morritt, D.; Stefanoudis, P. V.; Pearce, D.; Crimmen, O. A.; Clark, P. F. Plastic in the Thames: A River Runs through It. Marine Pollution Bulletin 2014, 78 (1–2), 196–200. https://doi.org/10.1016/j.marpolbul.2013.10.035.

Müller, Y. K.; Wernicke, T.; Pittroff, M.; Witzig, C. S.; Storck, F. R.; Klinger, J.; Zumbülte, N. Microplastic Analysis—Are We Measuring the Same? Results on the First Global Comparative Study for Microplastic Analysis in a Water Sample. Anal Bioanal Chem 2020, 412 (3), 555–560. https://doi.org/10.1007/s00216-019-02311-1.

Muncke, J. Exposure to Endocrine Disrupting Compounds via the Food Chain: Is Packaging a Relevant Source? Sci. Total Environ. 2009, 407 (16), 4549–4559. https://doi.org/10.1016/j.scitotenv.2009.05.006.

Murphy, F.; Ewins, C.; Carbonnier, F.; Quinn, B. Wastewater Treatment Works (WwTW) as a Source of Microplastics in the Aquatic Environment. Environ. Sci. Technol. 2016, 50 (11), 5800–5808. https://doi.org/10.1021/acs.est.5b05416.

NanoSight. NanoSight NTA 2.1 Analytical Software. Operating Manual. 2010.

Napper, I. E.; Bakir, A.; Rowland, S. J.; Thompson, R. C. Characterisation, quantity and sorptive properties of microplastics extracted from cosmetics. Mar. Pollut. Bull. 2015, 99, 178–185 DOI: 10.1016/j.marpolbul.2015.07.029.

Nasr-Esfahani, M.; Mehrabanian, M. HA/Nylon 6,6 Porous Scaffolds Fabricated by Salt-Leaching/Solvent Casting Technique: Effect of Nano-Sized Filler Content on Scaffold Properties. Int. J. Nanomedicine 2011, 1651. https://doi.org/10.2147/IJN.S21203.

Nel, H. A.; Chetwynd, A. J.; Kelleher, L.; Lynch, I.; Mansfield, I.; Margenat, H.; Onoja, S.; Goldberg Oppenheimer, P.; Sambrook Smith, G. H.; Krause, S. Detection Limits Are Central to Improve Reporting Standards When Using Nile Red for Microplastic Quantification. Chemosphere 2021, 263, 127953. https://doi.org/10.1016/j.chemosphere.2020.127953.

Neves, D.; Sobral, P.; Ferreira, J. L.; Pereira, T. Ingestion of Microplastics by Commercial Fish off the Portuguese Coast. Mar. Pollut. Bull. 2015, 101 (1), 119–126. https://doi.org/10.1016/j.marpolbul.2015.11.008.

Ng, K. L.; Obbard, J. P. Prevalence of Microplastics in Singapore's Coastal Marine Environment. Marine Pollution Bulletin 2006, 52 (7), 761–767. https://doi.org/10.1016/j.marpolbul.2005.11.017.

Nguyen, B.; Claveau-Mallet, D.; Hernandez, L. M.; Xu, E. G.; Farner, J. M.; Tufenkji, N. Separation and Analysis of Microplastics and Nanoplastics in Complex Environmental Samples. Acc. Chem. Res. 2019, 52 (4), 858–866. https://doi.org/10.1021/acs.accounts.8b00602.

Nizzetto, L.; Futter, M.; Langaas, S. Are Agricultural Soils Dumps for Microplastics of Urban Origin? Environmental Science & Technology 2016, 50 (20), 10777–10779. https://doi.org/10.1021/acs.est.6b04140.

Noda, I.; Dowrey, A. E.; Haynes, J. L.; Marcott, C. Group Frequency Assignments for Major Infrared Bands Observed in Common Synthetic Polymers. In Physical Properties of Polymers Handbook; Mark, J. E., Ed.; Springer New York: New York, NY, 2007; pp 395–406. https://doi.org/10.1007/978-0-387-69002-5_22.

Novotna, K.; Cermakova, L.; Pivokonska, L.; Cajthaml, T.; Pivokonsky, M. Microplastics in Drinking Water Treatment – Current Knowledge and Research Needs. Science of The Total Environment 2019, 667, 730–740. https://doi.org/10.1016/j.scitotenv.2019.02.431.

O'Brien, S.; Okoffo, E. D.; O'Brien, J. W.; Ribeiro, F.; Wang, X.; Wright, S. L.; Samanipour, S.; Rauert, C.; Toapanta, T. Y. A.; Albarracin, R.; Thomas, K. V. Airborne Emissions of Microplastic Fibres from Domestic Laundry Dryers. Science of The Total Environment 2020, 747, 141175. https://doi.org/10.1016/j.scitotenv.2020.141175.

Oberdörster, G.; Oberdörster, E.; Oberdörster, J. Nanotoxicology: an emerging discipline evolving from studies of ultrafine particles. Environ. Health Perspect. 2005, 113, 823–839.

OECD. Nanosafety at the OECD: The First Five Years 2006-2010; Better Policies for Better Lives; France, 2011.

Oecd. Test No. 202: *Daphnia* Sp. Acute Immobilisation Test; 2004; Vol. 1.

Oßmann, B. E.; Sarau, G.; Holtmannspötter, H.; Pischetsrieder, M.; Christiansen, S. H.; Dicke, W. Small-Sized Microplastics and Pigmented Particles in Bottled Mineral Water. Water Research 2018, 141, 307–316. https://doi.org/10.1016/j.watres.2018.05.027.

Panko, J. M.; Chu, J.; Kreider, M. L.; Unice, K. M. Measurement of Airborne Concentrations of Tire and Road Wear Particles in Urban and Rural Areas of France, Japan, and the United States. Atmospheric Environment 2013, 72, 192–199. https://doi.org/10.1016/j.atmosenv.2013.01.040.

Pegram, J. E.; Andrady, A. L. Outdoor Weathering of Selected Polymeric Materials under Marine Exposure Conditions. Polym. Degrad. Stab. 1989, 26 (4), 333–345. https://doi.org/10.1016/0141-3910(89)90112-2.

Peixoto, D.; Pinheiro, C.; Amorim, J.; Oliva-Teles, L.; Guilhermino, L.; Vieira, M. N. Microplastic Pollution in Commercial Salt for Human Consumption: A Review. Estuarine, Coastal and Shelf Science 2019, 219, 161–168. https://doi.org/10.1016/j.ecss.2019.02.018.

Pekka Sinervo. Small is Different: A Science Perspective on the Regulatory Challenges of the Nanoscale; Council of Canadian Academies: Ottawa, ON, Canada, 2008.

Physical electronics ULVAC-PHI. Phi NanoTOF II.

Pikuda, O.; Xu, E. G.; Berk, D.; Tufenkji, N. Toxicity Assessments of Micro- and Nanoplastics Can Be Confounded by Preservatives in Commercial Formulations. Environ. Sci. Technol. Lett. 2018. https://doi.org/10.1021/acs.estlett.8b00614.

Pitt, J. A.; Kozal, J. S.; Jayasundara, N.; Massarsky, A.; Trevisan, R.; Geitner, N.; Wiesner, M.; Levin, E. D.; Di Giulio, R. T. Uptake, Tissue Distribution, and Toxicity of Polystyrene

Nanoparticles in Developing Zebrafish (Danio Rerio). Aquat. Toxicol. 2018, 194, 185–194. https://doi.org/10.1016/j.aquatox.2017.11.017.

Pivokonsky, M.; Cermakova, L.; Novotna, K.; Peer, P.; Cajthaml, T.; Janda, V. Occurrence of Microplastics in Raw and Treated Drinking Water. Sci. Total Environ. 2018, 643, 1644–1651. https://doi.org/10.1016/j.scitotenv.2018.08.102.

Prata, J. C.; Alves, J. R.; da Costa, J. P.; Duarte, A. C.; Rocha-Santos, T. Major Factors Influencing the Quantification of Nile Red Stained Microplastics and Improved Automatic Quantification (MP-VAT 2.0). Science of The Total Environment 2020, 719, 137498. https://doi.org/10.1016/j.scitotenv.2020.137498.

Ranjan, V. P.; Joseph, A.; Goel, S. Microplastics and Other Harmful Substances Released from Disposable Paper Cups into Hot Water. Journal of Hazardous Materials 2021, 404, 124118. https://doi.org/10.1016/j.jhazmat.2020.124118.

Rasch, M. R.; Rossinyol, E.; Hueso, J. L.; Goodfellow, B. W.; Arbiol, J.; Korgel, B. A. Hydrophobic Gold Nanoparticle Self-Assembly with Phosphatidylcholine Lipid: Membrane-Loaded and Janus Vesicles. Nano Lett. 2010, 10, 3733–3739 DOI: 10.1021/nl102387n.

Raval, N.; Maheshwari, R.; Kalyane, D.; Youngren-Ortiz, S. R.; Chougule, M. B.; Tekade, R. K. Importance of Physicochemical Characterization of Nanoparticles in Pharmaceutical Product Development. In Basic Fundamentals of Drug Delivery; Elsevier, 2019; pp 369–400. https://doi.org/10.1016/B978-0-12-817909-3.00010-8.

Ray, A.; Das, S.; Chattopadhyay, N. Aggregation of Nile Red in Water: Prevention through Encapsulation in β-Cyclodextrin. ACS Omega 2019, 4 (1), 15–24. https://doi.org/10.1021/acsomega.8b02503.

Renner, G.; Schmidt, T. C.; Schram, J. Analytical Methodologies for Monitoring Micro(Nano)Plastics: Which Are Fit for Purpose? Current Opinion in Environmental Science & Health 2018, 1, 55–61. https://doi.org/10.1016/j.coesh.2017.11.001.

Ribeiro-Claro, P.; Nolasco, M. M.; Araújo, C. Characterization of Microplastics by Raman Spectroscopy. In Comprehensive Analytical Chemistry; Elsevier, 2017; Vol. 75, pp 119–151. https://doi.org/10.1016/bs.coac.2016.10.001.

Rillig, M. C.; Kim, S. W.; Kim, T.-Y.; Waldman, W. R. The Global Plastic Toxicity Debt. Environ. Sci. Technol. 2021, 55 (5), 2717–2719. https://doi.org/10.1021/acs.est.0c07781.

Rios*, L. M.; Jones, P. R.; Moore, C.; Narayan, U. V. Quantitation of persistent organic pollutants adsorbed on plastic debris from the Northern Pacific Gyre's "eastern garbage patch." J. Environ. Monit. 2010, 12, 2226 DOI: 10.1039/c0em00239a.

Rocha-Santos, T.; Duarte, A. C. A Critical Overview of the Analytical Approaches to the Occurrence, the Fate and the Behavior of Microplastics in the Environment. TrAC Trends in Analytical Chemistry 2015, 65, 47–53. https://doi.org/10.1016/j.trac.2014.10.011.

Rochman, C. M.; Hoh, E.; Kurobe, T.; Teh, S. J. Ingested plastic transfers hazardous chemicals to fish and induces hepatic stress. Sci. Rep. 2013, 3 DOI: 10.1038/srep03263.

Rochman, C. M.; Kross, S. M.; Armstrong, J. B.; Bogan, M. T.; Darling, E. S.; Green, S. J.; Smyth, A. R.; Veríssimo, D. Scientific Evidence Supports a Ban on Microbeads. Environ. Sci. Technol. 2015, 49 (18), 10759–10761. https://doi.org/10.1021/acs.est.5b03909.

Rochman, C. M.; Tahir, A.; Williams, S. L.; Baxa, D. V.; Lam, R.; Miller, J. T.; Teh, F.-C.; Werorilangi, S.; Teh, S. J. Anthropogenic Debris in Seafood: Plastic Debris and Fibers from

Textiles in Fish and Bivalves Sold for Human Consumption. Sci Rep 2015, 5 (1), 14340. https://doi.org/10.1038/srep14340.

Rolsky, C.; Kelkar, V.; Driver, E.; Halden, R. U. Municipal Sewage Sludge as a Source of Microplastics in the Environment. Current Opinion in Environmental Science & Health 2020, 14, 16–22. https://doi.org/10.1016/j.coesh.2019.12.001.

Ross, P. S.; Chastain, S.; Vassilenko, E.; Etemadifar, A.; Zimmermann, S.; Quesnel, S.-A.; Eert, J.; Solomon, E.; Patankar, S.; Posacka, A. M.; Williams, B. Pervasive Distribution of Polyester Fibres in the Arctic Ocean Is Driven by Atlantic Inputs. Nat Commun 2021, 12 (1), 106. https://doi.org/10.1038/s41467-020-20347-1.

Roussis, S. G.; Fedora, J. W. Use of a Thermal Extraction Unit for Furnace-Type Pyrolysis: Suitability for the Analysis of Polymers by Pyrolysis/GC/MS. Rapid Communications in Mass Spectrometry 1996, 10 (1), 82–90. https://doi.org/10.1002/(SICI)1097-0231(19960115)10:1<82::AID-RCM449>3.0.CO;2-N.

Sadler, G. W. Ultraviolet Radiation at Edmonton, Alberta, Canada. Solar Energy 1992, 49 (1), 13–17. https://doi.org/10.1016/0038-092X(92)90121-P.

Sait, S. T. L.; Sørensen, L.; Kubowicz, S.; Vike-Jonas, K.; Gonzalez, S. V.; Asimakopoulos, A. G.; Booth, A. M. Microplastic Fibres from Synthetic Textiles: Environmental Degradation and Additive Chemical Content. Environmental Pollution 2021, 268, 115745. https://doi.org/10.1016/j.envpol.2020.115745.

Sanchez, W.; Bender, C.; Porcher, J.-M. Wild Gudgeons (Gobio Gobio) from French Rivers Are Contaminated by Microplastics: Preliminary Study and First Evidence. Environ. Res. 2014, 128, 98–100. https://doi.org/10.1016/j.envres.2013.11.004.

SB-1422 California Safe Drinking Water Act: Microplastics.

Schirinzi, G. F.; Pérez-Pomeda, I.; Sanchís, J.; Rossini, C.; Farré, M.; Barceló, D. Cytotoxic Effects of Commonly Used Nanomaterials and Microplastics on Cerebral and Epithelial Human Cells. Environ. Res. 2017, 159, 579–587. https://doi.org/10.1016/j.envres.2017.08.043.

Schunk, P. F. T.; Kalil, I. C.; Pimentel-Schmitt, E. F.; Lenz, D.; de Andrade, T. U.; Ribeiro, J. S.; Endringer, D. C. ICP-OES and Micronucleus Test to Evaluate Heavy Metal Contamination in Commercially Available Brazilian Herbal Teas. Biol. Trace Elem. Res. 2016, 172 (1), 258–265. https://doi.org/10.1007/s12011-015-0566-2.

Schwabl, P.; Köppel, S.; Königshofer, P.; Bucsics, T.; Trauner, M.; Reiberger, T.; Liebmann, B. Detection of Various Microplastics in Human Stool: A Prospective Case Series. Ann Intern Med 2019, 171 (7), 453. https://doi.org/10.7326/M19-0618.

Schymanski, D.; Goldbeck, C.; Humpf, H.-U.; Fürst, P. Analysis of Microplastics in Water by Micro-Raman Spectroscopy: Release of Plastic Particles from Different Packaging into Mineral Water. Water Research 2018, 129, 154–162. https://doi.org/10.1016/j.watres.2017.11.011.

Shim, W. J.; Hong, S. H.; Eo, S. E. Identification Methods in Microplastic Analysis: A Review. Anal. Methods 2017, 9 (9), 1384–1391. https://doi.org/10.1039/C6AY02558G.

Shruti, V. C.; Pérez-Guevara, F.; Elizalde-Martínez, I.; Kutralam-Muniasamy, G. Toward a Unified Framework for Investigating Micro(Nano)Plastics in Packaged Beverages Intended for Human Consumption. Environmental Pollution 2021, 268, 115811. https://doi.org/10.1016/j.envpol.2020.115811.

Silva, A. B.; Bastos, A. S.; Justino, C. I. L.; da Costa, J. P.; Duarte, A. C.; Rocha-Santos, T. A. P. Microplastics in the Environment: Challenges in Analytical Chemistry - A Review. Analytica Chimica Acta 2018, 1017, 1–19. https://doi.org/10.1016/j.aca.2018.02.043.

Simon, M.; van Alst, N.; Vollertsen, J. Quantification of Microplastic Mass and Removal Rates at Wastewater Treatment Plants Applying Focal Plane Array (FPA)-Based Fourier Transform Infrared (FT-IR) Imaging. Water Research 2018, 142, 1–9. https://doi.org/10.1016/j.watres.2018.05.019.

Singh, T. Generation of Microplastics from the Opening and Closing of Disposable Plastic Water Bottles. Journal of Water and Health 2021, 19 (3), 488–498. https://doi.org/10.2166/wh.2021.025.

Sturm, M. T.; Horn, H.; Schuhen, K. The Potential of Fluorescent Dyes—Comparative Study of Nile Red and Three Derivatives for the Detection of Microplastics. Anal Bioanal Chem 2021, 413 (4), 1059–1071. https://doi.org/10.1007/s00216-020-03066-w.

Tagg, A. S.; Harrison, J. P.; Ju-Nam, Y.; Sapp, M.; Bradley, E. L.; Sinclair, C. J.; Ojeda, J. J. Fenton's Reagent for the Rapid and Efficient Isolation of Microplastics from Wastewater. Chem. Commun. 2017, 53 (2), 372–375. https://doi.org/10.1039/C6CC08798A.

Talvitie, J.; Mikola, A.; Koistinen, A.; Setälä, O. Solutions to Microplastic Pollution – Removal of Microplastics from Wastewater Effluent with Advanced Wastewater Treatment Technologies. Water Research 2017, 123, 401–407. https://doi.org/10.1016/j.watres.2017.07.005.

Tea Fact Sheet – 2018-2019; Fact sheet; Tea Association of the USA, 2019.

Tegge, G. Handbook of Adhesives. Starch - Stärke 1964, 16 (1), 38–38. https://doi.org/10.1002/star.19640160117.

Thompson, R. C. Lost at Sea: Where Is All the Plastic? Science 2004, 304 (5672), 838–838. https://doi.org/10.1126/science.1094559.

Trevor Nace. UK To Ban All Plastic Straws, Cotton Swabs, And Single-Use Plastics. Forbes. April 2018.

Tsuge, S.; Ohtani, H.; Watanabe, C. Pyrolysis - GC/MS Data Book of Synthetic Polymers: Pyrograms, Thermograms and MS of Pyrolyzates; Elsevier, 2011.

United States of America 114th congress (2015-2016). Microbead-Free Waters Act of 2015; 2015.

Van Cauwenberghe, L.; Claessens, M.; Vandegehuchte, M. B.; Janssen, C. R. Microplastics Are Taken up by Mussels (Mytilus Edulis) and Lugworms (Arenicola Marina) Living in Natural Habitats. Environmental Pollution 2015, 199, 10–17. https://doi.org/10.1016/j.envpol.2015.01.008.

Velzeboer, I.; Kwadijk, C. J. A. F.; Koelmans, A. A. Strong Sorption of PCBs to Nanoplastics, Microplastics, Carbon Nanotubes, and Fullerenes. Environ. Sci. Technol. 2014, 48, 4869–4876 DOI: 10.1021/es405721v.

Venkatachalam, S.; Shilpa, G.; Jayprakash, V.; Prashant, R.; Krishna, R.; Anil, K. Degradation and Recyclability of Poly (Ethylene Terephthalate). In Polyester; Saleh, H. E.-D., Ed.; InTech, 2012. https://doi.org/10.5772/48612.

Veselá, Š.; Ondruška, V.; Kuča, K.; Patočka, J. Freshwater Microcrustacean *Daphnia Magna Straus* as an Early Screen Model to Compare Toxicity of Acetylcholinesterase Inhibitors. J. Appl. Biomed. 2006, 4 (2), 105–110. https://doi.org/10.32725/jab.2006.010.

Vilaplana, F.; Ribes-Greus, A.; Karlsson, S. Degradation of Recycled High-Impact Polystyrene. Simulation by Reprocessing and Thermo-Oxidation. Polymer Degradation and Stability 2006, 91 (9), 2163–2170. https://doi.org/10.1016/j.polymdegradstab.2006.01.007.

Villegas-Navarro, A.; Rosas-L, E.; Reyes, J. L. The Heart of *Daphnia Magna*: Effects of Four Cardioactive Drugs. Comp. Biochem. Physiol. Toxicol. Pharmacol. CBP 2003, 136 (2), 127–134.

von Moos, N.; Burkhardt-Holm, P.; Köhler, A. Uptake and Effects of Microplastics on Cells and Tissue of the Blue Mussel Mytilus edulis L. after an Experimental Exposure. Environ. Sci. Technol. 2012, 46, 11327–11335 DOI: 10.1021/es302332w.

Wagner, M.; Scherer, C.; Alvarez-Muñoz, D.; Brennholt, N.; Bourrain, X.; Buchinger, S.; Fries, E.; Grosbois, C.; Klasmeier, J.; Marti, T.; Rodriguez-Mozaz, S.; Urbatzka, R.; Vethaak, A.D.; Winther-Nielsen, M.; Reifferscheid, G. Microplastics in Freshwater Ecosystems: What We Know and What We Need to Know. Environ. Sci. Eur. 2014, 26 (1). https://doi.org/10.1186/s12302-014-0012-7.

Wagner, S.; Reemtsma, T. Things We Know and Don't Know about Nanoplastic in the Environment. Nat. Nanotechnol. 2019, 14 (4), 300–301. https://doi.org/10.1038/s41565-019-0424-z.

Wang, J.; Zhou, G.; Chen, C.; Yu, H.; Wang, T.; Ma, Y.; Jia, G.; Gao, Y.; Li, B.; Sun, J. Acute Toxicity and Biodistribution of Different Sized Titanium Dioxide Particles in Mice after Oral Administration. Toxicol. Lett. 2007, 168 (2), 176–185. https://doi.org/10.1016/j.toxlet.2006.12.001.

Wang, W.; Ge, J.; Yu, X. Bioavailability and Toxicity of Microplastics to Fish Species: A Review. Ecotoxicology and Environmental Safety 2020, 189, 109913. https://doi.org/10.1016/j.ecoenv.2019.109913.

Warheit, D. B.; Donner, E. M. Risk Assessment Strategies for Nanoscale and Fine-Sized Titanium Dioxide Particles: Recognizing Hazard and Exposure Issues. Food Chem. Toxicol. 2015, 85, 138–147. https://doi.org/10.1016/j.fct.2015.07.001.

Watts, A. J. R.; Urbina, M. A.; Goodhead, R.; Moger, J.; Lewis, C.; Galloway, T. S. Effect of Microplastic on the Gills of the Shore Crab Carcinus Maenas. Environmental Science & Technology 2016, 50 (10), 5364–5369. https://doi.org/10.1021/acs.est.6b01187.

Witzig, C. S.; Földi, C.; Wörle, K.; Habermehl, P.; Pittroff, M.; Müller, Y. K.; Lauschke, T.; Fiener, P.; Dierkes, G.; Freier, K. P.; Zumbülte, N. When Good Intentions Go Bad—False Positive Microplastic Detection Caused by Disposable Gloves. Environ. Sci. Technol. 2020, 54 (19), 12164–12172. https://doi.org/10.1021/acs.est.0c03742.

World Economic Forum. The New Plastics Economy - Rethinking the Future of Plastics; 2016.

World Health Organization. Microplastics in Drinking Water; Switzerland, 2019.

Wright, S. L.; Kelly, F. J. Plastic and Human Health: A Micro Issue? Environ. Sci. Technol. 2017, 51 (12), 6634–6647. https://doi.org/10.1021/acs.est.7b00423.

Yang, D.; Shi, H.; Li, L.; Li, J.; Jabeen, K.; Kolandhasamy, P. Microplastic Pollution in Table Salts from China. Environ. Sci. Technol. 2015, 49 (22), 13622–13627. https://doi.org/10.1021/acs.est.5b03163.

Yin, L.; Chen, B.; Xia, B.; Shi, X.; Qu, K. Polystyrene Microplastics Alter the Behavior, Energy Reserve and Nutritional Composition of Marine Jacopever (Sebastes Schlegelii). Journal of Hazardous Materials 2018, 360, 97–105. https://doi.org/10.1016/j.jhazmat.2018.07.110.

Yousefi, N.; Tufenkji, N. Probing the Interaction between Nanoparticles and Lipid Membranes by Quartz Crystal Microbalance with Dissipation Monitoring. Front. Chem. 2016, 4 DOI: 10.3389/fchem.2016.00046.

Yousefi, N.; Wargenau, A.; Tufenkji, N. Toward More Free-Floating Model Cell Membranes: Method Development and Application to Their Interaction with Nanoparticles. ACS Appl. Mater. Interfaces 2016, 8, 14339–14348 DOI: 10.1021/acsami.6b00775.

Zalasiewicz, J.; Waters, C. N.; Ivar do Sul, J. A.; Corcoran, P. L.; Barnosky, A. D.; Cearreta, A.; Edgeworth, M.; Gałuszka, A.; Jeandel, C.; Leinfelder, R.; McNeill, J. R.; Steffen, W.; Summerhayes, C.; Wagreich, M.; Williams, M.; Wolfe, A. P.; Yonan, Y. The Geological Cycle of Plastics and Their Use as a Stratigraphic Indicator of the Anthropocene. Anthropocene 2016, 13, 4–17. https://doi.org/10.1016/j.ancene.2016.01.002.

Zhang, T.-R.; Wang, C.-X.; Dong, F.-Q.; Gao, Z.-Y.; Zhang, C.-J.; Zhang, X.-J.; Fu, L.-M.; Wang, Y.; Zhang, J.-P. Uptake and Translocation of Styrene Maleic Anhydride Nanoparticles in Murraya Exotica Plants As Revealed by Noninvasive, Real-Time Optical Bioimaging. Environ. Sci. Technol. 2019, 53 (3), 1471–1481. https://doi.org/10.1021/acs.est.8b05689.

Zhang, Z.; Chen, Y. Effects of Microplastics on Wastewater and Sewage Sludge Treatment and Their Removal: A Review. Chemical Engineering Journal 2020, 382, 122955. https://doi.org/10.1016/j.cej.2019.122955.

Zhong, H.; Yang, S.; Zhu, L.; Liu, C.; Zhang, Y.; Zhang, Y. Effect of Microplastics in Sludge Impacts on the Vermicomposting. Bioresource Technology 2021, 326, 124777. https://doi.org/10.1016/j.biortech.2021.124777.

Zhu, L.; Zhao, S.; Bittar, T. B.; Stubbins, A.; Li, D. Photochemical Dissolution of Buoyant Microplastics to Dissolved Organic Carbon: Rates and Microbial Impacts. Journal of Hazardous Materials 2020, 383, 121065. https://doi.org/10.1016/j.jhazmat.2019.121065.

Ziajahromi, S.; Neale, P. A.; Rintoul, L.; Leusch, F. D. L. Wastewater Treatment Plants as a Pathway for Microplastics: Development of a New Approach to Sample Wastewater-Based Microplastics. Water Research 2017, 112, 93–99. https://doi.org/10.1016/j.watres.2017.01.042.

Zubris, K. A. V.; Richards, B. K. Synthetic Fibers as an Indicator of Land Application of Sludge. Environmental Pollution 2005, 138 (2), 201–211. https://doi.org/10.1016/j.envpol.2005.04.013.